

Integrating Chromatin Structure and Global Chromosome Dynamics

By

RANA AHMAD SULEIMAN ALMUHUR

A thesis submitted to
The University of Birmingham
For the degree of
DOCTOR OF PHILOSOPHY

School of Bioscience
University of Birmingham
September 2014

UNIVERSITY OF
BIRMINGHAM

University of Birmingham Research Archive

e-theses repository

This unpublished thesis/dissertation is copyright of the author and/or third parties. The intellectual property rights of the author or third parties in respect of this work are as defined by The Copyright Designs and Patents Act 1988 or as modified by any successor legislation.

Any use made of information contained in this thesis/dissertation must be in accordance with that legislation and must be properly acknowledged. Further distribution or reproduction in any format is prohibited without the permission of the copyright holder.

Abstract

DNA associates with proteins to form chromatin which is essential for the compaction of the DNA into the cell nucleus and is highly dynamic in order to allow the different biological processes of the DNA to occur. Chromatin compaction is achieved at different hierarchical levels: the 10nm fibre (DNA associates to nucleosomes formed by different histones), the Higher Order Chromatin fibre and the 300 nm chromosome structures. This study has shown that both H1 and H4 histones play a crucial role in preserving meiotic as well as mitotic chromosome structure and functional genome integrity in *Arabidopsis*. The role of the different linker histone H1 isoforms as well as the core histone H4 in *Arabidopsis thaliana* was investigated using T-DNA and RNAi mutant lines which showed different meiotic defects. Chromosomal breaks as well as non-homologous connections in the *h4^{RNAi}* were linked to 45S/5S rDNA disorganisation, suggesting that H4 preserves chromosome integrity at these rDNA regions. *Ath1.1* mutant presented univalents and reduced chiasma frequency at metaphase I, linked to a severe defect in ASY1 localisation on the meiotic chromosome axes. Thus, indicating that histone H1.1 is vital for proper chromatin axis organization that permit normal loading of recombination machinery proteins in *Arabidopsis*.

ACKNOWLEDGEMENTS

My greatest thanks for Almighty ALLAH help and support, which not only enabled me to meet my project goals within the PhD programmed time, but also supplied me with self-motivation and potency required for keeping my academic progress on, even though at hard times, and up to bringing this thesis to light.

I would like to thank Dr. Eugenio Sanchez-Moran for this chance to do such an advanced project on chromatin components using advanced molecular and cytological techniques. I appreciate a lot his extraordinary supervision. Moreover, I am so grateful for him for all discussions that I had with him, which definitely added a global and deeper value to the whole work. Besides, his guidance allowed me to present my project within United Kingdom as well as international conferences, which added a lot to both my academic knowledge as well as my future career.

My warmest thank is to Prof. Chris Franklin, for his supervision and support. Besides to, all valuable discussions that we had during my PhD meetings, which always ended with a broaden figure for my project outcome in relation to new research findings.

I would like to thank Dr. Susan Armstrong and Dr. Kim Osman who have shared their time, experience, support and advice over the years.

I am so thankful for Claire Bauckham for all of her technical support and guidance during my project as well as her close friendship which helped me a lot during hard work times. I would thank Steve Price for his technical support with the FISH probes,

Ruth Perry for her valuable help and support throughout my PhD and Karen Staples for support at "Green House". I will never forget to be thankful to all colleagues, especially Allan West, and staff; within Eugenio Sanchez-Moran, Chris Franklin, Susan Amstrong and Franklin-Tong joint labs, as well as Juliate Coates lab, for all help, support, and sharing times.

I am so grateful and thankful for the Islamic Development Bank (IDB) manager and staff, for rewarding me with this Merit Scholarship for Excellence, to complete my PhD study, without it, my PhD study could not have been achieved.

Finally, my deepest and heartfelt thanks is for my family, especially my husband Mohammad Barakat, for his love and support, as well as my little angels, Yazeed, Saed and Yamen, whom although were cheeky at day and night time, but still their love supply me with super powers to continue my PhD.

List of Contents

CHAPTER 1

1 INTRODUCTION	1
1.1. BIOLOGICAL SIGNIFICANCE OF THE CHROMATIN	2
1.2. CHROMATIN STRUCTURE	2
1.2.1. The nucleosome fibre	4
1.2.1.1. Histones	6
1.2.1.2. Histone variants	9
1.2.1.3. Histone exchange	11
1.2.1.4. Histone modification	13
1.2.2. The Higher Order Chromatin Fibre	16
1.2.2.1. The 30 nm fibre could be polymorphic	16
1.2.2.2. Linker histones putative role in the formation of the higher order chromatin fibre structure	19
1.2.3. The 300nm Chromatin Fibre and the Chromosome Axis	28
1.3. CHROMATIN ROLE IN DNA-ASSOCIATED BIOLOGICAL PROCESSES	32
1.3.1. Replication	32
1.3.2. Transcription	33
1.3.3. Repair	34
1.3.4. Mitosis	37
1.3.4.1. Sister chromatid cohesion	40
1.3.5. Meiosis	43
1.3.5.1. Meiosis I and II	44
1.3.5.2. Chromosomes axes establishment	48
1.3.5.3. Homologous chromosomes pairing and synapsis	49
1.3.5.4. Meiotic recombination	53
1.3.5.4.1. DNA double strand breaks (DSB) formation	54
1.3.5.4.2. DNA DSBs processing	55
1.3.5.4.3. Single strand invasion	56
1.3.5.4.4. NCOs vs COs	57
1.3.5.4.5. CO interference and Class I & II COs	58
1.3.5.4.6. dHj structure processing	60
1.3.5.5. Meiotic recombination in the context of chromosome axes	60

1.3.5.6 COs link to chromatin-----	64
1.4. <i>ARABIDOPSIS</i> AS A MODEL SPECIES-----	65
1.5. PROJECT AIMS-----	65

CHAPTER 2

2 MATERIALS AND METHODS-----	67
2.1. PLANT MATERIAL-----	68
2.1.1. Growth conditions of plant material-----	68
2.1.2. Seeds sterilization for growing on MS media-----	70
2.1.3. Cisplatin treatment-----	70
2.2. MOLECULAR GENETICS TECHNIQUES-----	70
2.2.1. DNA extraction from plant leaves-----	70
2.2.2. RNA extraction from plant tissues-----	71
2.2.3. cDNA synthesis-----	72
2.2.4. DNA agarose gel electrophoresis-----	72
2.2.5. Primer design-----	73
2.2.6. DNA amplification by Polymerase Chain Reaction (PCR)-----	75
2.2.7. DNA band extraction from gel-----	76
2.2.8. DNA sequencing-----	76
2.2.9. DNA sequence analysis-----	77
2.2.10. Cloning-----	77
2.2.11. Preparation of competent <i>E.coli</i> cells-----	80
2.2.12. Restriction Enzyme digestions-----	80
2.3. CYTOLOGY-----	81
2.3.1. Meiotic Cytology Preparations-----	81
2.3.2. Fluorescence <i>in situ</i> hybridization (FISH) 45S/5S probes preparation-----	82
2.3.3. Fluorescence in situ hybridization-----	83
2.3.4 Immunolocalization-----	85
2.3.4.1. Squash Immunolocalization Method in <i>Arabidopsis</i> -----	85
2.3.4.2. Spreading Immunolocalization method in <i>Arabidopsis</i> -----	86
2.3.5. Pollen viability Assessment by using Alexander Stain (Alexander, 1969)-----	87
2.3.6 Fluorescence microscopy and image analysis-----	87
2.4. GENETIC CROSSING OF PLANTS-----	87
2.5. DATA STATISTICAL ANALYSIS-----	88

2.6. List of Websites-----	88
----------------------------	----

CHAPTER 3

3 KNOCKING DOWN HISTONE H4 IN *ARABIDOPSIS*-----90

3.1. INTRODUCTION-----	91
------------------------	----

3.2. <i>IN SILICO</i> ANALYSIS-----	93
-------------------------------------	----

3.2.1. <i>Arabidopsis</i> histone H4 isoforms have identical sequence-----	93
--	----

3.2.2. Characterization of an $h4^{RNAi}$ mutant line-----	97
--	----

3.2.3. $h4^{RNAi}$ mutant phenotype-----	98
--	----

3.2.4. Fertility analysis of <i>Arabidopsis thaliana</i> $h4$ knock-down mutant lines-----	99
--	----

3.2.5. Meiotic cytological analysis of histone $h4^{RNAi}$ mutant line -----	100
--	-----

3.2.6. Fluorescence <i>in situ</i> hybridization (FISH) analysis of <i>Arabidopsis</i> histone $h4^{RNAi}$ line-----	103
--	-----

3.2.7. Mitotic cytological analysis of <i>Arabidopsis</i> histone $h4^{RNAi}$ mutant line-----	104
--	-----

3.2.8. $h4^{RNAi}$ seeds are cisplatin sensitive-----	105
---	-----

3.3. ANALYSIS OF <i>ARABIDOPSIS</i> HISTONE H3-H4 CHAPERON complex-----	108
---	-----

3.3.1 <i>fas</i> mutants phenotype-----	109
---	-----

3.3.2. Fertility analysis of <i>fas</i> mutants-----	110
--	-----

3.3.3. Cytological analysis of <i>fas</i> mutants-----	111
--	-----

3.3.3.1. Meiosis of <i>fas</i> 1-3 mutant-----	112
--	-----

3.3.3.2. Meiosis of <i>fas</i> 2-3 mutant-----	114
--	-----

3.3.3.3. <i>fas</i> 1-3 mitotic defects-----	115
--	-----

3.3.3.4. <i>fas</i> 2-3 mitotic defects-----	115
--	-----

3.3.4. <i>fas</i> mutants sensitivity to cisplatin -----	116
--	-----

3.3.4.1. <i>fas</i> 2-3 seeds are cisplatin sensitive.-----	116
---	-----

3.3.4.2. <i>fas</i> 2-3 seeds are cisplatin sensitive.-----	119
---	-----

3.4. DISCUSSION-----	122
----------------------	-----

3.4.1. <i>Arabidopsis</i> genome encodes for eight isoforms of histone H4-----	122
--	-----

3.4.2. Histone $h4^{RNAi}$ mutant show abnormal meiosis-----	123
--	-----

3.4.3. Histone $h4^{RNAi}$ mutants show NORs organization defects-----	125
--	-----

3.4.4. <i>fas</i> mutants displayed developmental defects-----	127
--	-----

3.4.5. <i>fas</i> mutants show semi-sterile phenotype-----	128
--	-----

3.4.6. <i>fas</i> 1-3 and <i>fas</i> 2-3 semi-sterile phenotype has meiotic origin-----	129
---	-----

3.4.7. <i>fas</i> mutants have similar defects to $h4^{RNAi}$ mutants-----	132
--	-----

3.4.8. Histone H4 is needed for mitotic chromosome architecture-----	133
3.4.9. Mutants of <i>h4^{RNAi}</i> and <i>fas1&2</i> are sensitive to cisplatin-----	135

CHAPTER 4

4 Genetic Analysis of HISTONE H1 Isoforms in <i>Arabidopsis</i> -----	138
4.1. INTRODUCTION-----	139
4.2. RESULTS-----	141
4.2.1. <i>In Silico</i> Analysis of histone H1 isoforms in <i>Arabidopsis</i> -----	141
4.2.1.1. Identification of histone H1 isoforms in <i>Arabidopsis</i> -----	141
4.2.1.2. Expression pattern of the linker histone H1 genes-----	145
4.2.2. Characterisation of the <i>Arabidopsis</i> AtH1A isoform-----	146
4.2.2.1. Phenotypic characterisation of <i>Ath1a</i> mutant plants-----	146
4.2.2.2. Fertility of <i>Ath1a</i> mutant plants-----	147
4.2.3. Characterisation of the <i>Arabidopsis</i> AtH1B isoform -----	148
4.2.3.1. Phenotypic characterisation of <i>Ath1b</i> mutant plants-----	149
4.2.3.2. Fertility of <i>Ath1b</i> mutant plants-----	150
4.2.4 Characterisation of the <i>Arabidopsis</i> AtH1C isoform -----	151
4.2.4.1. Phenotypic characterisation of <i>Ath1c</i> mutant plants-----	152
4.2.4.2. Fertility of <i>Ath1c</i> mutant plants-----	153
4.2.5. Characterisation of the <i>Arabidopsis</i> AtH1D isoform-----	154
4.2.5.1. Phenotypic characterisation of <i>Ath1d</i> mutant plants-----	155
4.2.5.2. Fertility of <i>Ath1d</i> mutant plants-----	155
4.2.6. Characterisation of the <i>Arabidopsis</i> AtH1.1 isoform-----	157
4.2.6.1. Phenotypic characterisation of <i>Ath1.1</i> mutant plants-----	160
4.2.6.1.1. Phenotypic characterisation of <i>Ath1.1-1</i> mutant plants-----	160
4.2.6.1.2. Phenotypic characterisation of <i>Ath1.1-2</i> mutant plants-----	162
4.2.6.1.3. Phenotypic characterisation of <i>Ath1.1^{RNAi}</i> mutant plants-----	163
4.2.6.2. Fertility of <i>Ath1.1</i> mutant plants-----	165
4.2.6.2.1. Fertility of <i>Ath1.1-1</i> mutant plants-----	165
4.2.6.2.2. Fertility of <i>Ath1.1-2</i> mutant plants-----	166
4.2.6.2.3. Fertility of <i>Ath1.1^{RNAi}</i> mutant plants-----	167
4.2.7. Characterisation of the <i>Arabidopsis</i> AtH1.2 isoform-----	169
4.2.7.1. Phenotypic characterisation of <i>Ath1.2</i> mutant plants-----	170
4.2.7.2. Fertility of <i>Ath1.2</i> mutant plants-----	170

4.2.8. Characterisation of the <i>Arabidopsis</i> Ath1.3 isoform-----	172
4.2.8.1. Phenotypic characterisation of <i>Ath1.3</i> mutant plants-----	173
4.2.8.2. Fertility of <i>Ath1.3</i> mutant plants-----	174
4.2.9. Characterisation of the <i>Arabidopsis</i> AthON4 isoform-----	175
4.2.9.1. Phenotypic characterisation of <i>Athon4</i> mutant plants-----	176
4.2.9.2. Fertility of <i>Athon4</i> mutant plants-----	177
4.2.10. Characterisation of the <i>Arabidopsis</i> AthON5 isoform-----	178
4.2.10.1. Phenotypic characterisation of <i>Athon5</i> mutant plants-----	179
4.2.9.10. Fertility of <i>Athon5</i> mutant plants-----	180
4.3 DISCUSSION-----	182
4.3.1 <i>Arabidopsis</i> Linker histone H1s isoforms affect the flowering time of the plant-----	182
4.3.2 Histones play a role in proper timing of plant development-----	183
4.3.3 Histone H1 gene duplication allows H1 compensation in the single Knock-Out T-DNA mutants-----	185
4.3.4 Loss of H1 like proteins prevents normal fertility-----	186
4.4 FUTURE WORK-----	189
4.4.1 H1s Redundancy effect-----	189

CHAPTER 5

5 H1.1 ROLE IN MITOTIC AND MEIOTIC CHROMOSOME AXIS ORGANIZATION-190	
5.1. INTRODUCTION-----	191
5.2. CYTOLOGICAL ANALYSIS OF MITOSIS IN <i>Ath1.1</i> MUTANTS-----	192
5.3. <i>Ath1.1</i> EXPRESSION IS NOT SPECIFIC TO MITOSIS-----	194
5.4. CYTOLOGICAL ANALYSIS OF MEIOSIS IN <i>ARABIDOPSIS</i> WILD-TYPE AND <i>Ath1.1</i> MUTANTS-----	196
5.4.1. Meiotic cytology of <i>Arabidopsis</i> wild-type-----	196
5.4.2. Meiotic cytology of <i>Ath1.1-1</i> -----	199
5.4.3. Meiotic cytology of <i>Ath1.1-2</i> -----	203
5.4.4. Meiotic cytology of <i>h1.1^{RNAi}</i> mutant lines-----	206
5.5. VERIFICATION OF <i>Ath1.1</i> MUTANTS PHENOTYPE-----	209
5.5.1. Fluorescence <i>in situ</i> hybridization (FISH) analysis of the T-DNA insertion in <i>Ath1.1</i> mutants-----	209
5.5.2. Allelism test-----	211

5.5.2.1. Phenotypic observation of the <i>Ath1.1-2</i> ^{+/-} / <i>Ath1.1-1</i> ^{+/-} double heterozygote plant-----	211
5.5.2.2. Fertility analysis of <i>Ath1.1-2</i> ^{+/-} / <i>Ath1.1-1</i> ^{+/-} -----	212
5.5.2.3. Meiotic cytology of <i>Ath1.1-2</i> ^{+/-} / <i>Ath1.1-1</i> ^{+/-} -----	214
5.6. ANALYSIS OF THE MEIOTIC CHROMOSOME AXIS AND SC PROTEINS LOCALISATION IN WILD-TYPE AND <i>Ath1.1-1</i> MUTANTS-----	217
5.7. MEIOTIC COHESION COMPONENTS; ATSYN1, AtSMC1 AND ATSMC3 ARE NORMALLY LOCALIZED IN <i>Ath1.1-1</i> -----	225
5.8. CHIASMA FREQUENCY ANALYSIS IN WILD-TYPE AND <i>Ath1.1</i> MUTANTS----	228
5.8.1. Chiasma frequency analysis in <i>Arabidopsis</i> wild-type metaphase I meiocytes-----	230
5.8.2. Chiasma frequency analysis in <i>Ath1.1-1</i> metaphase I meiocytes-----	230
5.8.3. Chiasma frequency analysis in <i>Ath1.1-2</i> metaphase I meiocytes-----	233
5.8.4. Chiasma frequency analysis in <i>h1.1</i> ^{RNAi} metaphase I meiocytes-----	236
5.9. ANALYSIS OF RECOMBINATION PROTEINS IN <i>Ath1.1-1</i> -----	239
5.10. DISCUSSION-----	244
5.10.1. Developmental defects in <i>Ath1.1</i> mutants could be a consequence of epigenetic changes-----	244
5.10.2. Chromosome axis architecture is aberrant in the <i>Ath1.1</i> mutants; <i>Ath1.1-1</i> , <i>Ath1.1-2</i> , <i>h1.1</i> ^{RNAi} -----	245
5.10.3. Homologous chromosome pairing and synapsis is aberrant in <i>Ath1.1</i> mutants-----	247
5.10.4. <i>Ath1.1</i> differ significantly in chiasma frequency and their distribution from <i>Ath1.1-2</i> and <i>h1.1</i> ^{RNAi} -----	252
5.10.5. AtH1.1-1 and chromosome axes morphogenesis-----	258
5.10.6. AtH1.1 is required for normal ASY1 localization on the axes to allow normal meiotic recombination progression-----	259
5.10.7. H1.1 and meiotic chromosome axis organization within the homologous recombination context-----	262

CHAPTER 6

6 GENERAL DISCUSSION-----	265
6.1. INTRODUCTION-----	266
6.2. The core histone H4-----	268

6.2.1. Meiosis is affected in the <i>h4^{RNAi}</i> mutants-----	268
6.2.2. Histone H4 is needed for proper meiotic chromosome organisation-----	271
6.2.3. Histone H4 is needed for mitotic chromosome architecture-----	273
6.3. THE LINKER HISTONE -----	274
6.3.1. Linker histones are involved in plant development-----	274
6.3.2. Chromosome axis architecture is disturbed in <i>Ath1.1</i> mutants; <i>Ath1.1-1</i> , <i>Ath1.1-2</i> , <i>h1.1^{RNAi}</i> -----	275
6.3.3. AtH1.1 is needed for proper meiosis-----	277
6.3.4. <i>Ath1.1-1</i> mutants show disturbed meiotic chromosome axes-----	280
6.3.5. AtH1.1 is needed for proper COs-----	281
6.4. OVERVIEW OF CHROMATIN ASSOCIATED-HISTONES AND CHROMATIN--	282
6.5. FUTURE WORK-----	284
6.5.1. Core histone H4-----	284
6.5.2. Linker histone H1-----	285
6.6. CONCLUSION-----	287

CHAPTER 7

7 REFERENCES-----	290
-------------------	-----

FIGURES

Figure 1.1: The current chromatin compaction model	4
Figure 1.2: Nucleosome structure.....	5
Figure 1.3: Schematic representation of the C-terminus histone fold in the nucleosome core histones.....	7
Figure 1.4: The Histone modification map.....	16
Figure 1.5: Different structural models proposed for the higher order chromatin fibre...	18
Figure 1.6: A model for the linker histone H1 role in the higher order chromatin fibre formation.....	19
Figure 1.7: Histone H1 role in the polymorphic chromatin dynamics.....	23
Figure 1.8: Diagram of the two pathways of non-homologous end joining: the canonical KU Dependent NHEJ (D-NHEJ) and the Backup NHEJ (B-NHEJ) pathways.....	28
Figure 1.9: 300 nm Higher Order Chromatin structure and chromosome scaffold.....	31
Figure 1.10: Schematic diagram representing the mitotic nuclear division.....	39
Figure 1.11: Schematic diagram of mitotic and meiotic cohesion complex.....	43
Figure 1.12: Schematic diagram represents meiosis nuclear division stages.....	47
Figure 1.13: (A) Chromosome organisation during prophase I. (B) Synaptonemal complex structure.....	52
Figure 1.14: Schematic representation of the DNA DSB repair pathway in meiosis.....	54
Figure 2.1: pDRIVE Cloning Vector.....	79
Figure 3.1: BlastP alignment (NCBI) of Histone H4 protein sequence in human (Hs) and Arabidopsis (AT).....	92
Figure 3.2: <i>Arabidopsis</i> Histone H4 genes map.....	94
Figure 3.3: Clustalw2 alignment of <i>Arabidopsis</i> Histone H4 CDs.....	95
Figure 3.4 A: Wu Blastp alignment of <i>Arabidopsis</i> histones H4 protein sequences.....	96
Figure 3.4 B: WU-Blast (TAIR) alignment of <i>Arabidopsis</i> Histone H4 proteins.....	96
Figure 3.5: <i>Arabidopsis thaliana</i> Histone H4 genes microarray profile.....	97
Figure 3.6: ChromDB H4 genomic model.....	98
Figure 3.7: HF01 ds RNA construct (T-DNA region).....	98
Figure 3.8: Phenotype of h4RNAi mutant in comparison to wild-type plants.....	99
Figure 3.9: Fertility of <i>Arabidopsis</i> histone $h4^{RNAi}$ mutant line in comparison to wild-type plants.....	100
Figure 3.10: Meiotic cytology of $h4^{RNAi}$ PMCs vs wild-type.....	102

Figure 3.11: FISH analysis of NORs of the <i>h4^{RNAi}</i> and wild-type <i>Arabidopsis</i> plants.....	104
Figure 3.12: Mitosis in <i>A. thaliana h4^{RNAi}</i> mutant plants.....	105
Figure 3.13: Cisplatin sensitivity phenotype of wild-type and <i>h4^{RNAi}</i> seeds.....	107
Figure 3.14: Cisplatin sensitivity analysis of wild-type and <i>h4^{RNAi}</i>	108
Figure 3.15: Genevestigator diagram showing FAS proteins expression.....	109
Figure 3.16: Phenotype of <i>fas</i> mutants; <i>fas 1-3</i> and <i>fas 2-3</i> , in comparison to wild-type plants.....	110
Figure 3.17: Fertility of <i>fas</i> mutants; <i>fas 1-3</i> & <i>fas 2-3</i> , and the corresponding wild-type (WT).....	111
Figure 3.18: Meiosis of <i>fas 1-3</i> PMCs.....	113
Figure 3.19: Meiotic atlas of <i>fas 2-3</i> PMCs.....	114
Figure 3.20: Mitotic defects of <i>fas 1-3</i> mutant line at anaphase.....	115
Figure 3.21: Mitotic defects of <i>fas 2-3</i> mutant line.....	116
Figure 3.22: Cisplatin sensitivity phenotype of wild-type and <i>fas 1-3</i> seeds.....	118
Figure 3.23: Cisplatin sensitivity analysis of wild-type and <i>fas 1-3</i> seeds.....	119
Figure 3.24: Cisplatin sensitivity phenotype of wild-type and <i>fas 2-3</i> seeds.....	121
Figure 3.25: Cisplatin sensitivity analysis of wild-type and <i>fas 2-3</i> seeds.....	122
Figure 3.26: Comparison of seed set per silique mean in <i>h4^{RNAi}</i> and <i>fas</i> mutants vs wild-type.....	133
Figure 4.1: Histone H1 structural role in higher order chromatin structures formation.....	144
Figure 4.2: Localization of histone H1 genes at the <i>Arabidopsis</i> chromosomes.....	143
Figure 4.3: Homology protein sequence alignment of <i>Arabidopsis</i> histone H1 proteins.....	144
Figure 4.4: Expression profile of <i>Arabidopsis</i> histone H1 genes during plant developmental stages.....	145
Figure 4.5: Schematic diagram of At1g54260 locus showing T-DNA insertion localization.....	146
Figure 4.6: Phenotypic characterisation of <i>Ath1a</i> mutant plants.....	147
Figure 4.7: Fertility of <i>Ath1a</i> in comparison to Wild-type plants.....	148
Figure 4.8: Schematic diagram of At5g08780 locus showing the T-DNA insertion localization.....	149
Figure 4.9: Phenotypic characterisation of <i>Ath1b</i> mutant plants.....	150
Figure 4.10: Fertility of <i>Ath1b</i> in comparison to Wild-type plants.....	151

Figure 4.11: Schematic diagram of At1g48610 locus showing T-DNA insertion localisation.....	152
Figure 4.12: Phenotypic characterisation of <i>Ath1c</i> mutant plants.....	153
Figure 4.13: Fertility of <i>Ath1c</i> in comparison to Wild-type plants.....	154
Figure 4.14: Schematic diagram of At1g72740 locus showing T-DNA insertion localisation.....	155
Figure 4.15: Fertility of <i>Ath1d</i> in comparison to Wild-type plants.....	165
Figure 4.16: Schematic diagram of At1g06760 locus showing two different T-DNA insertion localisations.....	158
Figure 4.17: ChromDB model of HON1 ds RNA construct (T-DNA region).....	158
Figure 4.18: ChromDB blot analysis of <i>h1.1^{RNAi}</i> mutant lines.....	159
Figure 4.19: Phenotypic characterisation of <i>Arabidopsis Ath1.1-1</i> mutant plants in comparison to WT.....	161
Figure 4.20: Phenotypic characterisation of <i>Arabidopsis Ath1.1-2</i> mutant plants in comparison to WT.....	162
Figure 4.21: Phenotypic characterisation of <i>Arabidopsis h1.1^{RNAi}</i> mutant plants in comparison to WT.....	164
Figure 4.22: Fertility of <i>Ath1.1-1</i> mutant plants in comparison to Wild-type plants.....	166
Figure 4.23: Fertility of <i>Ath1.1-2</i> mutant plants in comparison to Wild-type plants.....	167
Figure 4.24: Fertility of <i>h1.1^{RNAi}</i> mutant plants in comparison to Wild-type plants.....	169
Figure 4.25: Schematic diagram of AT2G30620 locus showing T-DNA insertion localisation.....	170
Figure 4.26: Fertility of <i>Ath1.2</i> mutant plants in comparison to Wild-type plants.....	172
Figure 4.27: Schematic diagram of At2g18050 locus showing T-DNA insertion localisation.....	173
Figure 4.28: Phenotypic characterisation of <i>Ath1.3</i> mutant plants.....	174
Figure 4.29: Fertility of <i>Ath1.3</i> mutant plants in comparison to WT plants.....	175
Figure 4.30: Schematic diagram of At3g18035 locus showing T-DNA insertion localisation.....	176
Figure 4.31: Phenotypic characterisation of <i>Athon4</i> mutant plants.....	177
Figure 4.32: Fertility of <i>Athon4</i> in comparison to WT plants.....	178
Figure 4.33: Schematic diagram of At1g48620 locus showing T-DNA insertion localization.....	179
Figure 4.34: Phenotypic characterisation of <i>Athon5</i> mutant plants.....	179
Figure 4.35: Fertility of <i>Athon5</i> mutant plants in comparison to WT plants.....	181

Figure 4.36: Comparison between <i>Arabidopsis Ath1s</i> single T-DNA mutants and wild-type plants in flowering time delay.....	185
Figure 4.37: Fertility change in percentage for <i>Arabidopsis</i> histone <i>Ath1s</i> single mutant lines.....	187
Figure 5.1: Mitotic defect analysis in <i>Ath1.1</i> mutants; <i>Ath1.1-1</i> , <i>Ath1.1-2</i> and <i>h1.1^{RNAi}</i> , in comparison to WT.....	193
Figure 5.2: Genevestigator expression profile of <i>Arabidopsis</i> <i>Ath1.1</i> gene.....	195
Figure 5.3: Meiotic atlas of wild-type PMCs.....	198
Figure 5.4: Meiotic atlas of <i>Ath1.1-1</i> PMCs.....	201
Figure 5.5: Metaphase I defects observed in <i>Ath1.1-1</i> in comparison to WT.....	202
Figure 5.6: Meiotic atlas of <i>Ath1.1-2</i> PMCs.....	205
Figure 5.7: Meiotic atlas of <i>h1.1^{RNAi}</i> PMCs.....	208
Figure 5.8: FISH verification of <i>Ath1.1</i> TDNA insert.....	210
Figure 5.9: Phenotypic observation of <i>Ath1.1-2^{+/-}/Ath1.1-1^{+/-}</i>	212
Figure 5.10: Fertility of <i>Ath1.1-2^{+/-}/Ath1.1-1^{+/-}</i> in comparison to Wild-type plants.....	214
Figure 5.11: Meiotic defects of <i>Ath1.1-2^{+/-}/Ath1.1-1^{+/-}</i>	216
Figure 5.12: Dual Immunolocalization of ASY1, ZYP1 in WT meiocytes.....	219
Figure 5.13: Dual Immunolocalization of ASY1, on <i>Ath1.1-1</i> meiocytes.....	221-222
Figure 5.14: Immunolocalization of ASY1 (green) at zygotene on <i>Ath1.1-1</i> compared to WT cell.....	224
Figure 5.15: Dual Immunolocalization of ASY3 and ASY1 in WT and <i>Ath1.1-1</i> meiocytes.....	225
Figure 5.16 A: Immunolocalization of cohesion proteins SMC3 in the <i>Ath1.1-1</i> comparable to WT.....	226
Figure 5.16 B: Immunolocalization of cohesion proteins SMC1 in the <i>Ath1.1-1</i> comparable to WT.....	227
Figure 5.16 C: Immunolocalization of cohesion proteins SYN1 in the <i>Ath1.1-1</i> comparable to WT.....	227
Figure 5.17: FISH analysis of chiasmata in <i>Arabidopsis</i> WT and <i>Ath1.1</i> mutants at metaphase I.....	229
Figure 5.18: Chiasma analysis in <i>Ath1.1-1</i> in comparison to WT.....	232
Figure 5.19: Chiasma analysis in <i>Ath1.1-2</i> in comparison to WT.....	235
Figure 5.20: Chiasma analysis in <i>h1.1^{RNAi}</i> in comparison to WT.....	238
Figure 5.21A: Dual immunolocalization of RAD51 and ASY1 in the <i>Ath1.1-1</i> and WT.....	240

Figure 5.21 B: Dual immunolocalization of DMC1 and ASY1 in the <i>Ath1.1-1</i> and WT.....	241
Figure 5.22: Dual immunolocalization of MSH4 and ASY1 in the <i>Ath1.1-1</i> and WT....	242
Figure 5.23: Dual immunolocalization of MLH1 and ZYP1 in the <i>Ath1.1-1</i> and WT....	243
Figure 5.24: Comparison of chiasma frequency and distribution between <i>Ath1.1</i> mutants.....	257
Figure 5.25: Comparison of ASY1 and ZYP1 localisation on the <i>Ath1.1-1</i> and WT meiocytes.....	264

TABLES

Table 2.1: Data of Seeds analysed for Histones H1, H4 and related mutants: Gene locus and mutants lines studied.....	69
Table 2.2: Specific primer sequences histones mutant lines genotyping.....	74
Table 2.3: Primer sequences used to amplify T-DNA insertions, (LB: left border of T-DNA insertion).....	75
Table 2.4: Standard PCR reaction (T _m =melting temperature).....	76
Table 2.5: DNA sequencing reaction.....	77
Table 2.6: Cloning mixture preparation.....	78
Table 2.7: DNA transformation to DH5α competent cells.....	79
Table 2.8: Restriction enzymes: Requirements and conditions.....	81
Table 2.9: Plasmid description for the 45S/5S rDNA probes production.....	83
Table 2.10: rDNA probe labelling mixture.....	83
Table 2.11: rDNA probe labelling procedure.....	83
Table 2.12: Data sources web links.....	89
Table 3.1: Conserved domains of <i>Arabidopsis</i> histone H4 genes.....	94
Table 3.2: Summary of meiotic defects in the h4RNAi mutant.....	102
Table 3.3: comparison of sterility level intra fas mutants in reference to wild-type plants.....	129
Table 4.1: Histone H1s T-DNA mutant lines vs their given names through the research.....	144
Table 4.2: Summary of <i>Arabidopsis</i> histone Ath1s mutant lines phenotypic changes..	188
Table 4.3: Suggested double Histone Ath1 mutant lines crosses based on protein sequence homology.....	189
Table 5.1: Summary of defects seen in the mitosis of <i>Ath1.1</i> mutants.....	194
Table 5.2: Chiasma distribution in wild-type and <i>Ath1.1-1</i>	231
Table 5.3: Chiasma distribution in wild-type and <i>Ath1.1-1</i>	234
Table 5.4: Comparison of chiasma frequency and distribution in <i>Ath1.1-1</i> and <i>Ath1.1-2</i> null mutants.....	236
Table 5.5: Chiasma distribution in wild-type and <i>h1.1^{RNAi}</i>	237
Table 5.6: Summary of meiotic defects seen in the <i>Ath1.1</i> mutants.....	251
Table 5.7: Metaphase I defects seen in <i>Ath1.1</i> mutants comparable to WT.....	252
Table 6.1: Summary of meiotic defects in <i>Arabidopsis h4^{RNAi}</i> and <i>fas</i> mutants; <i>fas1-3</i> and <i>fas 2-3</i>	271

Table 6.2: Summary of mitotic defects in Ath1.1 mutants.....	276
Table 6.3: Summary of meiosis defects in the Ath1.1 mutants.....	279

List of Abbreviations

AB	Antibody
AE	Axial element
ASY1/3	Asynaptic1/3
At	<i>Arabidopsis thaliana</i>
ATP	Adenosine tri-phosphate
BAR	BASTA resistant gene
Bdf2	Bromodomain factor
BIO	Biotin
bp	Base pair
BrdU	Bromodeoxyuridine
BSA	Bovine serum albumin
CAC	Chromatin Assembly Complex
CAF1	Chromatin Assembly Factor-1
cDNA	copy DNA
CDC	Cell-Division-Cycle
chH5	Chicken Differentiation-Specific Histone H5
CO	CO
Col-0	<i>Arabidopsis thaliana</i> ecotype Columbia
COM	Chromosome Oscillatory Movement
C-terminal	Carboxyl-terminal
CTD	Carboxyl Terminal Domain
DAPI	4,6-Diaminido-2-Phenylindole
DDR	DNA Damage Response
DEPEC	Diethyl Pro-Carbonate
dHj	Double Holliday Junction
DIG	Digoxigenin
D-loop	Displacement Loop
DMC1	Disruption of Meiotic Control 1
DNA	Deoxyribonucleic Acid
DSB	Double-Strand Break
EDTA	Ethylene-Diamine-Tetra-Acetic Acid
EdU	5-Ethynyl-2-Deoxyuridine
EM	Electron Microscopy
EME1	Essential Meiotic Endonuclease 1
FAS	Fasciata
FISH	Fluorescent <i>In Situ</i> Hybridisation
FITC	Fluorescein Isothiocyanate
FLC	Flowering Locus C
FRAP	Fluorescence Recovery After Photobleaching
GD	Globular Domain
GFP	Green Fluorescent Protein
HOP1	Homologue Pairing 1
HADC	Histone Deacetylase Complex
HATs	Histone Acetylases
HMG	High Mobility Group
HORMA	Domain known in: Hop 1p, Rev7p and MAD2
HR	Homologous Recombination

HTMs	Histone Methyl Transferases
H2AX	Histone Variant of H2A
IPTG	Isopropyl-D-1-Thiogalactopyranoside
LB	Lysogeny Broth
LE	Lateral Element
ME12	Meiosis Gene 2
MER	Meiotic Recombination Defective
MLH1/3	MutL Homologue 1/3
MMS4	Methyl Methanesulfonate Sensitive 4
MER11	Meiotic Recombination 11
mRNA	Messenger RNA
MS	Murashige and Skoog
MSH4/5	MutS Homolog 4/5
MSI1	Multicopy Suppressor of IRA1
MUS81	MMS and UV Sensitive 81
MYB	Myloblastosis
NAP-1	Nucleosome Assembly Protein-1
NASC	National Arabidopsis Stock Center
NCO	Non Crossover
NHEJ	NON-Homologous End Joining
NORs	Nucleolar Organizing Regions
NRL	Nucleosomal Repeat Length
N-terminal	Amino-Terminal
NTD	Amino-Terminal Domain
O/N	Overnight
PBS	Phosphate Buffered Saline
PCH2	Pachytene Checkpoint 2
PCR	Polymerase Chain Reaction
PMC	Pollen Mother Cell
PTMs	Post Translational Modifications
rDNA	Ribosomal DNA
RAD	Radiation Sensitive Protein
RAM	Root Apical Meristem
REC	Abnormal recombination
RED1	Reduction Division Defective 1
RNA	Ribonucleic Acid
RNAi	RNA Interference
RT	Room Temperature
SAIL	Syngenta Arabidopsis Insertion Library
SAM	Shoot Apical Meristem
SAXS	Small Angle X-Ray Crystallography and X-Ray Scattering
SC	Synaptonemal Complex
SCC	Sister Chromatid Cohesion Protein
SCR	SCARECREW
SDSA	Synthesis-Dependent Strand Annealing
SDW	Sterile Distilled Water
SEI	Single End Invasion
siRNAs	Post-Translational Gene Silencing
SMC	Structural Maintenance of Chromosomes
SNF	Sucrose Non-Fermenting

SPO11	Sporulation Specific Protein 11
ssDNA	Single Stranded DNA
SWI	Switching
SYCP	Synaptonemal Complex Protein
SYN1	Synapsis 1
T-DNA	Transfer DNA
TF	Transverse Filament
TopoII	Topoisimerase II
WT	Wild-Type
WUS	WUSHEL
XH1	Xenopus Differentiation-Specific histone 1
XH1A	Xenopus Somatic Variant (xH1A)
XRCC	X-Ray Repair Comlementing Defective Repair In Chinese
XRS2	X-Ray Sensitive 2
ZYP1	Synaptonemal Complex Protein 1

CHAPTER 1
INTRODUCTION

1.1. Biological Significance of the Chromatin

The genetic inheritance inter species is preserved along an individual life span, due to the genetic material packed into every cell in the form of DNA (Deoxyribonucleic Acid). The DNA itself is responsible for the organisation of the cellular mechanisms. Thus, DNA has to be accessible in order to be replicated, translated, repaired and transmitted to future generations. The fact that the length of the naked DNA is about ten thousand times the diameter of the nucleus, in human cells (Annunziato, 2008) shows that DNA has to be highly packed inside this nucleus. Proteins associate to the nuclear DNA to allow this packaging and thus forming the chromatin (Woodcock, 2005). The organisation of DNA into chromatin is very important, to DNA spatial fit within the nucleus (Annunziato, 2008), besides to, the functional and metabolic activities of the DNA progress (Deal and Henikoff, 2010).

1.2. Chromatin Structure

Chromatin is formed by DNA and proteins; histones and non-histone proteins. Non-histone proteins include a wide range of nuclear proteins, more than 1,000 non-histone proteins types, including: transcription factors, polymerases, hormone receptors and other nuclear enzymes (Barrett, and Gould, 1973; Stein *et al.*, 1974; Laemmli *et al.*, 1987; Huang and Berger, 2008). Histones-DNA association forms the first level of DNA compaction in a structure termed nucleosome. The nucleosome, which “is the basic repeating structural and functional unit of the chromatin” (Sanchez-Moran, 2013), is composed of eight small positively charged histone proteins wrapped by around 146 base pairs (bp) of DNA (Kornberg, 1974; Van Holde, 1988). This histone octomer is composed of two copies of each of the four

conserved core histones (H2A, H2B, H3 and H4) bind tightly to around 146 bp of DNA (Kornberg and Thomas, 1974; Luger *et al.*, 1997; Wolffe, 1999). This protein-DNA association permits the DNA (about 2m in length in humans) to be packed in the nucleus (about 10 μ m in diameter) as chromatin in a hierarchical manner (reviewed by Sanchez-Moran, 2013), by different compaction levels, from the linear 10 nm nucleosome fibre structure (5 folds compaction) (Luger *et al.*, 1997), to the higher order (30 nm) chromatin fibre (about 40 fold compaction) (Finch and Klug, 1976; reviewed by Maeshima *et al.*, 2014), up to chromatin loops (300 nm) (about 200 folds compaction) attached at the base to the chromosome scaffold axes proteins (Paulson and Laemmli, 1977). During cell cycle it is believed that chromatin loops associate with scaffold axes at the interphase stage, which is copied during DNA replication. As a nucleus passes from prophase stage to metaphase, chromatin loops arrange in a helical way that permits extra chromatin folding, to produce a compaction of 700 nm per chromatid at metaphase chromosomes (10,000-20,000 fold compaction) (Marsden and Laemmli, 1979; Nelson *et al.*, 1986). **Figure 1.1** Represents the most advanced proposed model of chromatin compaction (reviewed by Sanchez-Moran, 2013).

The DNA-protein interactions within the chromatin organization context within the chromosome remain a mystery (Belmont, 2006). Therefore, more research on chromatin should be done at basic level, by studying the chromatin components. Hence the analysis of the chromatin structural and functional units; the nucleosomes, is a key point to identify novel chromatin proteins and protein interactions responsible for the nucleosome fibre structure compaction into the higher order chromatin fibre.

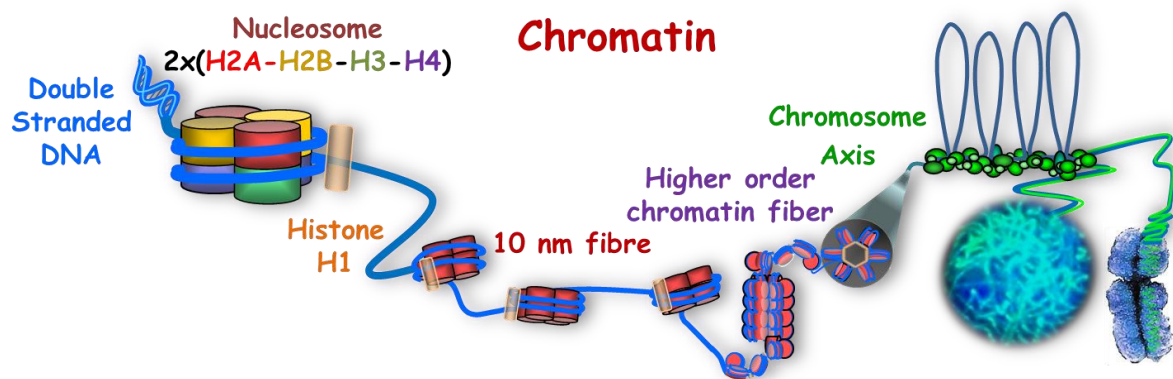


Figure (1.1): The current chromatin compaction model.

Chromatin is composed of nucleosomes monomers, each contains two copies for the core histones (H2A, H2B, H3 and H4), adjacent nucleosomes attach with the linker DNA to which the linker histone (H1) associate. The chromatin is a dynamic structure which is able to compact from the nucleosome fiber structure (10 nm, resemble an open or highly active chromatin), to higher order structures (30 nm), allowing further organisation into loops (300 nm) and further chromosomal compaction into 1400 nm structures (Figure based on Sanchez-Moran, 2013).

1.2.1. The nucleosome fibre

Chromatin has a repetitive nature (Hewish and Burgoyne, 1973; Phillip *et al.*, 1977). Different experiments using a nuclease to digest chromatin have resulted in 180-200 bp of DNA fragments that were protected from the nuclease activity (Williamson, 1970; Hewish and Burgoyne, 1973; Rill and Nelson, 1978). It was proposed to be protected by a complex protein-DNA association (Axel *et al.*, 1974; Sahasrabudhe and van Holde, 1974). These complexes presented a “beads on a string” structure under the electron microscopy (Woodcock, 1973; Olins and Olins, 1974; Olins and Olins, 2003; Annunziato, 2008). And, it was proposed that the DNA was wrapped around eight subunits of histone proteins forming the nucleosome structure (Kornberg, 1974). The nucleosome was proposed to be composed of a H3-H4 tetramer and two dimers of H2A-H2B (Richmond *et al.*, 1984; Arents *et al.*, 1991; Arents and Moudrianakis, 1993; Luger *et al.*, 1997). This chemical cross-linking of

histones “the subunit theory of chromatin” (reviewed by Woodcock, 2005) and its appearance under the electron microscope (EM) as a “string of beads” (Olins and Olins, 1974; Olins and Olins, 2003) suggested that a chromosome, which is about 100 million bp, is packaged into hundreds of thousands of these functional nucleosomes (Luger, 2001) (**Figure 1.2 A&B**). Adjacent nucleosomes are linked together via a variable length of DNA (10-60 bp) called linker DNA, and so forming the 10 nm chromatin fibre structure “beads on a string” (Peterson, 2004) (**Figure 1.2 C**).

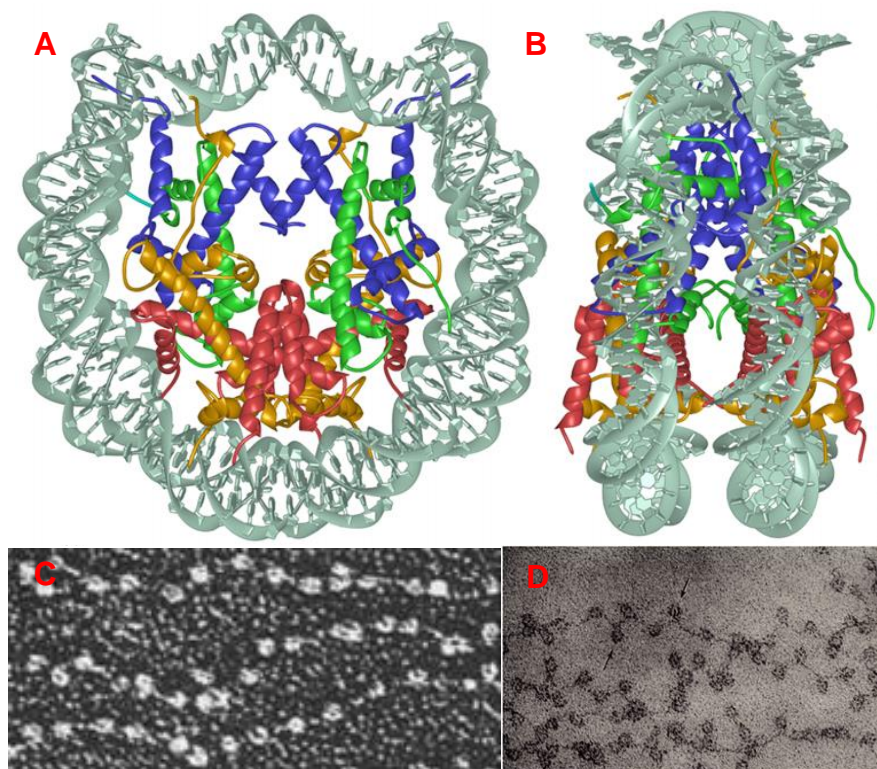


Figure (1.2): Nucleosome structure

(A&B) Crystallographic structure of the nucleosome. Nucleosome structure is formed of a histone octamer; 2X(H2A, H2B, H3, H4) associated to around 146 bp of naked DNA. (The DNA helices are represented in grey, histone H3 in blue, histone H4 in green, histone H2A in yellow, histone H2B in red. (B) The disc-like shape of the nucleosome particle is formed by rotating the nucleosome structure in A by 90 around the Y-axis Adapted from Luger, (2001). (C&D) Adjacent nucleosomes are joined by linker DNA, hence chromatin appears as a string of beads under the electron microscope EM. Nucleosomes are indicated by a black arrow at D. (A&B) are adapted from Luger (2001). (C) is adapted from (<http://sgi.bls.umkc.edu/waterborg/chromat/chroma09.html>). (D) is adapted from (Olins and Olins, 2003).

1.2.1.1. Histones

Research on histones has shown that histones are small proteins (MW=11-16 KDa), which has a positive charge due to the presence of high percentage of basic amino acids in their sequences, 20% of its sequence is mostly occupied by argenines and lysines (van Holde, 1988). Histones possess domains at both the N-terminus as well as the C-terminus (**Figure 1.3**) (reviewed by Downs *et al.*, 2007). A “histone fold domain”, at their carboxyl terminal end (C-terminus), allows interactions intra histones as well as between histones and DNA within the nucleosome (reviewed by Downs *et al.*, 2007). Such interactions permit the electrostatic forces balance required to stabilize the nucleosome unit (reviewed by Downs *et al.*, 2007). And “flexible amino-terminal domain” at the (N-terminus) (Downs *et al.*, 2007). The C-terminus is composed of three helices (α_1 , α_2 , α_3) linked via two linkers (L1 & L2) (**Figure 1.3**). It was proposed that the C-terminus play a role in the intra-histones interactions as well as DNA-histones interactions (Ammelburg and Lupas, 2007). Luger *et al.* (1997) reported that the C-terminus α -2 helices resemble the sites where histones dimerize. The nucleosome structure integrity and stability depends on both the histone-histone interactions as well as DNA-histones interactions. Hydrophobic forces between histones H2B and H4 allow the H2A-H2B dimer binding to the H3-H4 tetramer (Luger *et al.*, 1997). The electrostatic interactions between the positively charged arginine residues on the core histones and the negatively charged DNA backbone stabilizes the nucleosome structure (Wolffe *et al.*, 1998). In addition to this, the N-terminus is suggested to have different interactions with other components of the chromatin (Zheng and Hayes, 2003). The core histone N-terminus has showed a potential for several posttranslational modifications (Strahl and Allis, 2000; Jenuwein and Allis,

2001). Over a hundred of histone-DNA interactions have been recorded, including both hydrophilic and hydrophobic reactions (Davey *et al.*, 2002).

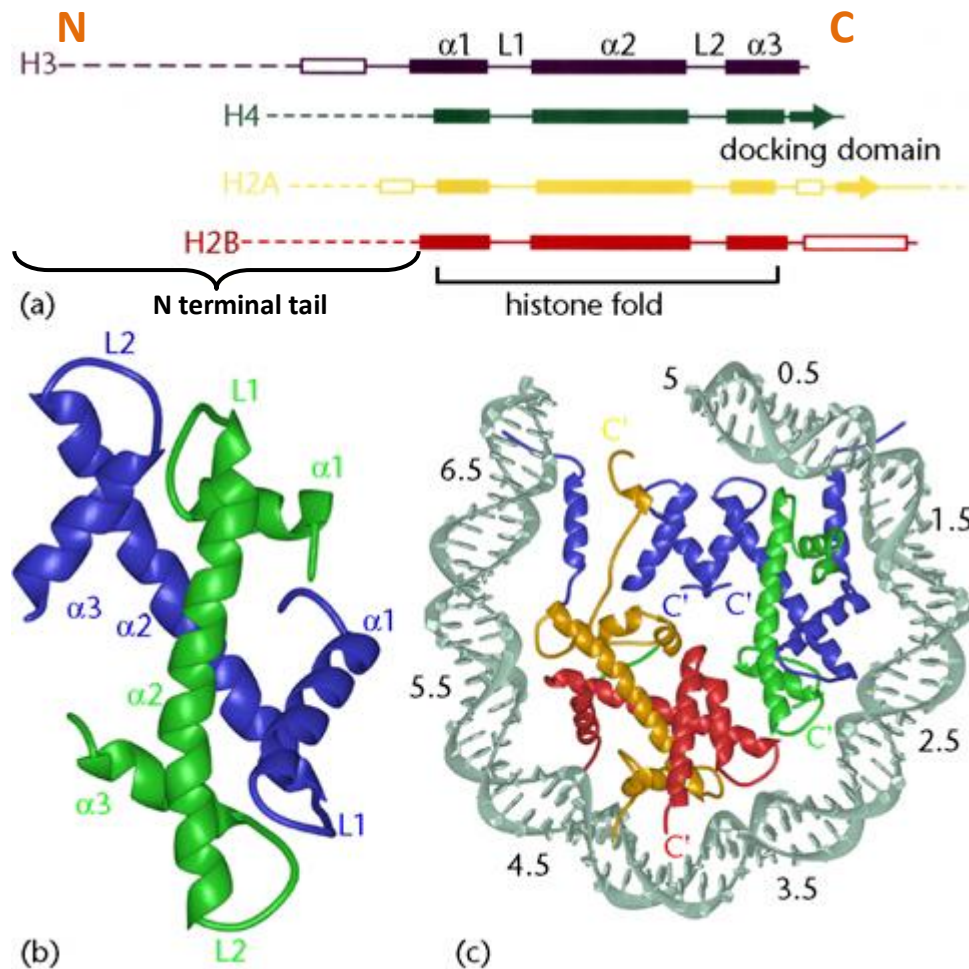


Figure (1.3): Schematic representation of the C-terminus histone fold in the nucleosome core histones.

(A & B) Histone folds in H3, H4, H2A and H2B are represented as helices and strands. (A) C-terminus of histone folds compose of three helices ($\alpha 1$ & $\alpha 2$ & $\alpha 3$) interlinked by two linkers (L1 & L2). (B) The antiparallel arrangement of histone folds in two histones (e.g H3 & H4) permits their histone folds to dimerize. (C) Histone folds arrangement of half of the core histones inside the nucleosome particle. Numbers on the DNA indicates sites of DNA-protein interactions. Histone fold helices are shown as solid boxes, strands as solid lines, extensions as empty boxes, tail chains as dots. Histone H3 is represented in blue, histone H4 in green, histone H2A in yellow and histone H2B in red. Adapted from Luger (2001).

Histone H4 is one out of the four histone proteins; H2A, H2B, H3 and H4; that build up the eukaryotic nucleosome core (Wolffe, 1998). Its position and association within

the nucleosome in (H3-H4)₂ tetramer and along with the two H2A-H2B dimers enables DNA-Histones into the nucleosome. Histone H4 can be subjected to different posttranslational modifications (**Figure 1.4**); among others, biotinylation, acetylation and methylation. Previous reports showed that biotinylation of H4 K8 and K12 might enable nuclear response to DNA double strand breaks (DSBs) and proper chromosomal condensation during mitosis in human cells (Kothapalli *et al.*, 2005; Kothapalli and Zemleni, 2005; Zemleni, 2005). Acetylation of lysine 16 on H4 allows gene transcription machinery to work by either changing the higher order chromatin structure organisation or altering interactions of proteins associated with chromatin (Shogren-Knaak and Peterson, 2006). Fraga *et al.* (2005) reported that H4 K16 acetylation loss is mostly seen in some cancers. Moreover, a study by Corsini and Sattler (2007) showed that Histone H4 dimethylated lysine 20 (H4K20me₂) plays a role in DNA damage repair by recruiting the DNA damage repair factor 53BP1 to DNA DSBs sites. H4K20 plays a role as a transcriptional control (Corsini and Sattler, 2007).

The fact that histone H4 core proteins are highly conserved during evolution, human histone H4 is nearly identical to the plant *Arabidopsis thaliana* H4 (only 2 amino acids changes), shows the important basic role of histone H4 in chromatin compaction and functionality.

Histones associated with chromosomes are one of the most highly conserved protein molecules in the eukaryotic cells (Cox *et al.*, 2005), which are not only vital for the packaging of DNA into chromosomes, within the nucleus, but also are important for

the chromosome stabilization and gene expression. In addition to these highly conserved histone proteins, some reports showed that the presence of histone variants (with some variation in the amino acid sequence) play clear roles in chromatin remodelling, gene inactivation and DNA replication (Ahmad and Henikoff, 2002; Jedrusik and Schulze, 2001; Meneghini *et al.*, 2003; Talbert *et al.*, 2002)

Histones could be grouped into two categories according to their timing of deposition on the chromatin (Tagami *et al.*, 2004) replication dependent (Singh *et al.*, 2013) or replication independent (Ahmad and Henikoff, 2002). Replication dependent histones include all histone proteins which are deposited on the chromatin during DNA replication which includes the core histone proteins and their isoforms (H2A, H2B, H3 and H4). Whereas the replication independent histones are deposited on the chromatin after DNA replication and during the cell cycle depending on the tissue specificity and/or the cell cycle stage, and it includes histone variants, which have differences in the amino acid sequence for its specific functional roles within the chromatin (reviewed by Sanchez-Moran, 2013).

1.2.1.2. Histone variants

The core histone proteins are encoded as multi-gene families, in which some are identical copies of the same gene; however others are similar but not identical genes (Walsh and Stephan, 2001; Eirn-Lopez., *et al* 2004). Zimmermann *et al.* (2004) showed that each histone protein is encoded by several genes in *Arabidopsis* genome. Histone H4 is encoded by eight different loci, histone H3 has five loci encoding for the core H3, and another five loci encoding for different H3 histone

variants. Furthermore, we identified thirteen loci encoding for H2A histones and eleven for H2B histones. The linker histone H1 is encoded by eleven different loci (reviewed by Sanchez-Moran, 2013). Okada *et al.* (2005) published the results of a BLASTX search against the *Arabidopsis* Information Resource (TAIR) database, fifteen histone H3 genes in the *Arabidopsis* genome were found; five histone H3.1 genes, three histone H3.3 genes and five histone H3.3-like genes. The analysis of gene structure revealed that gene duplication might have caused redundancy of these histone H3s. 13 out of the 15 *Arabidopsis* H3 genes have a highly conserved sequence. Five of *Arabidopsis* histones H3 are major histone H3s (H3.1), and the rest three are histone H3 variants (H3.3) (Chaubet *et al.*, 1992). In addition, Talbert *et al.* (2002) reported that HRT12/At1g01370 is a centromeric H3 variant which has a highly diverse sequence. Six novel H3 variant genes are present. Five of these H3 proteins are clustered in H3.3 groups, showing the same amino acid substitution found in the variant H3.3, at positions 31, 87 and 90 (Malik and Henikoff, 2003).

CENH3 is a centromere-specific histone H3 variant, which is utilised as a universal marker for centromeric chromatin (Henikoff *et al.*, 2001) with an important role in the kinetochore stabilization (Irvine *et al.*, 2004). Furthermore, some species specific euchromatic features or binding domains have been found for these variants (Cam *et al.*, 2005; Lam *et al.*, 2006).

H2AX, a conserved H2A-variant, forms 2-25% of H2A amount depending on the organism and cell type (Redon *et al.*, 2002; Rogakou *et al.*, 1998). H2AX has a unique carboxyl tail with a serine residue which can be phosphorylated (ser 139) resulting in the phosphorylated H2AX form also known as gamma H2AX (γ H2AX)

(Redon *et al.*, 2002). H2AX plays a central role in the chromatin stability in two ways, the first by inducing the DNA DSB repair cascade involving several processes: The recruitment of DNA repair proteins onto the DSB (Fernandez-Capetillo *et al.*, 2003; Fillingham *et al.*, 2006; Paull *et al.*, 2000), an ubiquitin ligase cascade, an accumulation of cohesins around the DSB (Unal *et al.*, 2004), and chromatin remodelling complex recruitment (Ikura *et al.*, 2007). Another role has been reported in enhancing programmed cell death in cases of DNA repair mechanism failure (Lu *et al.*, 2006; Mukherjee *et al.*, 2006).

1.2.1.3. Histone exchange

The nucleosome structure is very important since alterations in its structure can affect DNA accessibility for different biological functions. Different factors have been found to cause changes in the nucleosome structure, these are: histone posttranslational modifications, chromatin remodelling, and deposition of histone variants (reviewed by Jin *et al.*, 2005). Jin *et al.* (2005) reported that nuclear processes which demand DNA-histones interactions dissociation, or events with either partial or full removal of core histones, results in an increases in the RNA polymerase II dependent transcription, DNA replication and DNA repair. Chromatin dynamics demands nucleosomes formation and dissociation in a way that permits DNA to carry on replication and transcription processes easily. Several reports related histones chaperones importance for nucleosome assembly and chromatin dynamics (Akey and Luger, 2003; Tagami *et al.*, 2004). One of these histone chaperones is the Nucleosome Assembly Protein -1 (NAP-1), which play several roles during cellular transcription. NAP-1 binds H2A-H2B forming a complex capable to remove H2A-H2B

dimers during transcription (Walter *et al.*, 1995; Levchenko and Jackson, 2004 Park *et al.*, 2005) hence facilitates spacial binding of the transcriptional factors to nucleosomes. NAP-1 is also involved in histone exchange, through which the removed H2A-H2B dimers are replaced from adjacent nucleosomes, and so causing nucleosomes sliding along the DNA. NAP-1 was reported to act in the H2A.Z-H2B heterodimer exchange in yeast (Mizuguchi *et al.*, 2004). NAP-1 mediated histone H2A-H2B exchange and nucleosome sliding are ATP-free processes which actually explains their slow kinetics. So the actual role for NAP-1 in chromatin remodelling is not fully understood. Suggestions were made that NAP-1 might play a role in activating ATP-dependent chromatin remodellers (Bruno *et al.*, 2003). Moreover, it was reported that histones tails modifications, mainly acetylation, mediates nucleosome dissociation through NAP-1-H2A-H2B association (Ito *et al.*, 2000; Mizuguchi *et al.*, 2004). Furthermore, several reports pointed out that nucleosome remodelling complexes could exchange or remove histones in an ATP dependent manner. SWI/SNF, RSC and ISWIb, are chromatin remodelling complexes which facilitate ATP-dependent H2A-H2B dimers exchange (Bruno *et al.*, 2003), suggesting that these remodelling complexes change chromatin composition and or chromatin structure (Bruno *et al.*, 2003).

Chromatin remodelling, switching from open to compact state, is controlled via different components. The ATP-dependent nucleosome remodelling complexes (e.g the SWICH2 [SW12]/ SUCR+OSE NON-FERMINTING 2 [SNF2]) is one way to achieve these changes. Furthermore, histone modifications can control it too (e.g histone deacytalase complex [HDAC]). The open state has historically been

associated with the transcriptional machinery and the formation of euchromatin. Whereas, the heterochromatin has been associated with the compact state in which transcription is inactivated or reduced (Olins and Olins, 2003). The dynamic changes of chromatin compaction are a consequence for the responding genetic regions to different activators or repressors. The histone code hypothesis (Strahl and Allis, 2000; Turner, 2000) explains the role of histone's tail covalent modifications via acetylation, methylation, and phosphorylation (among others) in the induction of specific proteins to bind the chromatin forming a complex that either activate or repress these genomic DNA regions.

1.2.1.4. Histone modification

Histone H3 has the highest known number of post translational modifications (PTMs) among the core histones, including H3-acetylation, H3-methylation, and H3-phosphorylation (Espino *et al.*, 2005; reviewed by Perez-Cadahia *et al.*, 2009). Reports showed that the N terminal tail of H3 is subjected to phosphorylation at four residues: Thr3, Ser10, Thr11, and Ser28 (Hendzel *et al.*, 1997; Gernand *et al.*, 2003; Preuss *et al.*, 2003). Residues showed different phosphorylation roles during interphase, mitosis and meiosis. Research on different species showed that they have a similar distribution pattern during the cell cycle, with low or undetectable amount during interphase, and an increase during the prophase stage of mitosis and decrease at anaphase and telophase (Zhang *et al.*, 2005). However the global H3 phosphorylation is different in terms of distribution and timing, its consequences are not yet understood. Dai *et al.* (2005) suggested that mitotic histone H3 phosphorylation might play one out of three roles that impact the chromosome: affect

the nucleosome packing, create a binding site for chromosome condensing proteins or could induce modifications of other histone proteins.

Histone H4 as well as the other histone proteins is subjected to be modified to serve specific nuclear functions. Histone H4 methylation, acetylation and biotinylation are the most studied modifications. Two biotinylation sites were identified on histone H4; K8 and K12 (Camporeale *et al.*, 2004). Both biotinylation sites have vital nuclear roles. An evidence has been recorded that biotinylation of K8 and K12 in histone H4 could have an initial interference or response to the DNA DSB occurrence, as well as the condensation pattern of mitotic chromosomes in the human cell cycle (Kothapalli *et al.*, 2005; Kothapalli and Zempleni, 2005; Zempleni, 2005). Recent reports have showed that K12-biotinylated histone H4 (K12 Bio H4) and might be K8-biotinylated histone H4 (K8 Bio H4) are pericentromeric heterochromatin markers and show a transcriptionally down regulated chromatin in human lymphoblastoma cells (Camporeale *et al.*, 2007).

Another modification is methylation of histone H4 at lysine or arginine residues. Histone methyl transferases (HTMs) can methylate lysine residues at different levels; monomethylated, dimethylated, or trimethylated (Peterson and Laniel, 2004). Histone H4-K20 is a site that shows different patterns of methylation levels during development (Karanchentsev *et al.*, 2007). Two known enzymes can regulate lysine methylation status; the first PRSet7 (or Set 8) HMT which is responsible for H4-K20 monomethylation (Nishioka *et al.*, 2002; Fang *et al.*, 2002; Couture *et al.*, 2005; Xiao *et al.*, 2005), and the other enzyme is Suv4-20 which trimethylates H4-K20 (Schotta

et al., 2004). The importance of these two enzymes on chromatin is shown on their evolutionary conservation among species; from flies to human, except *S. pombe* which is methylated at H4-K20 by Set 9 HMT. HeLa cells PR-Set 7 expression shows the least values of expression at G1/S while goes to maximum level in G2/M phase of the cell cycle and peaks at mitosis (Rice *et al.*, 2002). Moreover, mono- and trimethylation of H4-lysine 20 is associated with repressed chromatin (Karachentsev *et al.*, 2006).

Histone H4 acetylation has been also associated with its chromatin status. The reversible acetylation of amino terminus of H4 lysines 5, 8, 12, and 16 allows less compact chromatin and accessible nucleosomes (Loidl, 1988; Loidl, 1994; Garcia-Ramirez *et al.*, 1995), open chromatin with accessibility to transcription machinery via RNA polymerases II or III (Lee *et al.*, 1993; Vettese-Dadey *et al.*, 1996). Acetylation of mammalian H4 is found in euchromatin that bypasses early replication and transcription (Sadoni *et al.*, 1999). Heterochromatin has lower acetylation comparable to euchromatin (open chromatin) in endosperm nuclei of *Gagea lutea* (Buzek *et al.*, 1998).

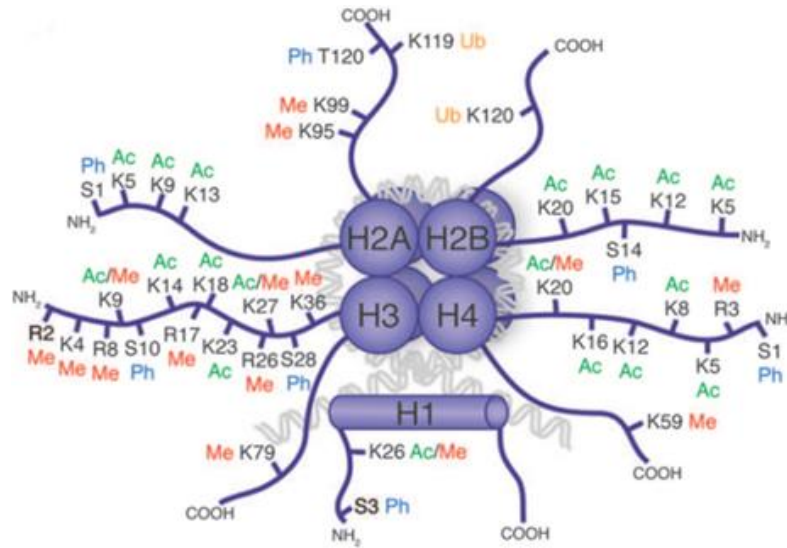


Figure (1.4): The Histone Modification Map.

Modifications of core histones (H2A, H2B, H3 and H4); acetylation, phosphorylation, methylation and ubiquitination, mediates chromosome dynamics during the various nuclear functions, allowing chromatin shift between open and compact phases in both directions. Ac stands for acetylation, Me for methylation, Ph for phosphorylation, and Ub for ubiquitination (Cota *et al.*, 2013).

1.2.2. The Higher Order Chromatin Fibre

1.2.2.1. The 30 nm fibre could be polymorphic

The utilization of the transmission electron microscope (EM) in 1976 enabled Finch and Klug to see that nucleosome fibres, which are 10 nm in diameter, were able to fold into chromatin fibres of 30 nm in diameter, by either the addition of histone H1 or Mg⁺² ions. Different models were proposed for the 30-nm chromatin fibres structures (**Figure 1.5**); the “Solenoid”, in which adjacent nucleosomes bind to each other in a helical way known as “one start helix” (Finch and Klug, 1976). The second model is called “Zigzag”, where nucleosomes attach to each other in a “Two start helix” manner forming a zigzag like structure, suggesting that each nucleosome is attached to a second nucleosome (Woodcock *et al.*, 1984; Bassett *et al.*, 2009). Another model is the crossed linker model, in which the fibre axis is perpendicular with the linker DNA orientation (Williams *et al.*, 1986; Smith *et al.*, 1990). Later on, several

other models were proposed to clarify the 30-nm fibre structure (van Holde and Zaltanova, 2007). The usage of different techniques to analyse the 30-nm fibre structure; biochemistry, biophysically, using X-ray crystallography, conventional EM, Cryo-EM, small angle X-ray crystallography and X-ray scattering (SAXS), have showed that no definite structure could be observed, suggesting that the 30 nm structure is variable (reviewed by Maeshima *et al.*, 2014). So, the Zigzag or the solenoid 30-nm structure was found to be affected by the nucleosomal linker DNA length in different species (Routh *et al.*, 2008). The impact of linker DNA length on the nucleosome fibre folding was confirmed. The length of 1bp was thought to result in 36° rotation of one nucleosome comparable to the adjacent nucleosomes binding to it (van Holde and Zlatanova, 2007).

The linker DNA was proposed to play a role in the zigzag model by binding to nucleosomes backwards and forwards to allow the binding of two nucleosome rows (Bendar *et al.*, 1998; Schalch *et al.*, 2005). It was suggested that chromatin at higher order is compacted at different levels, suggesting the co-presence of the different higher order chromatin structures *in vivo* (Robinson and Rhodes, 2006). The impact of linker histone H1 on the higher order is not clear yet, since it was found that H2A and H4 histones interactions might play a role in the higher order chromatin formation, regardless of the histone H1 (Schalch *et al.*, 2005). However, several reports confirmed a role for linker histones in the higher order chromatin in eukaryotes (Maresca *et al.*, 2005; Freedman and Heald, 2010) besides to the Mg²⁺ and nucleosome interactions (Grigoryeva *et al.*, 2009). Up to now research on the higher order chromatin structure is not confirmed *in vivo*, due to the limited

capabilities of the techniques to visualize the higher order chromatin structures *in vivo* (Tremethick, 2007).

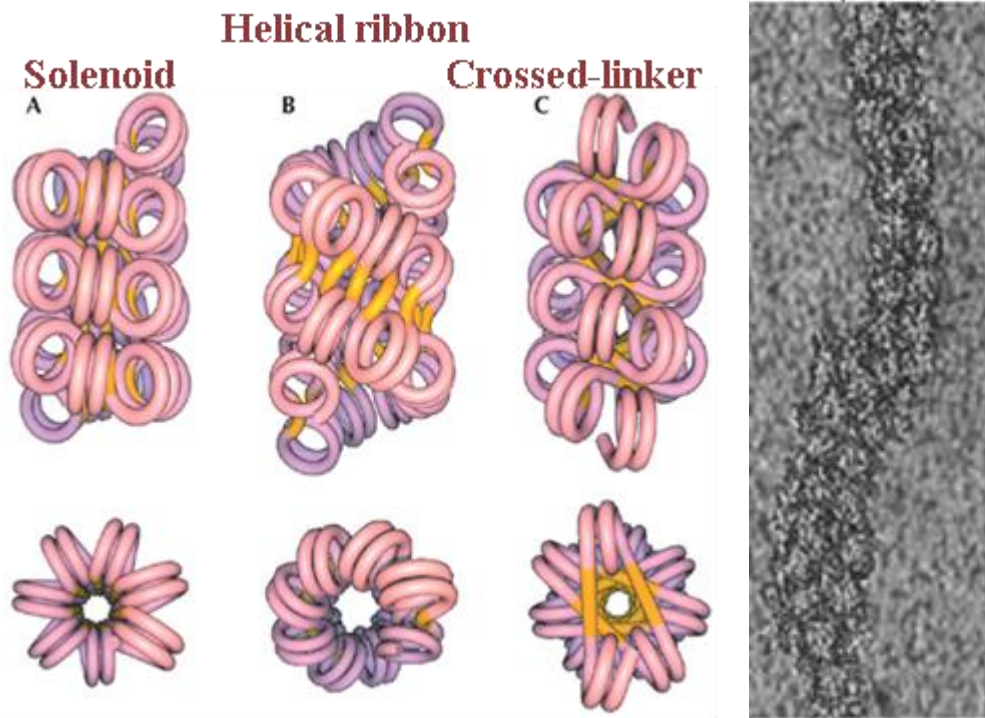


Figure (1.5): Different structural models proposed for the higher order chromatin fibre.

The way nucleosomes bind together along the nucleosome fibre controls the expected higher order chromatin structure formed. (A) If adjacent nucleosomes are joined together with one start helix then a solenoid-30 nm will be formed. (B) However if nucleosomes starts with two start helix where nucleosomes attach by allowing the binding of nucleosome from each helix per a time forming a Zigzag model. (C) And the Crossed linker forms when the linker DNA is at angel (0° - 50° with the fibre axis) (Wu *et al.*, 2007). (D) The higher order chromatin fibre structure under the EM. Adapted from <http://sgi.bls.umkc.edu/waterborg/chromat/chroma09.html>) (Olins and Olins, 2003).

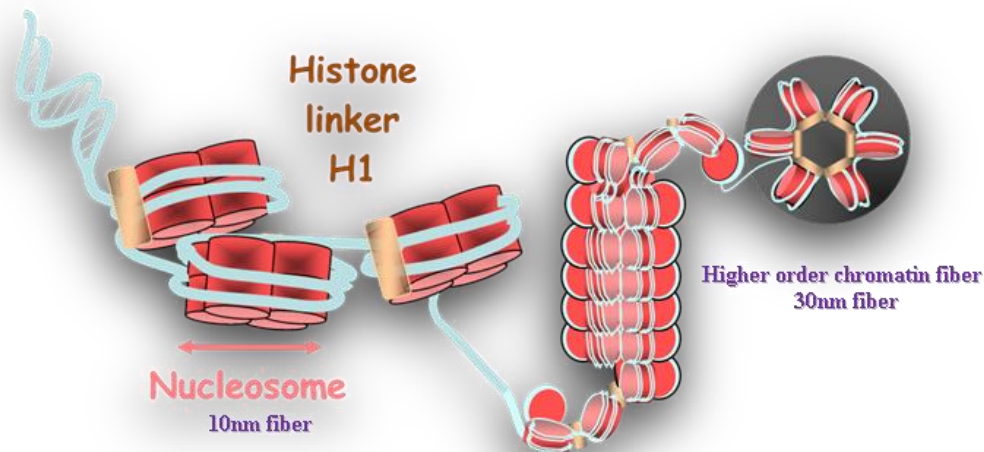


Figure (1.6): A model for the linker histone H1 role in the higher order chromatin fibre formation.

The linker histone H1 binds the linker DNA at the entry-exit position of the nucleosome. Histone H1 interaction with other chromatin proteins allows the nucleosome fibre (10 nm fibre) folding into the higher order chromatin fibre (about 30 nm in some species) (Model created by Sanchez-Moran, 2010)

1.2.2.2. Linker histones have a putative role in the higher order chromatin fibre structure

Linker histone H1 has been denominated as the chromatin architectural protein (McBryant *et al.*, 2006). It has a tripartite amino acid structure in higher eukaryotes: with an “amino-terminal domain” (NTD), a “central globular domain” (GD), and a “carboxyl terminal domain” (CTD) (Allan *et al.*, 1980). The NTD is a short domain; compose of 13-40 amino acids in length. However, the CTD is composed mainly of 100 amino acids with a high lysine, serine and proline composition, whereas, the globular domain is about 80 amino acids in composition (Allan *et al.*, 1980). This central globular domain has two DNA-binding sites (Clore *et al.*, 1987; Graziano *et al.*, 1990; Ramakrishnan *et al.*, 1993). The classical winged-helix motif and the basic

residues cluster, which permits the linker histones to bind different DNA molecules, resulting in tram-trak like structures (Thomas *et al.*, 1992), binding DNA crossovers (Krylov *et al.*, 1993), four-way junctions (Varga-Weisz *et al.*, 1993), asymmetrical binding of the linker histones to the DNA entry and exit sites of the nucleosomes (Hayes and Wolffe, 1993; An *et al.*, 1998; Hayes *et al.*, 1999), and the nucleosome protection against micrococcal nuclease (Noll and Komberg, 1977). Several reports showed that the amino terminus domains (NTD) are not required for linker histones – chromatin association (reviewed by Happel and Doenecke, 2009). However, although the C-terminus is not conserved among linker histones isoforms, but it might be playing a vital role in chromatin condensation (reviewed by Happel and Doenecke, 2009).

Linker histones besides having a role in chromosome architecture, might influence chromatin dynamics in two different ways: The first is by stabilizing the 30-nm diameter fibre. And the second is by communicating with many different nuclear non-histone proteins. H1 is one of the linker histones which play a dual stabilization role for both assembled nucleosome as well as the higher order chromatin structure (McBryant *et al.*, 2010).

Linker histones H1 are considered to be a family of related proteins with specifications in terms of: tissue and development within the same species. The conservation of histone H1 N and C terminal tails among species gives a clue about a possibility of distinct function for each of H1 variants (reviewed by Izzo *et al.*, 2008). Several reports gave attention to the role of the H1 C-terminal domain interaction

with chromatin, showing that it allows H1s high binding ability (Patterton *et al.*, 1998). Furthermore, the C terminal domain impact on the higher order chromatin structure formation and stabilization has been studied extensively (Shen *et al.*, 1995)

The locus family of linker H1 histones is highly divergent in sequence compared to that of the core histones. The human genome shows eleven different H1 loci of which: seven are somatic (H1.1-H1.5, H1^o and H1x) (Parseghian *et al.*, 1994; Albig *et al.*, 1997; Ausio and Abbott, 2004; Happel *et al.*, 2005) three are spermatogenic variants: H1t (Seyedin and Kistler, 1980), H1T2 (Martianov *et al.*, 2005) and HILS1 (Iguchi *et al.*, 2003; Yan *et al.*, 2003) and one is oocyte-specific H1foo (Tanaka *et al.*, 2003). These isoforms could be grouped in two categories according to the expression and timing-patterns: Somatic cells versus germ cells, suggesting that linker histones isoforms are expressed differentially depending on cell type and function (reviewed by Happel and Doenecke, 2009). Moreover, replication-dependent linker histones are expressed prior to the other histone H1 variants (reviewed by Happel and Doenecke, 2009). Although histone H1 is evolutionary conserved (Kasinsky *et al.*, 2001; Jerzmanowski, 2004), and has a discriminative DNA-binding location associated to the linker DNA at the entry exit site of the nucleosome (Zhuo *et al.*, 2000) its biological function is not well understood. Barra and collaborators (2000) observed that the deletion of H1 in the fungus *Ascobolus immerses*, reduced its life span and the global DNA hypermethylation. The *in vivo* examination of globular linker histone in plants and animals is difficult as their genomes encode for several redundant H1 isoforms which can compensate each other. Wierzbicki and Jerzmanoski (2005) found out that more than 90% reduction in H1 expression in

Arabidopsis thaliana resulted in great defects in the developmental stages of the plant. In this research we will investigate the role of each one of the linker H1 variants in *Arabidopsis thaliana* on the global chromosome dynamics and chromatin compaction.

The old view that H1 is a static chromatin component is now completely invalid. H1-GFP expression in living cells and photobleaching experiments brought to light that H1s are transient molecules and that its binding to nucleosomes is not static but highly dynamic (Lever *et al.*, 2000; Misteli *et al.*, 2000). The fluorescence recovery after photobleaching (FRAP) technique revealed that H1 has two phases in the context of chromatin: a “stop” stage and a “go” stage. In the “stop” stage, H1 associates to the binding site of the chromatin for a limited time, and its dissociation resembles the “go” stage. H1 residence on the nucleosome is longer than its dissociation, recording 220 seconds for its “stop” stage. The switch from one phase to the other shows continuous exchange of the H1 molecules to different nucleosomes. These findings show that there is not one H1 molecule which is statically bound to a specific nucleosome. Furthermore, in higher eukaryotes there is a complex community of histone H1 isoforms and variants that can replace one another after each “go” stage (reviewed by Bustin *et al.*, 2005). In addition, posttranslational modifications of H1 can control the time needed for H1-association at the chromatin (Lever *et al.*, 2000) and also by nuclear proteins competing with H1 for nucleosomal binding sites (Catez *et al.*, 2004).

The specificity of linker histone H1 position on the linker DNA and its capability to lock the nucleosomal unit (**Figure 1.7**) has brought attention to the real impact of

histone H1 on the nucleosomal repeat length (NRL). The NRL is affected by the H1/nucleosome ratio, in which, NRL increase when H1 level raise up and the NRL decrease if H1 content per nucleosome is reduced (Woodcock *et al.*, 2006; Fan *et al.*, 2005; Hashimoto *et al.*, 2010). The NRL is an indicator for chromatin status, “active chromatin” (eg. In ES cells) has shorter NRL however, “compact chromatin”, (such as in mature cells) has longer NRL (Berkowitz and Riggs, 1981; Perisic *et al.*, 2010).

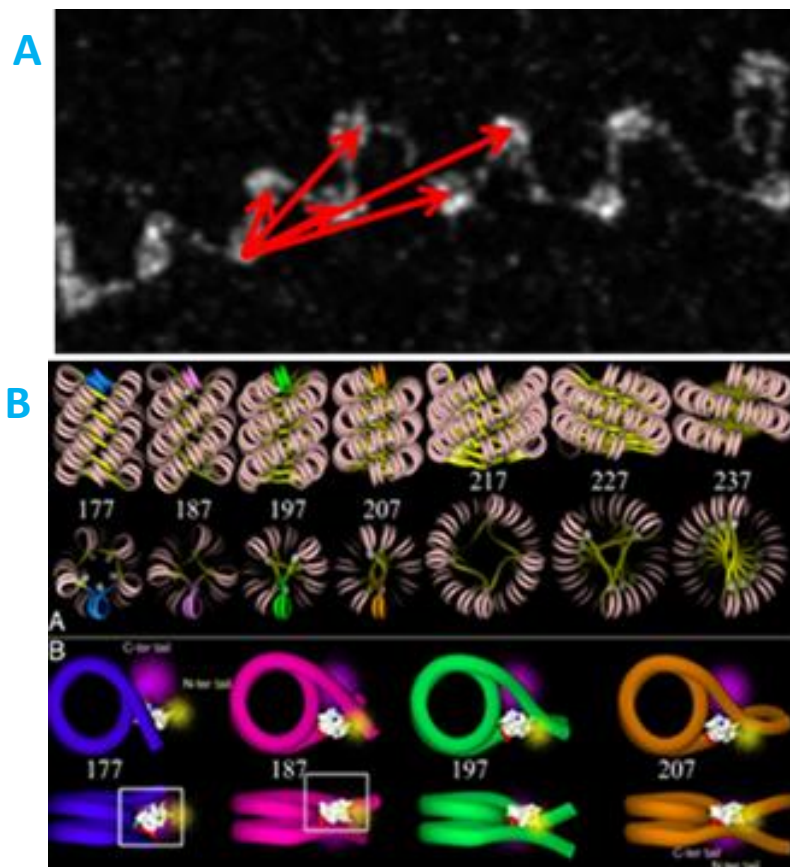


Figure (1.7): Histone H1 role in the polymorphic chromatin dynamics

Histone H1 linking between different nucleosomes was suggested to have a role in the formation of higher order structures. Different models for the higher order structures could apply depending on the intra nucleosomal links created via the linker histone (H1). The models above are showing a putative role for H1 as an “adjustable clip” which mediates intra nucleosomal associations during chromatin shift from 10 nm structure to the more compact (30 nm) fiber. Red arrows in resemble association (link) between different nucleosomes. Squares are marking the histone H1. (A) Adapted from (Lavelle *et al.*, 2010). (B) Adapted from (Wong *et al.*, 2007).

A recent study by *Oberg et al.* (2012) shed some light on the relation between histone variants and chromatin formation and organization showed that linker histone H1 subtypes of higher eukaryotes has a different impact on the nucleosomal spacing *in vivo*. The recorded NRL value after reconstitution of different eukaryotic histone linkers: chicken differentiation-specific histone H5 (chH5), *Xenopus* differentiation-specific (xH1), *Xenopus* somatic variant (xH1A), and human somatic subtypes (hH1.2 & hH1.3 & hH1.4 & hH1.5) in the *Xenopus* oocyte showed that there was an increase in the NRL when these histones were added except for the hH1.5. A NRL increase of 13-20 was found in hH1.4, xH1 and xH1A. chH5 showed around similar effect. However, both hH1.2 and hH1.3 showed less effect with just a 4.5-7 increase in the NRL. This subtype variation in NRL within the same species suggests that H1-chromatin modulation is isoform/variant dependent. A study by *Fan et al.* (2005) showed that knocking out three of histone H1 genes in mouse embryonic stem cells with a 50% decrease in the H1 level caused a reduction in both the nucleosome spacing and chromatin compaction status.

It has been reported that linker histones PTM are vital for nuclear functions. H1-phosphorylation during cell cycle G1-S-G2 shift the chromatin to its open phase, making it exposed to the different functional cellular factors; transcriptional proteins and repair proteins (reviewed by *Izzo et al.*, 2008). However, linker histone methylation is linked with the closed-phase of chromatin, which shows disabled accessibility (reviewed by *Izzo et al.*, 2008).

Several studies suggested that Histone H1 can regulate gene expression. H1 depletion affected the transcription machinery in the context of chromatin by either enhancing or repressing the expression process of distinct genes. H1 modulates the transcription process at two levels: the first is at the level of the higher order chromatin status in which H1 stabilizes the compact structure and prevent chromatin regulators to access the nucleosome. The second is at the level of the nucleosomal status, with the binding of both transcriptional regulators (activators and repressors) to their target (gene) site on the nucleosome and how H1 can affect by its association with the nucleosome.

Epigenome code studies including histone proteins dynamics within covalent modifications and replacement of linker histones, linking epigenetic silencing and gene expression have enabled a better understanding of the cell fate. The linker histones interactions through the nucleosomal fibers leading to the higher order structures seems to be essential for proper gene regulation (Wolffe, 2000). The linker histone is replaced by other variants during early embryogenesis in higher organisms like: flies, sea urchins, frogs and mice (Wolffe *et al.*, 1997; Tanaka *et al.*, 2001). In *Xenopus*, B4 which is an embryonic linker histone that exist in eggs is replaced by somatic H1 variants, initially H1A after midblastula stage synchronizing zygotic gene activation (Smith *et al.*, 1988; Ohsumi and Katagiri, 1991). Functional differences between the embryonic linker B4 and the somatic linker H1A in affecting chromatin structure and dynamics is revealed by the usage of linker histone chaperone, nucleosome assembly protein-1(NAP-1) showed that histone B4 influences the ATP-dependent chromatin remodeling factor pathway however the somatic linker histone

impeded this remodeling. Suggesting that the linker histone subtypes are changing developmentally to preserve the significance of the cell stage.

The linker histone H1 was considered as an essential factor that direct the assembly of mitotic chromosomes. This belief is based on two points of view: The first, is its role in the chromatin compaction status, hence, the formation of the higher order chromatin structure (30 nm fiber) (Thoma and Koller, 1977). The second finding is that the human master mitotic kinase cdc2/cyclin B does hyperphosphorylate histone H1 (Boggs *et al.*, 2000). Later on Maresca *et al.* (2005) showed that H1 depleted extracts of *Xenopus* eggs resulted in severe structural defects, showing more than 50% increase in chromosome length compared with control chromosomes. Furthermore, the H1 depleted chromosomes lack the normal alignment of mitotic chromosomes on the equatorial line, nor have the proper segregation at anaphase stage. These findings together with the fact that H1 depleted chromosomes defects could be rescued by the addition of purified *Xenopus* or bovine Histone H1 supported the idea that H1 directs the compaction of chromosome arms in *Xenopus* egg extracts and that it is needed to achieve proper (normal) mitosis.

A study by Prymakowska-Bosak *et al.* (1999) showed that the production of cDNA transgenic tobacco plants with around one quarter the normal amount of the somatic histone variants: H1A and H1B resulted in a noticeable increase in the minor variants: H1C, H1D, H1E and H1F. Although the plants growth was within the normal level, their flowers were 20% to 30% smaller than the controls, with smaller petals and stamens, with defects in fruit production and seed development. Defects in male

gametogenesis were confirmed by cytological analysis, in which signs of improper pairing and or segregation of homologous chromosomes were found. These results emphasize that the linker histone H1 variants might have a role in gametogenesis, and that might be crucial for normal levels of plant fertility.

The linker Histone H1 is thought to play a role in the Backup pathway of Non-Homologous End Joining (B-NHEJ) process (**Figure 1.8**). An *in vitro* End Joining analysis of HeLa cells treated with Ionizing Radiation (IR) and using recombinant human histone H1.2 suggested that H1 not only acts as an alignment factor for the B-NHEJ process, but also enhances the DNA end ligation, by activating PARP1 and ligase III components of B-NHEJ. Although, it seems that it stimulates ligase IV to a lesser degree (Rosidi *et al.*, 2008). Moreover, Downs *et al.* (2003) demonstrated that Hho1p, a yeast H1 homolog, deletion inhibits DNA-repair through the homologous recombination (HR) pathway.

Histone H1 protein structure in lower eukaryotes is different from higher eukaryotes. For example, the linker histone globular domain is missing in lower eukaryotes like *Tetrahymena*. However, *S. cerevisiae* linker histone, Hho1p, has an extra globular domain (reviewed by Izzo *et al.*, 2008). Several studies have showed that histone H1 is not vital for the cell cycle progression in unicellular eukaryotes (Patterton *et al.*, 1998; Ramon *et al.*, 2000; Shen *et al.*, 1995; Ushinsky *et al.*, 1997).

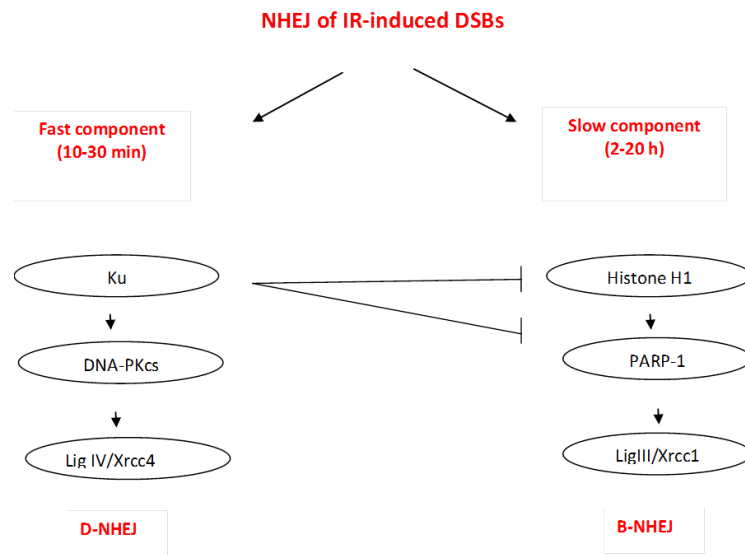


Figure (1.8): Diagram of the two pathways of non-homologous end joining: the canonical KU Dependent NHEJ (D-NHEJ) and the Backup NHEJ (B-NHEJ) pathways.

The D-NHEJ is dependent of the Ku protein complex and DNA-PKs for alignment and runs ligation by the usage of the Ligase IV / XRCC4 complex. However, alignment in B-NHEJ is carried out by histone H1 and the end ligation is dependent of Ligase III / XRCCI complex through PARP-1 activation. These results were obtained in Human Hela cells exposed to ionizing radiation (IR) to produce DSBs. Adapted from (Rosidi *et al.*, 2008).

1.2.3. The 300 nm Chromatin Fibre and the chromosome axes

The nucleosome fibre formed by the association of the histone octamer with the DNA (Goll and Bestor, 2002) can be further compacted into a higher order chromatin fibre (about 30 nm). This higher order chromatin fibre is arranged into loops attached to a proteinaceous structure named the chromosome axis. This further compaction manages to pack the DNA into a higher order 300 nm chromatin fibre structure (Luger *et al.*, 1997).

The chromatin organization in the interphase nuclei is not well understood yet, however several reports have tried to model the possible organization of the

chromatin at metaphase chromosomes (Marsden and Laemmli 1979; Paulson and Laemmli, 1977). Different models have been proposed for the organization of metaphase chromosomes. These models were; random fibre folding (Dupraw, 1966), a scaffold and loop arrangement (Laemmli et al., 1978) and helical coiling (Sedat and Manuelides 1977). The coiled nature of metaphase chromosomes were proofed through cytological preparations of meiotic chromosome spreads in plants as well as in animals (reviewed in White, 1973; Ronne, 1977; Geradia and David, 1977). Attention was directed to the zigzag or spiral nature of chromatid after results obtained from research on human by Onnuki (1968). Meanwhile, the “radial loop” model of metaphase chromosomes was accepted (Adolph *et al.*, 1977; Laemmli *et al.*, 1987). The “radial loop” proposes that DNA loops are arranged in a way that interferes with the proteinaceous scaffold formed at the chromatid central axis. The loop and scaffold structure were observed in histone-depleted chromosomes micrographs showing that the scaffold length is equal to the length of the condensed metaphase chromatid. The paradox between the zigzag nature of chromatid observed by Onnuki (1968) and the radial loop model were resolved by Rattner and Lin (1985) who suggested that the metaphase chromosome is packaged via coiling of 200-300 nm fibre in a helical manner and in a way that forms radial loops, a thing which permits formation of an organized scaffold elements and loop association.

The electron micrographs of histone-depleted Hela cells at metaphase showed loops of 30 to 90 Kb of DNA associated to a proteinaceous scaffold in each chromatid (Paulson and Laemmli, 1977). Chromatin loops are composed of 180-300 nucleosomes arranged in a 30 nm coiled fibre structure (Marsden and Laemmli,

1979). The DNA present on the loop is packaged into 700 folds relative to the chromosome axis length. Loops arrange along the chromosome axis of metaphase scaffold in a spiral helix (Marsden and Laemmli, 1979), which forms 15-18 chromatin loops per turn and that is about 1.2 million bp of DNA (Nelson *et al.*, 1986). Hence, it was predicted that a cylinder of chromatin loops forms at metaphase showing a thickness of about 800-1000 nm, was perfectly in accordance to the metaphase chromosome thickness (Marsden and Laemmli, 1979; Nelson *et al.*, 1986). Hence, allows the DNA helices to compact 10,000 folds in length and 400-500 folds in thickness to form the metaphase chromosomes.

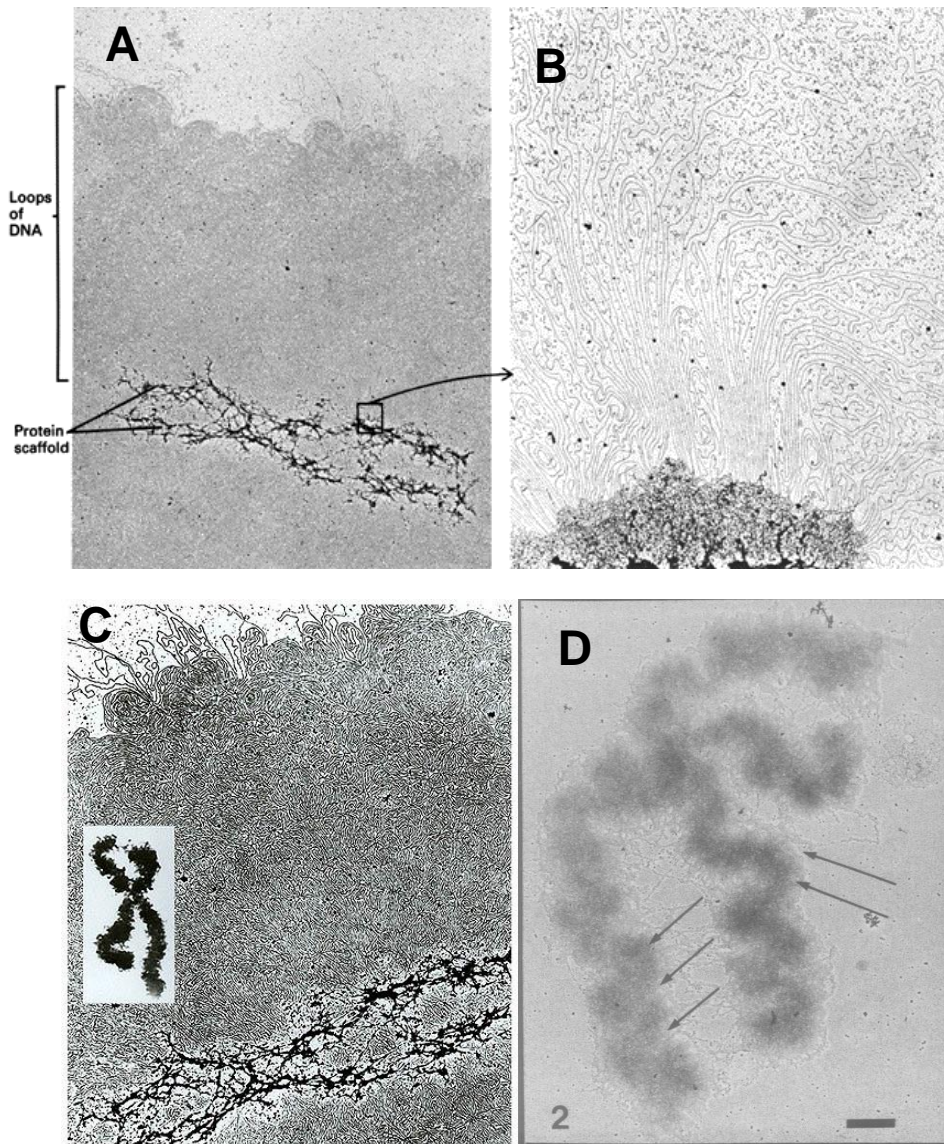


Figure (1.9): 300 nm Higher Order Chromatin structure and chromosome scaffold.

The 30 nm chromatin fibre undergo further compaction to allow DNA to fit in the nucleus. (A) The 30 nm chromatin fibre coiling into loops attached to the chromosome scaffold permit the 300 nm higher order chromatin formation. (A) Chromatin loops and scaffold formation. (B) Closer view of (A). (C) Chromatin loops coiling along the chromosome scaffold in a spiral helix pattern allow metaphase chromosome to be compacted as 10,000 times of the original DNA molecule and be as 400-500 times thicker. (D) Radial loops formation in the metaphase chromosome via chromatin coiling. (A&B) Adapted from (Griffiths *et al.*, 1996). http://www.pha.jhu.edu/~ghzheng/old/webct/note6_3.htm (C) Adapted from http://is.muni.cz/do/sci/UEBBiol/DNA-FTBcz/pics/29/16638_nohistone_dna.jpg (D) Adapted from (Rattner and Lin, 1985).

1.3. Chromatin Role in DNA associated Biological Processes

The genetic DNA material controls different vital cellular activities: replication, transcription, repair, recombination and segregation. Thus a highly dynamic change in the chromosomal compaction level controls the occurrence of the cellular division during meiosis and mitosis (Deal and Henikoff, 2010). The molecular mechanisms of chromatin condensation are highly conserved among eukaryotic species. So, although there are great differences in the eukaryotic chromosome size and organization, there are similar key proteins and structures involved in the chromatin compaction.

1.3.1. Replication

DNA replication is a highly conserved process through which genetic information transmits accurately through different divisions, which demands chromatin disassembly and reassembly to ensure that the genetic material fits inside the nucleus (Budhavarapu *et al.*, 2013). For each round of the cell cycle, it is necessary the production of core histones enough to form about 20 million new nucleosomes needed in the packaging of the newly formed DNA strand. For that, canonical core histones are synthesized during the cell cycle (Marzluff and Duronio, 2002; Gunjan *et al.*, 2005). Histone levels were found to play a role in the progress of the cell cycle. In *S. cerevisiae*, cell cycle arrest was recorded as a consequence of reduced histone levels (Han *et al.*, 1987; Kim *et al.*, 1988), although, the S-phase was just constrained in mammalian cells (Nelson *et al.*, 2002). In addition to that, an increase in histone levels resulted in DNA defects and genome instability (Gunjan and Verreault, 2003).

Chromatin assembly and disassembly is regulated by histone chaperons and ATP-dependent chromatin remodelling complexes (Macapline and Almouzni, 2013). Histone variants assembly on the chromatin allow diversity on the chromatin structure and function (Ahmad and Henikoff 2002a; Kamakaka and Biggins 2005; Probst *et al.*, 2009). These variants deposit on the chromatin either in a replication dependent or replication independent manner (Macapline and Almouzni, 2013).

During DNA replication half of the histones are gained from the parental chromatin (like a semiconservative manner) whereas the rest is newly formed. How the epigenetic code gets transmitted from the parental chromatin to the newly synthesized histones is still a mystery. Recently, it was reported that parental histone modifying enzymes associates with parental chromatin during replication, and so re-establish the parental pattern of histone epigenetic modification style on the newly formed chromatin (Budhavarapu *et al.*, 2013).

1.3.2. Transcription

A study by Dion *et al.* (2005) in budding yeast showed that the acetylation code of histone H4 tail lysines: K16, K5, K8, K12 can affect gene expression differently. Merely, lysine 16 (k16) mutation affect transcription of ~ 100 genes specifically. However lysines 5, 8 and 12 showed a cumulative effect on transcription in which its consequence depends on the total number of mutations. K16 acetylation status can control chromatin silencing, in which Sas2- acetylated- K16 to Sir2-deacytelated- K16 ratio direct the degree of telomere silencing (Kimura *et al.*, 2002; Suka *et al.*, 2002). That is partly due to the affinity of Sir3 to H4-deacetylated K16 (Carmen *et al.*, 2002).

Moreover, the bromodomain factor Bdf1 bind to H4-deacetylated K16 (Kurdistani *et al.*, 2004). However, the other lysine residues role is still to be clarified. Histone H4 di-acetylated at lysines 5 and 12 are noticed in many organisms (Sobel *et al.*, 1995). In addition, Bdf2; the bromodomain factor, binds to H4-acetylated-K12 in human cells (Kanno *et al.*, 2004). However, H4 acetylated K8 recruits hSwi/snf of IFN- β (Agalioti *et al.*, 2002). It was recorded that yeast mutants with the histone H4 tails lacking lysine residues showed abnormal G2/M cell cycle. Nevertheless, the addition of a single lysine could correct this defect (Megee *et al.*, 1995).

1.3.3. Repair

Several endogenous and exogenous factors have been found to produce DNA damages (Finkel and Holbrook, 2000; Marnett and Plastaras, 2001). The genome integrity is maintained by the proper responding to genetic lesions before each cell division (Kastan and Bartek, 2004). Usually DNA damage directs the cell to activate cell cycle arrest and the DNA repair pathways, whereas severe lesions result in cell apoptosis (Lownders and Murguia, 2000). Reports have showed that chromatin structure components and its organization is intrinsically linked to the DNA damage response (DDR) (reviewed by Costelloe *et al.*, 2006). Posttranslational modifications to both core histone proteins as well as histone variants, besides to ATP-dependent chromatin remodelling complexes are important in DNA damage signalling and repair specially at DNA DSBs (Berger, 2002; Lydall and Whitehall, 2005; Saha *et al.*, 2006; and reviewed by Costelloe *et al.*, 2006). γ H2A(X) role is essential in the DDR (Fernandez-Capetillo *et al.*, 2004; Foster and Downs, 2005; Lownders and Toh, 2005; Thiriet and Hayes, 2005; Stucki and Jackson, 2006; Wurtele and Verreault,

2006). As a response of DNA DSBs H2AX phosphorylates (γ H2AX) at the C-terminus serine 139 in higher eukaryotes or serine residue 129 in yeast (Turner, 2005), its phosphorylation extends to about 60 kb in yeast and 1 kb in higher eukaryotes (Lownders and Toh, 2005), and since DSBs induce this H2AX phosphorylation, γ H2AX is a well-known DSB marker (Foster and Downs, 2006; Stucki and Jackson, 2006).

Furthermore, methylation of histone H3 at lysine 79 (H3K79me) was found also to be linked to DDR (Huyen *et al.*, 2004; Giannattasio, *et al.*, 2005; Wysocki *et al.*, 2005). The H3K79me is present constitutively on euchromatin in human cells (reviewed by Costelloe *et al.*, 2006). Whereas, 90% of *S. cerevisiae* chromatin is methylated at K79 of histone H3 (Van *et al.*, 2002). H3K79me was found to peak at G1/S stage, possibly due to DOT1, the conserved methyltransferase enzyme which methylate histone 3 at lysine 79 (reviewed by Costelloe *et al.*, 2006). The H3K79me was found to play a role in DNA DSBs induced recruitment of 53BP1 in human and Rad9, homologue of 53BP1 in budding yeast through the K79me binding to their Tudor domain hydrophobic site (Maurer-Stroh *et al.*, 2003). A model was proposed showing that chromatin induced DSB site causes the higher order chromatin relaxation next to the break site, a thing which permits the 53BP1 in human, Rad9 in budding yeast, to bind to the methylated 79 lysine on histone H3, and hence act as an early marker for DDR, which induce recruitment of other proteins needed for the checkpoint response (Huyen *et al.*, 2004; Giannattasio, *et al.*, 2005; Wysocki *et al.*, 2005). Since H3 is constitutively methylated at K79, it acts as a “ready-made mark” for the DDR (reviewed by Costelloe *et al.*, 2006). Moreover, it was reported that at G2 both

γ H2AX and H3K79me recruit Rad9, which enhance the homologous recombination pathway of DSB (Wysocki *et al.*, 2005; Toh *et al.*, 2006).

Histone acetylation has also been linked to chromatin transition from highly compacted structures to more relaxed structures at the DSBs sites (Tamburini and Tyler, 2005). Several histone acetylase (HATs) enzymes were found to be recruited to 5 Kb region around the DSB site (Bird *et al.*, 2002; Teng *et al.*, 2002; Down *et al.*, 2004; Tamburini and Tyler, 2005; Qin and Parthun, 2006). Hence, acetylation increase was reported at the histone H3 lysine residues; K9, K14, K18, K23 and K27, as well as histone H4 residues; K5, K8, K12, and K16 (Tamburini and Tyler, 2005). Suggesting that histones H3 and H4 residues acetylation permit proteins involved in the DSB repair to access the DNA break site via moving the compact higher order chromatin into a relaxed and open chromatin (Downey and Durocher, 2006). Moreover, histone H4 acetylation levels at N-terminus were found to direct alternative repair pathways, so acetylation of one lysine residue in the H4-N-terminus in yeast result in the activation of the replication coupled repair pathway, but NHEJ is the choice if more than one lysine residue is acetylated (Bird *et al.*, 2002). Furthermore, the highest acetylation levels have been reported during HR (Tamburini and Tyler, 2005).

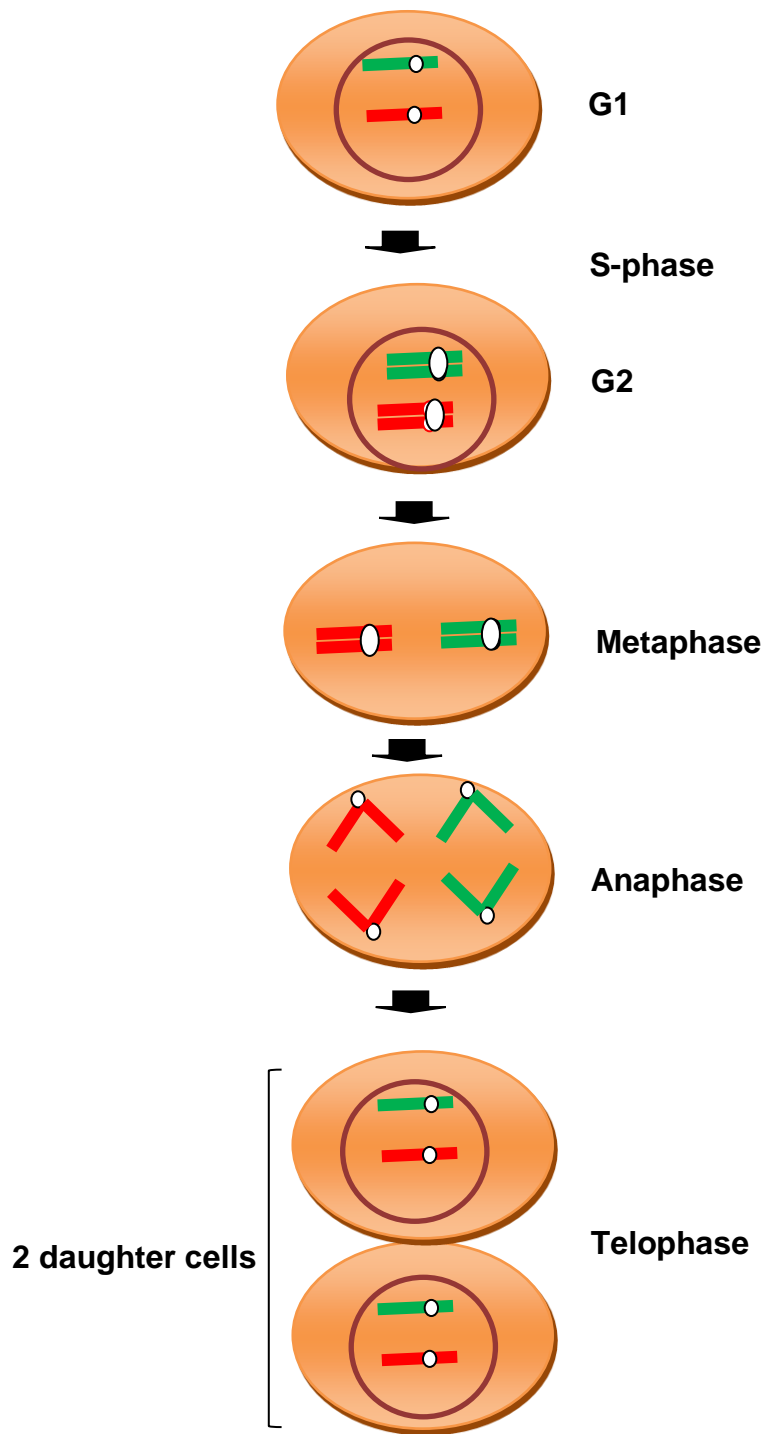
Several reports have indicated that ATP-dependent chromatin remodelling complexes play also a role in the DNA damage response (reviewed by Costello *et al.*, 2006), through nucleosome modulation either by dissolution, sliding or histone exchange (Cairns *et al.*, 1996; Owen-Hughes *et al.*, 1996; Shen *et al.*, 2000;

Mizuguchi *et al.*, 2004; Saha *et al.*, 2006). The chromatin remodelling complexes; INO80, RSC, SWI/SNF and SWR-C complexes, were found to be recruited to the DSBs induced by HO endonuclease in *S. cerevisiae* (Downs, *et al.*, 2004; Chai *et al.*, 2005; Nakamura *et al.*, 2005; Shim *et al.*, 2005). INO80 and SWR-C complex are recruited to the DSB via γ H2AX dependent manner (Downs *et al.*, 2004; Marrison *et al.*, 2004; van Attikum *et al.*, 2004). INO80 mediates nucleosome displacement at DSB (Tsukuda *et al.*, 2005), and so allow single strand DNA (ssDNA) formation (van Attikum *et al.*, 2004), suggesting that it has a role in the homologous recombination single strand invasion. The SWI/SNF complex as well was found to be needed in the strand invasion by mediating homology search (Chai *et al.*, 2005). Moreover, RSC complex is recruited by Mre11 and Ku70 (Shim *et al.*, 2005) indicating that RSC complex play a role in the donor strand dissociation prior to strands ligation during HR pathway of DNA repair (Chai *et al.*, 2005). The RSC complex induced by H2AX – Mre11 interaction allows cohesion loading at the break site (Chai *et al.*, 2005 Shim *et al.*, 2005).

1.3.4. Mitosis

Mitosis is the nuclear process where two newly formed cells arise from a single parent cell with identical genetic information (**Figure 1.10**) (Zickler and Kleckner, 1998; Cnudde and Greats, 2005). Prior to mitosis, the DNA is replicated at the Synthesis (S) phase producing two copies for each chromosome also known as sister chromatids. Cohesion protein complexes load between the sister chromatids as the DNA is replicated and keep them as a unit (chromosome) during prophase, pro-metaphase and metaphase stages (Nasmyth, 2001). At metaphase, the

chromosomes align on the equatorial plate with their centromeric kinetochores attached to the microtubule spindle fibres. At anaphase, sister chromatid cohesion gets dissociated allowing each sister chromatid to segregate and move to opposite poles of the cell. After telophase the nuclear division is completed, and after cytokinesis two cells have been formed with identical genetic information (**Figure 1.10**).



Figuer (1.10): Schematic diagram representing the mitotic nuclear division.

Parental cell with diploid number of chromosomes pass one round of DNA replication and separates the equally the sister chromatids formed to produce two identical daughter cells. Paternal chromosome is represented in green and maternal homologue is represented in red.

1.3.4.1. Sister chromatid Cohesion

After DNA replication the sister chromatids stay together by protein complexes denominated cohesion complexes or cohesins (Guacci *et al.*, 1994) (**Figure 1.3 A&B**). Cohesion establishment between sister chromatids had been implied in several reports using both genetic and biochemical analysis (Dej and Orr-Weaver, 2000; Hirano, T., 2000; Jones and Sgouros, 2001; Koshland and Guacci, 2000; Nasmyth *et al.*, 2000; Losada and Hirano, 2001; Van Heemst and Heyting, 2000). The early loading of cohesins at G2 stage implies a vital role for this sister chromatid organisation. Cohesins are involved in protecteing yeast DNA from damage stimulated by irradiation (Birkenbihi and subramani, 1995), and it mediates DNA DSB repair via sister chromatid recombination (Sjogren and Nasmyth, 2001). Moreover, cohesion is involved in sister chromatids attachment to the mitotic spindle allowing balanced segregation of chromosomes to opposite poles of the nucleus at anaphase (Tanaka *et al.*, 2000) and during the meiotic anaphase II (Uhlmann and Nasmyth,1998). The cohesin complex is evolutionary conserved, it is composed of two Structural Maintenance (SMC) proteins; SMC1&3, and two Sister Chromatid Cohesion (SCC) proteins; SCC 1&3 (Nasmyth and Haerring, 2009). The SMC1 and SMC3 as well as the SMC protein family members are composed of five domain structures, N and C terminal ATP binding motifs; Walker A motif and Walker B motif (Losada and Hirano, 2005). The SMC protein folds backwards forming antiparallel coiled coils in a way distinguishing hinge domain as the head and Walker A and Walker B motifs heads at ends. When the SMC1/ SMC3 hinge domains dimerize a stable v-shaped heterodimer forms (Hearing *et al.*, 2004). The V-shaped structure shifts to a 40 nm ring like-structure capable to hold the sister chromatid as a unit

when the SMC1 head interact with the carboxy terminal regions of SCC1/Mcd1/Rad21 (Haering *et al.*, 2002) and the SMC3 head interact with the amino terminal regions of the SCC1/Mcd1/Rad21 (Gruber *et al.*, 2003). The Cohesin complexes have two phases; mitotic and meiotic, both are characterised with SMC1/SMC3 heterodimer V-shaped, which shifts to the ring shape when SCC3 interacts with SCC1 in mitosis, and Rec8 interact with SCC3 in meiosis (**Figure 1.11 A**). The SCC1 cleavage during metaphase shift to anaphase directs sister chromatid dissociation to the opposite poles (Uhlmann *et al.*, 1999). Showing that SCC1 plays a dual role; structural and functional, in the vicinity of mitotic cohesions. Rec8 cohesin releases during meiosis I at metaphase I from between the arms and distal to chiasmata, while keeping centromeric sister chromatid cohesions, allow homologous chromosomes segregation. At meiosis II the cleavage of the remaining centromeric Rec8 cohesin during metaphase II results in an equal segregation of sister chromatids to each gamete (**Figure 1.11 B**). Cohesin protein sequences are evolutionary conserved from yeast to humans. Immunolocalization studies showed that cohesins loading on the chromosome occur as early as S phase. Foci signal in yeast *REC8* was observed at leptotene and zygotene while pachytene stage showed signal at chromosomes arms and centromere (Klein *et al.*, 1999; Watanabe and Nurse, 1999). The meiotic mammalian *REC8* appears as foci at S phase, which localize entirely along the chromosomes at pachytene (Prieto *et al.*, 2004). Klein *et al.* (1999) reported that the SMC3 colocalize with *REC8* at early prophase showing SMC3-*REC8* dual signal appearance along chromosomes arms at pachytene, which dissociate partially at metaphase I, whereas the remaining signal colocalize on the metaphase II centromeric region indicating its role in preserving sister chromatid

cohesion. Similar results were seen in the dual immunolocalization experiments of the mammalian meiotic cohesins SMC1 β and SMC3 (Eijpe *et al.*, 2003). The meiotic SMC3 normal loading in *rec8* mutants suggests that SMC3 loads on the chromosomes prior to REC8 loading (Xu *et al.*, 2005). Lam (2005) reported that SMC3 signal observed at the microtubule of spindles after metaphase I and until telophase I indicates a SMC3 suggested role in the microtubules assembly as well as glue sister chromatids as a unit. Studies on AtSYN1, the *Arabidopsis* meiotic homologue of *REC8* in yeast (Bai *et al.*, 1999), showed that *syn1* mutants have normal somatic growth, however, reproduction was abnormal, cytological analysis showed chromosome fragments were visualised at metaphase I, and bridges at anaphase II leading to polyads formation (Bai *et al.*, 1999; Bhatt *et al.*, 1999). Similar results were observed in mutants of other Rec8 homologues; maize *afd1* (Yu and Dawe, 2000), *Sordaria sm-rec8* (Pasierbek *et al.*, 2001), mouse *rec8* (Xu *et al.*, 2005), worm *rec8* (Storlazzi *et al.*, 2008) and rice *Osrad21-4* mutant line (Zhang *et al.*, 2006). SYN1 localization in *Arabidopsis* meiocytes indicated its presence on chromosome arms but not centromeres during interphase-anaphase I (Cai *et al.*, 2003) On another hand, a strong evidence for AtSSC3's role as one of the sister chromatid cohesins came from immunolocalization studies indicated that, it persist on chromosomes from leptotene to metaphase I, similar to other cohesion complex proteins. The *Atssc3* mutant cytological characteristics showed chromosome fragments and bridges at metaphase I suggesting that AtSSC3 role in the normal meiotic chromosomes phenotype (Chelysheva, 2005).

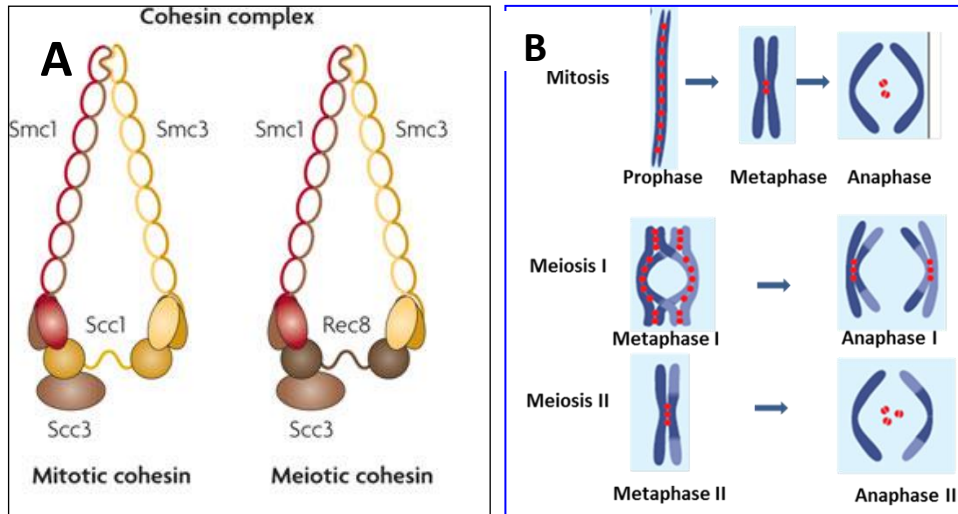


Figure (1.11): Schematic diagram of mitotic and meiotic cohesin complex.

(A) Cohesin complex is a ring-like structure composed of two subunits of each SMC and SCC proteins. Meiotic cohesin differs from the mitotic one in that the Rec8 replaces the mitotic SCC1 function. (B) Cohesin complex loading between sister chromatids in mitotic as well as meiotic cells glue chromosomes sister chromatids, and hence, keeping them preserved until the proper timing of chromosomes spatial organisation at anaphase, where their disassembly as well as kinetochores mechanical forces aid their separation to the opposite poles. (A) Adapted from (Wood, 2010). (B) Modified from (Uhlmann, 2001).

1.3.5. Meiosis

Eukaryotic sexual cell division cycles are called meiosis. Each meiotic process passes two rounds of nuclear divisions termed as meiosis I and meiosis II respectively. Meiosis I and meiosis II are subdivided into four stages each, depending on the chromosomal organization and status, these are: prophase, metaphase, anaphase and telophase. Meiosis is a highly conserved process among eukaryotes. Its necessity comes from the role it plays in species preservation through ages, by conserving chromosomal set number. After one round of DNA replication during interphase, two rounds of nuclear meiotic divisions follow. In meiosis I homologous chromosomes separation allows chromosomal reduction by half; however through meiosis II sister chromatid separates to end up with haploid

gametes. The conjugation of the two haploid gametes through fertilization allows retaining the diploid individual. And so, meiosis phases are the key for understanding sexual reproduction.

Meiosis is a dynamic process. Genetic variation seen within gametes and hence in the progeny is introduced by the recombination scenario, in which reciprocal genetic material exchange between parental homologous chromosomes during meiosis I opens the gate widely for recombination machinery proteins loading on the chromatin axis, mediating the parental physical genetic exchange and so enhancing new allelic combinations to appear.

1.3.5.1. Meiosis I and II:

DNA replication during Interphase-S stage is a prerequisite to meiosis machinery to proceed normally. Studies on meiosis in *Arabidopsis* showed that it takes 33 hrs to be completed (Armstrong *et al.*, 2003). Meiosis I has four distinct substages; prophase I, metaphase I, anaphase I and telophase I, respectively. Prophase I is the longest stage during meiosis, it takes about 30 hours to be completed in *Arabidopsis* (Armstrong *et al.*, 2003). Cytological analysis showed five discriminate phases for the prophase I chromosomes: leptotene stage, zygotene stage, pachytene stage, diplotene stage, and diakinesis stage. (**Figure 1.12**) is a schematic diagram that represents chromosomal phases within the context of meiosis process including meiosis I and II stages. Leptotene, chromosomes condense, hence thin thread-like structures termed as chromatids appear. Early cohesion loading between sister chromatids keep them stuck tightly together as a unit (Sjorgren and Nasmyth, 2001).

Leptotene stage is so vital and complicated stage, as chromosome axis proteins start loading on the axis, recombination initiates at distinct chromosomal sites, allowing chromosomes to search for their homologue. Homologous chromosomes initial pairing permits the synaptonemal complex (SC) structure formation. During zygotene stage, homologous chromosomes pairing and synapsis proceed along the entire chromosome axis. At pachytene stage, thick-fully synapsed homologous chromosomes are visible at this stage, marked as thicker linear structures. Diplotene stage comes afterwards, leading to synaptonemal complex disassemble. Then diakinesis stage continues with a discriminate homologous chromosomes shapes, known as bivalents, in which homologues are held only at crossover (COs) sites, the points where reciprocal parental genetic segments exchange occur and known as chiasmata. Bivalents condensation followed by kinetochore formation at centromeric region of the chromosomes, which later aid in the proper positioning of the bivalents at the equatorial site of the meiotic cell at metaphase I stage. Through anaphase I stage, separated homologous chromosomes moves to the opposite poles of the cell. Bivalents disjunction is initiated by the mechanical forces created by kinetochore spindles on the centromeres. After that, telophase I stage takes place, resulting in dyads, at which two de-condensed chromosome nuclei are seen. By that, the first meiotic nuclear division is completed, two nuclei with half chromosomal set number are distinguished. The second round of nuclear division during meiosis is highly similar to mitotic division. In Prophase II stage, re-condensation of chromosomes occur forming thread like structures. Each of the two nuclear poles is occupied by either one of the parental homologous chromosomes. At metaphase II stage, sister chromatids move to the equatorial region. Spindle fibre attachment at the centromeric

region creates physical and mechanical power which helps sister chromatid separation and migration to the poles during anaphase II stage. Thus, at telophase II stage, after nuclear envelope regeneration, followed with cytoplasmic division, four cells form, each containing haploid chromosomal set number.

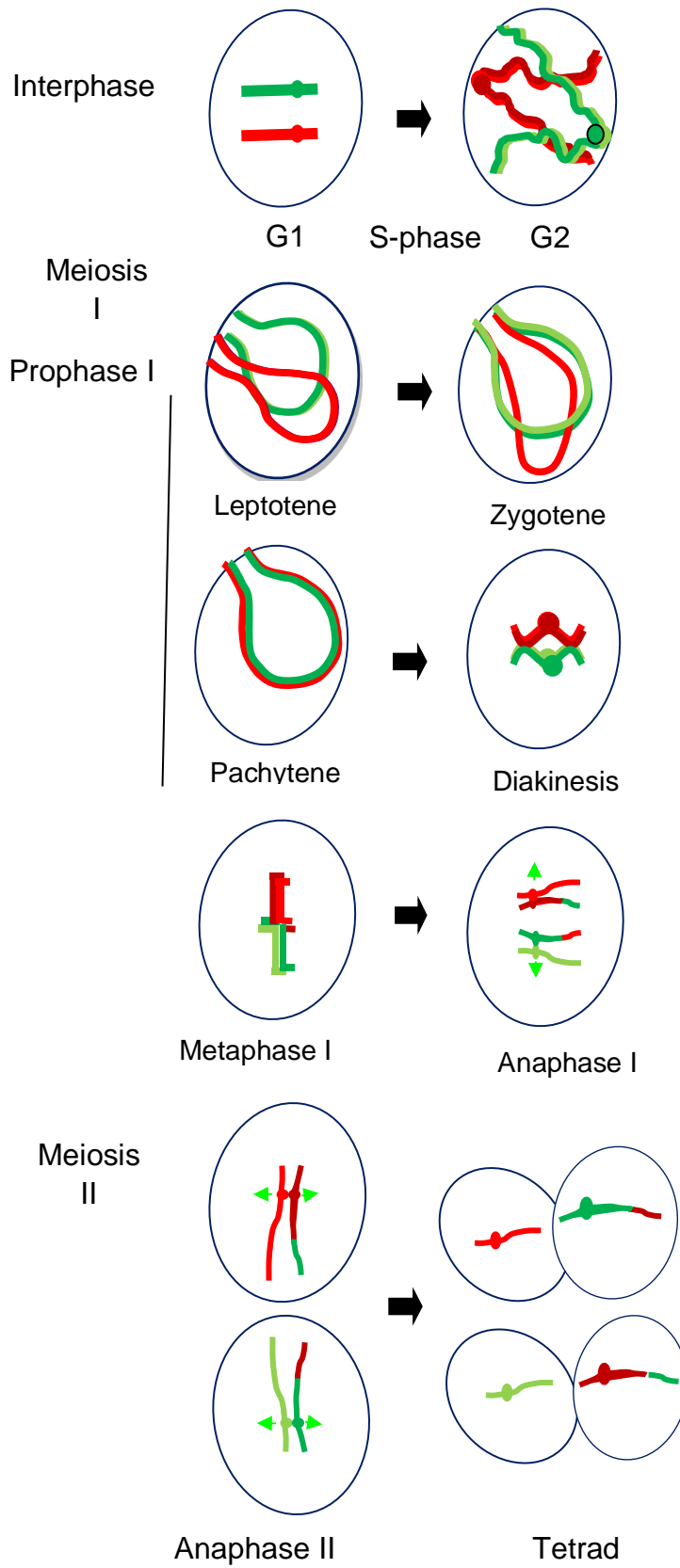


Figure (1.12): Schematic diagram represents meiosis nuclear division stages.

Prior to meiosis initiation DNA duplicates at the interphase S-phase. Meiosis follow that, with two rounds of nuclear divisions ending up with four genetically different haploid gametes. Meiosis I is the key phase through which chromosomes number per cell halves and so named “reductional division”, whereas meiosis II is similar to the mitotic division hence is known as “equational division”. Meiosis I importance is due to the highly active prophase I stage, where homologous chromosomes organization, pairing, synapsis and recombination context exceeds the creation of newly formed allelic combinations, to the preservation of their chromosomal integrity needed through their alignment at metaphase I and separation at anaphase I. Hence, dyads, the products of meiosis I could continue meiosis II normally, and allowing proper alignment of chromosomes at metaphase II and sister chromatids separation at anaphase II, else, gamete production is affected.

1.3.5.2. Chromosome axis establishment

Chromosomes are highly organised structures. Sister chromatid chromatin arranges during prophase I into loops series, which associates with the chromosome axis proteins at their base (**Figure 1.10 A**) (Kleckner, 2006). These loops density are conserved among organisms, showing 20 loops per micron of chromosome axis length (Zickler and Kleckner, 1999). Several reports indicated that loop density is constant via the adjustment of loop size depending on the chromosome axis length (Revenkova *et al.*, 2004; Tease and Hulten, 2004; Novak *et al.*, 2008). Although of the high advances made in chromosome study, however, up to now the chromosome context is mysterious, further research is still needed to carry on to show a deeper view of protein-protein, as well as, protein-DNA networking during chromosome axis organization context, a thing which led Andrew Belmont to write describing chromosomes “A riddle, wrapped in a mystery, inside an enigma” (Belmont, 2006). Cohesins role in holding sister chromatids during meiosis and mitosis suggested a role for them in the organisation of chromatin loop (Novak *et al.*, 2008). The loading of cohesins to the meiotic axis (Cai *et al.*, 2003; Severson *et al.*, 2009), besides to the defects observed in chromosome axis formation in the mutants of cohesins subunits (Bhatt *et al.*, 1999; Klein *et al.*, 1999; Bannister *et al.*, 2004; Xu *et al.*, 2005; Novak *et al.*, 2008), suggested a role for cohesins in the development of

chromosome axes. The importance of chromatin organisation into loops is that chromosome axis starts to form. Several proteins are needed for the chromosome axis formation. Loading of Topoisomerase II (Topo II) leads to mitotic chromosome axes development (Saitoh and Laemmli, 1994; Novak *et al.*, 2008). Also, it has been reported that loading of SYCP3 in mammals, Red1/Hop1 in budding Yeast and ASY3/ASY1 in *Arabidopsis* play a role in their meiotic chromosome axis formation (Saitoh and Laemmli, 1994; Kleckner, 2006; Novak *et al.*, 2008, Ferdous *et al.*, 2012).

1.3.5.3. Homologous chromosomes pairing and synapsis

Homologous chromosomes starts pairing at early prophase I. The telomeres had been reported that it mediates homologue recognition and pairing. It was found that chromosomes transfer from “Rabl” orientation (Zickler and Kleckner, 1998) to “bouquet” formation (Bass *et al.*, 2000; Scherthan, 2001) mediates homologues recognition and pairing in some species (Bass *et al.*, 2000; Golubovskaya *et al.*, 2002; Harper *et al.*, 2004). Bouquet formation in wheat had a confirmed role in subtelomeric pairing, which continues along homologous chromosomes (Lukaszewski, 1997). A recent study on barley (*Hordeum vulgare L*) suggested that telomeres pairing in a bouquet at G2 (Higgins *et al.*, 2012). Moreover, the axis protein ASY1 showed continuous signal at subtelomeric region while interstitial regions showed foci. Interestingly, the SC initiated at the subtelomeric region polymerize along homologues during zygotene where telomeres were found to be clustered. From this, it was proposed that telomeres clustering in Barley aid pairing and synapsis at the subtelomeric region (Higgins *et al.*, 2012). This is not the case in all species, bouquet had no role in homologue pairing in *Sordaria macrospora* (Storlazzi *et al.*,

2003) since pairing was observed prior to homologue pairing. For that, further research on bouquets role is still required. In *Arabidopsis*, the usual bouquet was not seen; meiotic telomeres were found to cluster while associated to the nucleolus rather than the nuclear envelope at G2-leptotene (Armstrong *et al.*, 2001). In the same study, FISH analysis using probes for subtelomeric region showed that telomeres of homologous chromosomes pair while they associated to the nucleolus. From these results, Armstrong *et al.* (2001) suggested that telomeres cluster while they still associated to the nucleolus, somehow, facilitates homologue pairing similar to bouquet formation in some species. Some recent studies suggest that the telomere-led rapid prophase movement (RPMs) enhance meiotic chromosomes pairing (Lee *et al.*, 2012; Sheehan and Pawlowski, 2009), suggesting that these telomere-led movements aid in homologues pairing by bringing them in a close proximity, and so mediate homologues search and recognition. Moreover, the RPMs were suggested to aid in resolving chromosomal interlocks (Koszul and Kleckner, 2009). The HORMA-domain axis associated proteins; Hho1p in yeast (Borner *et al.*, 2008) and HORMAD 1 and 2 in mammals (Wojtasz *et al.*, 2009; Daniel *et al.*, 2011) are part of so called axial elements (AE) in meiosis. As synapsis initiates, homologous chromosomes start to interconnect via the polymerization of the synaptonemal complex (SC) transverse filament (TF) along the axial elements (AE) that pass to be called lateral elements (LE), as reviewed by (Zickler and Kleckner, 1999). (**Figure 1.13 B**). As SC polymerization occurs along the chromosomes, the fully polymerized LE proteins (Hop1, Hormad1/2) removal occurs. It has been reported that AAA+ ATPase Trip 13 has a role in the removal of HORMAD1 and 2 from the synapsed mammalian chromosomes (Wojtasz *et al.*, 2009). Moreover, it has been suggested that the mammalian chromosome axis protein HORMAD1 and the SC transverse filament protein SYPC1 affects meiotic progression differently, so

HORMAD1 enhance homologous chromosomes alignment and synapsis, whereas the SYPC1 cause HORMAD1 depletion on the axis (Daniel *et al.*, 2011). The meiotic chromosome axis proteins; ASY1, ASY3, HORMAD1 and Red1/Hop1, importance exceeds the temporal axis structure formation during early prophase I, to achieve successful meiotic recombination event. Several reports suggested that chromosome axis establishment mediates recombination, as was reviewed by (Kleckner, 2006), which was confirmed by several studies showing that the recombination protein complexes are axis associated (Carpenter, 1975; Blat *et al.*, 2002; Tesse *et al.*, 2003; Moens *et al.*, 2007). Although recombination occurs at the chromosome axis (Kleckner, 2006), it was suggested that the introductory DSB events occur in the chromatin (yet to be determined if initially is axis associated or chromatin loops associated) to appear later on the axis (Blat *et al.*, 2002; Storlazzi *et al.*, 2003; Kim *et al.*, 2010).

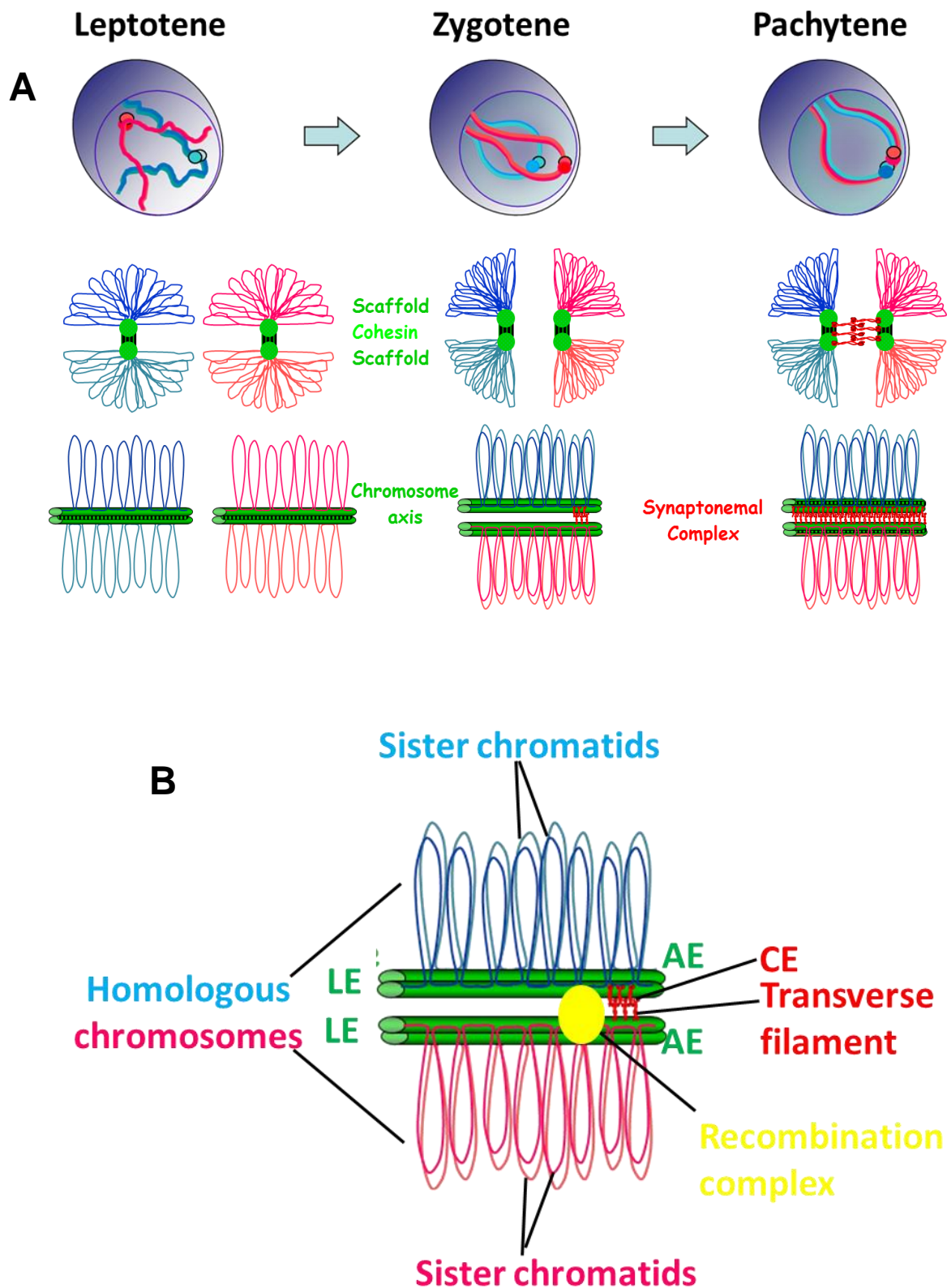


Figure (1.13): (A) Chromosome organisation during prophase I. (B) Synaptonemal complex structure.

(A) During early leptotene stage chromatin is arranged into loops. Cohesion loading between the sister chromatids loops allow their pairing. Meanwhile prophase I progress, loops in each of the homologous chromosomes associates to the protenaceous chromosome axes structure, knowing that by the end of leptotene chromosome axis is linearized. Synapsis initiates by the end of leptotene stage via loading of the transverse elements along homologues axis. Through chromosomes transition from zygotene stage to pachytene stage; the transverse element associates to the lateral element (LE) from one side and to the central element (CE) from the other side. And by the end of pachytene stage the synaptonemal complex (SC) is fully polymerized, forming SC structure of 100 nm in diameter. Modified from (Sanchez-Moran, 2008)

1.3.5.4. Meiotic recombination

Meiosis significance relies on the production of new genetic composition. Genetic variation results from successful parental homologues crossovers. Meiotic recombination events are conserved inter species. Recombination initiates when the double strand breaks (DSBs) form as early as G₂, followed with the 5' strand resection step, afterwards, recombinases-mediated single strand invasion allow intermediate structures formation, which if resolved properly, mature crossovers form **(Figure 1.14)**.

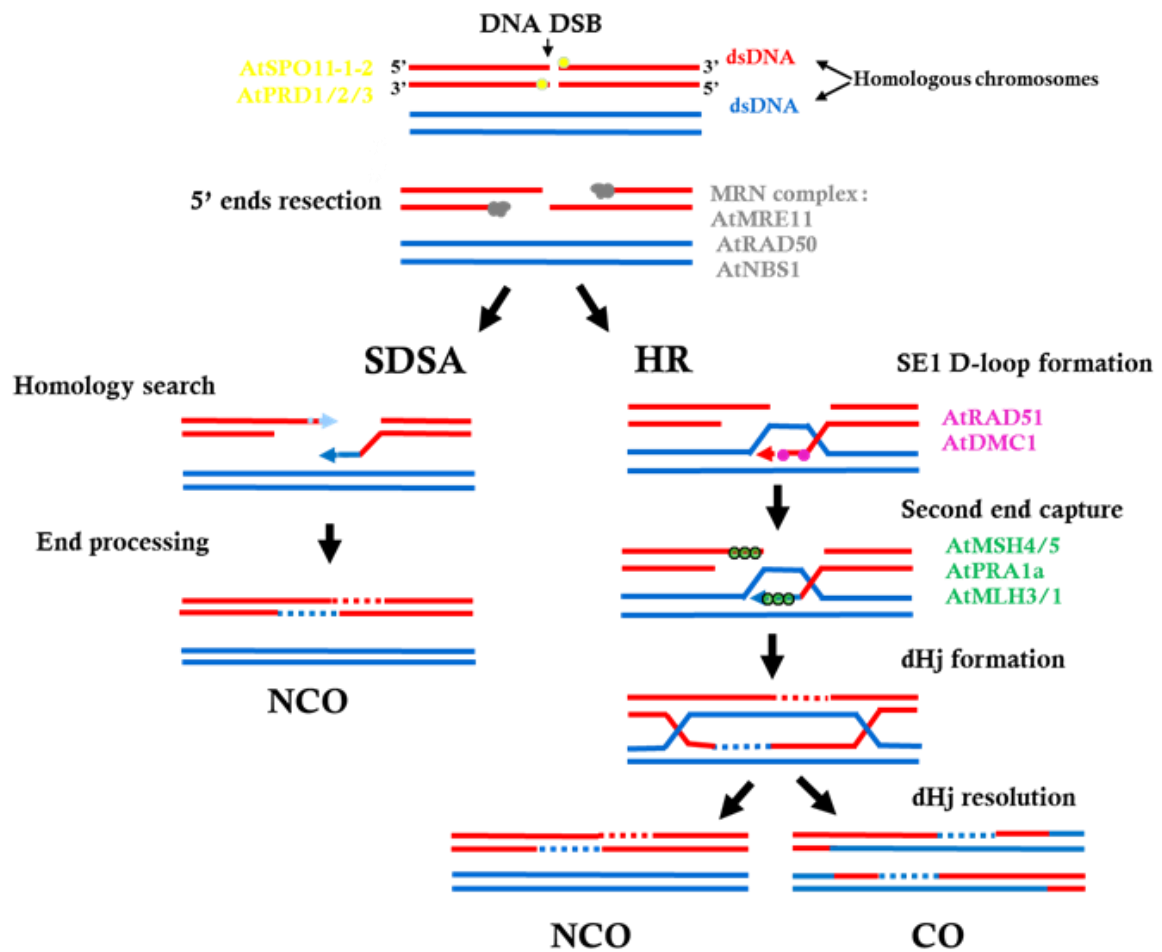


Figure (1.14): Schematic representation of the DNA DSB repair pathway in meiosis
 Meiotic recombination initiates after DSB induced formation by SPO11 protein, after that the MRN complex allow the 5` DNA DSB end resection, forming 3` ssDNA molecules. After that, D-loops form as a result of recombinases mediated 3`ssDNA invasion to its homologue. D-loops could be repaired either by synthesis-dependent strand annealing pathway (SDSA) where non crossovers (NCOs) is their fate, or it continues homologous recombination pathway, where D-loops stabilization allow second end capture proceeding to the stable double holliday junction (dHj) structures. The mature dHjs are resolved as COs, whereas the non-mature dissolve and generate NCOs. Adapted from Osman *et al.*(2011)

1.3.5.4.1. DNA double strand breaks (DSBs) formation

DSBs formation at early leptotene results in recombination initiation (Sun *et al.*, 1989). SPO11, a topoisomerase type VI, allow DSBs since its tyrosine residue which ligates and dissociates with DNA to promote break formation (Keeney *et al.*, 1997). The DNA-SPO11 association lead to the enhancement of the recombination via

recruiting γ H2AX to the DSBs sites. Several studies showed that SPO11 protein is intra-species conserved. *Arabidopsis* possess three paralogues of SPO11; SPO11-1, SPO11-2 and SPO11-3 (Hartung and Puchta, 2000; Grelon *et al.*, 2001; Stacey *et al.*, 2006). Studies on *spo11-1* mutants as well as *spo11-2* mutants showed that both had fertility defects, neither pairing, synapsis or homologous recombination take place in these mutants (Stacey *et al.*, 2006; Sanchez-Moran *et al.*, 2007). From these findings, it was proposed that both AtSPO11-1 and AtSPO11-2 are needed for DSBs formation, and that they work synergistically as a heterodimer (Sanchez-Moran *et al.*, 2007; Stacey *et al.*, 2006). On the other hand, reports indicated that the AtSPO11-3 plays a role in DNA repair during DNA replication (Stacey *et al.*, 2006)

Several other proteins were found to show a similar phenotype to *Atspo11* mutants. Recombination blockage in the *Atprd-1*, *Atprd-2* and *Atprd-3* mutants confirmed the role of AtPRD1, AtPRD2 and AtPRD3 in DSB formation (De Muyt *et al.*, 2009). Moreover, research on yeast showed that DSBs formation requires nine more proteins besides to SPO11. These proteins were; Mre11, Rad50, Xrs2, Mer2, Mei4, Ski8, Rec102, Rec104, and Rec 114 (Grelon *et al.*, 2001; Keeney, 2001). These results as well as the presence of other proteins which mutants mimic *Atspo11* phenotype suggest that, likely, other proteins are involved in DSBs formation in *Arabidopsis*, yet to be confirmed; hence extra work should be done to emphasize this.

1.3.5.4.2. DNA DSBs processing

Once DSBs are formed, the phosphorylated form of H2AX (γ H2AX) at serine 139 is recruited to the DSB site (Shroff *et al.*, 2004). By that time, SPO11 association to the

5`end of the break, allows resection of the 5` end, and so results in 3` ends single stranded DNA (ssDNA) formation. The 5` DNA resection is done by MRX/N complex; MRE11, RAD50, and XRS2/NBS1, in budding and fission yeast (Puizina *et al.*, 2004; Bleuyard *et al.*, 2004; Waterworth *et al.*, 2007). The yeast MRN/X complex role in DSBs 5`end resection was confirmed in several reports (Nairz and Klein, 1997; Usui *et al.*, 1998; Hartsuiker *et al.*, 2009a; Nicolette *et al.*, 2010). *Arabidopsis* homologues of the MRX/N complex were referred to as MRN complex (Bundock and Hooykaas, 2002; Gallego and White, 2005; Uanschou *et al.*, 2007). The fact that *Arabidopsis* MRN complex is not needed for DSBs formation (Puizina *et al.*, 2004) was confirmed by the fragments observed at early prophase I in the *Atmre11* and *Atrad50* mutants in *Arabidopsis*, showing defects in DSB repair rather than formation (Bleuyard *et al.*, 2004; Puizina *et al.*, 2004; Unaschou *et al.*, 2007). Moreover, analysis of *Atmre11/Atspo11-1* double mutant showed a phenotype which lacks fragmentation, thus indicating that AtMRE11 allow DSB processing and do not play a role in its formation (Puizina, 2004).

1.3.5.4.3. Single strand invasion

The product of DSBs processing is 3`ssDNA end at both sides of the DSBs. Once the 3`ssDNA are formed, RecA-related recombinases; RAD51 and DMC1, attachment lead to the nucleoprotein filament formation, which allow strand invasion (Bishop and Zickler, 2004). Research on *Arabidopsis* recombinases showed the presence of six paralogues for RAD51, these are: AtRAD51, AtRAD51B, AtRAD51C, AtRAD51D, AtXRCC2 and AtXRCC3, however, one homologue is present for DMC1; AtDMC1 (Klimyuk and Jones, 1997; Doutriaux *et al.*, 1998; Osakabe *et al.*, 2002; Bleuyard *et al.*, 2005). RAD51 in budding yeast showed a mitotic role, DNA repair

using the sister chromatid as a template (Bishop *et al.*, 1992; Shinohara *et al.*, 1992), whereas in *Arabidopsis* two AtRAD51 paralogues; AtRAD51C and AtXRCC3, showed a role during meiotic homologous recombination (Bleuyard and White, 2004; Li, 2005). However, AtDMC1 is needed for meiotic single strand invasion (Neale and Keeney, 2006). *rad51* mutants in *Arabidopsis* showed synapsis defects, besides of chromosome fragmentation, suggesting that the SPO11 induced DSBs were not repaired (Li *et al.*, 2004), however, although mutants of *dmc1* in *Arabidopsis* showed similarly asynaptic phenotype, leading to univalent at metaphase I, but cells did not show chromosomes fragmentation (Couteau *et al.*, 1999), suggesting that DNA repair at the DSBs using sister chromatid as template (Siaud *et al.*, 2004). These results show the importance of both recombinases, RAD51 and DMC1, for meiotic recombination in *Arabidopsis*. Recent studies on budding yeast showed a role for another protein; RPA, in meiotic recombination. RPA protein allows RAD51 loading at the ssDNA site suggesting that it might deal with secondary structures at the ssDNA (Alani *et al.*, 1992). A study by Osman *et al.* (2009) reported that *Arabidopsis* possess five homologues for RPA, and that one of these proteins, RPA1a, plays a role in meiotic recombination.

1.3.5.4.4. NCOS vs COs

Once a D-loop structure is formed its fate to proceed to homologous recombination pathway depends on the presence of some protein complexes, which stabilize the D-loop structure and allow the second end capture, proceeding to double holiday junction (dHj) structures, which could be resolved to COs or to NCOs. D-loops, the products of single end intermediates (SEI), are not stabilized, then it will be removed and synthesis strand annealing (SDSA) pathway of DNA repair will progress (**Figure**

1.14) ending up with NCOs. The high number of DSBs compared to COs emphasize that most of DSBs are resolved as NCOS. A round 10% of these 140 DSBs per meiocyte develop to COs (Sanchez-Moran *et al.*, 2002), hence the rest (90%) are resolved as NCOs. Some reports indicated that CO to NCO pathway is decided at two steps; the first is at the SEI (Borner *et al.*, 2004), where ZMM could play a role in SEI stabilization, since ZMM mutants in budding yeast show normal DSBs whereas abnormal SEI, and the second is after dHj formation, where AtMRI1/BLAP75 and AtTOP3a (Hartung *et al.*, 2008) could act as a backup for the unsuccessful dHjs, leading to form NCOs. Moreover, Osman *et al.* (2011) reported that the recombination proteins foci at zygotene are three times more than COs. Suggesting that the excess foci have other functions rather than COs formation.

1.3.5.4.5. CO interference and Class I & II COs

COs distribution on chromosomes is nonrandom (Jones and Franklin, 2006), since bivalents which are CO free, are unlikely to be seen in the normal meiosis (CO obligation) (Jones and Franklin, 2006). Hence, the CO interference concept was set, when the CO is formed, it is unlikely to have other COs adjacent to it, however, the chance to have other COs increase at sites away from the original site (Jones and Franklin, 2006). Different interpretations were put to explain the CO interference context. Three models have been proposed the mechanical stress model (Kleckner, 2004), the counting model (Stahl *et al.*, 2004), and recently the chromosome oscillatory movement (COM) model (Hulten, 2011). Studies on yeast showed that CO interference is not seen in all COs (de los Santos *et al.*, 2003). Moreover, a previous study by Copenhaver *et al.* (1998) on *Arabidopsis* suggests that 85% of COs show interference. From these results, COs distribution is thought to be two types; CO

class I and CO class II. And that Class I COs resemble COs sensitive to interference (de los Santos *et al.*, 2003), which is the majority of COs in *Arabidopsis* (Higgins *et al.*, 2004), whereas Class II COs resembles COs which are interference insensitive (de Los Santos *et al.*, 2003). The ZMM proteins; Zip1, Zip2, Zip3, Zip4, Mer3, Msh4 and Msh5, are thought to play a role in class I COs (Borner *et al.*, 2004). A study by Snowden *et al.* (2004) on the ZMM homologues in *Arabidopsis* AtMSH4/5 complex showed that AtMSH4/MSH5 stabilizes SEI and allows it to form mature dHj structure. Moreover, an Immunolocalization analysis for the AtMSH4/MSH5 localization during prophase I showed that it forms 30 foci at leptotene, which is reduced to 8 foci at pachytene (about the CO frequency estimated per cell) and that these foci are DSB dependent (Higgins *et al.*, 2004; Higgins *et al.* 2008a), and their mutants (*msh4*, *msh5*) have complete synapsis (Higgins *et al.*, 2004; Higgins *et al.* 2008a). Besides that, other proteins were proposed to have a role during class I of CO pathway; these are the bacteria MutL homologues; MLH3 and MLH1. Dion *et al.* (2007) reported that MLH3 has a meiotic role, however MLH1 is involved in mitotic DNA repair besides to its meiotic role. A study by Jackson *et al.* (2006) showed that pachytene cells have 9-10 foci for the AtMLH1 and AtMLH3, working as COs markers. Moreover Franklin *et al.* (2006) reported that mutants of *Atmlh1* and *Atmlh3* have normal SC, besides that the AtMSH5 localization show a normal phenotype, hence, proposed that MLH3 and MLH1 is important in the final stages of meiotic recombination. Since the MutL complexes were thought to play a role in dHjs conversion to COs. The class II COs were thought to involve MUS 81, and MMS4/EME1 proteins (de Los Santos *et al.*, 2003; Berchowitz *et al.*, 2007; Higgins *et al.*, 2008b). Although *Atmus81* mutants have normal phenotype, however analysis of the *Atmsh4/Atmus81* double mutant showed that ~1.25 COs were observed in the single *Atmsh4* mutant whereas ~ 0.8 in the double mutant, suggesting that the extra reduction is due to AtMUS81 in Class II

CO pathway (Berchowitz and Copenhaver, 2008; Higgins *et al.*, 2008b). Moreover, Oh *et al.* (2008) reported that MUS81 in budding yeast works as a back-up for unsuccessful Class I CO pathway.

1.3.5.4.6. dHj structure processing

The progress of homologous chromosomes to COs depends on the resolvases which process the dHj structures. It was reported that GEN1 and YEN1 act as dHj resolvases in mammals and budding yeast (Ip *et al.*, 2008). Moreover, GEN1 has a role in CO formation, since it was found that it is able to rescue *mus81* phenotype (Lorenz *et al.*, 2010). The ability of RuvC, a bacterial resolvase, to rescue the *mus81* phenotype suggests that MUS81 has a resolvase role (Ip *et al.*, 2008).

1.3.5.5. Meiotic recombination in the context of chromosome axes

As recombination complexes proceed from early prophase I to pachytene, its association with the axis keeps SC association, leading to CO development, and allowing the NCO factors to dissociates from the SC (Moens *et al.*, 2007; Terasawa *et al.*, 2007). In *Arabidopsis*, after the SPO11 initiates DBSs, H2AX phosphorylation is triggered, acting as a marker for DSBs (Shroff *et al.*, 2004) on the axes (Sanchez-Moran *et al.*, 2007). Mutants of the axis associated components; Red1, Hop1, besides to cohesion Rec8, showed abnormal DBSs localization on the axis, suggesting a role for the chromosome axis proteins in DSBs distribution and positioning (Blat *et al.*, 2002; Glynn *et al.*, 2004). The AEs were not seen in the yeast *red1* mutants (Rockmill and Roeder, 1990), besides to that, recombination defects were linked to the loss of 75% of the normal DSBs (Xu *et al.*, 1997). The *Arabidopsis* chromosome axis protein, ASY1, (a HORMA domain containing protein) has a

confirmed localization on the AEs through both the immunolocalization as well as the immunogold electron microscopy (EM) (Armstrong *et al.*, 2002). Studies on the *asy1* mutants showed that chromosome axis is disrupted. Besides that homologous recombination is severely affected, as AtDMC1 foci on the chromosomes were highly decreased in comparison to wild-type as well as *chiamata* (Ross *et al.*, 1997; Sanchez-Moran *et al.*, 2001), suggesting a role for AtASY1 in enhancing biased inter-homologue recombination (Sanchez-Moran *et al.*, 2007). Similarly, the ASY3 protein in *Arabidopsis* was found to load on the chromosome axis (Ferdous *et al.*, 2012). The same study showed that the *asy3* mutants lack polymerization of ASY1 on the axis, however, *asy1* mutants showed normal ASY3 localization on the chromosome axis, suggesting that in *Arabidopsis* ASY1 is needed for normal ASY3 localization but not vice versa. (Ferdous *et al.*, 2012). Moreover, *asy3* mutants similarly to *asy1* mutants showed defects in the chiasma frequency, as well as confirmed defects in the recombination proteins loading on the axis in the *asy3* mutants comparable to wild-type (Ferdous *et al.*, 2012).

The *Arabidopsis* transverse filament protein AtZYP1 has been reported that it is involved in recombination. Since, the corresponding mutants in *Arabidopsis* with confirmed AtZYP1 depletion showed asynaptic phenotype besides to ~80% decline in CO in comparison to wild-type. Mutants analysis revealed COs presence between non-homologous chromosomes suggesting that AtZYP1 has a role in blocking the non-homologous recombination (Higgins *et al.*, 2005). ZEP1, the rice TF homologue, has a confirmed meiotic role (Wang *et al.*, 2010). Although ZEP1 mutants showed synapsis defects but their COs frequency was increased suggesting that ZEP1 has a role in interference (Wang *et al.*, 2010). Previously, results on budding yeast SC

showed that *zip* mutants were interference free (Sym and Roeder, 1994) suggesting that the SC plays a role in preserving interference. Although other studies showed that interference apply prior to SC polymerisation (Borner *et al.*, 2004). In addition to that the AtZYP1^{RNAi} mutants had shown meiotic interference phenotype (Higgiins *et al.*, 2005). From all of that the SC has showed that it does not mediate interference, else, further work is still needed to clarify the antagonistic SC roles seen in different species.

The recombination initiates as early as chromosome axes starts to polymerize. As the recombination starts it allows pairing of homologous chromosomes and hence synapsis. At 400 nm distance in between homologous chromosomes synapsis starts. Several reports indicated that homologous chromosomes pairing is linked with DSB formation in *Arabidopsis* (Grelon *et al.*, 2001) as well as in budding yeast (Rockmill *et al.*, 1995; Peoples *et al.*, 2002; Henderson and Keeney, 2004) and in *Sordaria* (Tesse *et al.*, 2003). DSBs formation is required for helping the homologous chromosomes alignment in *Sordaria*. Rad51foci mediates bridge formation between aligned homologues. RAD51 play a role in chromosome homology search required for homologues pairing (Rockmill *et al.*, 1995; Franklin *et al.*, 1999; Moens *et al.*, 2002; Tesse *et al.*, 2003; Clavente *et al.*, 2005). Chromosomes search to find its homologue aid in their DSBs association in the chromosomes loops (Tesse *et al.*, 2003). Several proteins play a role in homologues pairing besides to RAD51. Mer3, Msh4 and Mlh1, had shown a role in homologues pairing in *Sordaria* (Storlazz *et al.*, 2010).

The importance of meiotic recombination for homologous synapsis was proposed as synapsis initiates at eventual CO sites (Zickler *et al.*, 1992; Lichten, 2001; Mahadevaiah *et al.*, 2001; Fung *et al.*, 2004; Henderson and Keeney, 2004). A study on *spo11* mutants of budding and fission yeast showed that the SC is not properly formed (Keeney *et al.*, 1997). Later on, a study on yeast had revealed that DSBs rather than SPO11 are needed for synapsis, since defects seen in the *spo11* mutants were repaired after DSBs creation via radiation exposure (Celerin *et al.*, 2000). Moreover, experiments had been applied on *Arabidopsis Atspo11* mutants showed similar results (Grelon *et al.*, 2001; Sanchez-Moran *et al.*, 2007). Recombination progress is still affecting synapsis even though after its initiation, since recombination proteins are still needed to complete synapsis. The *Atmsh4* mutants showed reduced chiasma per meiocyte as well as synapsis delay (Higgins *et al.*, 2004). However, studies on some species showed that DSBs are not a synapsis prerequisite, as was seen in *Drosophilla* females as well as *C. elegans* (Dernburg *et al.*, 1998; Mckim *et al.*, 1998). A study showed that the quantification of Rad51 foci comparable to the eventual COs exist during prophase I revealed an excess in foci (Moens *et al.*, 2002). Suggesting that the extra Rad51 foci are needed to achieve pre-synaptic homologous chromosomes alignment, since the not needed foci dissociate from homologues as NCOs (Moens *et al.*, 2002). These results on mouse within synapsis context, were also observed in plant genomes, and because both are members of higher eukaryotes, which possess large genome, so, the Rad51 is needed not only to mediate sequence homology search between homologous chromosomes, but also to permit full synapsis within larger chromosomes, however, the extra Rad51 foci fate is NCOs (Anderson *et al.*, 2011).

1.3.5.6. COs link to chromatin

The genome sites that are most likely to have COs are known as hotspots (Jeffreys *et al.*, 2001; Myers *et al.*, 2008; McVean and Myers, 2010). It was reported that chromatin status in budding yeast is related to CO distribution, and that COs are mostly exist in the open chromatin regions (Ohta *et al.*, 1994; Wu and Lichten, 1994; Berchowitz *et al.*, 2009). Moreover, the epigenetic code of the histones on chromatin plays a role on DSBs distribution and formation. The H3K4me3 (histone H3 lysine 4 trimethylated) increase was reported around DSBs in budding yeast (Borde *et al.*, 2009), and that DSBs number decrease in the mutants of H3K4methyl transferase (Borde *et al.*, 2009). Besides that, Wanger *et al.* (2010) reported that H2AK5Ac (H2A lysine 5 acetylation) mark DSB distribution in *C.elegans*. In addition to this, chromatin modifying proteins play a role in DSBs formation. HIM-17, a modifier for meiotic H3K9me2 in *C.elegans* is needed for normal DSBs formation (Reddy and Villeneuve, 2004). Besides to all of that, the chromosomal structural proteins; cohesins and condensins, were found to affect DSBs distribution. Mutants of Rec8, the meiotic cohesion in budding yeast, affect DSB by blocking SPO11 (Kugou *et al.*, 2009), whereas the condensing subunit CAP-D2 affects DSB distribution in *C.elegans* by affecting the length of chromatin axis (Tsai *et al.*, 2008; Mets and Meyer, 2009).

The genetic DNA material controls different vital cellular activities: replication, transcription, repair, recombination, and segregation. Thus a dynamic change in the chromosomal compaction level controls the occurrence of the cellular division during meiosis and mitosis (Deal and Henikoff, 2010). The molecular mechanisms of chromatin condensation are highly conserved among eukaryotic species. So,

although there are great differences in the eukaryotic chromosome size and organization, there are similar key proteins and structures involved in the chromatin compaction.

1.4. *Arabidopsis* as a Model Species

Arabidopsis thaliana is a plant that has several traits making it a useful model for genetic, cellular and molecular biology. *Arabidopsis* is a model organism because of different key characteristics: it has only a six weeks-life cycle, it has a small size genome with about 157 million base pairs (Bennett *et al.*, 2003) and five chromosomes. Furthermore, the entire genome is sequenced completely in 2000 by the *Arabidopsis* Genome Initiative (The *Arabidopsis* Genome Initiative, 2000). In addition, the functions of its 27,000 genes and the 35,000 proteins they encode were studied extensively (Integr8–*A. thaliana* Genome Statistics). Moreover, the transformation protocol termed “floral dip” is carried routinely using *Agrobacterium tumefaciens* (Clough and Bent, 1998; Zhang *et al.*, 2006) without the need for tissue culture or regeneration. Recently, Sanchez-Moran *et al.* (2007) developed cytological and ultrastructural techniques based on molecular cytogenetic protocols for studying chromosome dynamics in *Arabidopsis*. For that all, *Arabidopsis thaliana* will be used in this research as a model to shed light on the role of histone proteins on the chromosome dynamics.

1.5. Project Aims

The chromatin histones play an essential role in preserving the meiotic and chromosome axis and organisation needed for meiotic recombination as well as

mitotic cell cycle. This project will focus on the analysis of two histone proteins isoforms in *Arabidopsis* during meiotic and mitotic phases. This is the first-in depth analysis of histones in this system. Although a few articles shed some light on histones role in mitotic chromosome structure in some organisms, but this is the first time to study histones role within cell cycle and meiosis of *Arabidopsis*. Moreover, these analyses are to fill the gap in the literature concerning histones role on chromatin dynamics within plants and higher eukaryotes.

The aims of this project are:

- To run an *in silico* analysis of both the linker histones isoforms as well as the core histone H4 copies in *Arabidopsis*.
- To analyse Histone H1s isoforms role within meiosis and mitosis in *Arabidopsis* by analysing their corresponding knock-out and knock-down mutants.
- To skip gene redundancy effect seen in the single H1 mutants via producing double histone H1 mutants and H4 identical forms in *Arabidopsis*.
- To study the Histone AtH1.1 role within meiotic context by running genetic, molecular, and cytological techniques.
- To investigate H4 role in carrying out the analysis of $h4^{RNAi}$ mutant lines, and H4 chaperon mutants.

CHAPTER 2
MATERIALS AND METHODS

2.1. Plant Material

Seeds of *Arabidopsis thaliana* ecotype Columbia-0 (Col-0) as wild-type control as well as for T-DNA and RNAi mutant lines of histones H1, and H4 as shown in the table (2.1) were obtained from the European *Arabidopsis* Stock Centre (NASC) <http://arabidopsis.info>. See **Table (2.1)** for the list of all mutant lines seeds used.

2.1.1 Growth conditions of plant material

Seeds were sown in soil compost with one seed per pot. Plants were sown in the glasshouse at 18-25° C under 16 to 8 hours of light to darkness cycle, and irrigated two times a day. The growing plants were checked on a weekly basis, in which their phenotypic observations were recorded and compared to that of the control plants.

Protein	Gene Locus	Mutant Type	Line
Histone H1	At5g08780	T-DNA	N659488- Salk_090072
Histone H1	At1g54260	T-DNA	N877696- Sail_883~_F09
Histone HON4	At3g18035	T-DNA	N599887- Salk_099887
Histone H1.3	At2g18050	T-DNA	N665594- Salk_025209
Histone H1	At1g48620	T-DNA	N656137- Salk_007422
Histone H1.2	At2g30620	T-DNA	N321948- GK-116E08
Histone H1.1-1	At1g06760	T-DNA	N521410- Salk_021410
HistoneH1.1-2	At1g06760	T-DNA	N654890- Salk_128430
Histone H1	At1g48610	T-DNA	N586260- Salk_086260
Histone H1	At1g72740	T-DNA	N657654- Salk_065267
Histone H1.1	At1g06760	RNAi	N23980- CS23980
Histone H4 (HF01)	At3g46320	RNAi	N31351- CS31351
FAS1	At1g65470	T-DNA	FAS 1-3 N9930
FAS 2	At5g64630	T-DNA	FAS 2-3 N9929
Drm1 Drm2 Met	Drm1 At1g28330 Drm2 At2g33830 Met1 At5g49160	Triple T- DNA	N16387
HDA6-7		T-DNA	N66154 CRS+S 1-1
FE1-0		T-DNA	N9995

Table (2.1): Data of Seeds analysed for Histones H1, H4 and related mutants: Gene locus and mutants lines studied.

2.1.2. Seeds sterilization for growing on MS media

Seeds were put to sterilize by immersing in 5% sodium hypochloride for 25 minutes, then were washed with 75% ethanol for 10 minutes. After that seeds were washed three times, 5 minutes each with sterile distilled water (SDW). A rotating shaker was used through sterilisation and washing steps to keep homogeneous seeds sterilization and washing. Sterilized seeds were placed on MS media. This day was recorded as day (0). The plates were left in fridge at 4° C for 3 days to vernalize. At day (3) plates were moved to 16° C room temperature and were checked on a weekly basis.

2.1.3. Cisplatin treatment

MS Plates previously prepared with 30 µM cisplatin were used to check DNA repair in Histone H1s selected mutant lines and Histone *h4^{RNAi}* line besides to related mutant lines as well as Columbia-0 (Col-0) as control. At the beginning seeds were sterilized and vernalized as in part 2.1.2. 50 seeds were put to germinate on each single plate. Afterwards vernalized seeds were checked on days 11, 14 and 17, and then number of viable seeds and number of leaves per seed were recorded. Besides that plant growth rate was assessed in time scale manner depending on mutant time delay needed to get a similar leaves count to (Col-0) wild type.

2.2. Molecular Genetics Techniques

2.2.1. DNA extraction from plant

Leaf discs were collected from histone *h1* and *h4* mutant plants as well as wild type plants by closing sterile 1.5 ml microtubes over leaves, the resulting circular sections of the leaves were kept on ice. Then, 40 µl of freshly made extraction buffer (1 M Tris HCl pH 7.5, 1 M NaCl, 0.5 M EDTA, 10% SDS) was added to the tubes. Samples were macerated using autoclaved plastic grinders. After that, another 400 µl of extraction buffer was added, vortexed for 5 seconds and then were centrifuged at 13,000 rpm for 5 minutes, forming a pellet of cellular debris and leaving the DNA in the supernatant. A total of 400 µl of the supernatant was transferred to a new sterile microtube, and 400 µl of cold isopropanol was added to precipitate the DNA. Tubes were shaken gently and left at room temperature for 2 minutes and then centrifuged at 13,000 rpm for 10 minutes to pellet the precipitated DNA. Supernatant was discarded, and 400 µl of 70% ethanol was added to the DNA pellet to wash and remove the salt. Samples were centrifuged at 13,000 rpm for 5 minutes and supernatant was discarded. The tubes were left open and inverted on a tissue paper to dry for about one hour, and then 50 µl of sterile deionized water (SDW) was added to each sample to dissolve the DNA. Samples were heated at 65° C for 10 minutes and centrifuged at 13,000 rpm for 5 seconds. Prepared samples were then stored at -20° C, in order to be used later for further analysis.

2.2.2. RNA extraction from plant tissues

This experiment was carried in RNase free environment in which all the needed stuff (tubes, pipette tips, SDW and pestles were exposed to diethyl pyrocarbonate (DEPEC) treatment to get away of any RNases effect in them. DEPEC prepared solution in SDW (0.1:100) was used to immerse the desired equipments for at least

two hours and then autoclaved to inactivate DEPEC, afterwards were left to dry before use. Total RNA was extracted from chosen histones mutants lines plants as well as the wild type Columbia-0 using RNase Miniprep kit (Qiagen) (<http://www.qiagen.com>) and following manufacturer`s instructions. Plant material of weight less than 100 mg immediately were placed in RNase-free, 2 ml microcentrifuge tube and immersed in liquid nitrogen, grind thoroughly with a pestle until powder was formed. Liquid nitrogen was allowed to evaporate without allowing tissue to thaw. The “RLT buffer” (Qiagen) was added to the sample, then vortexed to remove broken and open cells. The sample was then transferred to “QIAshredder spin column” (Qiagen) to separate cellular debris. Then passed through an “RNeasy mini column” (Qiagen), which has silica membrane with RNA binding affinity, which was then washed with “RW1 buffer” (Qiagen) containing ethanol and finally eluted by RNase free (DEPEC treated) water. Prepared RNA samples were stored at -80° C.

2.2.3. cDNA synthesis

cDNA was synthesised from RNA using cDNA synthesis (Eugenio protocol) following the manufacturer`s guideline. 2 µl of RNA sample was placed in RNase free eppindroff, to which 1 µl of Oligo (dt) primer and 1µl of dNTP mix (10 mM of each; dATP, dTTP, dCTP, dGTP) was added. RNase free water was added up to 12 µl. The samples were heated at 65° C for 5 minutes and immediately placed on ice.

2.2.4. DNA agarose gel electrophoresis

Agarose gels were prepared for the identification of DNA material in each of the mutants and wild type samples. 1%, 1.2%, and 0.8% agarose gels were used for DNA, CDNA and plasmid samples respectively. Agarose (Sigma) was dissolved in 0.5X TBE via heating in a microwave. Gels were cooled, and Red Safe was added to them allowing DNA detection later, and then put to set for 20 minutes. Ready gels were immersed with loading buffer (0.5XTBE) and DNA samples were loaded to the gel wells besides to 1 Kb Ladder which permits molecular weight determination of DNA bands. DNA PCR products were ready to be added immediately to gels, however cDNA and plasmid were mixed with 5X DNA loading buffer. Gels were run in Biorad electrophoresis set kits at 90 V for 45 minutes. Gel images were read by Gel-Doc XR imager using QuantityOne software.

2.2.5. Primer design

Primers were designed referring to the genomic DNA sequences and the TDNA insertion site of each specific mutant line. 18 - 21 nucleotide sequences were identified and selected to be used to match sites flanking TDNA sites. All primers in this study were supplied by Eurofins Genomics (**Table 2.2**) and (**Table 2.3**)

Line	Locus	Primers	Primer sequence
N659488 Salk_090072	At5g08780	Salk_090072_LP	CTTCGAGTTCACATCCTGGAG
		Salk_090072_RP	CGGGTGAGAAGAAGACTGTTG
N877696 Sail_883_F09	At1g54260	Sail_883_F09_LP	GGTATGATGCGATGGTTTTTG
		Sail_883_F09_RP	TGCCAACTCATTTCCTTC
N599887 Salk_099887	At3g18035 HON4	Salk_099887_LP	TTTGGACTGCAATTTGATTC
		Salk_099887_RP	TGTGTTAATCCGGCTTAATGG
N665594 Salk_025209	At2g18050 H1.3	Salk_025209_LP	CAAAGCCTCTCGGTAAATGTG
		Salk_025209_RP	TATTCTTCTTGTCTGCTGCC
N656137 Salk_007422	At1g48620	Salk_007422 LP	AGATGGGAAGCATGAACAATG
		Salk_007422 RP	ATTGTCTCTTTCGAGCGTGTG
N321948	At2g30620 H1.2	GK_116E08	GACCTCTTCATAGGTAGGGTGAGA
		GK_116E08_Rv	TCTTTGGTCGGATTCAACAAC
N521410 Salk_021410	At1g06760 H1.1-1	Salk_021410_LP	TCGGATGACCTTGACATGTG
		Salk_021410_RP	AATCCAAAATCAGAATCCGG
N654890 Salk_128430	At1g06760 H1.1-2	Salk_128430_LP	TTGAAATCCCACGTTTATTGG
		Salk_128430_RP	GGGAGTTTAAACGAGGCTTTG
N586260 Salk_086260	At1g48610	Salk_08260_LP	CCAGATTTGAGACCACCAGAG
		Salk_08260_RP	CGGCGTCTCAGCTACTGATAC
N657654 Salk_065267	At1g72740	Salk_065267_LP	ACCGATCCTTTACGAATCAGC
		Salk_065267_RP	TGGTCCATATCTGTCTGAGCC

Table (2.2): Specific primer sequences for histone mutant lines genotyping

Line	Locus	Primer	sequence
Salk-LBbi-3 T-DNA-BP	T-DNA	Salk-LBbi-3	ATTTTGCCGATTTTCGGAA
Sail-LB1 T-DNA-BP	T-DNA	Sail-LB1	GCCTTTTCAGAAATGGATAAATAGCCTTG CTTC
Gk08409	T-DNA	GK08409	ATATTGACCATCATACTCATTGC

Table (2.3): Primer sequences used to amplify T-DNA insertions, (LB: left border of T-DNA insertion).

2.2.6. DNA amplification by Polymerase Chain Reaction (PCR)

Amplification of genomic DNA, cDNA, and plasmid DNA was carried out through PCR. Taq DNA polymerase ReddyMix (Invitrogen) following the manufacturer's instructions was used with the designed primers for identification of plants genotype. Accurate amplification of definite nucleotide sequence was done by using proof reading Pfu DNA polymerase (Promega) following the manufacturer's guidelines. Primers were prepared in 0.2 μ M final concentration. PCR samples prepared by mixing 10 μ l of TaqDNA polymerase ReddyMix with 7 μ l SDW to which added 1 μ l of each primer in the primer combination; LP and RP or RP and BP, and 1 μ l of desired DNA sample. Samples were spun in a mini centrifuge for few seconds. Then were transferred to a PCR machine The PCR thermo cycler program started with an initial DNA denaturation at 94° C for 1 minute, followed with up to 35 cycles of DNA Denaturation, annealing and elongation respectively. And ended up with a final elongation for 10 minutes as is shown in **Table (2.4)**. Although DNA amplification via Pfu DNA polymerase was done following the same PCR program but PCR solution mix needed a hot start step at 94° C before the addition of the Pfu DNA polymerase.

PCR cycles	Temperature (°C)	Time (minutes)	Number of cycles
Initial Denaturation	94	2	1
Denaturation	94	1	35
Annealing	5° C below T _m of primers	1	
Elongation	72	1 minute per Kb	
Final Elongation	72	10	1

Table (2.4): Standard PCR reaction (T_m=melting temperature)

2.2.7. DNA band extraction from gel

DNA bands within agarose gel were identified using UV light illuminator. The desired DNA bands were cut with a clean sharp scalpel. DNA bands were extracted from the gel following QIAquick Gel Extraction Kit (QIAGEN) manufacturer's protocol. The cut DNA gel bands were dissolved in QG buffer by heating at 50° C for 10 minutes with vortexing intermittently. Isopropanol was added to the sample and then the sample was loaded to the QIAquick column and centrifuged at 13,000 rpm for 1 minute, a step which allows DNA binding to the QIAquick column. Then QIAquick column was washed with buffer PE and centrifuged at 13,000 rpm for 1 minute. DNA was eluted by applying buffer EB, centrifuged at 13,000 rpm for 1 minute then heated to 65° C for 10 minutes to remove any nucleases, spun and stored at -20° C.

2.2.8. DNA sequencing

DNA samples extracted from agarose gels for each of (*Ath1.1-1*, *Ath1.1-2*, and *Ath1.1-2 x Ath1.1-1*) were prepared for sequencing. 10 µl DNA sequencing reaction was prepared as shown in the **Table (2.5)**. Samples were sequenced by the Functional Genomics Laboratory in the University of Birmingham.

DNA Sequencing Reaction	Concentration
DNA template	2 µl
Primer LP or RP	3.2 µl (1pmol/µl)
Sigma water (nuclease free)	4.8 µl
Total Volume	10 µl

Table (2.5): DNA sequencing reaction.

2.2.9. DNA sequence analysis

The obtained DNA sequencing results were analysed with Chromas software. DNA sequences were checked for homology via TAIR search for the wild type bands, and TDNA express search for the mutant bands, and National Centre for Biotechnology Information (NCBI) (www.ncbi.nlm.nih.gov) used to search both genomic DNA and TDNA sequences.

2.2.10. Cloning

DNA was cloned into pDrive vector (Qiagen) (**Figure 2.1**) prior to sequencing. The Cloning mixture was prepared as in **Table (2.6)**, and then was left overnight at 15° C.

5µl of this cloning mixture was transformed into DH5α competent cells as in **Table (2.7)**. Afterwards, **100 µl** of the transformation mixture prepared in **Table (2.7)** was spread on LBA agar plates treated with (40 µg/ml) 5-bromo-4-chloro-3-indolyl-beta-D-galactopyranoside (Xgal), (100µg/ml) ampicillin and (0.1 mM) isopropyl beta-D-thiogalactopyranoside (IPTG). Plates were incubated overnight at 37° C. Next day the plates were checked for any growth. The DH5α cells with ampicillin resistance are the ones with successful pDRIVE transformation, hence the pDRIVE contains ampicillin resistance gene. The presence of white colonies on the plates is an indicative of successful transformation, since the DNA insertion in the lac Z gene (in the pDRIVE) will inactivate it, and so the Xgal substrate in the plates will not be changed. However, if the DNA insertion failed in the pDRIVE lac Z gene, so β-galactosidase will be expressed, which metabolise Xgal (with IPTG presence) producing a blue coloured product. The plasmid DNA isolation from the successfully transformed DH5α cells (white colonies) was carried out using the QIAprep Spin Miniprep Kit (Qiagen; <http://www.qiagen.com>). DNA sequencing and analysis was applied as in 2.2.8 and 2.2.9.

Cloning mixture	Volume (µl)
cDNA template	4
pDRIVE (Qiagen)	1
2X ligation buffer	5
Total volume	10

Table (2.6): Cloning mixture preparation.

DNA transformation to DH5α competent cells	Volume	Duration	Treatment
Cloning mixture (Table 2.6)	5 µl		
DH5α competent cells	1 ml	30 min(s)	ice
Heat shock		30 sec(s)	42° C
Allow heat shock proteins reactivation		2 min(s)	ice
Add LBB to allow cell recovery	250 µl	1 hour	Agitate at 37° C
100 µl The prepared mixture was spread onto agar plates treated with selective antibiotics. Ampicillin resistant colonies will grow on the plates.			

Table (2.7): DNA transformation to DH5α competent cells

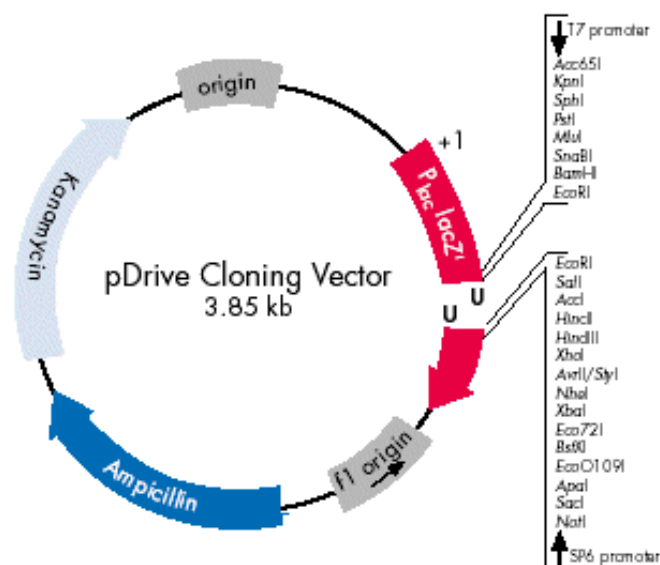


Figure (2.1): pDRIVE Cloning Vector.

3.5 Kb pDRIVE Vector contains multiple selection gene sites. Two dual antibiotic resistant genes for kanamycin and ampicillin antibiotics as selective markers. Besides to that, lacZ gene show blue/white colony selection. So, if the desired DNA was successfully ligated to the vector, inactive lacZ gene results in the appearance of white colonies. However, the blue colonies arise when the lacZ is

expressed, as the β -galactosidase converts the Xgal (under the induction of IPTG) into blue-coloured product.

2.2.11. Preparation of competent *E. coli* cells

Competent *E. coli* DH5 α from glycerol stocks was streaked on a Lysogeny Broth (LB) agar plates, then incubated overnight at 37° C. Single colonies were inoculated separately in 5 ml of LB media, and left to grow overnight at 37. 2 litre flask was inoculated with 100 ml of LB media, to which then 200 μ l of the formed culture solution was added and put to grow at 37° C with shaking at 250 rpm until optical density (OD₅₅₀) recorded was between 0.3-0.4. DH5 α cells was placed immediately on ice for 10 minutes and transferred to pre-cooled 50 ml centrifuge buckets. Cells were centrifuged for 5 minutes at 3000 rpm in 4° C Beckman Centrifuge. Supernatant was discarded however pellet with cells were re-suspended gently by swirling in 20 ml of ice-cold TFB1 and incubated on ice for 2 hours, then centrifuged for 5 minutes at 2000 rpm in 4° C Beckman centrifuge. After which supernatant removed, cells were re-suspended by swirling in 4 ml of ice-cold TFB2. 50 μ l aliquot of prepared *E. coli* DH5 α cells were transferred into 1.5 ml sterile microtubes gently. Tubes then were frozen rapidly in liquid nitrogen and stored at -80° C.

2.2.12. Restriction Enzyme digestions

The following table (**Table 2.8**) shows the restriction enzymes used in the experiments with their typical working conditions

Enzyme	Company	Requirements		Digestion temperature	Inactivation treatment	
		Buffer	BSA		Heating	Time
<i>XhoI</i>	Biolabs	4	BSA	37° C	65° C	15 minutes
<i>KpnI-HF</i>	Biolabs	4	No BSA	37° C	65° C	15 minutes

Table (2.8): Restriction enzymes: Requirements and conditions.

2.3. Cytology

2.3.1. Meiotic Cytology Preparations

Arabidopsis buds fixation and chromosome preparation was done referring to Armstrong *et al.* (2009). Immature *Arabidopsis* flower buds for both histones mutant lines and the control (Col-0) were removed from the plant and fixed in 3:1 fixative (3 ethanol: 1 glacial acetic acid). The inflorescences were fixed at room temperature. The fixative was replaced after 24 hours with freshly made fixative. Flower buds were washed in 0.01 M citrate buffer (pH 4.5) three times, five minutes each. Then the buds were separated from the inflorescences and digested (to break the cell wall) in 1% enzyme mix of 0.3% (w/v) pectolyase, 0.3% (w/v) cytohelicase, and 0.3% (w/v) cellulose dissolved in citrate buffer for 90 minutes at 37° C (Incubation in a moist chamber). Then, the enzymatic digestion was stopped by adding ice-cold water. Buds were transferred individually to clean slides with a small amount of buffer (using a glass Pasteur pipette) and then macerated with a needle. The cells were kept wet by adding buffer if needed. 10 µl of (60%) acetic acid was added to the slide, and it

was heated on a 45° C hotplate for 30/60 seconds. The slide was removed from the hotplate and an extra 10 µl of 60% acetic acid was added. Afterwards, 100 µl of freshly made cold fixative 3:1 was added to the slide, around and on top of the material area. The slide was washed with again with 100 µl of 3:1 fixative and dried with a hair drier. The cells were stained with 4',6'-Diamidino-2-phenylindole (DAPI) in Vectashield at 1µg/1µl; 7 µl of DAPI Vectashield solution was added on the top of the slide and covered with a coverslip. Prepared slides were kept in darkness, and checked using fluorescence microscope (Nikon90i) with a DAPI filter and NIS-Elements AR software.

2.3.2. Fluorescence *in situ* Hybridization (FISH) 45S/5S probes preparation

The meiotic chromosomal rDNA segments were labelled using labelled 45S/5S rDNA probes during FISH. Plasmids used in the production of the rDNA probes are described in **Table (2.9)**. rDNA labelling mixtures were prepared for each of the 45S and the 5S rDNAs as is shown in **Table (2.10)**. Prepared mixtures were then passed through the labelling procedure shown in **Table (2.11)**. Through this research the 45 S is labelled with DIG (appear as green signal under the epifluorescent microscope) and the 5S with BIO (appear as red signal under the epifluorescent microscope).

Probe	Plasmid (Ref)	Plasmid source/description
5S rDNA	pCT4.2 (Campell <i>et al.</i> , 1992)	500 bp of <i>A.thaliana</i> cloned in PBlu
45S rDNA	pTa71 (Gerlach and Bedbrook, 1979)	9 Kb of <i>EcoR1</i> fragment of <i>Triticum aestivum</i> compose of the rDNA genes; 18S-5.8S-25S and spacer regions)

Table (2.9): Plasmid description for the 45S/5S rDNA probes production

Material	Quantity (µl)
Plasmid Table (2.7)	3
Biotin (BIO) or Digoxigenin (DIG) Nick translation mix (Roche) (Biotin illuminate as red colour, and Digoxigenin as green)	4
SDW	13
Final volume	20

Table (2.10): rDNA probe labelling mixture.

rDNA labelling reaction	Temperature	Duration (min)
Incubation	15° C	90
To stop the reaction add 1µl of 0.5M EDTA (pH8.0), then heating	65° C (water bath)	10

Table (2.11): rDNA probe labelling procedure

2.3.3. Fluorescence *in situ* hybridization (FISH)

FISH was carried out according to protocols previously published (Fransz *et al.* 1998; Sanchez-Moran *et al.*, 2001; Armstrong and Jones 2003).

Meiotic metaphase I slides were washed in 100% ethanol for about five minutes, then washed in 4T (4XSSC-0.05 % Tween 20[®]) for one hour to remove antifading. Another washing with 2XSSC (0.3 M NaCl, 0.03 M Sodium Citrate, pH 7.0) at room temperature for ten minutes. After that digested with Pepsin (Sigma) (0.01 % in 0.01 % M HCl) at 37° C for 1.5 minutes. Then slides were washed in 2XSSC at room temperature for ten minutes, fixed in paraformaldehyde 4% pH 8 for ten minutes, washed in sterile deionized water for some seconds. Dehydrated through ethanol series, 70, 90, 100 %, respectively, for two minutes each, then slides were drained. 20 µl of 45S and 5S probes were added on each of the slides and sealed with a coverslip (22x22mm). Coverslip edges were glued and then slides were heated on a hotplate at 70° C for 4 minutes. The slides were incubated in a moist chamber at 37° C overnight allowing probes to hybridize. Then slides were washed three times, five minutes each in 50 % formamide-2XSSC at 45° C. After that washed once in 2XSSC at 45° C for five minutes, washed once in 4T (4XSSC-0.05 % Tween 20[®]) at 45° C for five minutes. Finally washed once in 4T at room temperature for five minutes. 20 µl per slide of decided antibodies was added to each slide; anti-DIG-FITC, Streptavidin-rhodamine- antibiotine texas red (5ng/µl). Slides were covered with parafilm and incubated in a moist chamber at 37° C for 30 minutes. Slides were washed in 4T, three times, five minutes each. One wash with SDW followed that. Slides were dehydrated by passing them in 70%, 85%, and 100% ethanol respectively, each for two minutes. FISH prepared slides were viewed with fluorescence microscope (Nikon E90i) having filters for DAPI, FITC and TRITC and equipped with an image capture and analysis system.

2.3.4. Immunolocalization

2.3.4.1 Squash Immunolocalization Method in *Arabidopsis*

Inflorescences of proper size at different meiotic stages were removed from both wild type and mutant plants and fixed in 4% paraformaldehyde (ice cold) pH7.3 for 10 - 20 minutes, then washed three times with PBS (0.1% Triton X-100) in total for ten minutes, followed by one wash with citrate buffer for few seconds, then were put for enzyme digestion using 1% cytohelicase at 37° C for 90 – 120 minutes , then washed three times with PBS (0.1% Triton X-100) in total for 10 minutes, five buds per slide were dissected to release anthers and after that slides with dissected anthers were put to digest with 1% cytohelicase at 37° C for ten minutes, 10 µl 1% lypsol was added on the slide with anthers, cover slip was put and squashed onto the slide and immersed in liquid nitrogen, then cover slips were removed from the slide with a razor blade very quickly and put to dry on the bench, slides were washed three times in PBS (0.1% Triton X-100) for ten minutes, next 50 µl for each slide of primary antibody prepared in the 1% BSA PBS Blocking solution was added, slides with primary antibody were incubated at 4° C (in the fridge) up to two days. Then slides were washed three times with PBS (0.1% Triton X-100) in total for ten minutes (on the shaker), next 50 µl for each slide of secondary antibody prepared in the 1% BSA PBS Blocking solution was added, slides with secondary antibody were incubated at room temperature for forty five minutes in a dark place, washed three times with PBS (0.1% Triton X-100) in total for ten minutes (on the shaker), and finally prepared slides were counterstained with DAPI, 7 µl of DAPI dissolved in Vectashield solution was added on the top of the slide and covered with a coverslip. Prepared slides

were kept in the fridge and checked using an epifluorescence microscope (Nikon90i) with a DAPI, FITC and TRITC filters and NIS-Elements AR software.

2.3.4.2 Spreading immunolocalization method in *Arabidopsis*

Buds of proper size for the meiotic stages to study were selected and dissected. The cut buds were put on a wet petri dish. 5 buds were left on each pre-washed slide (acetone, SDW, 70% ethanol respectively, 10 minutes each wash). Anthers were extracted from the buds in a drop 10 µl of Citrate Buffer. Exposed anthers were digested with 10 µl 1% cytohelicase mix in a moist chamber at 37° C hot plate for 10 min. Anthers were macerated with brass rod, then 10 µl of cytohelicase mix was added. Slides were put at 33C° hot plate for 4/5 minutes. Digested anthers were exposed to 10 µl of 1% lipsol. Meicytes area was marked with diamond pen then slides were put on a hot plate at 37° C for 4-6 minutes to allow meicytes spreading on the slides. Meicytes were fixed on the slides with 10 µl ice-cold 4% paraformaldehyde PH 8 and after that were left to dry for 2 hours. Slides were washed three times with PBS (0.1 % Triton X-100) five minutes each. Slides were immersed in 1 % BSA PBS solution at room temperature for 10-20 minutes as a blocking step. 50 µl (1/500) primary antibody blocking solution mix was put on a parafilm piece. Slides were sealed with parafilm and incubated at 4° C overnight in a moist chamber. Next day parafilm was peeled off and slides were washed three times with PBS (0.1 % Triton-X100), five minutes each. 50 µl of secondary antibody-Blocking solution mix was dropped on parafilm. Slides were incubated in dark at room temperature for 45 minutes. Slides were washed three times in PBS (0.1 %

Triton X-100). Slides were counterstained with DAPI. Slides were stored at 4C in fridge and later were checked with epifluorescence microscope (Nikon90i) with a FITC, DAPI and TRITC filters and NIS-Elements AR software.

2.3.5. Pollen viability Assessment by using Alexander Stain (Alexander, 1969)

Mature inflorescences were selected and removed from wild type and mutant plants. About six anthers from each inflorescence were put on each slide to which two drops of water were added before releasing anthers and then stained using 10µl of Alexander stain. Alexander stain is composed of 10ml Ethanol (95%), 1 ml Malachite Green (1% in 95% ethanol), 5ml Fuchsin Acid (1% in water), 0.5ml Orange G (1% in water), 5g Phenol, 5g Chloral Hydrate, 2 ml Glacial acetic acid, 25 ml Glycerol, 50 ml distilled water. Coverslips were used to release pollen grains from anthers via squash method. Then slides were stored at room temperature for at least 12 hours to permit enough time for the stain to penetrate into pollen grains and studied under light microscope.

2.3.6 Fluorescence microscopy and image analysis

Epifluorescent microscope was used in fluorescent cytological preparations study analysis, and Nikon digital camera for image capture. ELS Software Imaging System was applied in captured images analysis.

2.4. Genetic Crossing Of Plants

Knock-Out mutant lines with homozygous T-DNA insertions were crossed as shown in the table below. Crosses were done in reciprocal manner in which each line act as donor once and as recipient another time. In recipient plants, 3-4 inflorescences with proper size, nor small or mature, were selected and the ones that did not match were removed. Buds of the right size were emasculated using forceps under a light microscope, and all unwanted tissues and immature anthers surrounding the stigmata were taken out under sterile conditions. Donor plants containing mature flowers were used to pollinate the exposed stigmata under a binocular. Pollinated plants were labelled and allowed to grow under wet conditions for 2 days. 20 days later pollinated stigmata developed to mature siliques. Seeds were harvested and stored at 4° C in the cold room and were ready for sowing.

2.5. Data Statistical Analysis

Statistical calculations; means, standard deviations and standard error of the wild type and mutant plants were calculated and analysed using Microsoft Office Excel 2010. T-test was used to calculate the P-value, which indicates the significance of the difference of the means between the mutants and the wild type. T-test was used to compare the difference between the means of the silique size and the seed number of the mutant lines and the wild type plants using EXCEL software.

2.6. List of Websites

Source	Website
ChromDB	http://www.chromdb.org/org_specific.html?o=ARATH
Genevestigator for Protein expression: Microarray	https://www.genevestigator.com/gv/
Gene description	http://www.arabidopsis.org/cgi-bin/bulk/genes/gene_descriptions
RNAse Miniprep kit (Qiagen)	http://www.qiagen.com
NASC:	http://arabidopsis.info/
NCBI	http://www.ncbi.nlm.nih.gov/guide/
NCBI, BLAST	http://blast.ncbi.nlm.nih.gov/Blast.cgi
Sequence alignment:	http://www.ebi.ac.uk/Tools/msa/clustalw2/
T-DNA express	http://signal.salk.edu/cgi-bin/tdnaexpress
Tm calculator:	http://www6.appliedbiosystems.com/support/techtools/calc/

Table (2.12): Data sources web links.

Chapter 3
Knocking Down Histone H4 in *Arabidopsis*

3.1. Introduction

Histone H4 is one of the four core histone proteins (H2A, H2B, H3 and H4) that build up the eukaryotic nucleosome (Wolffe, 1998). DNA-Histone association permits the chromatin organization into the nucleosome fibre, which appearance is known as “beads on a string”. Chromatin dynamics permits its shifting between different chromatin compaction structures; 10 nm fibre, 30 nm fibre and 300 nm fibre. Thus DNA could carry on its vital processes in a flexible way; DNA replication, repair and transcription, as well as mitotic and meiotic divisions.

Histone H4 can be subjected to different modifications; biotinylation, acetylation and methylation. These different modifications have shown different histone H4 roles. Previous reports showed that biotinylation of H4 at residues K8 and K12 might enable cellular responses to DNA double strand breaks and proper chromosomal condensation during mitosis in human cells (Kkothapalli *et al.*, 2005; Kothapalli and Zemleni, 2005; Zemleni, 2005). Furthermore, acetylation of lysine 16 on H4 seems to allow gene transcription machinery to be activated either by changing the higher order chromatin structure organisation or altering interaction of nuclear proteins-chromatin association (Shogren-Knaak and Peterson, 2006). Moreover, Fraga *et al.* (2005) reported that the loss of H4 K16 acetylation is mostly seen in some cancers. In addition, a study by Corsini and Sattler (2007) showed that Histone H4 dimethylated lysine 20 (H4K20) plays a role in DNA damage repair by recruiting the DNA damage repair factor 53BP1 to DNA double-strand break sites. Furthermore, H4K20 seems to be able to control transcription (Corsini and Sattler, 2007).

Histone H4 protein sequence is highly conserved during eukaryotic evolution, to the point that in *Arabidopsis* there are eight loci encoding for histone H4 with nearly identical nucleotide sequences but with some differences, although these genes encode for a H4 protein that is identical for all. Furthermore, the Blast alignment of histone H4 protein sequences in human (HS) and *Arabidopsis* (AT) showed that their match reaches 98% identity only differing in two amino acids but keeping 100 % similar characteristics (**Figure 3.1**). Thus, in order to carry out a genetic analysis of H4 we analysed a histone H4 RNAi knock down mutant to investigate the role of H4 in *Arabidopsis*.

Score	Expect	Identities	Positives	Gaps
198 bits(504)	2e-71()	101/103(98%)	103/103(100%)	0/103(0%)

```

Hs (H4) 1  MSGRGKGGKGLGKGGAKRHRKVLRDNIQGITKPAIRRLARRGGVKRISGLIYEETRGVLK  60
          MSGRGKGGKGLGKGGAKRHRKVLRDNIQGITKPAIRRLARRGGVKRISGLIYEETRGVLK
AT (H4) 1  MSGRGKGGKGLGKGGAKRHRKVLRDNIQGITKPAIRRLARRGGVKRISGLIYEETRGVLK  60

Hs (H4) 61  V FLENVIRDAV TYTEHA K RKTVTAMDVVYALKRQGRTLYGFGG  103
          + FLENVIRDAV TYTEHA + RKTVTAMDVVYALKRQGRTLYGFGG
AT (H4) 61  I FLENVIRDAV TYTEHA R RKTVTAMDVVYALKRQGRTLYGFGG  103
  
```

Figure (3.1): BlastP alignment (NCBI) of Histone H4 protein sequence in human (Hs) and *Arabidopsis* (AT).

Although H4 protein sequence Blast in Hs and AT showed that they differ in two amino acids (98% identity), but still their H4 amino acids share 100% similar characteristics (100% positives). Amino acids shaded with greenish background are non-identical. The positive sign (+) resembles different amino acids but still sharing the positive charge.

3.2. *In silico* analysis

3.2.1. *Arabidopsis* histone H4 isoforms have identical sequence.

The *in silico* analysis of *Arabidopsis* genome showed the presence of eight genes coding for histone H4: At1g07660, At1g07820, At2g28740, At3g45930, At3g46320, At3g53730, At5g59690, and At5g59970 (**Figure 3.2**). The protein sequence analysis showed that all of H4 isoforms were identical (**Table 3.1**), (**Figures 3.3 & 3.4 A&B**). The identical amino acid sequence and the constitutive expression of all the H4 isoforms in *Arabidopsis* suggest a redundancy of these genes. Thus, a T-DNA insertion *h4* mutation for one of these isoforms will not show a visible phenotype in *Arabidopsis* as other isoforms would be perfectly functional (redundant). The possibility to obtain a plant with the eight H4 isoforms mutated is very low. The expression of histone H4 proteins using Genevestigator has showed that histone H4 is expressed constitutively during all of the *Arabidopsis* developmental stages; from seeds to siliques, as is shown by **Figure (3.5)**.

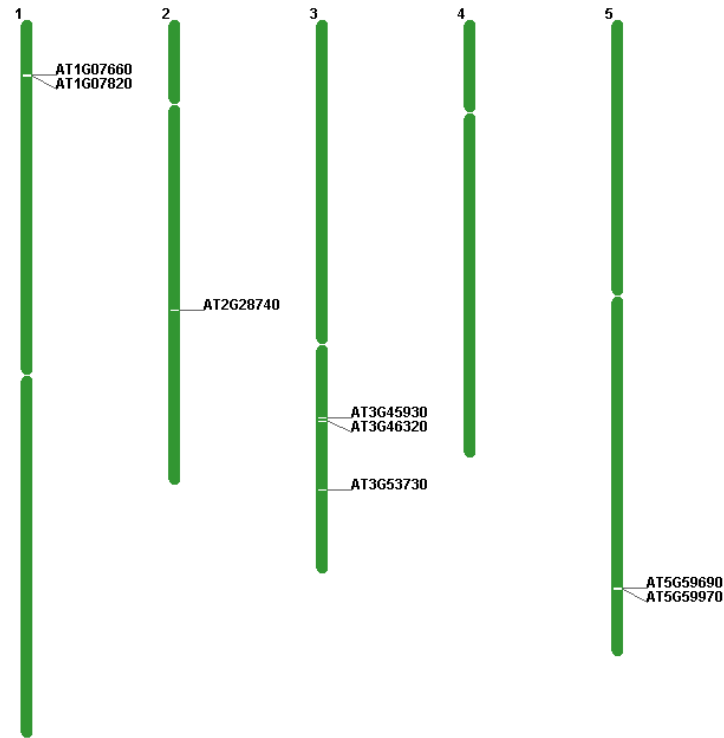


Figure (3.2): Arabidopsis Histone H4 genes map.

Arabidopsis thaliana has eight genes encode for the Histone H4 protein, localized on four chromosomes out of the five *Arabidopsis* chromosomes, two genes on chromosome one (At1g07660, At1g07820), one gene on chromosome two (At2g28740), three genes on chromosome three (At3g45930, At3g46320, At3g53730) and two genes on chromosome five (At5g59690, At5g59970).

<http://www.arabidopsis.org/servlets/ViewChromosomes>

ocus Identifier	Representative Gene Model Name	Gene Conserved Domains	Gene Model Type	Other names
AT5G59690	AT5G59690.1	DOMAIN/s: Histone H4 conserved site (InterPro:IPR019809), Histone-fold (InterPro:IPR009072), Histone core (InterPro:IPR007125), Histone H4 (InterPro:IPR001951)	protein_coding	
AT1G07820	AT1G07820.1	DOMAIN/s: Histone H4 conserved site (InterPro:IPR019809), Histone-fold (InterPro:IPR009072), Histone core (InterPro:IPR007125), Histone H4 (InterPro:IPR001951)	protein_coding	F24B9.8
AT3G45930	AT3G45930.1	DOMAIN/s: Histone H4 conserved site (InterPro:IPR019809), Histone-fold (InterPro:IPR009072), Histone core (InterPro:IPR007125), Histone H4 (InterPro:IPR001951)	protein_coding	F16L2.140
AT3G53730	AT3G53730.1	DOMAIN/s: Histone H conserved site (InterPro:IPR019809), Histone-fold (InterPro:IPR009072), Histone core (InterPro:IPR007125), Histone H4 (InterPro:IPR001951)	protein_coding	F5K20.30
AT3G46320	AT3G46320.1	DOMAIN/s: Histone H4 conserved site (InterPro:IPR019809), Histone-fold (InterPro:IPR009072), Histone core (InterPro:IPR007125), Histone H4 (InterPro:IPR001951)	protein_coding	F18L15.40
AT5G59970	AT5G59970.1	DOMAIN/s: Histone H4 conserved site (InterPro:IPR019809), Histone-fold (InterPro:IPR009072), Histone core (InterPro:IPR007125), Histone H4 (InterPro:IPR001951)	protein_coding	MMN10.3
AT1G07660	AT1G07660.1	DOMAIN/s: Histone H conserved site (InterPro:IPR019809), Histone-fold (InterPro:IPR009072), Histone core (InterPro:IPR007125), Histone H4 (InterPro:IPR001951)	protein_coding	F24B9.25
AT2G28740	AT2G28740.1	histone 4	protein_coding	F8N16.2 F8N16_2 HIS4 HISTONE H4

Table (3.1): Conserved domains of Arabidopsis histone H4 genes.

All of Arabidopsis histone H4 genes have identical domains: “conserved site (InterPro:IPR019809)”, “histone fold (InterPro:IPR009072)”, “histone core (InterPro:IPR007125)” and “histone H4 (InterPro:IPR001951)”, TAIR, http://www.arabidopsis.org/cgi-bin/bulk/genes/gene_descriptions

```

AT1G07660.1 ATGTCAGGAAGAGGAAAGGGAGGAAAAAGGATTGGGAAAAGGAGGAGCGAAGAGGCACAGG 60
AT1G07820.1 ATGTCGGGAAAGAGGAAAGGGAGGAAAAAGGATTGGGAAAAGGAGGAGCGAAGAGGCACAGG 60
AT3G45930.1 ATGTCAGGTCGTGGAAAGGGAGGCAAAAGGTTTGGGCAAAAGGTGGAGCCAAACGTCATAGG 60
AT3G46320.1 ATGTCAGGTCGTGGAAAGGGAGGCAAAAGGTTTGGGCAAAAGGTGGAGCCAAACGTCATAGG 60
AT5G59690.1 ATGTCGGGTCGTGGAAAGGGAGGAAAAAGGTTTGGGTAAAGGAGGAGCCAAACGTCACAGG 60
AT5G59970.1 ATGTCGTGGTCGTGGAAAGGGAGGAAAAAGGCTTGGGTAAAGGAGGAGCCAAACGTCACAGG 60
AT2G28740.1 ATGTCAGGAAGAGGAAAGGGAGGAAAAAGGTTAGGCAAAAGGAGGAGCAAAAGAGACACAGA 60
AT3G53730.1 ATGTCAGGCCGAGGAAAGGGAGGAAAAAGGATTAGGAAAAGGAGGAGCCAAAGAGACATCGG 60
*****

AT1G07660.1 AAGGTTCTGAGGGATAACATTCAGGAATCACCAAGCCTGCTATTCGTCGCTTGGCTCGT120
AT1G07820.1 AAGGTTCTGAGGGATAACATTCAGGAATCACCAAGCCTGCCATTCGTCGCTTGGCTCGT120
AT3G45930.1 AAGGTTCTGAGAGACAACATCCCAAGGAATCACTAAACCGGCGATTTCGGAGATTGGCTCGT120
AT3G46320.1 AAGGTTCTGAGAGACAACATCCCAAGGAATCACTAAACCGGCGATTTCGGAGATTGGCTCGT120
AT5G59690.1 AAGGTTCTGAGAGACAACATCCCAAGGAATCACCAAGCCTGCGATTTCGAAGATTGGCTCGT120
AT5G59970.1 AAGGTTCTGAGAGACAACATCCCAAGGAATCACCAAGCCTGCCATTCGAAGATTGGCTCGT120
AT2G28740.1 AAGGTTCTAAGAGACAACATTCCAAGGAATCACAAAGCCAGCGATTTCGTCGCTTGGCTCGT120
AT3G53730.1 AAAGTACTCAGAGACAACATCCCAAGGATTACCAAACCTGCGATTTCGTCGCTTCGCGAGA120
*****

AT1G07660.1 AGAGGTGGTGTCAAGCGTATCAGTGGTCTCATCTACGAAGAGACCAGAGGTGTCCCTCAAG180
AT1G07820.1 AGAGGTGGTGTCAAGCGTATCAGTGGTCTCATCTACGAAGAGACCAGAGGTGTCCCTCAAG180
AT3G45930.1 AGAGGTGGTGTAAACGTAATTAGTGGTCTGATCTACGAAGAGACACGTGGCGTTCTCAAG180
AT3G46320.1 AGAGGTGGTGTAAACGTAATTAGTGGTGTGATCTACGAAGAGACACGTGGCGTTCTCAAG180
AT5G59690.1 AGAGGTGGAGTCAAGCGTATCAGTGGTCTCATCTACGAAGAGACTCGTGGCGTCCCTCAAG180
AT5G59970.1 AGAGGTGGAGTCAAGCGTATCAGTGGTCTCATCTACGAAGAGACACGTGGCGTCCCTCAAG180
AT2G28740.1 AGAGGAGGTGTGAAGAGAAATCAGTGGATTGATCTATGAAGAAACGAGAGGTGTGTTGAAG180
AT3G53730.1 AGAGGAGGCGTGAAGCGTATCAGTGGTGTGATCTATGAAGAGACTCGCGGCGTTCTCAAG180
*****

AT1G07660.1 ATCTTCTCGAGAAATGTTATCCGCTGACGCCGTTACCTACACTGAGCAGCCAGGAGGAAG240
AT1G07820.1 ATCTTCTCGAGAAATGTTATCCGCTGACGCCGTTACTTACACTGAGCAGCGTAGAAGGAAG240
AT3G45930.1 ATCTTTTTGGAGAAATGTTATCCGCTGACGCCGTTACTTACACTGAGCAGCGTCGGAGGAAG240
AT3G46320.1 ATCTTTTTGGAAAAATGTTATCCGCTGACGCCGTTACTTACACTGAGCAGCGTCGGAGGAAG240
AT5G59690.1 ATCTTCTCGAGAAACGTTATTCGCTGATGCTGTCACTTACACCGAGCAGCGTAGGAGGAAG240
AT5G59970.1 ATCTTCTCGAGAAACGTTATTCGCTGATGCTGTCACTTACACCGAGCAGCGTAGGAGGAAG240
AT2G28740.1 ATTTTTCTGGAGAAATGTAATTAGAGATGCTGTACTTACACTGAGCATGCGAGGAGGAAG240
AT3G53730.1 ATCTTCTCGAGAAACGTTATTCGCTGACGCCGTTACTTACACCGAGCAGCGTCGCCGGAAG240
*****

AT1G07660.1 ACGGTGACCGCCATGGATGTTGTCTACGCTTTGAAAGAGGCAAGGTCGTACTCTCTACGGT300
AT1G07820.1 ACGGTGACCGCCATGGATGTTGTCTACGCTTTGAAAGAGGCAAGGTCGTACTCTCTACGGT300
AT3G45930.1 ACGGTGACTGCTATGGATGTTGTTTATGCTCTTAAAGAGACAAGGAAGAACTCTCTACGGA300
AT3G46320.1 ACGGTGACTGCTATGGATGTTGTTTATGCTCTTAAAGAGACAAGGAAGAACTCTCTATGGA300
AT5G59690.1 ACTGTGACCGCCATGGATGTTGTCTACGCTCTCAAGAGGCAAGGAAGGACTCTTTACGGA300
AT5G59970.1 ACTGTGACCGCCATGGATGTTGTCTACGCTCTCAAGAGGCAAGGAAGGACTCTCTACGGA300
AT2G28740.1 ACGGTGACTGCTATGGATGTTGTTTATGCCTTGAAGAGACAAGGAAGAACTCTATATGGA300
AT3G53730.1 ACTGTTACGGCGATGGACGTCGTTTACGCTCTCAAGAGACAAGGACGAACCTTGTATGGA300
*****

AT1G07660.1 TTCGGAGGTTAA 312
AT1G07820.1 TTCGGAGGTTAA 312
AT3G45930.1 TTCGGCGGCTAG 312
AT3G46320.1 TTCGGTGGTTGA 312
AT5G59690.1 TTCGGTGGTTAA 312
AT5G59970.1 TTCGGCGGTTAA 312
AT2G28740.1 TTTGGTGGTTGA 312
AT3G53730.1 TTCGGCGGCTAA 312
*****

```

Figure (3.3): Clustalw2 alignment of *Arabidopsis* Histone H4 CDs.

The eight H4 gene sequences are similar. “*” marks identical residues along the aligned sequences.

<http://www.ebi.ac.uk/Tools/services/web/toolresult.ebi?jobId=clustalw2-E20120621-104132-0454-84544598-pg&tool=clustalw2&analysis=alignments>.

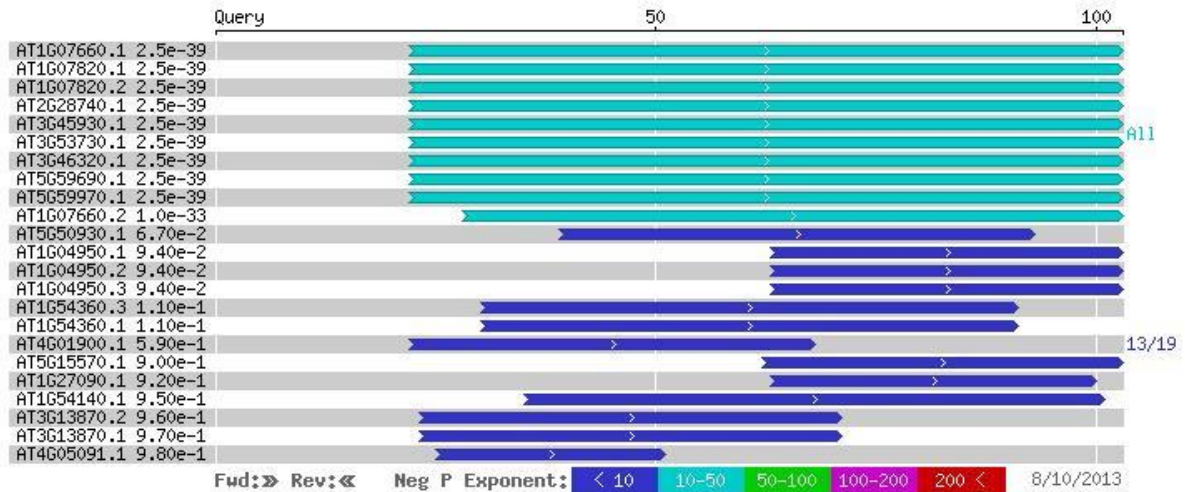


Figure (3.4 A): Wu Blastp alignment of *Arabidopsis* histones H4 protein sequences.
 The eight histone H4 proteins sequences show 100 % amino acid similarity or match. Wu-BLAST (TAIR).

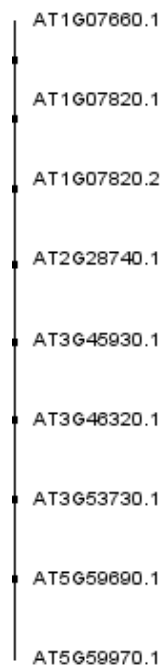


Figure (3.4 B): WU-Blast (TAIR) alignment of *Arabidopsis* Histone H4 proteins.
 The eight H4 proteins are identical in terms of protein sequence.
<http://www.ncbi.nlm.nih.gov/tools/cobalt/cobalt.cgi>

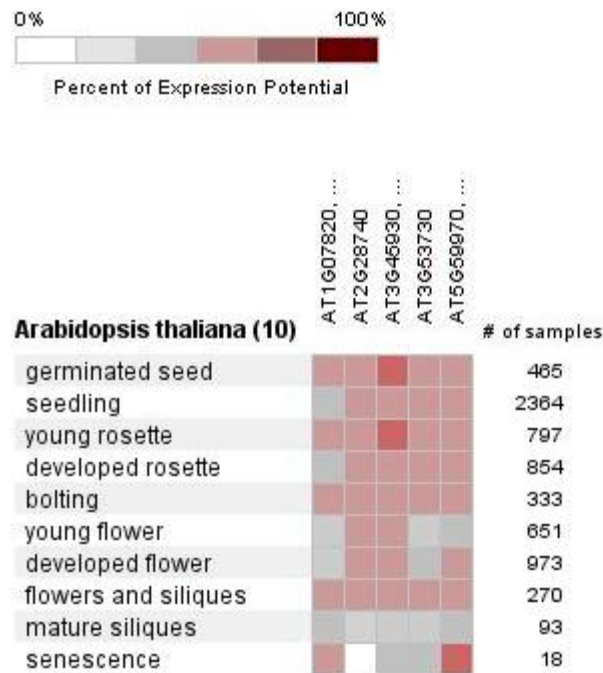


Figure (3.5): Arabidopsis thaliana Histone H4 genes microarray profile.

Geneinvestigator assessment of histone H4 expression through *Arabidopsis* developmental stages showed constitutive H4 proteins production through all stages following seed germination, passing seedling, rosette, flower and silique stages and up to seed senescence stage. Histone H4 expression intensity indicated high level of expression among all stages depending on the expression mean value calculation using the shown sample numbers studied for each gene at a certain developmental stage. The *Arabidopsis* H4 microarray profile shows five genes out of eight because some genes shows identical expression pattern as is shown in the following H4 pairs: (At1g07820 & At1g07660), (At3g45930 & At3g46320), (At5g59970 & At5g59690). Vertical dotted line represents the presence of other genes with identical expression (Hruz *et al.*, 2008).

3.2.2. Characterization of an $h4^{RNAi}$ mutant line

The *in silico* analysis of *Arabidopsis* histone H4 protein showed that the eight H4 proteins are identical and expressed through all the plant development stages. Hence, the best strategy to analyse H4 role within the nucleus would be by obtaining a knock-down mutant affected in all these isoforms. Therefore, a ChromDB $h4^{RNAi}$ line (CS31351-N3135) was analysed. The RNAi line was produced using the cDNA of the At3g46320 H4 gene (**Figure 3.6**). The constructs of $h4^{RNAi}$ were prepared by

using the pFGC5941d vector for the build-up an HF01 (Histone Four 1) double stranded RNA construct as shown in **Figure 3.7**.

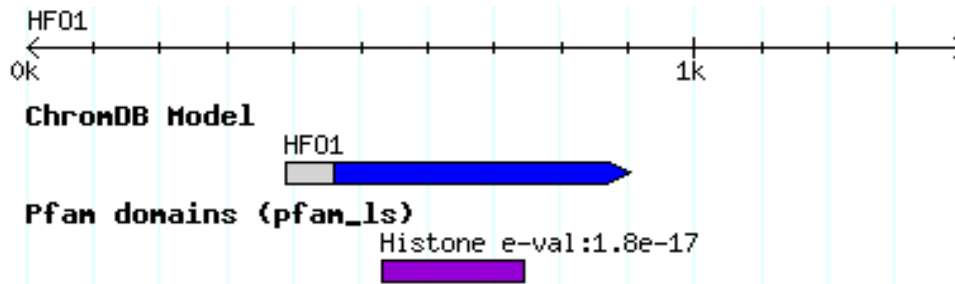


Figure: 3.6 ChromDB H4 genomic model.



Figure (3.7): HF01 ds RNA construct (T-DNA region).

The schematic diagram represents $h4^{RNAi}$; Ath13-CS31351, construct.

3.2.3. $h4^{RNAi}$ mutant phenotype

The investigation of histone $h4^{RNAi}$ mutant line showed differences from the wild-type phenotype. The $h4^{RNAi}$ developmental rate was faster than that observed in the wild-type plants (**Figure 3.8 A**). So that, the $h4^{RNAi}$ showed flower appearance, apical shoot growth and silique formation before that observed in the Wild-type plants. Later on when the seed pods mature, gaps were observed in some $h4^{RNAi}$ plants (**Figure 3.8 C**). The plants which showed these gaps were assessed later for their fertility level comparable to WT (**Figure 3.8 B**).

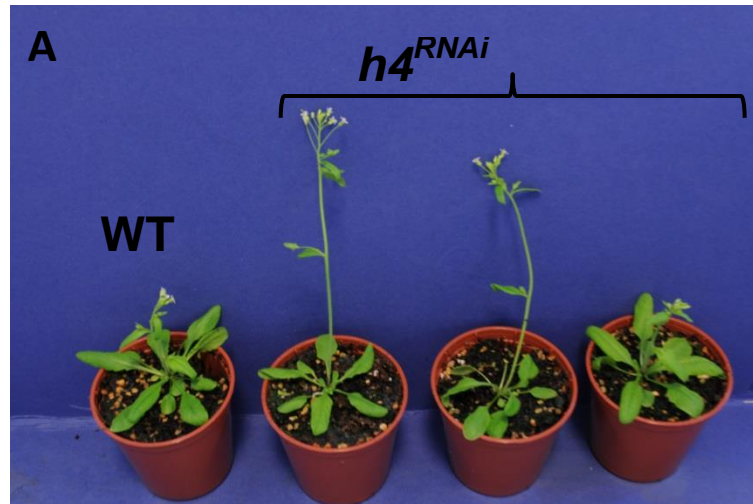


Figure (3.8): Phenotype of $h4^{RNAi}$ mutant in comparison to wild-type plants.

The $h4^{RNAi}$ plant showed (A) delayed faster flowering and growth than wild-type. (C) $h4^{RNAi}$ plants showed reduced siliques with little seed-set content (C) compared to WT. (B) WT silique. (C) $h4^{RNAi}$ silique. The $h4^{RNAi}$ line showed 47.3 % reduction in seed-set of the WT. Black arrows show gaps in between seeds.

3.2.4. Fertility analysis of *Arabidopsis thaliana* $h4$ knock-down mutant lines

Fertility level was assessed in different $h4^{RNAi}$ lines depending on seed sets and silique length in both mutant lines and the wild-type plants grown in parallel. The results showed that as these mutant lines presented different knocked down levels, and so plant phenotypes varied. Some plants showed a phenotype similar to the WT, whereas, others were a little affected and others severely affected. The results showed that $h4^{RNAi}$ mutant displayed 47.3 % seed set loss compared to wild type ($p=1.99135E-28$, T-test). Siliques of $h4^{RNAi}$ mutants showed about 23.56 % reduction

in length referring to wild-type ($p=1.654E-15$, T-test). **Figures (3.9 A) and (3.9 B)** shows siliques length mean and seed sets mean respectively for the *Arabidopsis* wild-type and $h4^{RNAi}$ line.

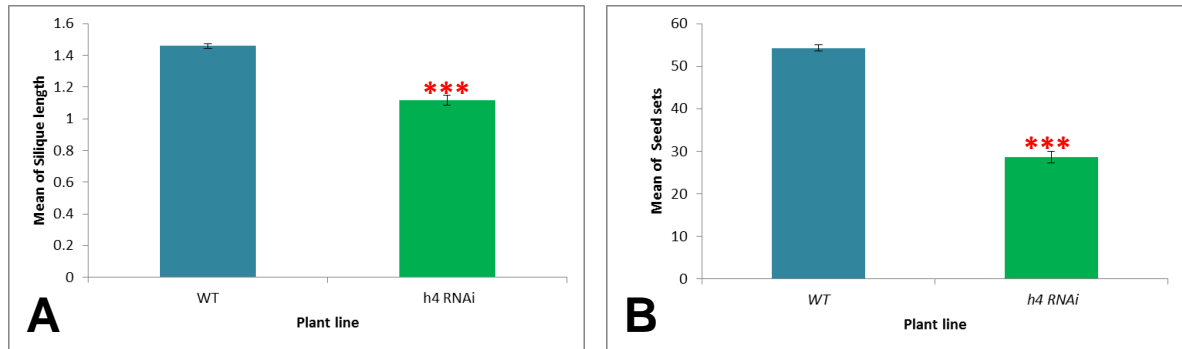


Figure (3.9): Fertility of *Arabidopsis* histone $h4^{RNAi}$ mutant line in comparison to wild-type plants.

(A) Silique length (N=50). (B) Seed set (N=50). ***=P<0.005, T-test. Error bars = standard error of the mean.

3.2.5. Meiotic cytological analysis of histone $h4^{RNAi}$ mutant line

The confirmed $h4^{RNAi}$ mutants reduced fertility phenotype indicated a possible role for H4 protein on *Arabidopsis* chromosomes behaviour through meiosis. To check this, cytological preparations were made from $h4^{RNAi}$ mutant lines and the corresponding wild-type plants. Several abnormalities were identified in histone $h4^{RNAi}$ line within meiosis compared to the wild type (**Figure 3.10**) (**Table 3.2**). Although at leptotene (**Figure 3.10 G**) appeared very similar to the wild type (**Figure 3.10 A**), however at zygotene (**Figure 3.10 H**) some chromatin fragmentation was observed comparable to the non-fragmented chromatin in the wild-type (**Figure 3.10 B**). Moreover, at pachytene more chromatin fragmentation was observed (**Figure 3.10 I&J**). Furthermore, homologous chromosomes discontinuous synapsis was also observed (**Figure 3.10 K**). Some pachytene meiocytes in $h4^{RNAi}$ mutants (**Figure 3.10 L&M**)

showed that the nucleolar organizing regions (NORs) located on chromosomes 2 and 4 were affected. The NORs appeared not as just one region like in wild-type but severely separated in different regions and showing a remarkable different condensation compared to wild-type (**Figure 3.10 C**). At diakinesis (**Figure 3.10 O**) abnormal non-homologous connections could be observed specially involving chromosomes 2 and 4 and their NORs compared to the wild-type (**Figure 3.10 D**). The abnormalities seen in $h4^{RNAi}$ mutants at prophase I proceeded on to the rest of the meiotic stages. Non-homologous inter-connections were visualised at anaphase II (**Figure 3.10 P&Q**) in comparison to the wild-type (**Figure 3.10 E**). At telophase II (**Figure 3.10 R**) the correct chromosome segregation in the four haploid meiotic products was often inadequate, whereas four haploid tetrads were formed in the wild-type (**Figure 3.10 F**).

Meiotic stage	Defects	Percentage ells
Zygotene-Pachytene	Chromatin breaks	60%
Pachytene	Chromosome clustering in more than one nuclei	2%
Diakinesis	Bivalent connections	30%

Table (3.2): Summary of meiotic defects in the $h4^{RNAi}$ mutant.

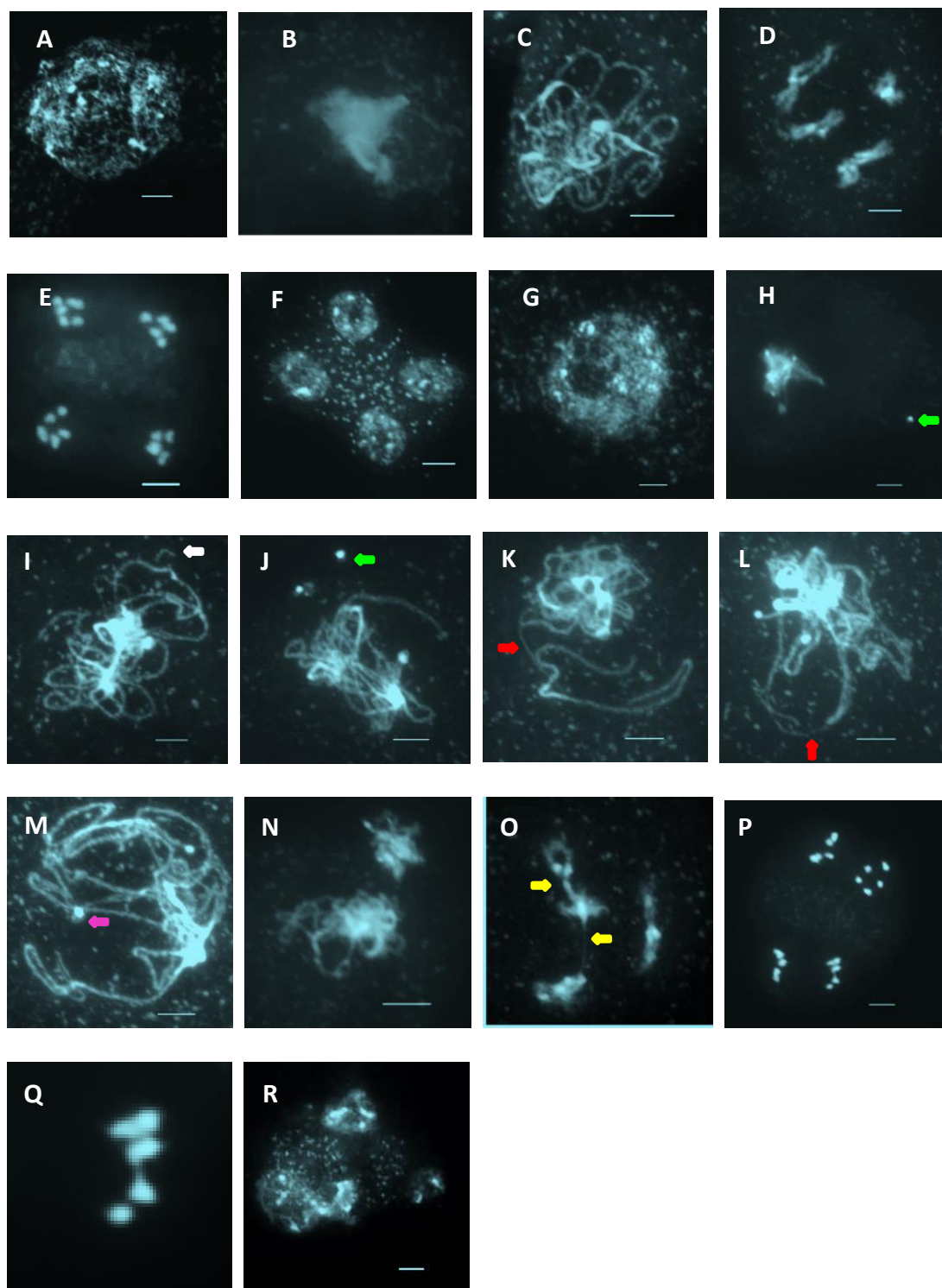


Figure (3.10): Meiotic cytology of $h4^{RNAi}$ PMCs vs wild-type.

(A-F) Dapi stained meiocytes of wild-type. (G-R) Dapi stained meiocytes of $h4$ kd mutants $h4^{RNAi}$. (A) Leptotene (B) Zygotene (C) Pachytene (D) Diakinesis (E) Anaphase II (F) Tetrad . (G) Normal-like leptotene. (H) Zygotene with fragmented chromatin. (I-N) Abnormal Pachytene. (I) Abnormal regions of broken chromatin. (J) One pachytene cell containing two micronuclei. (K) Incomplete or partial synapsis between homologous chromosomes. (L) A clear chromatin breakage of unsynapsed chromatin. (M) Nucleolar organizing region is abnormal. (N) Abnormal chromosomal clustering in two nuclei format. (O) Diakinesis showing abnormal chromosome joining. (P&Q) Anaphase II. (P)

Abnormal chromosome joining at anaphase II. (Q) A closer view of (P) showing anaphase II chromosomes joining together. (R) Telophase II shows aneuploidy. The four newly formed nuclei are imbalanced in terms of chromosomal numbers and set, hence the four nuclei lack the normal viable haploid gamete chromosomal style. White arrow indicates chromatin breakage. Green arrows indicate abnormal micronuclei. Red arrows indicate unsynapsed chromatin. Pink arrows indicate tangled nucleolus. Yellow arrows indicate connections between non-homologous chromosomes.

3.2.6. Fluorescence *in situ* hybridization (FISH) analysis of *Arabidopsis* histone $h4^{RNAi}$ line

Meiotic FISH analysis using 45S and 5S rDNA probes in the $h4^{RNAi}$ mutants showed a distinctive abnormality in the rDNA regions or NORs. Chromosomes 2 and 4 are easily discriminated as they bear the 45S rDNA gene repeats. A single NOR associated to the 45S signal appears usually during prophase I at zygotene/pachytene stages in the wild-type meiocytes (**Figure 3.11 A**), indicating that chromosomes 2 and 4 pairs are converging at the same position. However, $h4^{RNAi}$ mutants showed more than one NOR (45S rDNA signals) during prophase I (**Figure 3.11 B&C**). The appearance of fragmented 45S rDNA regions at diakinesis was also observed in the mutants (**Figure 3.11 E**). Moreover, the wild-type 5S rDNA signal at pachytene obviously shows two separate sites resembling the homologous pairs of chromosomes 3 and 5 separately (**Figure 3.11 A**). This two 5S rDNA signals continue until diakinesis (**Figure 3.11 D**). Whereas, $h4^{RNAi}$ pachytene meiocytes showed a fragmented 5S rDNA signal (**Figure 3.11 B&C&E**). In addition to this, the presence of chromosomal connections involving always 45S and/or 5S rDNA signals was frequently observed at diakinesis suggesting putative recombination events among rDNA sequences present between non-homologous chromosomes (**Figure 3.11 E**).

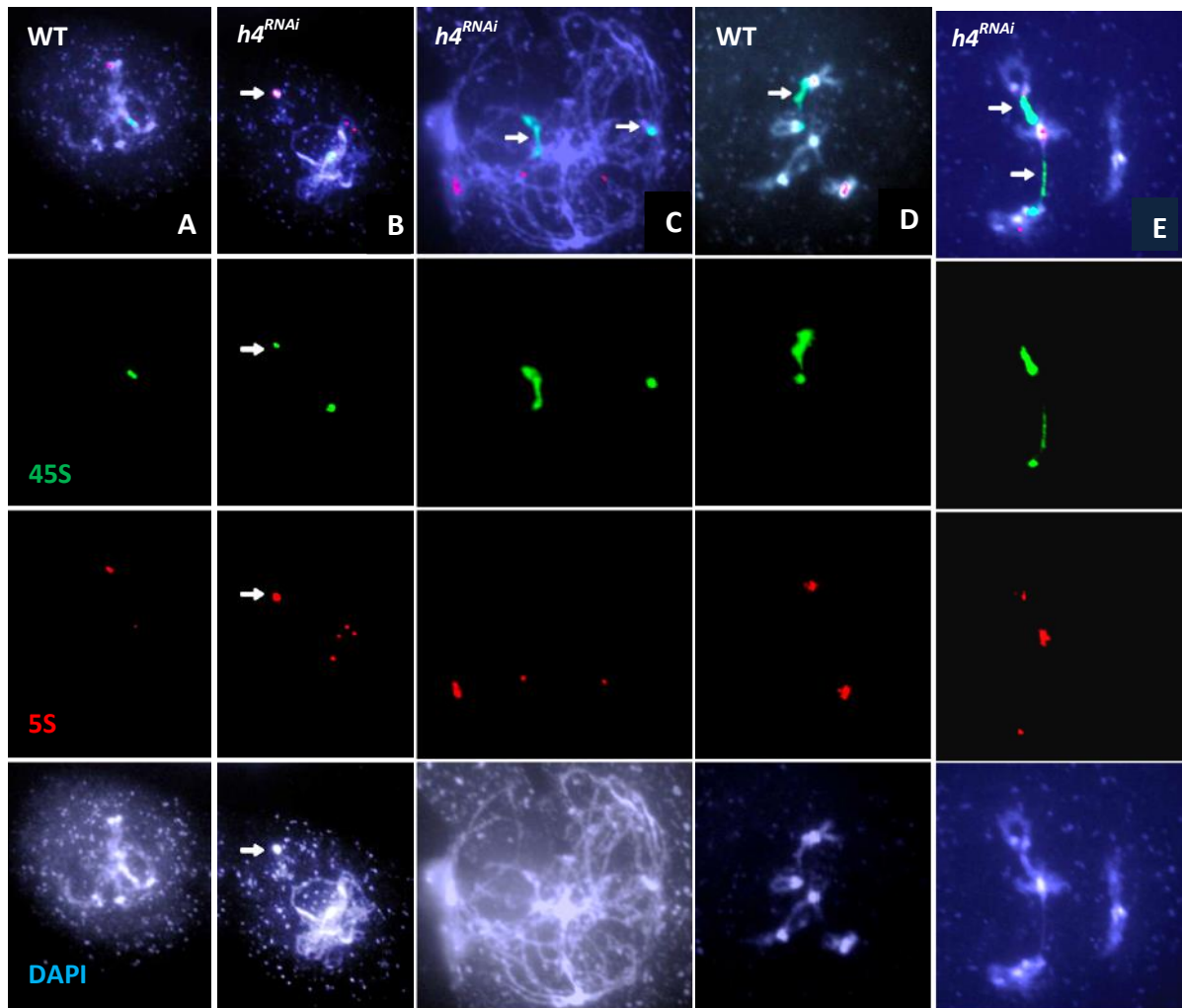


Figure (3.11) FISH analysis of NORs of the $h4^{RNAi}$ and wild-type *Arabidopsis* plants. (A&D) wild-type. (B&C&E) $h4^{RNAi}$. (A&B&C) Pachytene. (D&E) Diakinesis The nucleolus organizing region (NOR) is disrupted in the $h4^{RNAi}$ mutant. The 45S signal of chromosomes 2 and 4 is separate (B&C), whereas, in wild-type one signal is present (A). The 5S rDNA is fragmented in the $h4^{RNAi}$ mutant (B) while, no fragmentation is seen in the wild-type (A). Moreover, chromosome 5 connections with chromosomes 2&4 in the $h4^{RNAi}$ line indicate non-homologous recombination occurrence (E), whereas, that is not present in the wild-type (D).

3.2.7. Mitotic cytological analysis of *Arabidopsis* histone $h4^{RNAi}$ mutant

The vegetative $h4^{RNAi}$ mutants phenotype differed from that observed in the wild-type, $h4^{RNAi}$ mutants showed a consistent pattern of faster developmental rate compared to that of the wild-type as described in 3.2.3 (**Figure 3.8**), the fast growth of plant

organs (stem, inflorescence, and leaves), compared to wild-type, might suggest a putative mitotic role for *Arabidopsis* H4. Mitotic *Arabidopsis* chromosomes irregularities were visualised in $h4^{RNAi}$ mutant line, where some asynchronous sister chromatid separation was noticed (**Figure 3.12 A**). Defects in sister chromatid separation were also observed up to late anaphase-telophase stages (**Figure 3.12 B**) with some chromosomes lagging in the middle of the bi-oriented spindle poles.

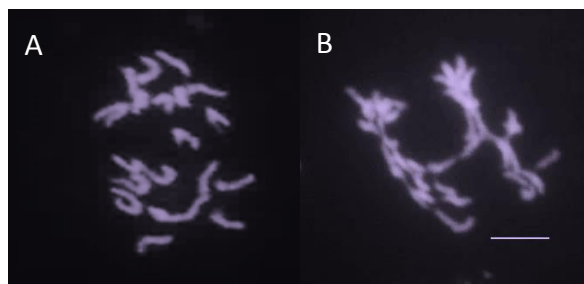


Figure (3.12): Mitosis in *A. thaliana* $h4^{RNAi}$ mutant plants. Dapi stained cells of $h4^{RNAi}$ line shows mitotic defects. (A&B) Anaphase. (A) chromosomes are out of synchrony. (B) Anaphase-Telophase bridge. Scale Bars are 5 μ m.

3.2.8. $h4^{RNAi}$ seeds are cisplatin sensitive.

The vegetative defects observed in the $h4^{RNAi}$ phenotype might suggest mitotic defects. This was confirmed in the chromosomal spreads prepared for the $h4^{RNAi}$ mutants comparable to wild-type. Anaphase bridges were observed in the mutant but not present on the wild-type. This suggested that histones H4 might play a role in the mitotic DNA lesions repair. And so, to verify this histone H4 role in DNA repair we characterised the sensitivity of the plants to cisplatin a DNA cross-linking drug which produces DNA breaks.

Cisplatin sensitivity was assessed by the quantification of the number of leaves per plant, as well as to the percentage of viable seeds on days 11, 14 and 17 by analysing the seed germination on Murashige and Skoog (MS) agar medium with and without 30 μ M of cisplatin. A hundred seeds from $h4^{RNAi}$ as well as the wild-type were placed on two MS agar plate (50 seeds each), and then incubated at 22° C growth room. The results showed that the $h4^{RNAi}$ mutant seeds are highly sensitive for the cisplatin. The $h4^{RNAi}$ mutant showed 12% viable seeds compared to 94% in the wild-type on day 11 of seed germination (**Figure 3.14 B**). The $h4^{RNAi}$ mutant formed 0.58 leaves per plant compared to 3.52 in the wild-type (**Figures 3.13 & 3.14 A**). Statistical analysis showed that this difference is significant ($P=4.300E-23$, T-test). Moreover, the $h4^{RNAi}$ seeds germination was also decrease on day 14 showing only 22% viable seeds compared to 96% in the wild-type (**Figure 3.14 C**). The $h4^{RNAi}$ mutant showed an average of 0.86 leaves per plant compared to 3.84 in the wild-type (**Figures 3.13 & 3.14 A**). Statistical analysis showed that these differences were significant ($3.78E-18$, T-test). And on day 17 the $h4^{RNAi}$ showed up to 24% viable seeds compared to 96% in the wild-type (**Figure 3.14 D**). The $h4^{RNAi}$ mutant showed significant reduction in leaves appearance showing 1.16 leaves average compared to 5.72 in wild-type ($4.152E-21$, T-test) (**Figures 3.13 & 3.14 A**).

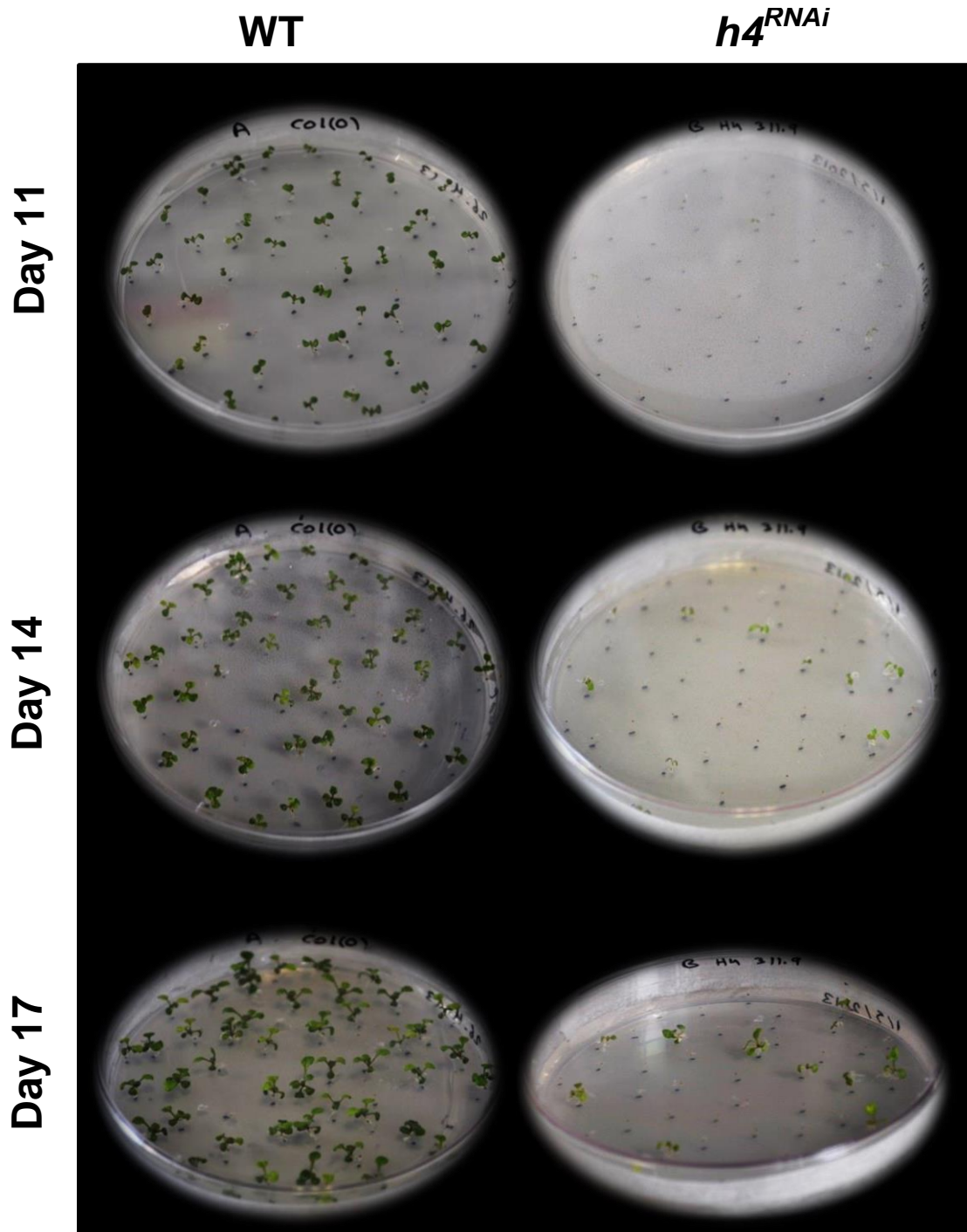


Figure (3.13): Cisplatin sensitivity phenotype of wild-type and *h4*^{RNAi} seeds. Seeds of wild-type and *h4*^{RNAi} plants were grown on MS plates containing 30 μ M cisplatin. Seeds were assessed on days 11, 14 and 17 after seed germination.

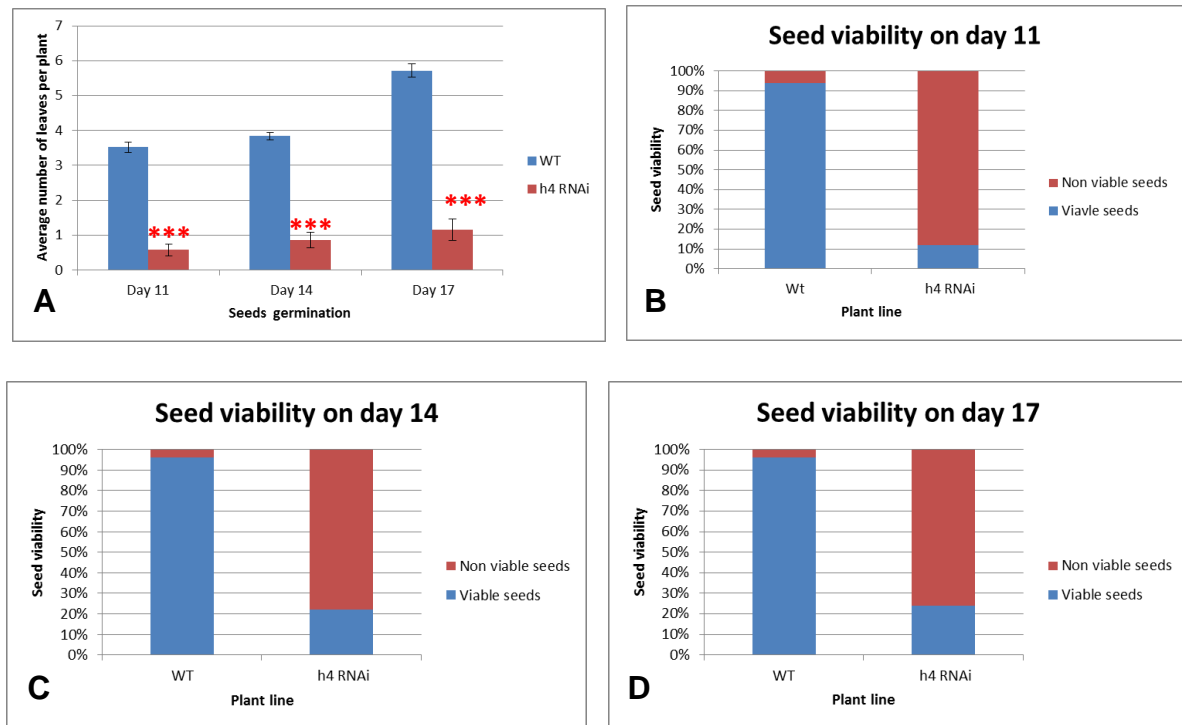


Figure (3.14): Cisplatin sensitivity analysis of wild-type and $h4^{RNAi}$.

(A -D) Seeds of wild-type and $h4^{RNAi}$ plants were grown on 30 μ M cisplatin treated MS medium. (A) Number of rosette/ leaves per plant was assessed in the wild-type and $h4^{RNAi}$ mutants on days; 11, 14, and 17 after seed germination. Statistical analysis showed that the number of leaves of the $h4^{RNAi}$ mutants was significantly decreased comparable to wild-type on days 11 (4.30E-23), 14 (3.787E-18) and 17 (4.152E-21). (B-D) Seed viability in percentage was assessed in the wild-type and $h4^{RNAi}$ mutants. The $h4^{RNAi}$ showed 12%, 22% and 24% compared to 94%, 96%, 96% in the wild-type on days 11, 14 and 17 after seed germination N=50. (***)= $P < 0.005$, T.test)

3.3. Analysis of *Arabidopsis* histone H3-H4 chaperone complex

In order to further understand these defects observed in the histone h4 knock-down mutant line, and to confirm the histone H4 role within chromatin, more analysis was carried out for *Arabidopsis* histone H4-related mutants. The Chromatin Assembly Factor – 1 (CAF1) complex is a tripartite chaperon complex that loads the budding yeast H3-H4 heterodimers onto DNA and nucleosomes (Haushalter and Kadonaga, 2003; Polo and Almouzni, 2006). The p150, p60 and p48 are human homologues of

CAF-1 complex subunits (Smith and Stillman, 1989; Kaufman *et al.*, 1995; Verreault *et al.*, 1996). In *Arabidopsis* these subunits are known as FAS1, FAS2 and MSC11 (Leyser and Furner, 1992; Kaya *et al.*, 2001; Hennig *et al.*, 2003; Ramirez-Parra and Gutierrez, 2007). The analysis of mutants for this histone H4 chaperone could add further details on the H4 depletion phenotype observed.

In silico analysis of FAS expression showed that it is constitutively expressed through the different plant developmental stages (**Figure 3.15**). Giving a clue how important it is for the proper cellular functions. This suggestion was further clarified through the defects observed in the *fas* mutants.



Figure (3.15): Genevestigator diagram showing FAS proteins expression.

The microarray analysis of Fas genes expression. FAS 1-3 (AT1G65470), and FAS 2-3 (AT5G64630) (Hruz *et al.*, 2008).

3.3.1 *fas* mutants Phenotype

The external physical features of *Arabidopsis fas* mutants were analysed and compared to the wild-type plants. The characterization of two T-DNA insertion mutants showed that both *fas 1-3* (**Figure 3.16 A**) and *fas 2-3* (**Figure 3.16 B**) mutants presented a delayed flowering phenotype compared to the wild-type. This

defect in *fas* mutants growth continued to later stages of development. *fas* mutants presented twisted stems with highly reduced number of leaves and siliques with reduced size compared to that of the wild-type (**Figure 3.16 C & D**). *fas* mutants phenotypic defects were also reported previously by Leyser *et al.* (1992), who showed plants with fused stems termed fasciated (thus, the name *fasciata* mutants or *fas*). Other plant defects observed include stems lacking apical meristem dominance, narrow leaf shape, disturbed root and floral growth changes Leyser *et al.* (1992).

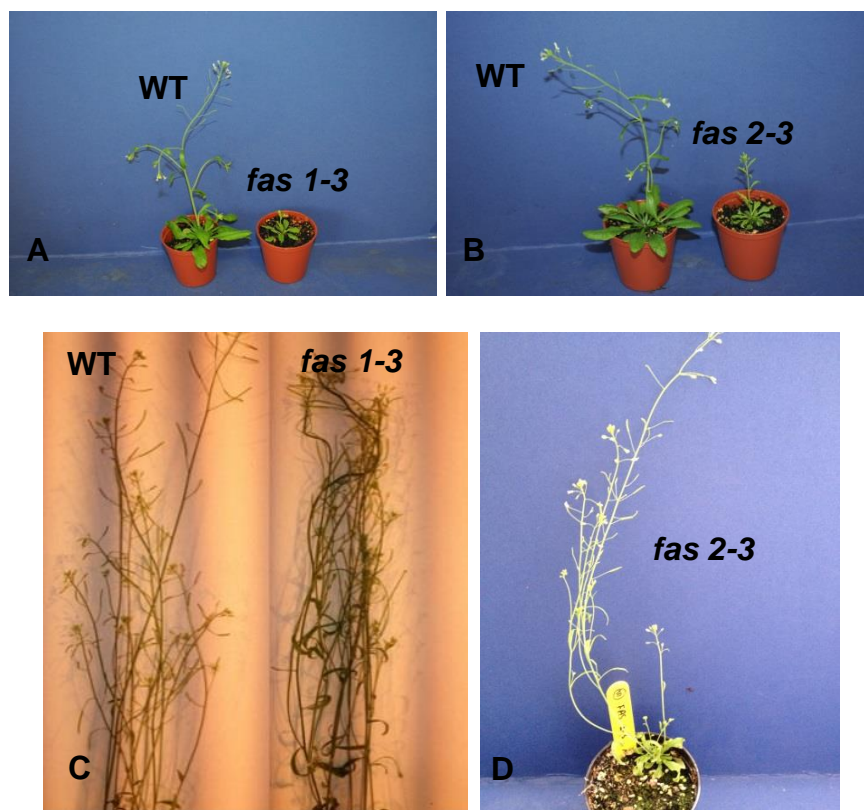


Figure (3.16): Phenotype of *fas* mutants; *fas 1-3* and *fas 2-3*, in comparison to wild-type plants. (A&C) *fas 1-3* vs WT. (B&D) *fas 2-3* vs WT. Delayed flowering and development in *fas* mutants (A) *fas 1-3* (B) *fas 2-3*. Twisted stems in *fas 1-3* (C). Reduced siliques in *fas 1-3* (C) and *fas 2-3* (D).

3.3.2. Fertility analysis of *fas* mutants

The fertility level was assessed in these mutant lines in *Arabidopsis*. These analysis showed a significant defect on the plant fruit product size (silique/ seed pod) (**Figure**

3.17). Silique measurements analysis in both *fas* mutant lines showed that *fas1-3* and *fas 2-3* plants exhibited 42.32% and 50.2% decrease in the average silique length, respectively (**Figure 3.17 A**). Moreover, the quantification of the seed set per pod (mean number of seeds per silique) in *fas 1-3* and *fas 2-3* recorded 79.3 % and 78.6% reduction from the WT, respectively (**Figure 3.17 B**). The significance of these results was confirmed by using a T-test statistical analysis showing P-values of 2.97791E-25 and 3.56241E-53 for *fas 1-3*, *fas 2-3* mean silique length respectively, and P-values of 4.37476E-49, 6.24001E-58 for *fas 1-3* and *fas 2-3* seed set mean respectively. Thus, Fas1 and Fas2 seem to have a role in maintaining the normal fertility levels in *Arabidopsis* plants.

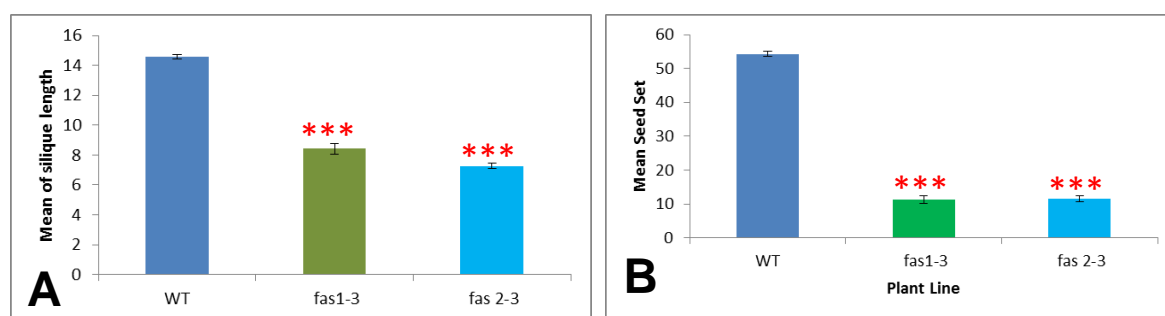


Figure (3.17): Fertility of *fas* mutants; *fas 1-3* & *fas 2-3*, and the corresponding wild-type (WT). (A) Silique length (n=50). (B) Seed set (n=50). (***)= $P < 0.005$, T.test). Error bars = Standard error of the mean.

3.3.3. Cytological analysis of *fas* mutants

The high reduction of fertility in *fas1/2* mutants demanded further cytological investigation to analyse these defects in more detail. Hence DAPI stained PMCs from *fas 1-3* and *fas 2-3* mutants and wild-type plants were characterised using an epifluorescence microscope.

3.3.3.1. Meiosis of *fas 1-3* mutant

Cytological preparations of *fas 1-3* PMCs showed differences from the wild-type meiocytes. Tangled nucleolus was observed at pachytene (**Figure 3.18 E**). Moreover, chromatin fragments were observed at different stages of meiosis; pachytene (**Figure 3.18 C&D**), diplotene (**Figure 3.18 F**) (**Figure 3.18 G**), prophase II (**Figure 3.18 J**) and metaphase II (**Figure 3.18 K**). Furthermore, *fas 1-3* diakinesis chromosomes showed unusual condensation, and also univalents were observed at this stage (**Figure 3.18 H**), allowing inappropriate chromosome orientation during homologues separation at anaphase I (**Figure 3.18 I**), and causing chromosome mis-segregation at metaphase II (**Figure 3.18 K**) leading to the formation of incorrect haploid gametes (**Figure 3.18 L**).

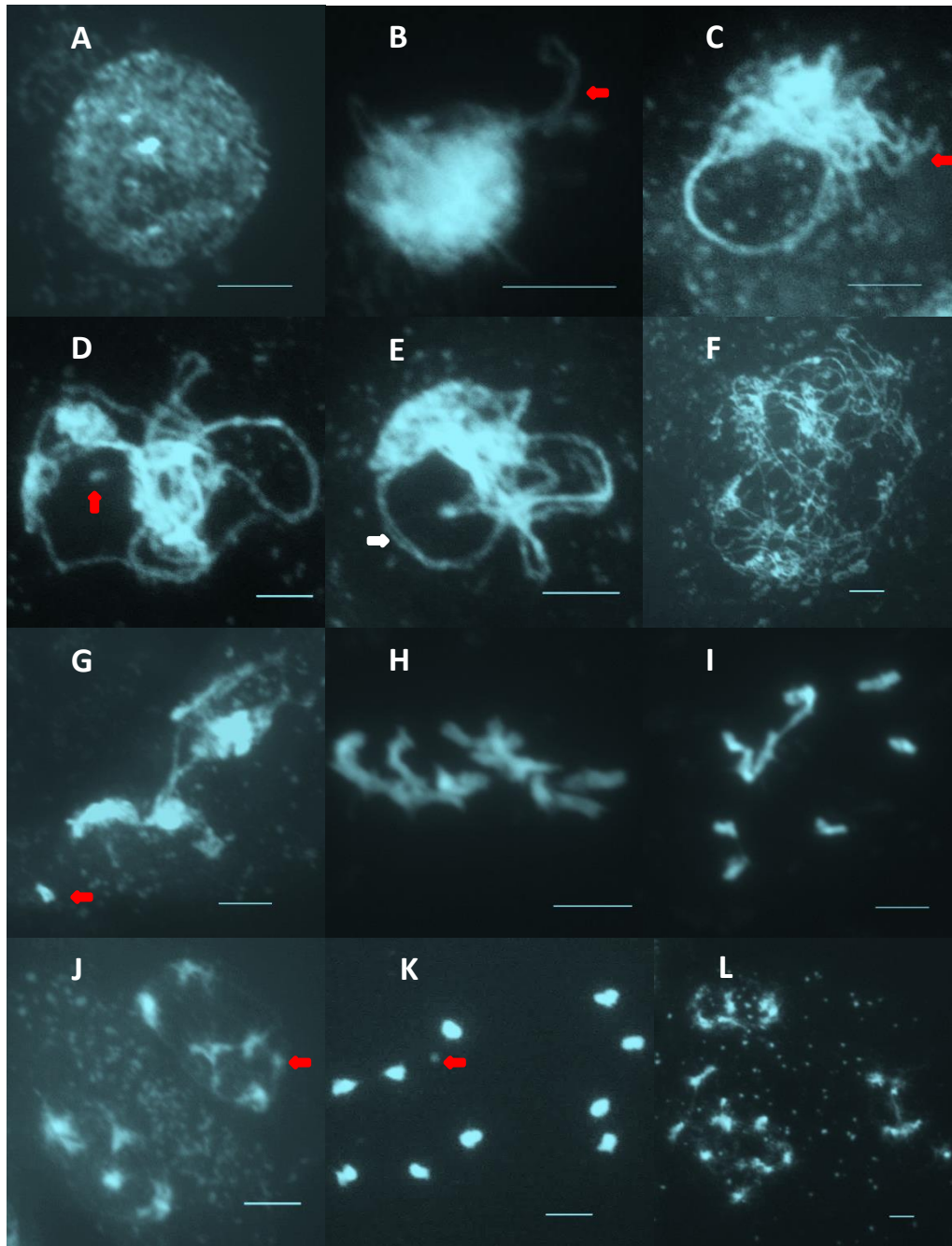


Figure (3.18): Meiosis of *fas 1-3* PMCs.

Defects were seen in the *fas 1-3* meiocytes. Fragmentation (C&D&F&G&J&K), tangled nucleolus (E), univalents (H), chromosome missegregation (I), and abnormal tetrad (L). Leptotene stage (A), Zygotene stage (B), Pachytene stage (C-E), Diplotene stage (F), diffuse stage (G), diakinesis stage (H), anaphase I stage (I), Prophase II stage (J), metaphase II stage (K), Telophase II stage (L). Red arrows indicate chromatin breakage. White arrow indicates unsynapsed chromatin. Bar= 5 μ m.

3.3.3.2. Meiosis of *fas 2-3* mutant

The meiotic preparations for *fas 2-3* were very difficult as the mutant inflorescences were not fully developed. Only a few meiotic cells have been able to be analysed. We were able to analyse some meiocytes at pachytene (**Figure 3.19 A&B**), metaphase I (**Figure 3.19 C**) and anaphase I (**Figure 3.19 D**) stages. Clearly, at pachytene, chromatin fragmentation was observed. At metaphase I, chromosomes showed a reduction in chiasma frequency losing the obligate chiasma in some cases showing univalents.

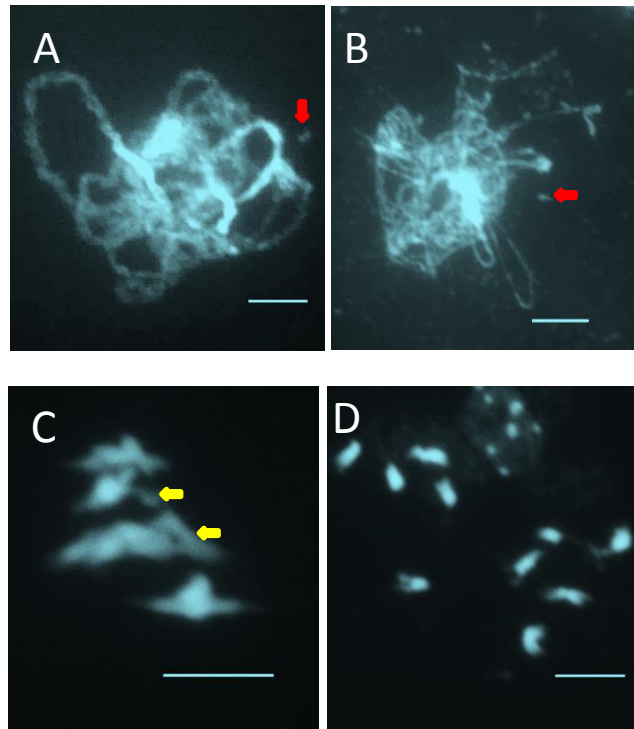


Figure (3.19): Meiotic atlas of *fas 2-3* PMCs.

The mutant showed fragmentation at pachytene stage (A). Chromatin fragments at diplotene stage (B). Reduction in the chiasmata per meiocytes were seen at metaphase I (univalents, low bivalents and rod shaped bivalents). Chromosomes were unable to create balanced haploid chromosomal set at anaphase I stage due to mis-segregation (C). un balanced homologous disjunction at anaphase I stage (D). Red arrows represent chromatin fragments. Yellow arrows represent univalents. Scale bar= 5 μ m.

3.3.3.3. *fas 1-3* mitotic defects

The observed phenotypic abnormalities in *fas* mutants have showed that mitotic disturbances could be predicted. So, mitotic stages were investigated in these mutants to clarify if their vegetative phenotype defects have derived from errors during mitotic divisions. The analysed mitotic *fas 1-3* cells showed genetic instability appearing as chromosomal fragmentation (**Figure 3.20 A**), lagged chromosomes (**Figure 3.20 B**), and anaphase bridges from anaphase up to telophase stages (**Figure 3.20 B&C**). These abnormal mitotic divisions fits very well with the mutant defective characters like; reduced organ parts (leaves) and silique size. Moreover, *fas 1-3* growth rate defects were also noticed in some plants.

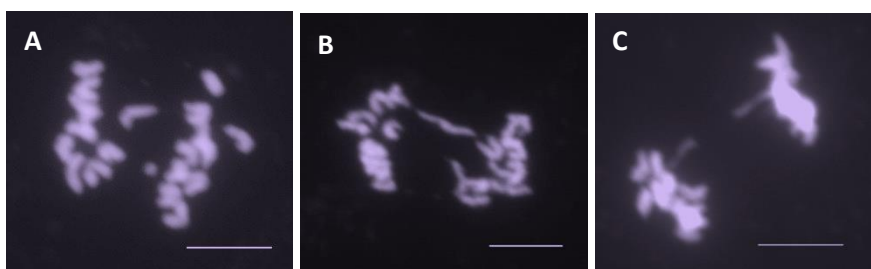


Figure (3.20): Mitotic defects of *fas 1-3* mutant line at anaphase.

(A&B) Anaphase. (C) Telophase. Chromosome fragments (A). Anaphase –bridge (B). (C) Delayed chromosome separation and condensation.

3.3.3.4. *fas 2-3* mitotic defects

The mitotic cells of *fas 2-3* mutants recorded some aberrant stages. The visible chromosomal defects showed chromosome interconnections at prophase (**Figure 3.21 A**) and chromosome missegregation at metaphase-anaphase (**Figure 3.21 B**). Furthermore, some anaphase bridges could be observed at late anaphase/early telophase stages (**Figure 3.21 C**).

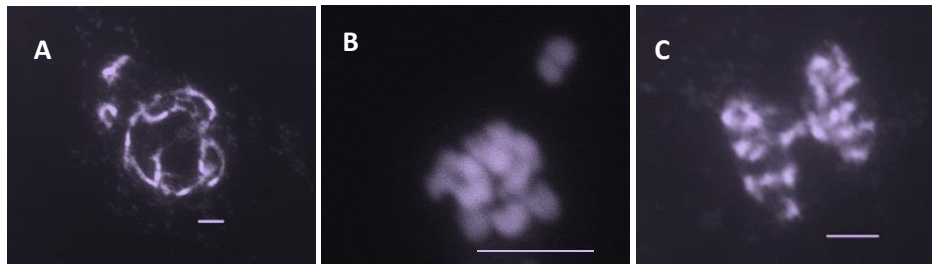


Figure (3.21): Mitotic defects of *fas 2-3* mutant line.

(A) Prophase: chromosomes interconnections are visible, besides some chromosomes do not position properly. (B) Metaphase: the mitotic chromosomal package does not align fully at cell equator. (C) Anaphase: The delayed chromosomes separation resulted in anaphase-bridge formation.

3.3.4.. *fas* mutants sensitivity to cisplatin

3.3.4.1. *fas 1-3* seeds are cisplatin sensitive.

The developmental defects observed in the *fas 1-3* phenotype suggested having a mitotic origin. This was confirmed in the mitotic chromosomal spreads prepared for the *fas 1-3* mutants comparable to wild-type. Anaphase bridges were present in the mutant. FAS 1 might play a role in the mitotic DNA lesions repair. Hence, FAS 1 role in the mitotic DNA repair was studied by using cisplatin-induced DNA cross-linking defects.

Cisplatin sensitivity was assessed by the quantification of the leaves number per plant, and the percentage of viable seeds on days 11, 14 and 17 by seeds germination on MS agar medium with 30 μ M cisplatin. A hundred seeds from *fas 1-3* as well as from the wild-type were placed on two MS agar plates (50 seeds on each plate), and then incubated at 22^o C growth room. The results showed that the *fas 1-3* mutant seeds were highly sensitive for the cisplatin. The *fas 1-3* mutant showed 66% viable seeds compared to 94% in the wild-type on day 11 of seed germination

(Figure 3.23 B). The *fas 1-3* mutant formed 1.288 leaves per plant compared to 3.52 in the wild-type (**Figures 3.22 & 3.23 A**). Statistical analysis showed that this differences were significant ($2.573E-18$, T-test). Moreover, the *fas 1-3* seeds germination on day 14 showed 70% of viable seeds compared to 96% in the wild-type (**Figure 23 C**). The *fas 1-3* mutant showed significant reduction in leaves formation showing 1.288 average leaves per plant compared to 3.84 in the wild-type ($1.141E-25$, T-test) (**Figures 3.22&3.23 A**). And on day 17 the *fas 1-3* showed 70% viable seeds compared to 96% in the wild-type (**Figure 3.23 D**). The *fas 1-3* mutant showed significant decline in leaves formation showing 1.40 leaves average compared to 5.72 in wild-type ($1.012E-31$, T-test) (**Figures 3.22 & 3.23 A**).

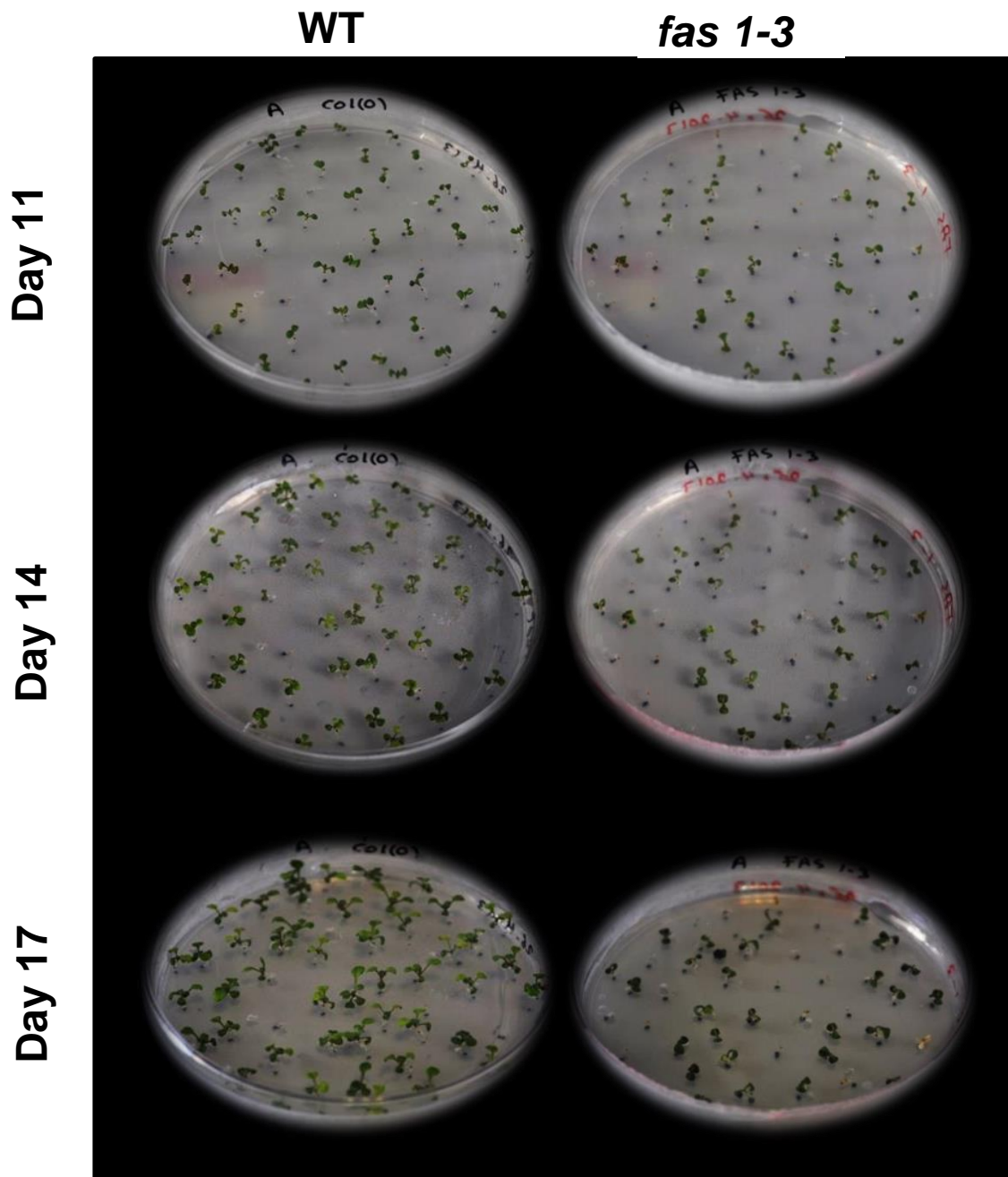


Figure (3.22): Cisplatin sensitivity phenotype of wild-type and *fas 1-3* seeds.

Seeds of wild-type and *fas 1-3* plants were grown on MS plates containing 30 μ M cisplatin. The wild-type and *fas1-3* mutant seeds were assessed on days 11, 14 and 17 after seed germination.

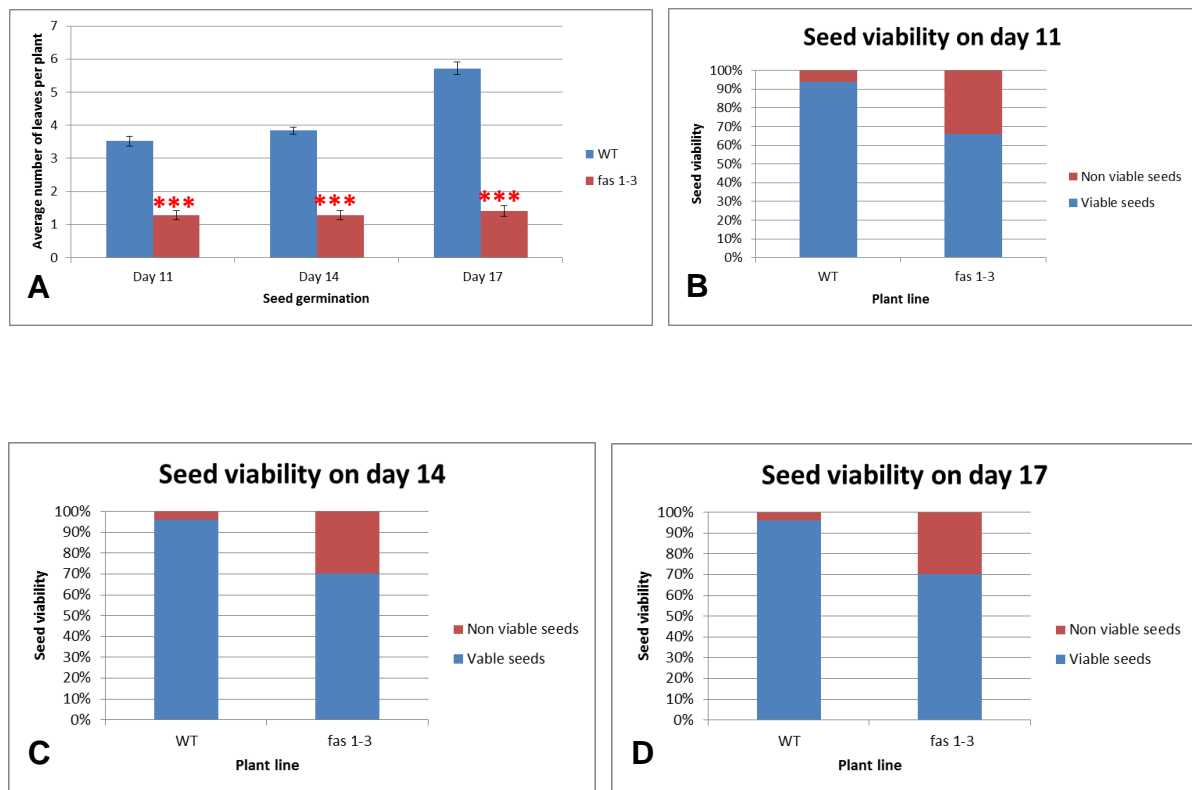


Figure (3.23): Cisplatin sensitivity analysis of wild-type and *fas 1-3* seeds.

(A -D) Seeds of wild-type and *fas 1-3* seeds were grown on 30 μ M cisplatin treated MS medium. (A) Number of rosette/ leaves per plant was assessed in the wild-type and *fas 1-3* mutants on days; 11, 14, and 17 after seed germination. Statistical analysis showed that the number of leaves of the *fas 1-3* mutants was significantly affected comparable to wild-type on days 11 (2.573E-18), 14 (1.141E-25) and 17 (1.012E-31). (B-D) Seed viability in percentage was assessed in the wild-type and *fas 1-3* mutants. The *fas 1-3* showed 66%, 70% and 70% compared to 94%, 96%, 96% in the wild-type on days 11, 14 and 17 after seed germination N=50. (***)=P<0.005, T.test)

3.3.4.2 *fas 2-3* seeds are cisplatin sensitive.

The characterisation of *fas 2-3* phenotype also suggested mitotic defects. This was verified in the mitotic atlas prepared to the *fas 2-3* mutants comparable to wild-type. Anaphase bridge formation was shown in *fas 2-3* mutant. This suggested that the FAS 2 protein also might play a role in the DNA repair during mitosis.

To further verify this, *fas 2-3* sensitivity to cisplatin was assessed by; the quantification of the number of leaves per plant and the percentage of viable seeds. Counts were taken on days 11, 14 and 17 of seeds germination on MS agar medium with 30 μ M cisplatin. A hundred seeds from *fas 2-3* as well as the wild-type were placed on two MS agar plate (50 seeds each), and then incubated at 22° C. The results showed that the *fas 2-3* mutant seeds were highly sensitive to the cisplatin. The *fas 2-3* mutant showed 48% viable seeds compared to 94% in the wild-type on day 11 of seed germination (**Figure 3.25 B**). The *fas 2-3* mutant formed 0.84 leaves per plant compared to 3.52 in the wild-type (**Figures 3.24 & 3.25 A**). Statistical analysis showed that these differences were significant ($1.347E-22$, T-test). Moreover, the *fas 2-3* seeds germination was highly reduced on day 14 showing 48% viable seeds compared to 96% in the wild-type (**Figure 3.25 C**). The *fas 2-3* mutant showed 0.96 average leaves per plant compared to 3.84 in the wild-type (**Figures 3.24 & 3.25 A**). Statistically these differences were also significant ($3.482E-28$, T-test). And on day 17 the *fas 2-3* showed 48% viable seeds compared to 96% in the wild-type (**Figure 3.25 D**). The *fas 2-3* mutant showed 0.96 leaves average compared to 5.72 in wild-type (**Figures 3.24 & 3.25 A**), indicating that *fas 2-3* are significantly different from the wild-type ($3.619E-35$, T-test).

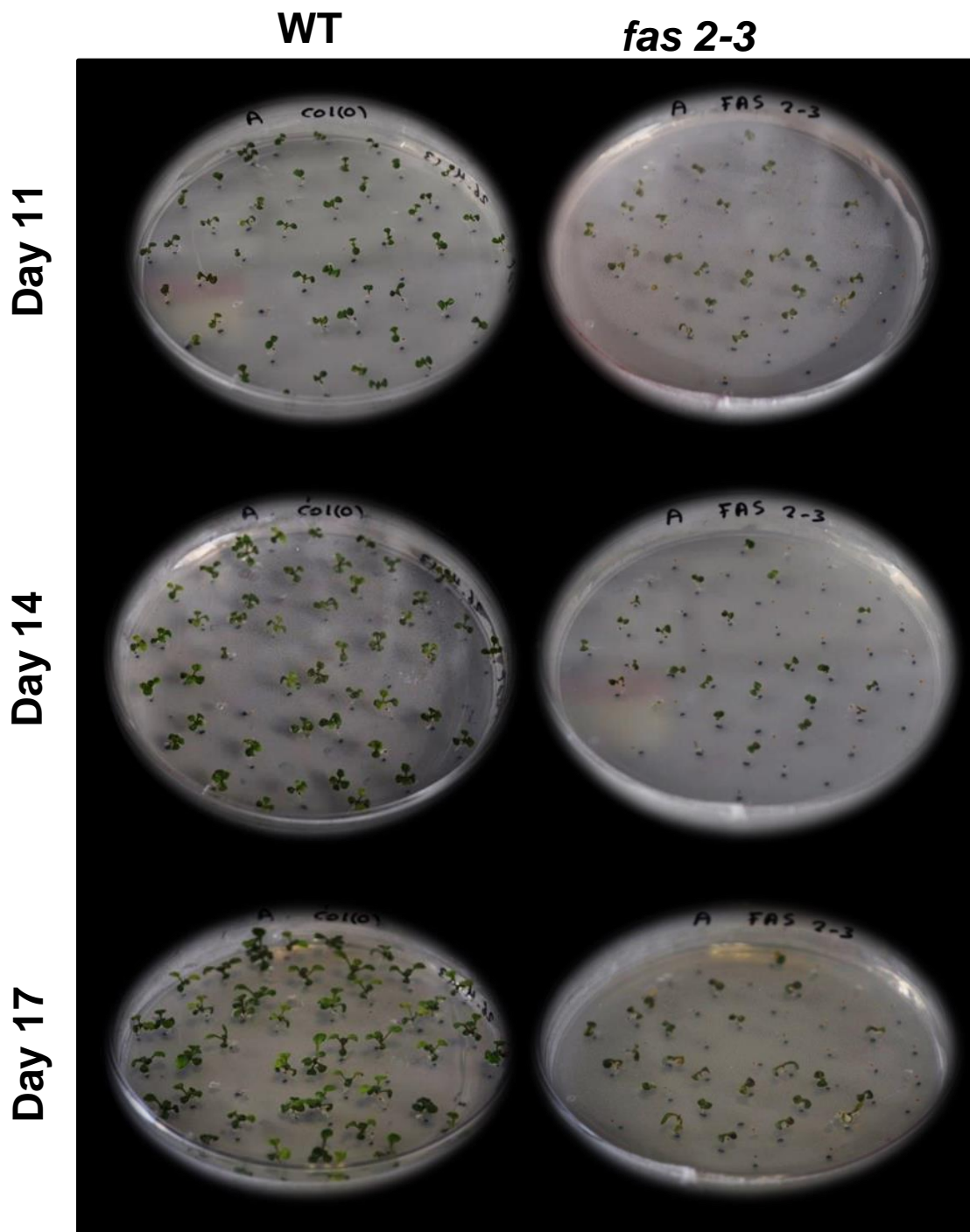


Figure (3.24): Cisplatin sensitivity phenotype of wild-type and *fas 2-3* seeds. Seeds of wild-type and *fas 2-3* plants were grown on MS plates containing 30 μ M cisplatin. Seeds were assessed on days 11, 14 and 17 after seed germination.

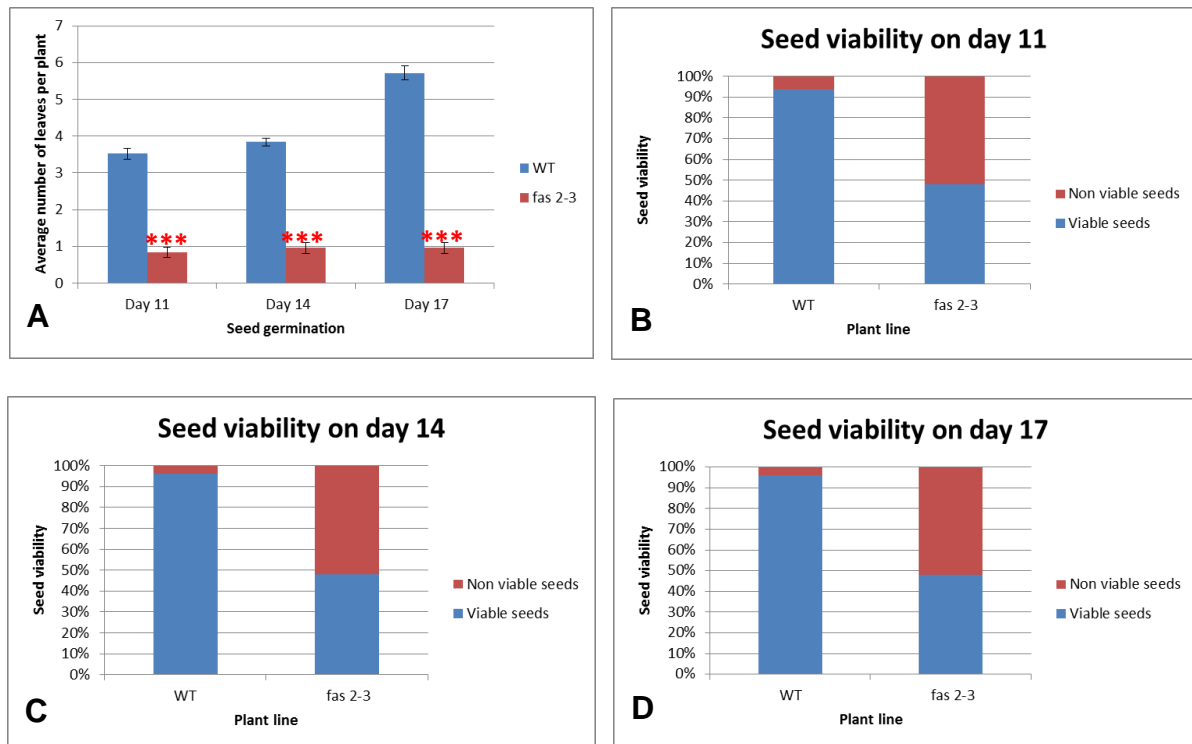


Figure (3.25): Cisplatin sensitivity analysis of wild-type and *fas 2-3* seeds.

(A - B) Seeds of wild-type and *fas 2-3* seeds were grown on 30 μ M cisplatin treated MS medium. (A) Number of rosette/ leaves per plant was assessed in the wild-type and *fas 2-3* mutants on days; 11, 14, and 17 after seed germination. Statistical analysis showed that the number of leaves of the *fas 2-3* mutants was significantly affected comparable to wild-type on days 11 (1.34723E-22), 14 (3.48239E-28) and 17 (3.61969E-35). (B-D) Seed viability in percentage was assessed in the wild-type and *fas 2-3* mutants. The *fas 2-3* showed consistant percentage of viable seeds of 48% compared to 94%, 96%, 96% in the wild-type on days 11, 14 and 17 after seed germination N=50. (***)= $P < 0.005$, T.test).

3.4. Discussion

3.4.1. *Arabidopsis* genome encodes for eight isoforms of histone H4

The eight *Arabidopsis* histone H4 proteins are identical, with the same amino acid sequence, suggesting similar protein functionality within the nucleus for all of these copies or isoforms. The fact that *Arabidopsis* possess eight identical copies for histone H4, invites us to ask ourselves some key questions about the importance of this protein. What functions it might play inside the nucleus? What is the need for multi-copies of this protein?

As *Arabidopsis* possesses eight identical copies of the H4 genes. And since, reports addressed gene redundancy effect in *Arabidopsis* (Nowak *et al.*, 1997). Hence, *H4* single gene knock-Out strategy would not show us any phenotypic effect. The presence of another seven wild-type *H4* genes is expected to compensate for the loss of single *H4* locus. Moreover, the other scenario of knocking out seven out of the eight *Arabidopsis* H4 genes is un-applicable; due to the gene inter chromosomal linkage distance. For all of that, H4 knock-Down mutants, $h4^{RNAi}$, is the best choice to see a possible phenotypic defect as a result of reduced histone H4 protein level in the nucleus.

3.4.2. Histone $h4^{RNAi}$ mutant show abnormal meiosis

Analysis of $h4^{RNAi}$ line and their progeny clearly indicated that histone *h4* mutants have reduced fertility in *Arabidopsis*. To understand the basis of these fertility defects seen in the $h4^{RNAi}$ line cytological preparations were studied in the mutant and their reference wild-type plants. The $h4^{RNAi}$ meiotic cells were investigated and compared to their corresponding wild-type phenotype. The semi sterile $h4^{RNAi}$ line phenotype meiotic origin was confirmed observing *h4* meiocytes abnormalities. Chromatin fragmentation was clearly visible through early meiotic stages at zygotene–pachytene- diplotene in $h4^{RNAi}$ line, but never seen in the wild-type. Moreover, non-homologous chromosomes connections were observed at diakinesis in $h4^{RNAi}$ mutant. The $h4^{RNAi}$ meiotic chromosomal abnormalities cause chromosome mis-segregation and hence, lead to nonviable aneuploid telophase II cells comparable to haploid viable tetrads in the wild-type. Nevertheless, the $h4^{RNAi}$ line also formed viable gametes with potential to develop seeds. As a result, the seed number per

silique was significantly reduced in the $h4^{RNAi}$ mutant with some gaps comparable to the wild-type. Analysis of large number of histone $h4^{RNAi}$ line for three generations showed that the seed production capability ranges between semi-sterile up to wild-type like plants (data not shown), which implied that the level of histone H4 reduction varied inter generation and intra generations suggesting that the h4 knock down RNAi level differ in-between some of the individual plants.

Defects in several *Arabidopsis* genes coding for the recombination proteins (AtDMC1 and AtSPO11-1) and DNA damage repair proteins (AtATM, ATXRCC3 and MEI1) had showed elevated non-viable gametophyte and abnormal fertility potential (Bleuyard and White, 2004; Couteau *et al*, 1999; Grelon *et al*, 2001, 2003; Garcia *et al*, 2003). In these mutants the semi-sterile phenotype observed was correlated with meiosis defects. Furthermore, chromosome fragmentation has also been shown to be responsible for meiotic defects in some mutants like *atxrcc3* (Bleuyard and White, 2004).

Moreover, some reports have addressed that histone H4 modification might play an important role in the signalling of DNA double strand break repair response (Kothapalli *et al.*, 2005; Corsini and Sattler, 2007). A study on human histone H4 showed that decrease in K12 biotinylation occurred temporally as a response to DSBs but it was not observed in DNA single strand breaks, hence it could act as an early DSB response signalling (Kothapalli *et al.*, 2005). Biotinylation of K12 was found to play a role in the reassembly of nucleosomes as a response to DNA repair (Kosmoski *et al.*, 2001). Cells response to DSBs demand alteration in the chromatin

structure (Bakkenist and Kastan, 2003). Chromatin structures relaxation mediated by histone modifications allows DNA repair factors access to DNA breaks sites (Fernandez-Capetillo *et al.*, 2004; Kothapalli *et al.*, 2005). Suggesting that histone H4 rapid K12 biotinylation was declined in response to DSBs mediates chromatin shift to open and relaxed phase, which permits DNA repair proteins access to the DSBs sites (Kothapalli *et al.*, 2005). Histone H4 biotinylated at K12 is known in the condensed chromatin (e.g. pericentromeric heterochromatin) (Hassan and Zempleni, 2006). This role is not yet addressed in *Arabidopsis*. Hence further research is needed to understand if the chromatin breakage visualised in the $h4^{RNAi}$ meiocytes is due to failure in DNA DSBs processing during meiosis as a result of chromatin structure accessibility defects or it is a result of structural defects in the meiotic chromosome.

3.4.3. Histone $h4^{RNAi}$ mutants show NORs organization defects

By comparing the $h4^{RNAi}$ meiotic stages to that of the wild-type an abnormal structure and location of the nucleolus organising region (NOR) was identified. Usually the NOR in the wild-type pachytene is compacted in a way that permits the 45S rDNA regions at chromosomes 2 and 4 to be associated in a unique transcription factory. This was proofed by 45S rDNA FISH analysis. The wild-type pachytene cell show one green 45S signal indicating chromosomes 2 and 4 joining at the NOR region. Whereas, the tangled NORs region in the $h4^{RNAi}$ line suggests that the improper compaction imbed NORs of chromosomes 2 and 4 association. This suggestion was approved as 45 S rDNA FISH showed two discrete signals at pachytene. A possible

role for H4 modifications might direct NOR compaction status and hence affecting intra chromosomes 2 and 4 association. Some reports showed that the normal mitotic histone H4 acetylation at lysines 5 and 12 in barely (*Hordeum vulgare*) shifts to less compact NOR and so easing its association (Wako *et al.*, 2005). Moreover, *in vitro* experiments showed that H4K16Ac is linked with chromatin decondensation (Shogren-Knaak *et al.*, 2006). The suggested impact of histone H4 on NOR compaction status and association was clear at pachytene and diakinesis stages, where histone H4 reduction resulted in two separate 45S rDNA signals. Besides to this, NOR fragmentation of chromosome 4 at pachytene suggests chromosomal translocation events to happen, a thing which is still seen at diakinesis, in which abnormal physical distance in-between the 45S and 5S signals of chromosome 4 indicates that the 5S region possibly could be involved in ectopic recombination events during meiosis.

A study by Prado and Aguilera (2005) showed that partial depletion of histone H4 in *Saccharomyces cerevisiae* resulted in 20 fold increase in the homologous recombination between ectopic DNA sequences compared to wild-type level. The increase in recombination in the H4 depleted cells was accompanied with Rad52-YFP foci accumulation. The Rad52-YFP foci are known as an indicator for the link between DNA replication and homologous recombination in response to S and G2/M DNA DSBs (Lisby *et al.*, 2001, 2003). The *Saccharomyces cerevisiae* depleted h4 cells showed delayed S and G2/M phases as well, suggesting that chromatin assembly was impaired due to H4 deposition depletion, leading to DNA synthesis

defects appeared as recombinogenic DNA structures, hence, consequently genomic instability increased (Prado and Aguilera, 2005).

The eukaryotic genomes contain hundreds of repetitive sequences arranged in 45S ribosomal RNA (rRNA) genes (45S rDNAs) which when transcribed by RNA polymerase I three rRNA structures; 18S, 5.8S and 28S are formed. Several reports proposed a role for the 45S rDNA in eukaryotic genome instability. In *Neurospora*, the nucleolus organized region (NOR) (crack) removal resulted in big terminal loss knowing that the exposed 45s rDNA terminus is capped with a telomeric repeats that imbed their termini union (Butler, 1992). Furthermore, 45S rDNA breaks in *Lolium rigidum* caused changes in 45S rDNA number and location sites showing chromosome rearrangement (Thomas *et al.*, 1996). Moreover, 45S rDNA sites in *Arabidopsis* with abnormal telomerase showed gene rearrangement, fusion and chromosome bridges (Siroky, 2003).

3.4.4. *fas* mutants displayed developmental defects

fas mutant plants phenotype was unusual compared to the wild-type *Arabidopsis* plants. Its stem appearance as flat and broad, reflecting the term *fasciata*, and it shows clearly that *fas* mutants are unable to grow normally. *fas* mutants developmental defects were stated previously by Leyser and Furner (1992). Histological analysis of *fas* mutants indicated that *fas1* and *fas2* mutants have showed abnormal shoot apical meristem (SAM) and root apical meristem (RAM) postembryonic organisation. And that the SAM and RAM mis-function seen in these

mutants were referred to mis-expression in WUSHEL (WUS) and SCARECREW (SCR) genes respectively (kaya *et al.*, 2001).

The *fas* mutant phenotypic defects suggested a role for mitotic genome behaviour. Instable mitotic chromosomes phenotype was noticed at anaphase-telophase. Defects were represented as anaphase bridges formation, anaphase chromosomes lagging and chromatin fragmentation. For this, we can say that mitosis instability is mostly the causative of this abnormal phenotype. FAS might be able to preserve genome integrity by allowing fast nucleosomes reconstitution to facilitate chromatin reformation after passing the replication fork. This prediction depends on results obtained by Ridgeway and Almouzni (2000) and Verreault (2000) where *in vivo* experiment on human proliferating cells showed CAF-1 association with newly formed H3.H4 histones and positioned on the replication foci meanwhile DNA replication indicating chromatin assembly activity and DNA repair. Smith and Stilman (1989) also showed that CAF-1 plays an role in nucleosomes assembly at the replicating DNA *in vitro*.

3.4.5. fAS mutants show semi-sterile phenotype

Quantification of seed set per silique in the *fas 1-3* and *fas 2-3* showed massive reduction comparable to the wild-type (**Table 3.2**). This phenotypic defect was expected as their siliques were highly reduced. Each time *fas 1-3*, *fas 2-3* and the wild-type plants were germinated a similar phenotype was observed, and even re-quantifications of the seed sets in a single silique showed similar average values.

These results confirmed a role for both *fas 1-3* and *fas 2-3* importance in *Arabidopsis* fertility. Moreover, running statistical analysis between *fas 1-3* and *fas2-3* in terms of either seed set average or silique length showed no significant difference in the seed set per pod, with p value of (0.928), however siliques length were significantly different with P-value of (0.003). And so, it seems that *fas 1-3* and *fas 2-3* have similar impact on seed formation in *Arabidopsis*. The significant silique length difference recorded between *fas 1-3* and *fas 2-3* mutants did not reflect significant difference on seed sets formation. Besides that, although *fas 1-3* showed longer siliques in reference to *fas 2-3* but, it contains lower seed sets mean. At the moment we cannot draw any conclusion from this. More analysis is needed to understand *fas 1-3* and *fas 2-3* individual roles on *Arabidopsis* development.

Plant Line	Seed no. per silique mean (A) N=50	P.value (A)	Silique length mean (B) N=50	P.value (B)
<i>fas 1-3</i>	11.22 ± 8.013 (A) 79.3 % (C)	4.37476E-49	8.42 ± 2.425 (B) 42.32% (D)	2.97791E-25
<i>fas 2-3</i>	11.62 ± 6.256 (A) 78.6% (C)	6.24001E-58	7.27 ± 1.225 (B) 50.2% (D)	3.56241E-53
WT	54.28 ± 5.503 (A)		14.6 ± 1.030 (B)	

Table (3.3): comparison of sterility level intra *fas* mutants in reference to wild-type plants.
(C) Percentage of reduction in seed sets per silique. (D) Percentage of reduction in silique length.

3.4.6. *fas 1-3* and *fas 2-3* semi-sterile phenotype has meiotic origin

The defects seen in the seed set number per pod gave a clue about FAS impact on meiosis. And by analysing meiocytes in both *fas 1-3* and *fas 2-3* mutants we found that this was true. Several defects were observed in the meiotic sub stages during MI and MII which finally produced gametes lacking the normal chromosomal number. Meiotic cells derived from *fas 1-3* mutants showed chromatin breakage and fragments through all the studied prophase I and at later stages at metaphase II, and also univalents were observed at metaphase I and chromosome mis-segregation at metaphase II. Hence, some of the final gamete products could not be viable. These chromosomal aberrations during meiosis are most likely the cause of the semi-fertility phenotype in *fas* mutants. As previous reports related fertility defects with meiosis progress (reviewed by Osman *et al*, 2011).

The meiotic errors seen in *fas 2-3* were not away from the ones observed in *fas 1-3*. Although meiotic preparations from *fas 2-3* were not successful as *fas 1-3*, but still the few *fas 2-3* meiocytes observed showed chromatin fragmentation at pachytene similar to that seen in *fas 1-3* pachytene. The meiotic aberrations similarity between *fas 1-3* and *fas 2-3* besides to the fact that statistically seed sterility level similarity might indicate that both FAS 1-3 and FAS 2-3 are needed for proper chromosomal behaviour through meiosis. And that each of FAS proteins has its specific meiotic role that cannot be replaced by one of the other. Moreover, FAS 1-3 and FAS 2-3 are predicted to be working in the same complex as independent subunits of each other, nevertheless, neither of the two mutations caused completely sterile plants, which suggest the presence of another factor that permits ascertain level of meiosis.

Hence, the third CAF-1 subunit (MSC11) might play this role. More investigation using double mutants would be needed to clarify this prediction.

The *Arabidopsis* chromosomal breakage observed in the studied *fas* mutants showed a suggested role for FAS in DSB maintenance. This prediction agrees with results reported previously showing elevated DNA repair proteins transcriptions in *fas* mutants. Endo *et al.* (2006) reported that *fas* mutants showed elevated DSBs in *fas 1-2* and *fas 2-2* mutants 40 times fold the number observed in wild-type *Arabidopsis*. Furthermore, chromatin fragmentation and breakage phenotype were consistent in several *Arabidopsis* mutants related to mal-function of one of the DSB repair mechanism proteins. All mutants of *mre11*, *rad51* and *xrcc3* showed meiotic chromatin fragments (Couteau *et al.*, 1999; Grelon *et al.*, 2001, Garcia *et al.*, 2003; Grelon *et al.*, 2003; Bleuyard and White, 2004; reviewed by Osman *et al.*, 2011). Although their fragmentation severity varied, all shared the fact that they are proteins involved in meiotic DNA repair machinery.

Moreover, the analysis of *Arabidopsis fas 1-4* mutant were found to show dramatic increase in the intrachromosomal homologous recombination by 96 fold even when expression of DNA repair genes like RAD50, MRE11 and RAD51 was not upregulated. These results together with the finding that *fas 1-4* showed reduced heterochromatin content allowed Kirik *et al.* (2006) to suggest that the DNase 1 hypersensitivity in the open chromatin structure could be responsible for the observed genome instability phenotype.

3.4.7. *fas* mutants have similar defects to *h4^{RNAi}* mutants

The phenotypic partial similarity between *h4^{RNAi}* mutant plants and *fas* mutants in terms of showing broad twisted stems in some cases was not strange, as both mutants share histone H4 deposition problems. Although, both mutants shared genomic stability failure as mitotic chromosomal errors were consistent in both mutants represented as anaphase bridge formation, but the fragmentation shown in *fas* mutants showed more severe mitotic defects. The more affected *fas* mutants phenotypic changes still need an extra analysis to confirm if the results obtained are due to histone H4 lack only, or other factors are involved since *fas* free cells retard the chromatin assembly complex formation and function.

Fertility reduction recorded in *h4^{RNAi}* and *fas* null mutants indicated that they are significantly different (**Figure 3.26**). T-test analysis of seed set per silique resulted in P- values of (7.8917E-17) and (7.81771E-18) for the difference between *h4^{RNAi}* and *fas1-3*, *h4^{RNAi}* and *fas 2-3* respectively. *fas 1-3* and *fas 2-3* were found to have 32% and 31.3% extra reduction in mutant ability to produce seeds. Suggesting that FAS might retain normal fertility levels by affecting or communicating with other proteins besides to H4. Since the further reduction in fertility in *fas* null mutants was not joined with a different meiotic defect from *h4^{RNAi}* mutant in the studied PMCs, as both *fas* and *h4^{RNAi}* mutants showed clearly meiotic chromatin fragmentation and breakage, we cannot draw more conclusion about FAS role in preserving meiotic structural chromosomes without analysing more mutant cells and analysing other related mutants, besides to carrying further proteomic analysis. We also have to keep in mind that the *h4^{RNAi}* mutant line that we studied has a depleted H4 protein which

means that nucleosomes build up is not fully retarded and hence normal nuclear structural components are still there to carry on the desired functions to some level.

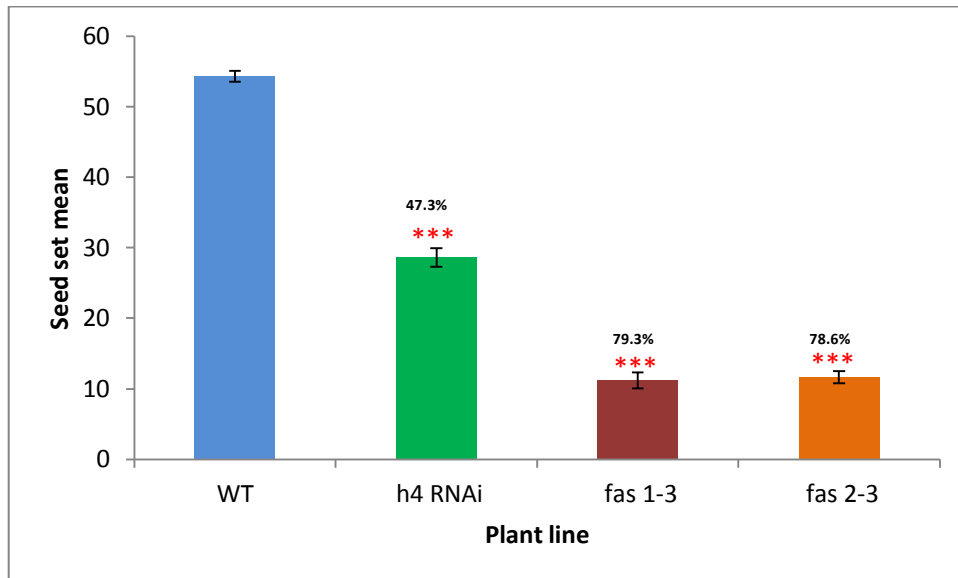


Figure (3.26): Comparison of seed set per silique mean in $h4^{RNAi}$ and *fas* mutants vs wild-type. Percentages show sterility frequency per plant line. (N=50). Error bars = standard error of the mean.

3.4.8. Histone H4 is needed for mitotic chromosome architecture

A defect seen in the mitotic cells of the $h4^{RNAi}$ mutants suggests a role for histone H4 in preserving the structural chromosomes integrity. Anaphase bridges were consistent in the $h4^{RNAi}$ as well as in the *fas* mutants showing a possibility of chromosome fragmentation or defects in the inter sister chromatid homologous recombination. Few reports suggested a link between histone H4 and the cell cycle (Megee *et al.*, 1995). In *Saccharomyces cerevisiae* the amino-terminal domain of histone H4 loss prevents nuclear division progress. Moreover, genome integrity in *Saccharomyces* is maintained in a lysine-dependent manner of histone H4. And that mutation in *Saccharomyces* lysines activates G2/M checkpoint RAD9-dependent

pathway (Megee *et al.*, 1995). Furthermore, Shogren-Knaak and Peterson (2006) proposed that histone H4 acetylation either has a role on the higher order chromatin organisation by shifting to transcriptionally active chromatin or cause alteration in the chromatin-proteins binding potential (yet to be studied). Loss of acetylation of the H4 K16 is known in several cancers, indicating that failure of the normal chromatin structure regulation impedes proper cell growth and division, hence resulting in the normal cells shift to cancer (Shogren-Knaak and Peterson, 2006). Interestingly, the histone epigenetic code changes were found to have a role in the chromatin structure shift from compact phase (highly organised) to loose phase of organisation and vice versa (Cimini *et al.*, 2003). Moreover, the deacetylated core histones H3 and H4 (H3-Deac and H4-Deac) were detected at the highly compact heterochromatin (reviewed by Cimini *et al.*, 2003). Hyperacetylation of H3 in the human primary fibroblasts was found to cause abnormal chromosome condensation and constrain mitotic progression *in vivo* as a result of an expected cell checkpoint activation. FISH analysis revealed the presence of anaphase chromatin bridges, suggesting that cohesion persistence along the sister chromatids arms beyond centromere separation constrain the normal sisters separation. On another hand, chromosome condensation defect resulted from hyperacetylated chromatin were suggested to cause improper sister chromatid resolution, and showing lagging chromosomes formation associated with depletion in the heterochromatin protein 1 and resulting in kinetochore-microtubules mis-attached in a reciprocal manner (Cimini *et al.*, 2003).

Several reports indicated that chromatin structure has a dynamic status. Chromatin dynamic is the result of its ability to be influenced by several factors; “chromatin-

modifying enzymatic complexes and by the action of several other enzymatic activities such as condensins and cohesins, topoisomerase II, and the securin/separin pathway” (reviewd by Cimini *et al.*, 2003). Further analysis is needed to understand the role of chromatin structure in the sister chromatid condensation and chromosome segregation to allow better understanding of chromatin role in the genomic instability.

It was reported that mutants of the CAF1 components, *fas1* and *fas2*, in *Arabidopsis* results in telomere shortening. Telomere shortening was associated with 45S rDNA loss, however, the other repetitive sequences; 5S rDNA, centromeric 180-bp repeat, CACTA, and Athila, were unchanged. Interestingly, the cytological phenotype of the *fas* mutants showed accumulation of anaphase bridges, suggesting that FAS is needed for the stability and maintenance of chromosomal telomeres and 45S rDNA sites (Mozgova *et al.*, 2010). Since reports indicated that CAF1 malfunction in plants has been associated to increase in the: DNA DSBs numbers, HR level, and upregulation of genes involved in HR (Endo *et al.*, 2006; Kirik *et al.*, 2006; Schonrock *et al.*, 2006; Ramirez-Parra and Gutierrez, 2007), hence it is suggested that 45S rDNA loss is the result of unbalanced level of the normal recombination events.

3.4.9. Mutants of *h4*^{RNAi} and *fas1&2* are sensitive to cisplatin

Moreover, the *h4*^{RNAi} mutants growth on 30 µM cisplatin plates was abnormal. The *h4*^{RNAi} mutants showed delayed vegetative growth as well as reduction in the number of viable seeds comparable to wild-type, suggesting that DNA repair induced in the

h4^{RNAi} mutants was out of function. Cisplatin (cis-Diamminedichloroplatinum II) is a chemotherapy which is used as a powerful treatment of a variety of human cancers (Loehrer, 1948; Muggia, 1991; Einhorn, 1994; Muggia and Muderspach, 1994). Cisplatin forms covalent platinum- DNA crosslinks that cause DNA damage (Wang and Lippard, 2004). Cisplatin application enhance various cellular responses; DNA repair, transcription inhibition, cell cycle arrest, and apoptosis, all processes that demands chromatin structural remodeling and dynamics (Nilsson *et al.*, 2010). Further analysis is needed to understand if the somatic viability defects observed in the *h4^{RNAi}* mutants are caused by H4 depletion or it is due to epigenetic deregulation caused by H4 depletion.

The significant decrease in seed viability besides to growth defects observed in *fas 1-2* and *fas 2-3* mutants suggests that the DNA repair is inefficient. A study by Nabatiyan *et al.* (2006) showed that *caf-1^{RNAi}* quiescent cells treated with bleocin in vivo showed significant reduction in cell viability associated with increase in DSBs. This allowed Nabatiyan *et al.* (2006) to suggest that CAF-1 play a role in the human quiescent cells response to DSBs via permitting chromatin reassembly afterwards DNA breaks repair. Several factors are causing eukaryotic DNA damage; ionizing radiation, mutagenic chemicals, and reactive oxygen species, which demands genome integrity maintenance by efficient DNA repair mechanisms (Lindahl and Wood. 1999; Caldecott, 2003; Friedberg, 2003). Besides to this, several reports indicated that besides to the DNA damage response, the chromatin accessibility and remodelling play a key role in the successful DNA damage response (Gontijo *et al.*, 2003; Peterson and Cote; 2003; Nabatiyan *et al.*, 2006), via allowing proper

responding to DNA damage; recognition and repair, in addition to restoring chromatin structure and information (Nabatiyan *et al.*, 2006)

CHAPTER 4
Genetic Analysis of Histone H1 Isoforms in
Arabidopsis

4.1 INTRODUCTION

Histone H1 is one of the most abundant nuclear proteins which is physically associated to the linker DNA between nucleosomes (Smith *et al.*, 1980). Histone H1 might act as an “adjustable clip” at this position and so H1 might have a role in the formation of higher order chromatin structures (**Figure 4.1**) by allowing the packaging of the dynamic nucleosome fiber (Rutledge *et al.*, 1981; Robinson and Rhodes, 2006). Histone H1 protein sequence is evolutionary conserved among higher eukaryotes. Nevertheless, several variant isoforms have been identified (Millan-Arino *et al.*, 2014), as well as different post-translational modifications (Wisniewski *et al.*, 2006). It has been postulated that H1 proteins have a general role in preserving the typical functionality of the nucleus, playing crucial roles in: DNA repair, DNA replication, transcription and cell division. Previous reports showed that H1 loss presented a significant impact to the vital nuclear processes that control the normal cellular and chromosomal integrity, ranging from homologous recombination blockage in yeast (Downs *et al.*, 2003), the reduction of fungal life span (*Ascobolus immerses*) (Barra *et al.*, 2000), aberrations in *Tobacco* male gametogenesis due to abnormality in homologues pairing and or segregation (Prymakowska-Bosak *et al.*, 1999) and presenting mitotic chromosomal structure defects (Maresca *et al.*, 2005). Moreover, the presence of several isoforms and copies for H1 gene in plants and animals (Fan *et al.*, 2001) presents a challenge, since the loss of one H1 isoform could be compensated by other H1 copy or isoform making difficult the analysis of each H1 isoform separately. Some publications have shed the light on the impact of individual histone H1s genes on the nuclear and chromatin organisation in different species. Nevertheless, there are very limited studies of H1s in *Arabidopsis* and plants

in general (Wierzbicki and Jerzmanowski, 2005; Rea *et al.*, 2012). In this chapter we are presenting a comprehensive genetic, phenotypic and molecular analysis of the different histone H1 isoforms present in *Arabidopsis*. The ability to study single knock-out mutants for each of the ten *Arabidopsis* H1s genes will help us to understand the role and importance of each H1 gene isoform in nuclear functionality. The presences of this number of histone H1 genes produce an increased complexity and a challenge to analyse each histone H1 specificity as it could be some functional redundancy among the different isoforms. The main aim of this study is to investigate the role of each H1 protein in *Arabidopsis*. Since the H1 protein sequence is, in an extent, evolutionary conserved, our findings could help in the understanding of histone H1s role in chromatin structure dynamic within the nucleus in other species including other plants, animals and, of course, human.

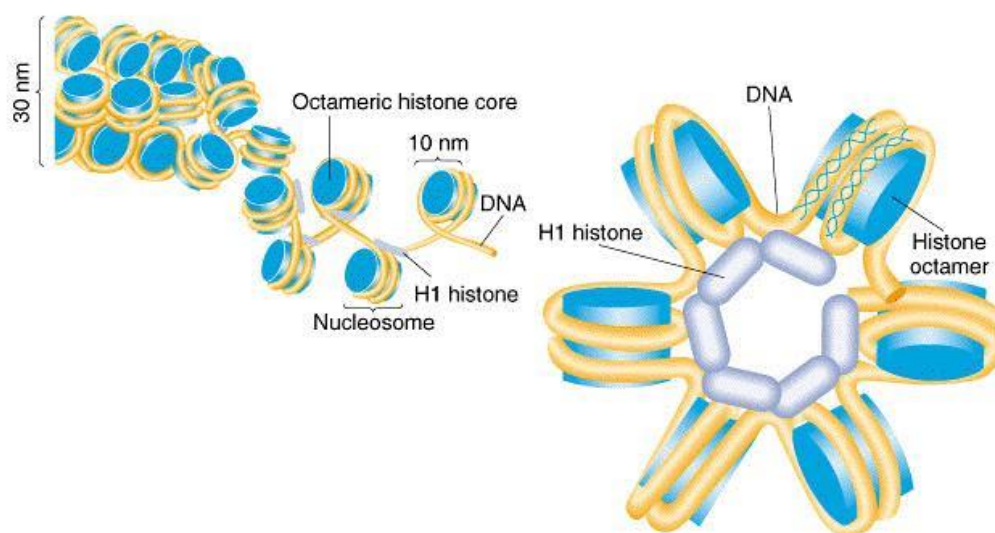


Figure (4.1): Histone H1 structural role in higher order chromatin structures formation.

Histone H1 associates to the linker DNA between adjacent nucleosome. It acts as “adjustable clip” which controls nucleosomes formation of the primary nucleosome fiber (10 nm), allowing it to proceed to higher compact chromatin structures (30 nm)

http://www.cbs.dtu.dk/courses/genomics_course/roanoke/genetics980218.html

4.2 RESULTS

4.2.1 *In Silico* Analysis of histone H1 isoforms in *Arabidopsis*

4.2.1.1 Identification of histone h1 isoforms in *Arabidopsis*

Ten non identical copies for histone H1 proteins were identified in *Arabidopsis* using WU-BLASTp in TAIR by their sequence similarity to histone H1 proteins from yeast and mammalian species: At1g06760, AT1G17520, AT1G48610, AT1g48620, AT1G54260, AT1G72740, AT2G18050 and AT2G30620, AT3G18035 and AT5G08780. The genes coding for these proteins were localised along the genome of *Arabidopsis thaliana*; 6 genes in chromosome 1, 2 genes in chromosome 2, 1 gene in chromosome 3 and 1 gene in chromosome 5 (**Figure 4.2**). A reverse genetic approach was followed to analyse the role of these genes by using T-DNA transformed mutant lines and RNAi technology. Our study focus on characterising any phenotypic changes observed on the different mutant plants. In order to simplify, throughout this chapter, AT1G06760, AT2G30620 and AT2G18050 will be referred to as H1.1, H1.2 and H1.3 respectively as previously described by Jerzmanowski and Wierzbicki, (2005). AT1G48620 and AT3G18035 will be referred to as HON5 and HON4 respectively according to The Arabidopsis Information Resource-TAIR (<http://www.arabidopsis.org>). And finally the genes AT1G54260, AT5G08780, AT1G48610, AT1G72740 and AT1G17520 we will be addressing them as H1A, H1B, H1C, H1D and H1E respectively (**Table 4.1**).

Linker Histone H1 proteins can be grouped into three categories in *Arabidopsis* according to their amino acid sequence of the conserved domains. These categories

are: HMG-LIKE, H1-LIKE and MYB-LIKE as it is shown in **(Figure 4.3)** (Eugenio Sanchez-Moran). The HMG-like group of linker histone H1 are proteins which share the high mobility group A (HMG A) characteristic domain, with the presence of an AT-hook, and AT-hook-like DNA binding motifs. The AT-hook motif is present in a wide range of nuclear proteins including; high mobility group (HMG) proteins (Reeves and Beckerbauer, 2001), DNA binding proteins (Meijer *et al.*, 1996) and the chromatin remodelling (SWI/SNF) complex (Singh *et al.*, 2006). The AT-hook domain consists of a conserved core sequence; proline-arginine-glycine-arginine-proline, flanked with different number of positively charged lysine and arginine residues (Reeves, 2001). The AT-hook name derived from its binding to the adenine-thymine (AT) rich DNA-minor groove in a way that forms crescent or hook (Reeves and Nissen, 1990).

The MYB-like domain group is the linker histone proteins which have MYB-like DNA binding domain. The name is derived from the retroviral oncogene v-myb, and its cellular counterpart c-myb. The plant MYB is an ortholog of the human MYB “Myeloblastosis”, an old name of a type of leukemia, of transcription factors. The human myb-*proto-oncogene* contains three domains; an N-terminal DNA binding domain, a central domain, and a C-terminal domain. MYB proteins contain 51 to 53 amino acid repeats termed R1, R2 and R3. Although all of the MYB motifs are DNA binding regions, the R2 R3 motifs have superior ability to bind to the DNA major groove directly. R2R3-type MYB domain has been characterized in the plant MYP protein family (Stracke *et al.*, 2001). Several reports on plants emphasized that the R2R3-type MYP proteins could act as gene regulator (Boddu *et al.*, 2006), or a suppressor (Lee and Harper, 2002).

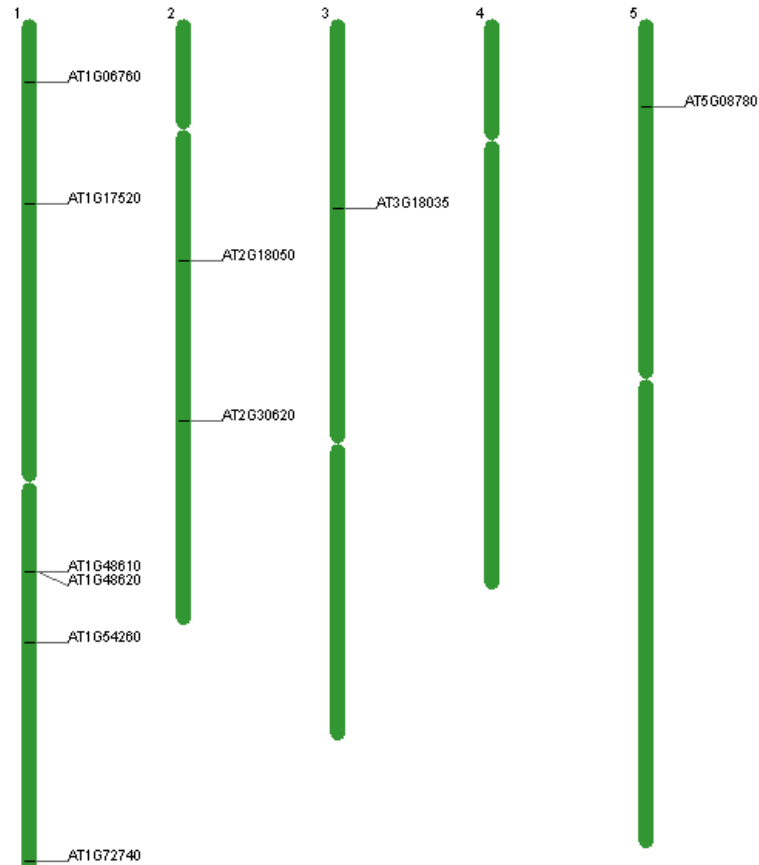


Figure (4.2): Localisation of histone H1 genes at the *Arabidopsis* chromosomes.

Arabidopsis thaliana possesses ten different genes coding for the Histone H1 protein isoforms. The chromosomal distribution for these genes is shown: six genes on chromosome one: AT1G06760 (H1.1), AT1G17520 (H1E), AT1G48610 (H1C), AT1g48620 (HON5), AT1G54260 (H1A) and AT1G72740 (H1D). Two genes on chromosome two: AT2G18050 (H1.3) and AT2G30620 (H1.2). One gene on chromosome three: AT3G18035 (HON4). And one gene on chromosome five: AT5G08780 (H1B). TAIR, Chromosome map tool, <http://www.arabidopsis.org/servlets/ViewChromosomes>

Histone H1 protein	Gene locus	T-DNA line
H1A	At1g54260	N877696-Sail_883_F09
H1B	At5g08780	N659488-salk_090072
H1C	At1g48610	N586260-Salk_086260
H1D	At1g72740	N65754-Salk_065267
H1.1-1	At1g06760	N521410-salk_021410
H1.1-2	At1g06760	N-654890-salk_128430
H1.2	At2g30620	N321948- GK-116E08
H1.3	At2g18050	N665594-Salk_025209
HON4	At3g18035	N599887-Salk_099887
HON5	At1g48620	N656137-salk_007422

Table (4.1): Histone H1s T-DNA mutant lines vs their given names through the research.

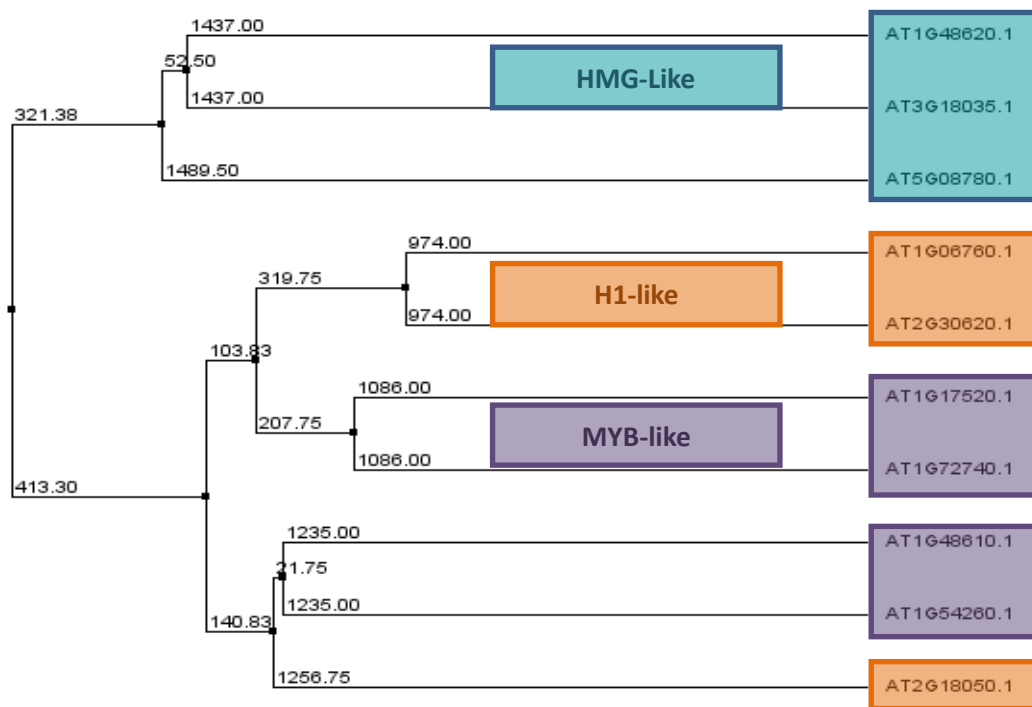


Figure (4.3): Homology protein sequence alignment of *Arabidopsis* histone H1 proteins.

Linker Histone H1 proteins can be grouped into three categories according to their amino acid conserved domain sequences present. The categories are: HMG-LIKE: At1g48620.1 (HON5), At3g18035.1 (HON4) and At5g08780.1 (H1B). H1- LIKE: At1g06760.1 (H1.1), At2g30620.1 (H1.2) and At2g18050.1 (H1.3). MYP-LIKE: At1g17520.1 (H1E), At1g72740.1 (H1D), At1g48610.1 (H1C) and At1g54260.1 (H1A). (Eugenio Sanchez-Moran)

4.2.1.2 Expression Pattern of the linker histone H1 genes

An expression analysis was carried out using Genevestigator, which enables information about specific *Arabidopsis* gene expression patterns referring to reported microarray data (Hruz *et al.*, 2008). This analysis showed that linker histone H1 genes; H1A, H1B, H1C, H1D, H1.1, H1.2, HON4 and HON5, are expressed in germinated seed, seedling, young rosette, developed rosette, buds, young flower, developed flower, flowers, siliques, and mature siliques (**Figure 4.4**). Thus, these findings confirm that these genes are expressed in both vegetative and reproductive tissues. However, H1.3 (At2g18050) seems to be expressed at the silique stage, indicating that it might play a specific role in the silique and or seed maturity (**Figure 4.4**). And H1C (At1g48610) expression seems to be increased at floral development (**Figure 4.4**).

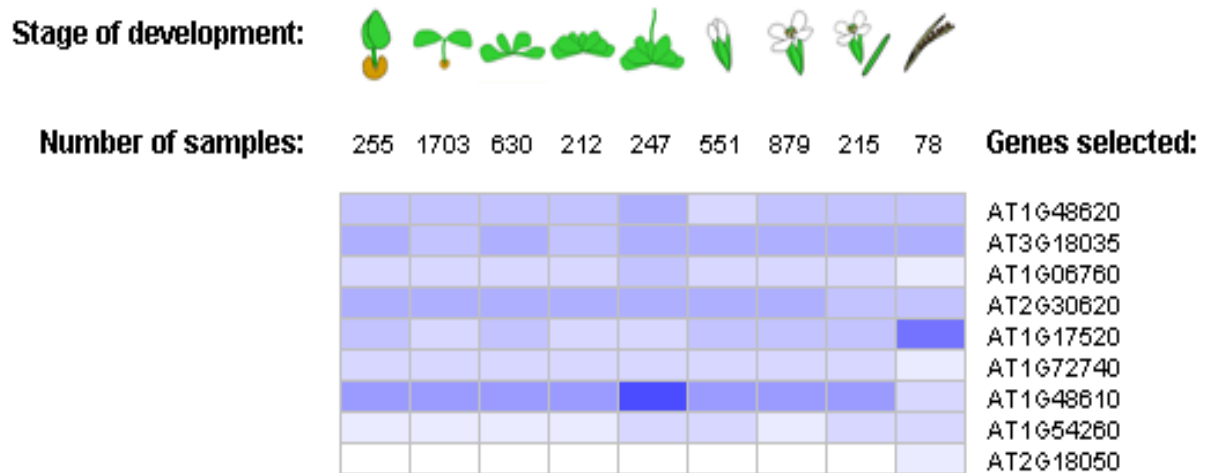


Figure (4.4): Expression profile of *Arabidopsis* histone H1 genes during plant developmental stages.

Eight of the histone H1 genes; At1g48620, At3g18035, At1g06760, At2g30620, At1g17520, At1g72740, At1g48610, At1g54260, expression is seen throughout the whole plant growth stages: seeds, seedling, rosette, buds, flowers and siliques, while one gene; At2g18050, is expressed at silique maturation only. <https://www.genevestigator.com/gv/index.jsp>. (Hruz *et al.*, 2008)

4.2.2. Characterisation of the *Arabidopsis* AtH1A isoform

H1A role within the nuclei was analysed using the N877696-Sail_883_F09 T-DNA insertion mutant brought from the NASC. The T-DNA express (Salk Institute) search showed that the *Ath1a* has a T-DNA insertion in the third intron at nucleotide 1170 of the *AtH1A* gene (**Figure 4.5**). Plants of the wild type and *Ath1a* mutants were genotyped via PCR using specific primers. LP-RP (**Table 2.2**) primers reaction showed the wild type band of about 1.133kb length on agarose gel however, RP-BP (**Table 2.3**) primers reaction showed the mutant band of about 0.485 kb on agarose gel. The double homozygote *Ath1a*T-DNA insertion mutant plants were analysed in parallel with the wild type plants in terms of phenotypic alterations and fertility quantification.

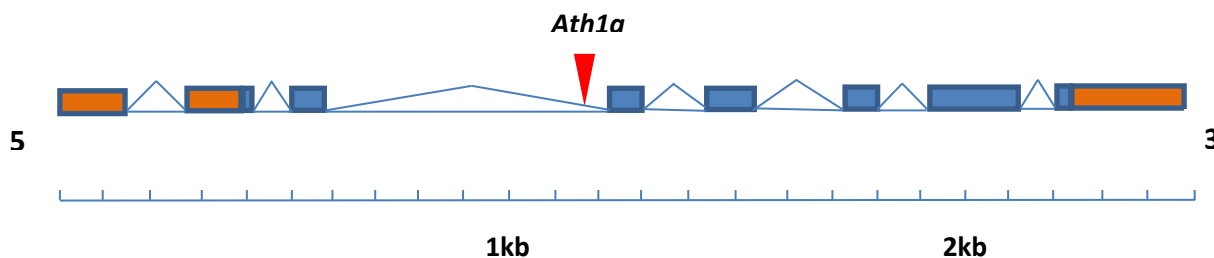


Figure (4.5): Schematic diagram of At1g54260 locus showing T-DNA insertion localisation.

2.482 kb of *AtH1A* sequence organisation into UTRs, exons and introns. Exons are represented with blue blocks, introns are shown as triangles and UTRs are diagrammed as orange blocks. N877696-Sail_883_F09 T-DNA insertion position is diagrammed as inverted red triangle. Diagram based on gene structure available on TAIR (www.arabidopsis.org).

4.2.2.1 Phenotypic observation of *Ath1a* mutant plants

The investigation of *Ath1a* N877696-Sail_883_F09 T-DNA homozygote mutant plants showed a normal growth in comparison to the wild-type plants. The *Ath1a* plants

were able to achieve normal development, as well as normal flowering time compared to wild type plants.



Figure (4.6): Phenotypic characterisation of *Ath1a* mutant plants
Ath1a mutant plants showed normal flowering similar to wild-type plants.

4.2.2.2 Fertility of *Ath1a* mutant plants

The assessment of fertility parameters in *Ath1a* N877696-Sail_883_F09 T-DNA and wild-type plants indicated that the *Ath1a* mutants had a normal level of fertility. Although the mean for the silique length in the *Ath1a* mutant in comparison to the wild type (**Figure 4.7 A**) were 13.27 mm and 14.14 mm respectively with a P-value of 0.0015 (T-test). But the average seed count for the *Ath1a* mutant compared to wild type (**Figure 4.7 B**) was 48.69 and 51.06 respectively with a P-value of 0.145 (T-test), suggesting that AtH1A does not affect seed production.

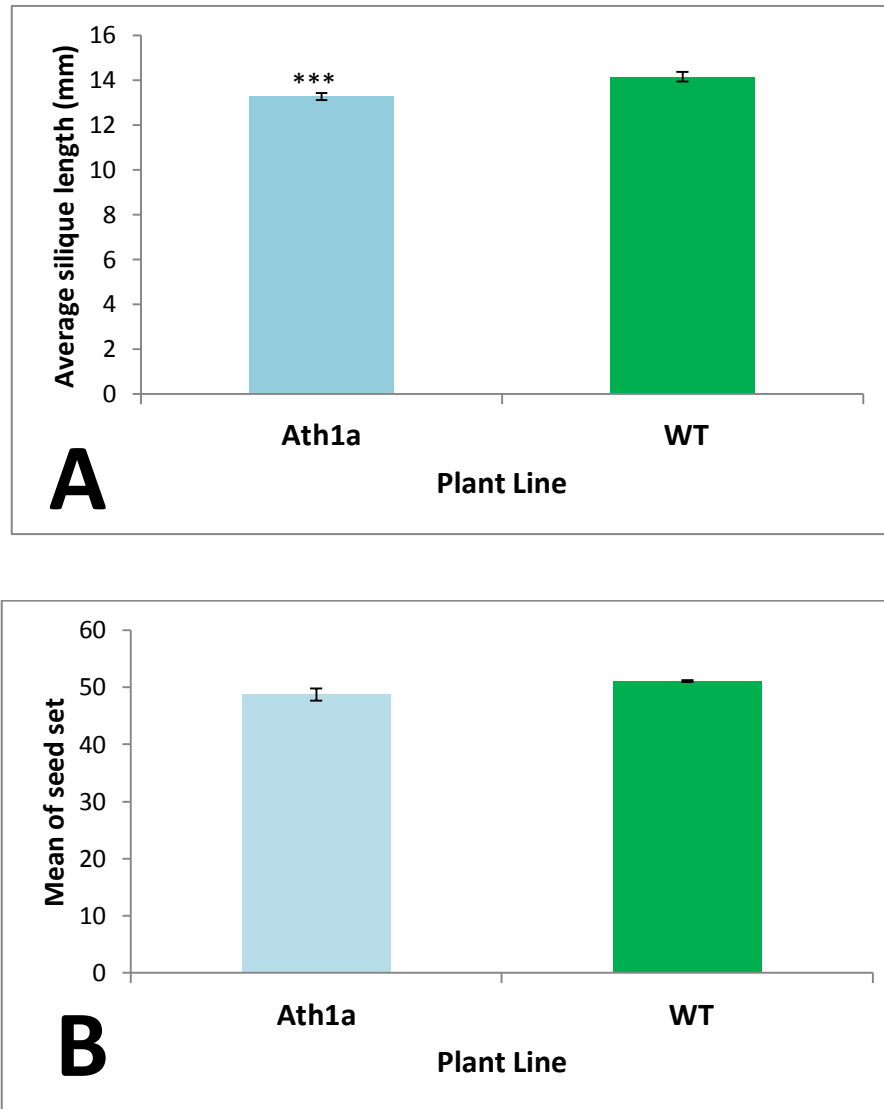


Figure (4.7): Fertility of *Ath1a* in comparison to Wild-type plants.

(A) Silique length Average (N=50). (B) Seed set mean (N=50). ***= P<0.005. Error bars = Standard error of the mean.

4.2.3 Characterisation of the *Arabidopsis* AtH1B isoform

To investigate the role of AtH1B protein a T-DNA insertion mutant line was purchased from NASC. *Ath1b* N659488- salk_090072 T-DNA mutant line contains T-DNA insertion in the third exon of *AtH1B* gene (**Figure 4.8**) at 1.230 kb from the start position of the gene. Seeds of this line as well as the wild type were grown at

the same time and under similar conditions. T-DNA insertions were identified using PCR. Genomic DNA was extracted from leaves of *Ath1b* salk_090072 T-DNA mutant line and wild type. PCR was carried out using specific primers for both sides of the wild type gene and the T-DNA. Primers for both the left and right sides of the insertion position (LP-RP) (**Table 2.2**) of the *Ath1B* gene were used as well as primers for the T-DNA left border (LBb1.3) (**Table 2.3**) were used to genotype the plants. Four out of ten plants showed homozygous T-DNA insertions presenting PCR bands of 0.359 kb in length on an agarose gel and did not present the genomic 0.997 kb band. Plants which are *Ath1b* homozygote for the T-DNA were chosen and studied extensively at different phenotypic levels; somatic appearance, fertility and growth development. Always comparing them to wild-type plants.

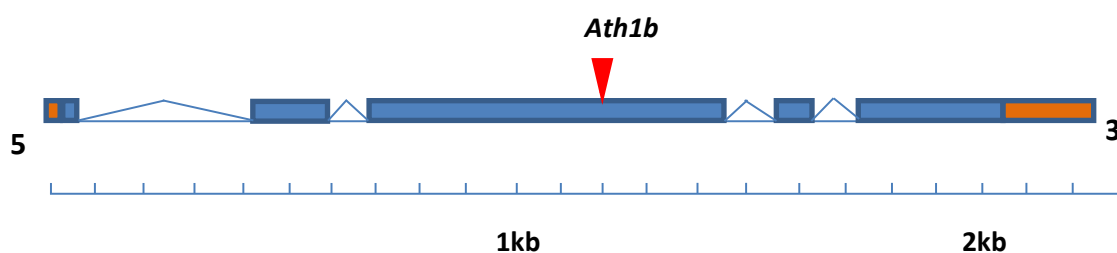


Figure (4.8): Schematic diagram of At5g08780 locus showing the T-DNA insertion localisation.

The structure of *Ath1B* gene (2.267 kb length) is represented showing the localisation of UTRs, exons and introns. Blue rectangles represent exons, orange rectangles represent UTRs, triangles represent introns, and *Ath1b* salk_090072 T-DNA insert is represented with an inverted red triangle.

4.2.3.1. Phenotypic characterization of *Ath1b* mutant plants

The *Ath1b* salk_090072 T-DNA mutant line presented a 75% of the mutant plants with a delay in their flowering time (**Figure 4.9**). However, 25% of the mutant plants showed a normal flowering time comparable to the wild-type. The delay observed in

the affected mutants continued for two to three weeks when the plants seemed to have dwarf phenotype comparable to the wild type. Nevertheless, after this time *Ath1b* mutant plants succeeded in progressing up to their mature life cycle stage and the normal growth.



Figure (4.9): Phenotypic characterisation of *Ath1b* mutant plants
75% of *Ath1b* showed delay in flowering time whereas the rest had normal flowering.

4.2.3.2 Fertility of *Ath1b* mutant plants

The fertility level of the plants was assessed by measuring the silique length and counting the seed number in both the *Ath1b* mutant line and the wild-type. The results showed that *Ath1b* salk_090072 T-DNA homozygous mutant plants were not far from normal fertility levels observed in the wild-type with a mean silique length of 16.42 mm and 14.14mm for *Ath1b* and wild-type respectively. And with a mean seed count per silique of 53.17 and 51.06 in the mutant and wild type respectively. P values (T-test) were 0.082 and 0.285 for both silique length and seed number

respectively, which indicates that both siliques and seed set are not significantly affected in *Ath1b* mutants. **Figure (4.10 A)** shows the average silique length of the wild type and *Ath1b* T-DNA mutant. And **Figure (4.10 B)** shows the average seed set for wild-type and *Ath1b* salk_090072 T-DNA null mutant

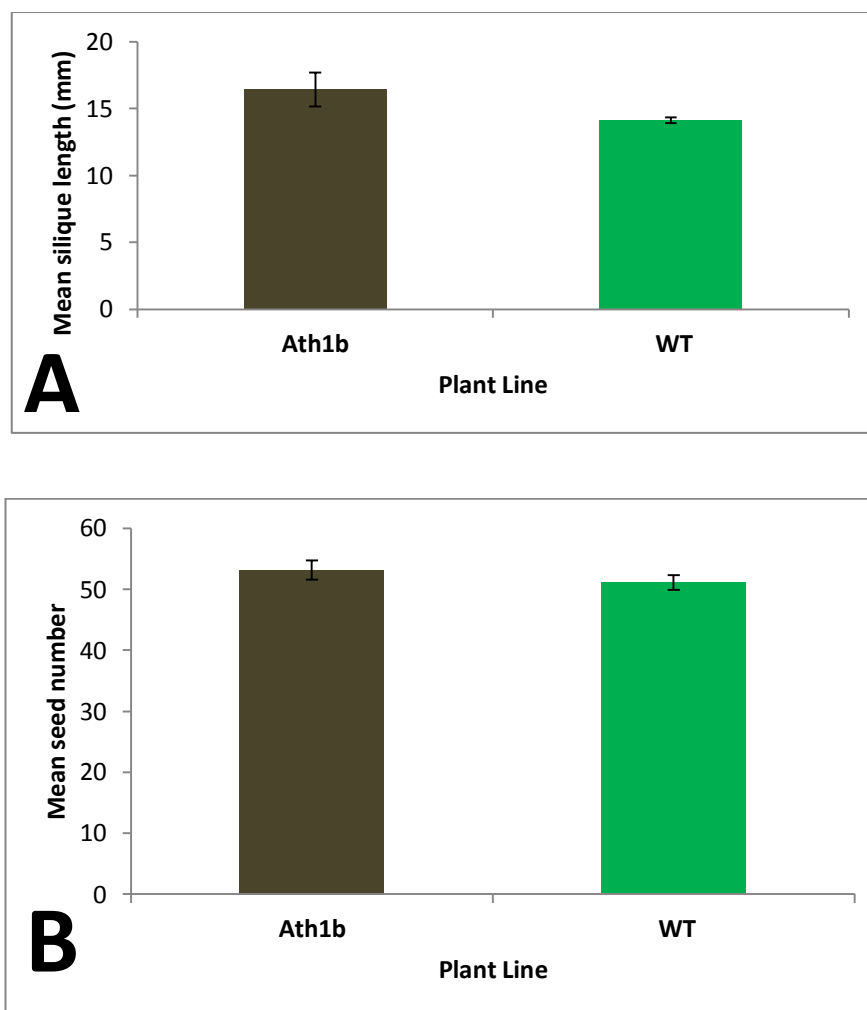


Figure (4.10): Fertility of *Ath1b* in comparison to Wild-type plants. (A) silique length Average (N=50). (B) Seed set mean (N=50). * = P<0.05. Error bars= Standard error of the mean.

4.2.4 Characterisation of the *Arabidopsis* AtH1C isoform

Analysis of the *AtH1C* gene in *Arabidopsis* was investigated by studying the T-DNA insertion line; N586260-Salk_086260 (NASC). The *Ath1c* mutant line has a T-DNA insert in the second intron of the *AtH1C* gene (**Figure 4.11**) at nucleotide position 1035 from the start position of the gene. The plants genotype was checked using PCR and a specific combination of primers, which reflects either the wild type locus gene of 1.159 kb in size (LP-RP primers reaction) (**Table 2.2**), or the mutant T-DNA insertion band (RP and BP primers reaction) (**Table 2.3**), which PCR product size is 0.429 kb. Plants with confirmed homozygous T-DNA insertion for the locus *Ath1c* were selected for further studies and compared to the wild-type plants.

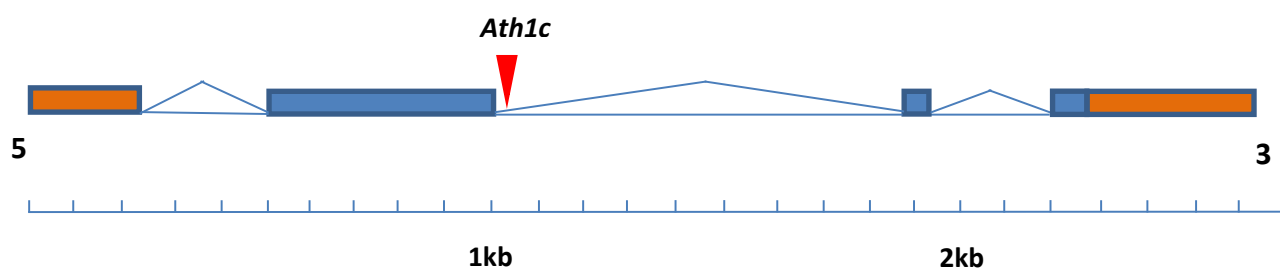


Figure (4.11): Schematic diagram of At1g48610 locus showing T-DNA insertion localisation. 2.626 kb of *AtH1C* organisation; UTRs, exons, introns. Orange boxes represent UTRs, blue boxes indicate exons and triangles represent introns. The position of *Ath1c* T-DNA insertion (N586260-Salk_086260) is represented on the diagram as an inverted red triangle.

4.2.4.1. Phenotypic characterisation of *Ath1c* mutant plants

The *Ath1c* N586260-Salk_086260 T-DNA mutant plants appearance showed variation in growth rate from that of the wild-type plants. About 43% of homozygous mutant plants presented a delay in initial flowering time comparable to wild-type plants (**Figure 4.12**).



Figure (4.12): Phenotypic characterisation of *Ath1c* mutant plants.

43% of *Ath1c* mutants showed a delay in their flowers appearance as well as developmental changes comparable to WT.

4.2.4.2. Fertility of *Ath1c* mutant plants

Fertility quantification of the *Ath1c* mutant plants compared to that of the WT plants indicated that *the* mutant had a similar level of fertility than the WT. The mean silique length was 13.80 mm for the *Ath1c* mutant compared to 14.14mm for WT (**Figure 4.13 A**). Whereas, the mean number of seeds per pod was 50.4 in *Ath1c* T-DNA mutant compared to 51.06 in the WT (**Figure 4.13 B**). The P-values (T-test) for the mean size of the siliques was 0.183 and for the mean number of seeds per pod was 0.768.

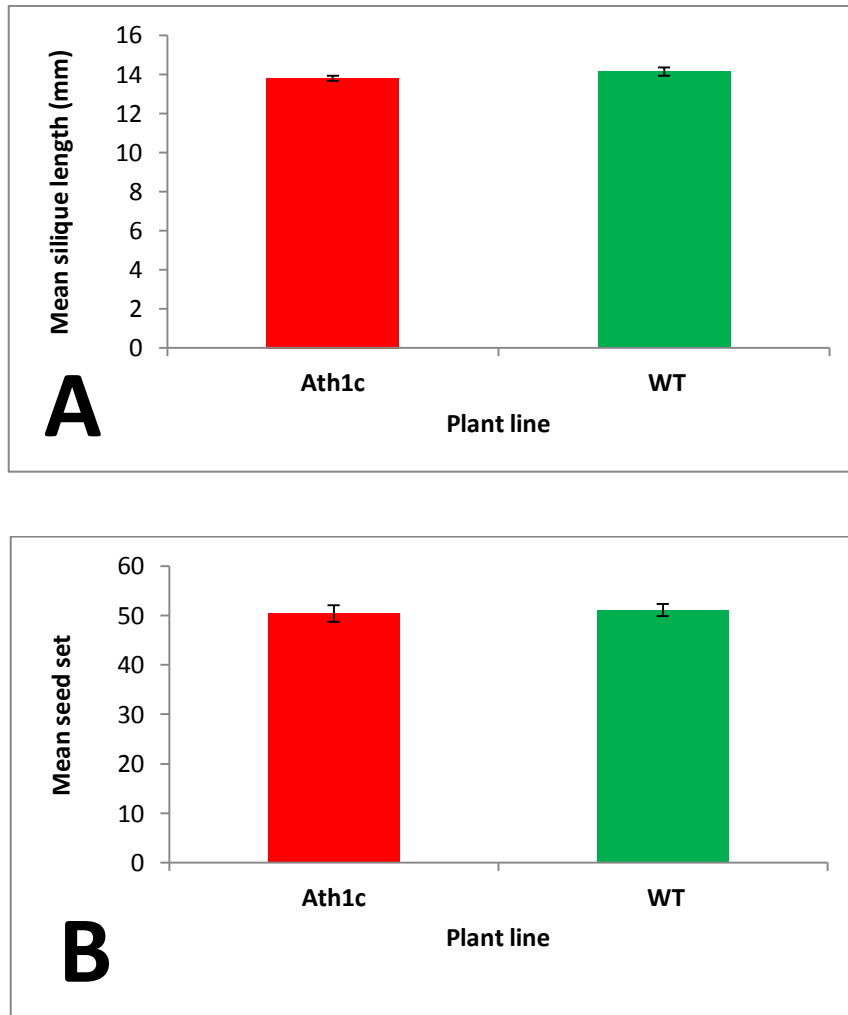


Figure (4. 13): Fertility of *Ath1c* in comparison to Wild-type plants.

(A) Silique length Average (N=50). (B) Seed set mean (N=50). ***= $P < 0.05$. Error bars = Standard error of the mean.

4.2.5. Characterisation of the *Arabidopsis* AtH1D isoform

To study the role of *Arabidopsis* *AtH1D* gene, we analysed an *Ath1d* T-DNA insert line; N65754-Salk_065267, which seeds were brought from NASC. *Ath1d* seeds were assessed at the same time as wild-type plants as control. The plants first were checked for having the *Ath1d* T-DNA insert within the fifth intron of *AtH1D* gene (**Figure 4.14**) at nucleotide positioned 2.369kb by running a PCR with primers

designed specifically to the *AtH1D* gene. Two primer combinations were used (LP-RP) (Table 2.2), (RP and BP) (Table 2.3); the first to show specifically the wild-type *AtH1D* gene with 1.194 kb band length on agarose gel, and the second indicates the *Ath1d* T-DNA with 0.488 kb band size on agarose gel. The plants which had confirmed homozygotes for the wild-type and *Ath1d* T-DNA insertion for the mutant were chosen to be studied phenotypically. And at later stages fertility potential was assessed in the mutant and wild-type plants.

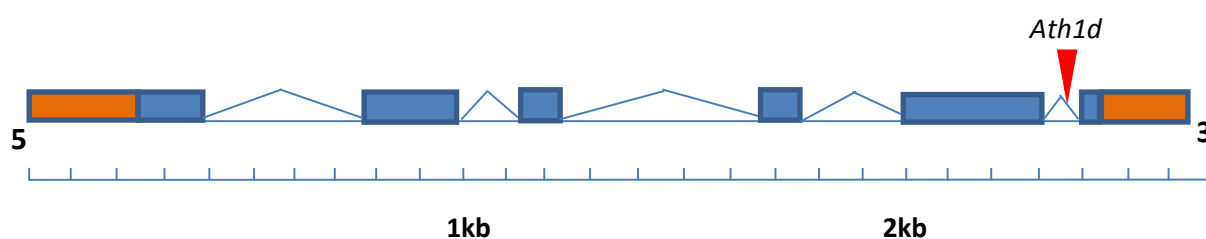


Figure (4.14): Schematic diagram of At1g72740 locus showing T-DNA insertion localisation . Diagrammatic representation of 2.631 kb of *AtH1D* organisation; UTRs, exons, introns. Orange boxes represent UTRs, blue boxes indicate exons and triangles represent introns. *Ath1d* salk-065267 T-DNA insert position is drawn as inverted red triangle.

4.2.5.1 Phenotypic observation of *Ath1d* mutant plants

The investigation of *Ath1d* null mutants in comparison to their control showed that the style of plant growth and development of the *Ath1d* and the wild-type plants were very similar. Leaf, shoot and flower development of *Ath1d* plants were alike to that seen in the wild-type. And so, suggesting that AtH1D loss has most likely no impact on *Arabidopsis* development.

4.2.5.2 Fertility analysis of *Ath1d* mutant plants

Assessment of mature pods and their contents in the *Ath1d* and their reference WT plants indicated that *Ath1d* plants retain the normal level of fertility. The mean of silique length of the *Ath1d* to wild-type was 14.94 mm and 14.14 mm respectively (**Figure 4.15 A**). Statistically, siliques length showed significant difference in comparison to WT (P value=0.016, T-test). However, the average seed sets per pod in *Ath1d* and wild type recorded were 51.96 and 51.06 respectively (**Figure 4.15 B**). And the P value calculated via T-test indicated that seeds counts are not far from that of the wild-type (P=0.629).

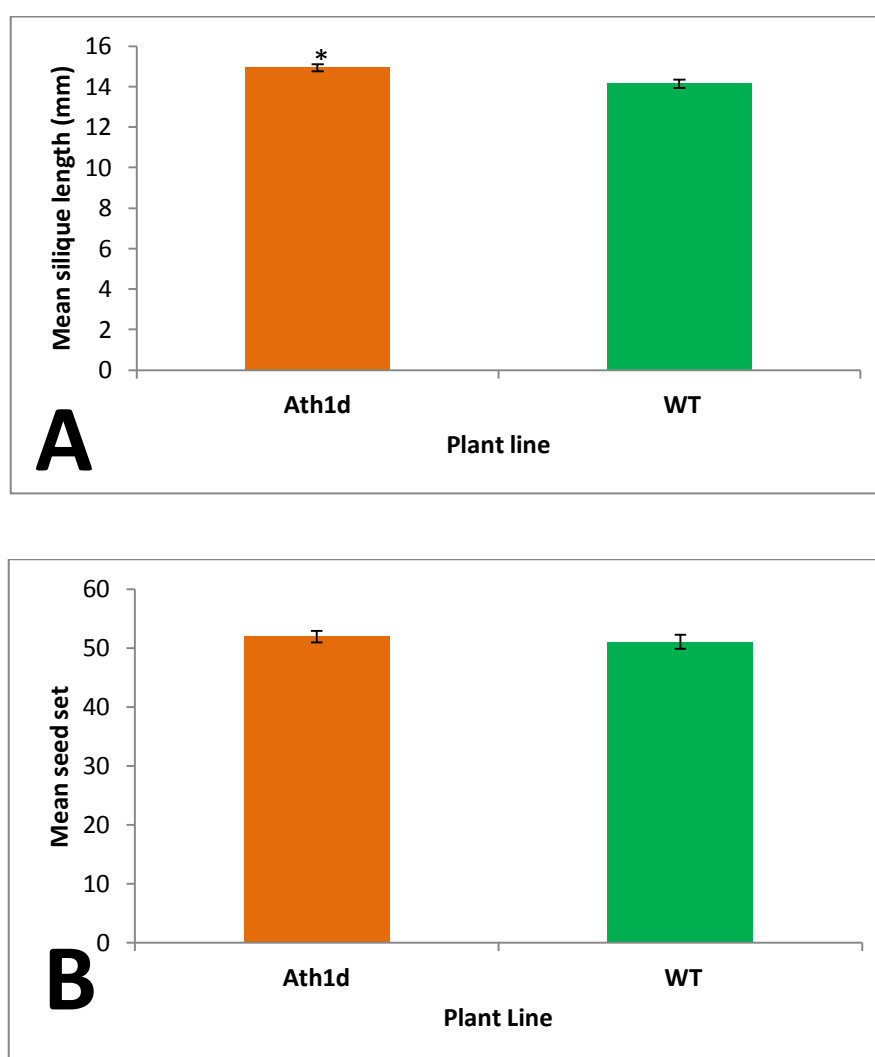


Figure (4.15): Fertility of *Ath1d* in comparison to Wild-type plants.

(A) Silique length Average (N=50). (B) Seed set mean (N=50). * = P<0.05. Error bars= Standard error of the mean.

4.2.6. Characterisation of the *Arabidopsis* AtH1.1 isoform

To investigate the role of AtH1.1 two TDNA insertion mutant lines were purchased from NASC (European Arabidopsis Stock Centre). Database showed that N521410-salk_021410 and N-654890-salk_128430 T-DNA mutant lines contain T-DNA insertions at nucleotide positions 40 up the 5' UTR and at nucleotide 160 at the end of the first exon of the H1.1 gene (**Figure 4.16**) respectively, which will be referred to in this study as *h1.1-1* for the first and *h1.1-2* for the second. Seeds of both mutant lines as well as the wild type were grown at the same time. Plants then were screened for having the T-DNA insertion using PCR. Genomic DNA extracted from the leaves of *Ath1.1-1* and *Ath1.1-2* T-DNA mutant lines and WT were screened using specific primers for both sides (LP: left border, RP; right border) as shown in **Table (2.2)**. (LP-RP) primer pair was used to check the wild type gene. However, RP and LBb1.3 (**Table 2.3**) primer pair was used to check the T-DNA insertion sites. The WT genomic band size on agarose gel for *Ath1.1-1* and *Ath1.1-2* were 1.134 kb and 1.105 kb respectively, and for the *Ath1.1-1* T-DNA and *Ath1.1-2* T-DNA insert bands were 0.388 kb and 0.413 kb respectively on agarose gel.

The plants with confirmed null *Ath1.1-1* and *Ath1.1-2* genotypes, besides to the WT ones as control were chosen and studied extensively. Plants were checked at different levels; phenotypic, fertility and growth development.

Moreover, a search via ChromDB for the presence of a knock-down mutant line for histone *Ath1.1* showed the existence of three *Ath1.1* RNAi lines; T-FGC993A-CS23979, T-FGC993B-CS23980 and T-FGC993Cm-CS23981. These lines were constructed via ChromDB in a pFGC5941 vector (**Figure 4.17**). The genomic DNA of the three lines was analysed using blot analysis using probes for both BASTA resistant gene (BAR) and OSC 3 (**Figure 4.18**). The analysis of T-FGC993B-CS23980 line showed the presence of one copy for each of the BAR and OSC3 probes and, therefore, it was chosen for analysing histone *Ath1.1* knock-down phenotype in *Arabidopsis*.

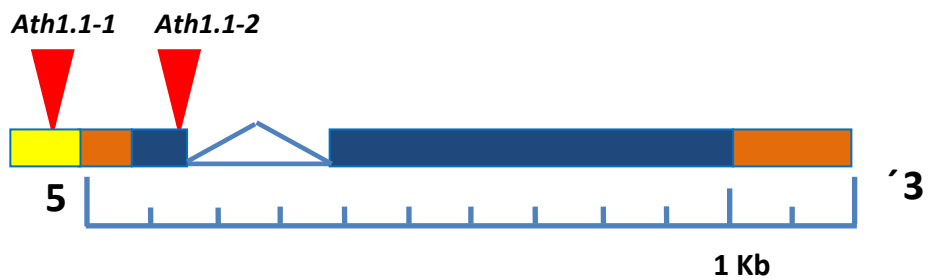


Figure (4.16): Schematic diagram of At1g06760 locus showing two different T-DNA insertion localisations.

1.95kb long *Ath1.1* gene organisation into UTRs, exons and introns. Exons are represented with blue blocks, introns are shown as triangles and UTRs are diagrammed as orange blocks. T-DNA insertion positions; N521410-salk_021410 (*Ath1.1-1*) and N-654890-salk_128430 (*Ath1.1-2*) are diagrammed as inverted red triangles. Upstream sequence is represented as a yellow block.

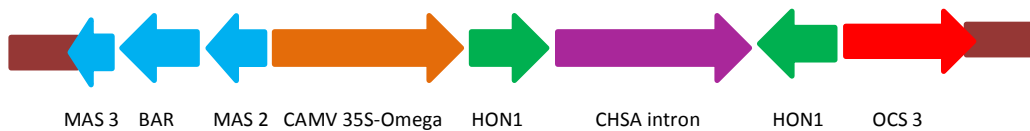


Figure (4.17): ChromDB model of HON1 ds RNA construct (T-DNA region).

The schematic diagram represents *h1.1^{RNAi}; Ath1.1-CS23980*, construct. MAS 3 and OCS 3 are polyadenylated signal sequences (*Agarobacterium tumefaciens*). MAS 2 is a plant promoter. CHSA intron (*Petunia hybrid*). BAR codes for BASTA herbicide resistance. The Omega fragment is a leader sequence (TMV).

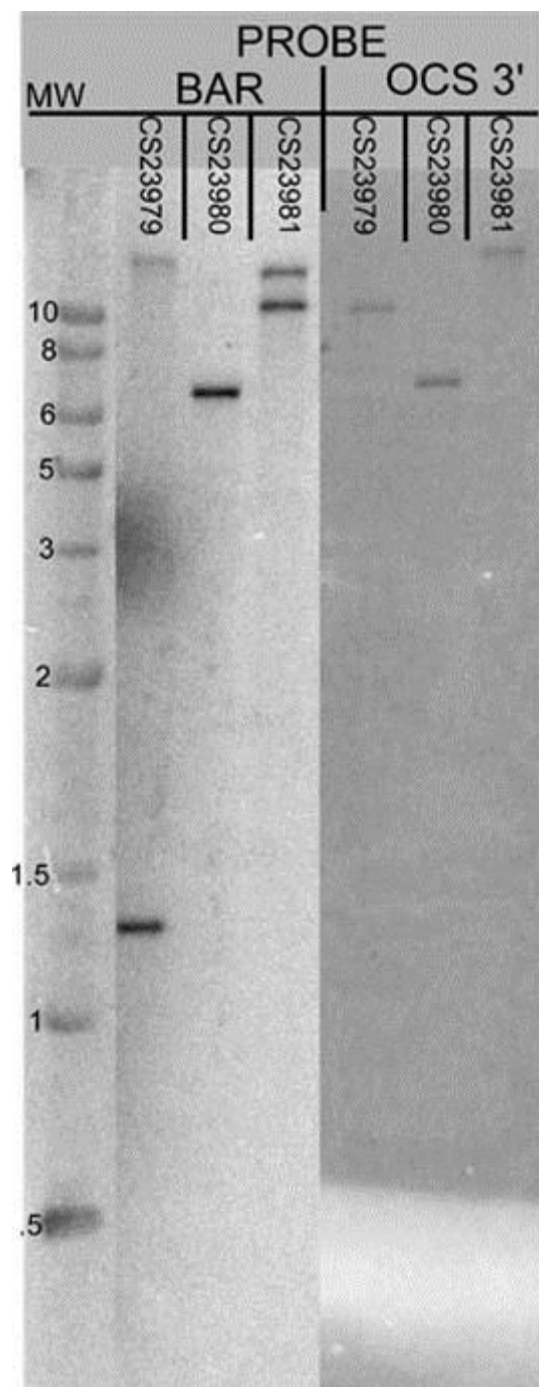


Figure (4.18): ChromDB blot analysis of *h1.1*^{RNAi} mutant lines.

Genomic DNA of T-FGC993A-CS23979, T-FGC993B-CS23980 and T-FGC993Cm-CS23981 was treated with the EcoRI (restriction digestion enzyme) and then blotted using BAR fragment (BASTA resistant gene) as in the left border probe and the OCS 3' fragment as in the right border probe. DNA ladder (MW= 1Kb). http://www.chromdb.org/org_specific.html?o=ARAT
H

4.2.6.1. Phenotypic characterisation of *Ath1.1* mutant plants

4.2.6.1.1. Phenotypic characterisation of *Ath1.1-1* mutant plants

The vegetative growth of *Ath1.1-1* mutants showed plants that lacked the normal growth style. The *Ath1.1-1* plants showed differences in their developmental potential comparable to WT (**Figure 4.19 A**). 95% flowering to 5% non-flowering phenotype was recorded in *Ath1.1-1* individual plants. Some mutants showed an initial developmental blockage. Where flowering stage was undistinguishable. Plants appeared as frozen at the rosette stage, lacking the ability to grow further and so flowers were not seen. Hence, plants appeared as few small leaves (**Figure 4.19 B**). Suggesting an error occur during cell cycle and vegetative development. However the flowering *Ath1.1-1* mutants showed plants with reduced size of both stems and leaves. Furthermore, low number of siliques per stem and small siliques were also observed (**Figure 4.19 D**) comparable to WT (**Figure 4.19 E**). Hence, a semi-sterile phenotype (**Figure 4.19 C**) was suggested and, therefore, a meiotic role could be predicted. The cytological analysis of this mutant confirmed some meiotic defects.

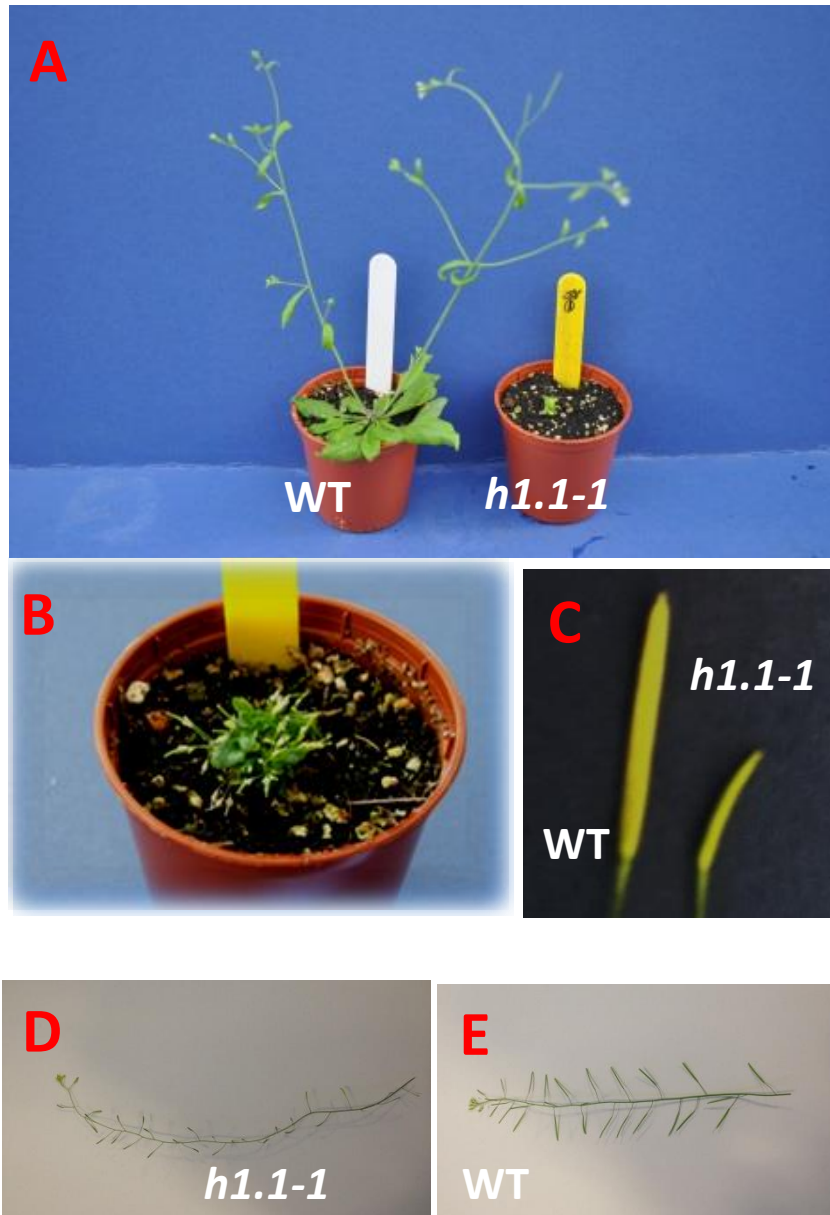


Figure (4.19): Phenotypic characterisation of *Arabidopsis Ath1.1-1* mutant plants in comparison to WT.

(A) Dwarf *Ath1.1-1* phenotype comparable to WT plants. (B) Closer view of *Ath1.1-1* T-DNA mutant. (C) Reduced Siliques in length of *Ath1.1-1* in comparison to WT siliques. (D&E) Seed pods phenotype of (D) *Ath1.1-1* T-DNA line and (E) WT.

4.2.6.1.2. Phenotypic characterisation of *Ath1.1-2* mutant plants

The investigation of *Ath1.1-2* null mutant phenotype showed that it was not far away from the wild type. The homozygous *Ath1.1-2* mutant plants showed normal growth rate comparable to wild type plants (**Figure 4.20 B**), their development pattern; leaves, flowers, stems were alike to that seen in the WT (**Figure 4.20 A**). Moreover, the *Ath1.1-2* and WT had 100% matches in their flowering time. At later stages the *Ath1.1-2* showed seed pods that have tiny reduction in siliques length comparable to the WT (**Figure 4.20 C&D**).

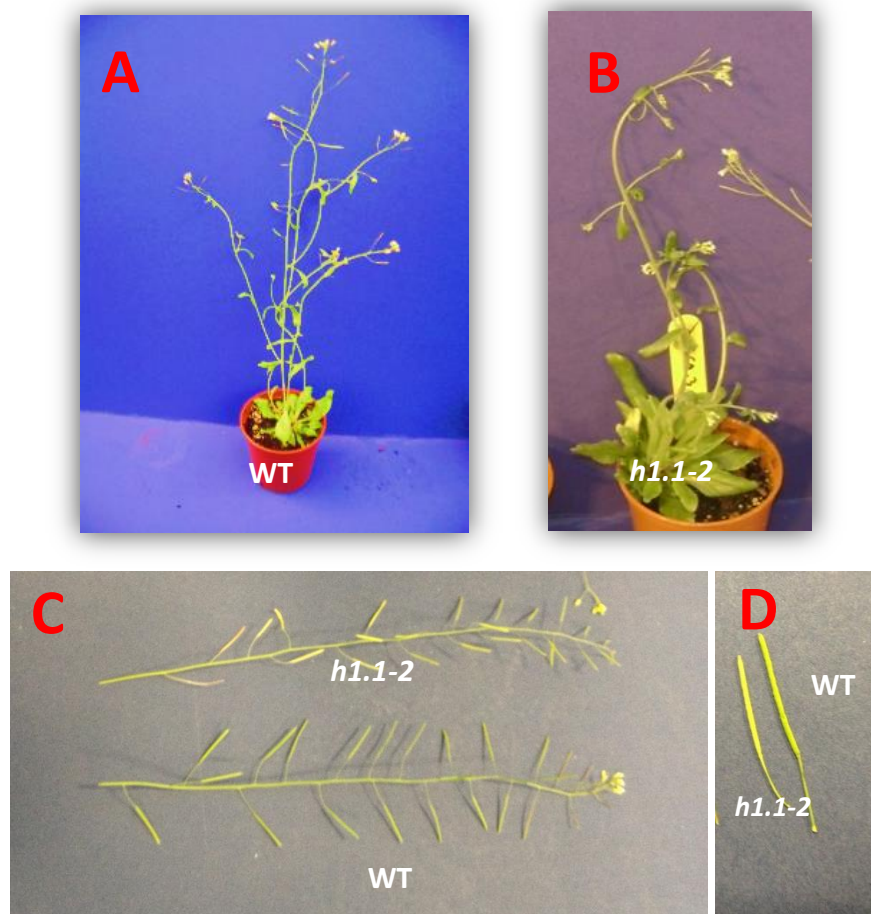


Figure (4.20): Phenotypic characterisation of *Arabidopsis Ath1.1-2* mutant plants in comparison to WT.

(A) WT phenotype. (B) *Ath1.1-2* phenotype. (C) Seed pods of *Ath1.1-2* and WT. (D) Comparison of silique length between *Ath1.1-2* and WT.

4.2.6.1.3. Phenotypic characterisation of *Ath1.1^{RNAi}* mutant plants

The observations of the *Ath1.1^{RNAi}* line mutant revealed distinct abnormality comparable to the WT plants. A total of 20% of *Ath1.1^{RNAi}* plants showed delay in flowering time comparable to wild type (**Figure 4.21 A**). Moreover, a noticed reduction in silique length was recorded (**Figure 4.21 D**) comparable to WT (**Figure 4.21 C**). Furthermore, gap appearance among the seeds within siliques was consistent in this mutant line (**Figure 4.21 F**) comparable to WT plants (**Figure 4.21 E**). Thus, suggesting a reduction in their seed content. Later on, *Ath1.1^{RNAi}* seed pods quantification confirmed their semi-sterile phenotype. In addition to this, two plants out of about a hundred analysed showed a fasciated (fused stem) phenotype (**Figure 4.21 B**), suggesting some kind of mitotic abnormalities. Defects in mitotic chromosomal segregation were confirmed later in this mutant line.

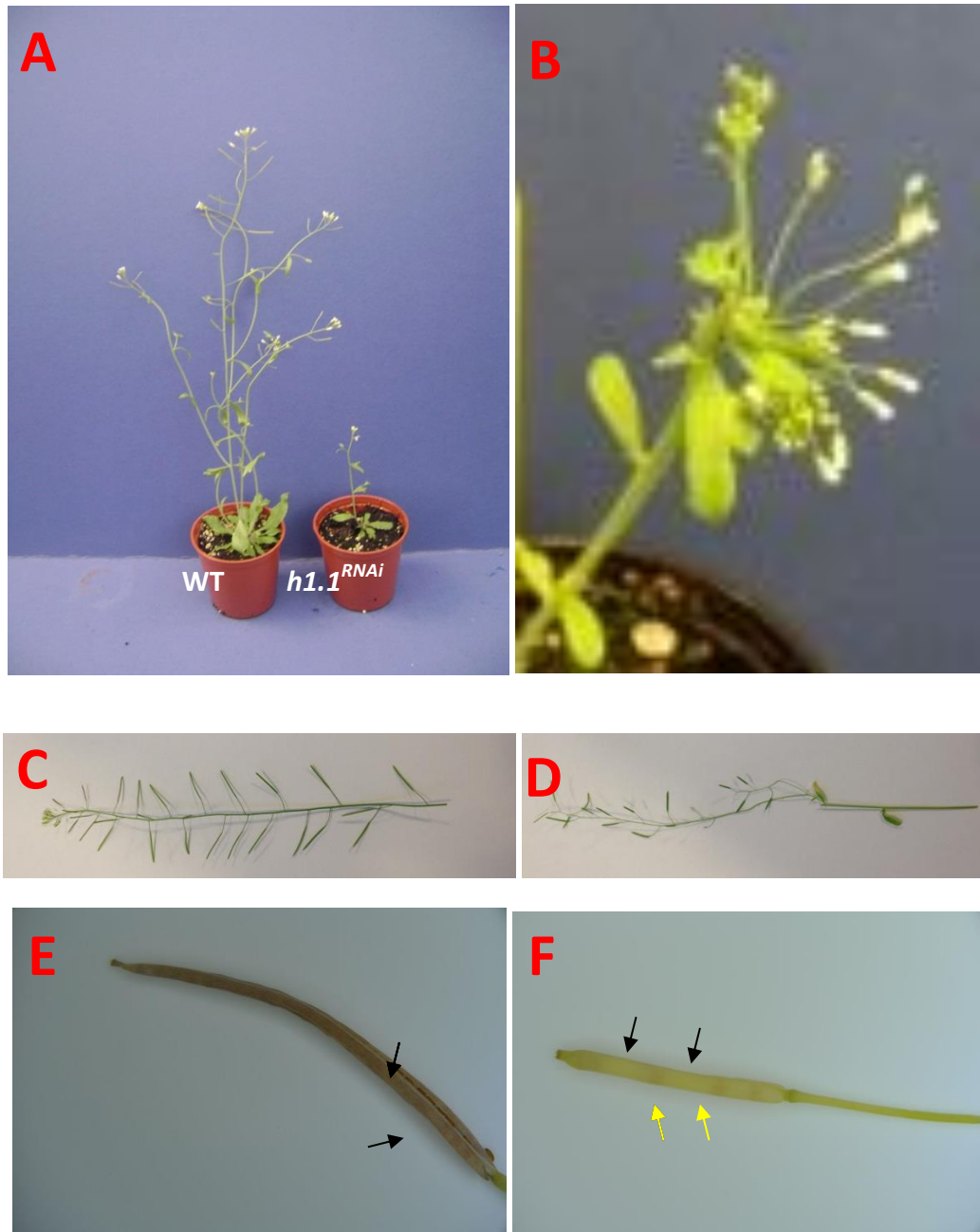


Figure (4.21): Phenotypic characterisation of *Arabidopsis Ath1.1^{RNAi}* mutant plants in comparison to WT.

(A) Flowering delay in *Ath1.1^{RNAi}* comparable to WT after five weeks of plant growth. (B) Fasciated-like phenotype of *Ath1.1^{RNAi}*. (C&D&E&F) Silique phenotype. (C&E) WT silique. (E) Showing fully seed pod. (D&F) *Ath1.1^{RNAi}* silique, Seed pod lacking the complete seed set as gaps appear in between seeds (F). Gaps are represented by black arrow. Seeds are represented with yellow arrow. E&F pictures are photographed under a light dissecting microscope (Nikon SMZ800).

4.2.6.2. Fertility of *Ath1.1* mutant plants

4.2.6.2.1 Fertility of *Ath1.1-1* mutant plants

Fertility level analysis in this mutant line and the wild-type was done via assessing seed sets and silique measurement. Data collected from fully dry siliques implied about 51% reduction in silique length compared to wild-type. ($p = 6.983E-46$, T-test). **Figure (4.22 A)** shows the average silique length for wild-type and *Ath1.1-1* plants. Moreover, *Ath1.1-1* T-DNA recorded 90% decline in seed number per silique referring to WT ($p = 1.672E-44$, T-test). **Figure (4.22 B)** shows the mean of seed set per silique in wild-type and *Ath1.1-1* T-DNA mutant plants. Analysis of pollen viability by using Alexander staining, revealed that a large number of pollen grains were lacking normal phenotype, showing several defects; incomplete cytoplasm, smaller size, variable sizes, and irregularly shaped pollen. Pollen viability was highly reduced in *Ath1.1-1* comparable to wild-type. The Alexander staining in the *Ath1.1-1* mutant showed that only 21.28% ($n=531$) of the total pollen was viable compared to 95.4 % ($n=500$) in the wild-type. These results come with the seed-sets and siliques defects seen in *Ath1.1-1* mutant, showing that *AtH1.1-1* is needed to retain normal fertility levels in *Arabidopsis*. These results also indicate a proposed potential meiotic defect in the *Ath1.1-1* mutant lines.

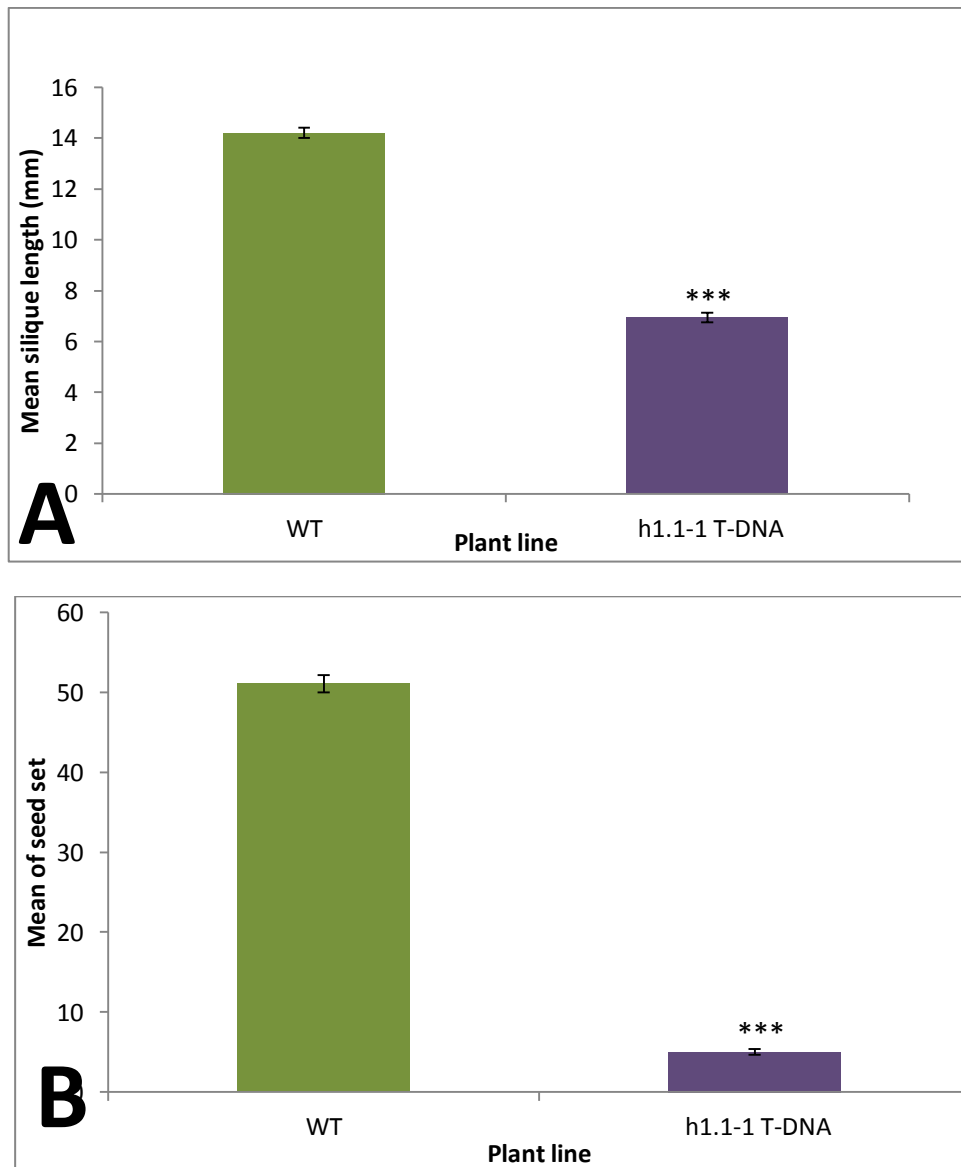


Figure (4.22): Fertility of *Ath1.1-1* mutant plants in comparison to Wild-type plants.

(A) Silique length Average (N=50). (B) Seed set mean (N=50). *** = $P < 0.005$. Error bars = Standard error of the mean.

4.2.6.2.2 Fertility of *Ath1.1-2* mutant plants

Analysis of *Ath1.1-2* T-DNA mutant line showed a reduction in the fertility levels compared to the wild-type. The mean silique length of the mutant and the wild-type were 13.14mm (n=50) and 14.21mm (n=50) respectively. Statistical analysis

indicated that the decrease was significant ($P=0.0002$, T-test). In addition to this the seed-set per silique mean was reduced too significantly, recording 42.06 ($n=50$) and 51.06 ($n=50$) for *Ath1.1-2* T-DNA and WT respectively ($p = 2.202E-08$, T-test). **Figure (4.23 A)** shows the mean silique length in *Ath1.1-1* T-DNA and WT plants. **Figure (4.23 B)** represents mean of seed sets in *Ath1.1-2* T-DNA mutant and WT plants.

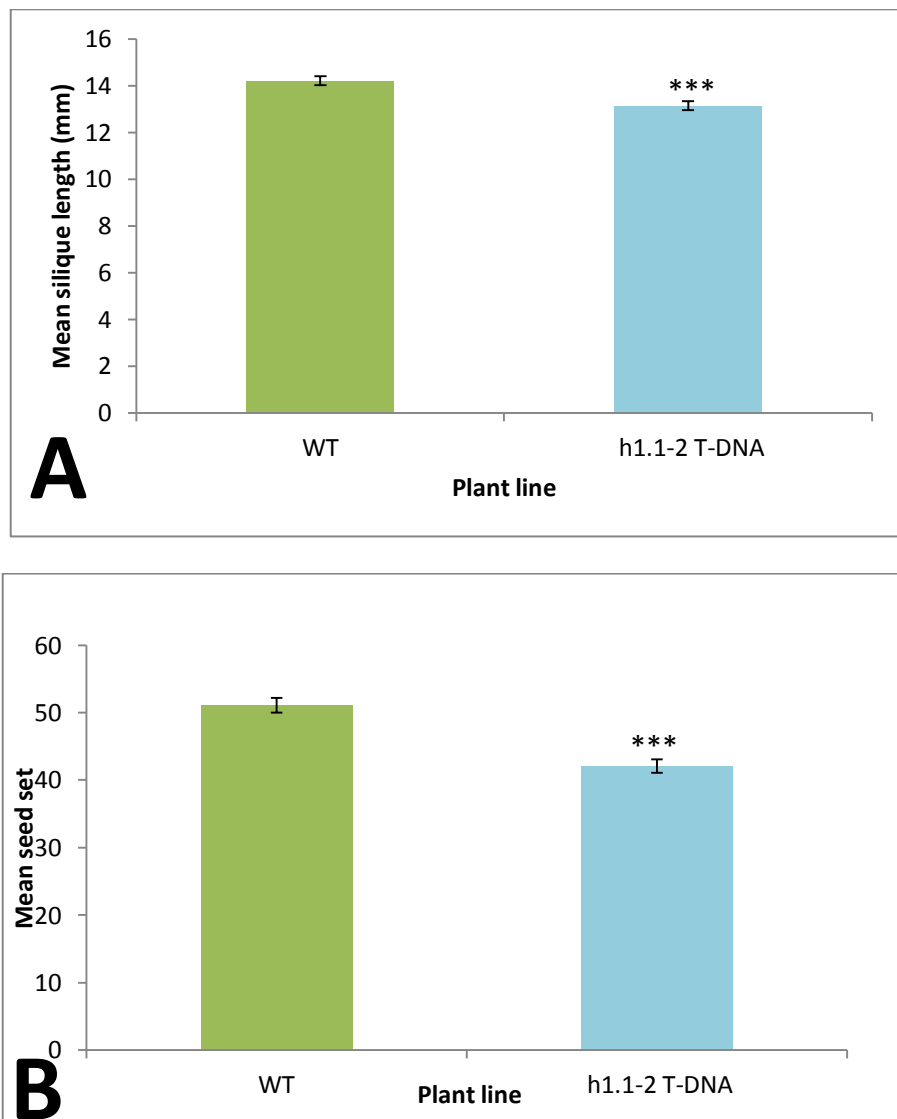


Figure (4.23): Fertility of *Ath1.1-2* mutant plants in comparison to Wild-type plants. (A) Silique length Average ($N=50$). (B) Seed set mean ($N=50$). *** = $P<0.005$. Error bars = Standard error of the mean.

4.2.6.2.3 Fertility of *Ath1.1^{RNAi}* mutant plants

To assess fertility level in *Ath1.1^{RNAi}* line, seed sets and siliques lengths were taken for both the mutant line as well as the wild type plants fully dry seed pods. Since the RNAi mutation strategy show phenotypic variation within mutant plants ranging from highly affected plants with short siliques up to about normal ones, so plants which showed defected phenotype of siliques that are short or with gaps were chosen for fertility assessment. The results showed that siliques of *Ath1.1^{RNAi}* showed about 44% reduction in length referring to WT ($p=4.776E-42$, T-test). Moreover, *Ath1.1^{RNAi}* had about 41% reduction in seed set compared to wild type ($p=1.542E-27$, T-test). **Figure (4.24 A)** shows silique length average for wild type and *Ath1.1^{RNAi}*. **Figure (4.24 B)** shows seed mean for the *Ath1.1^{RNAi}* and the WT.

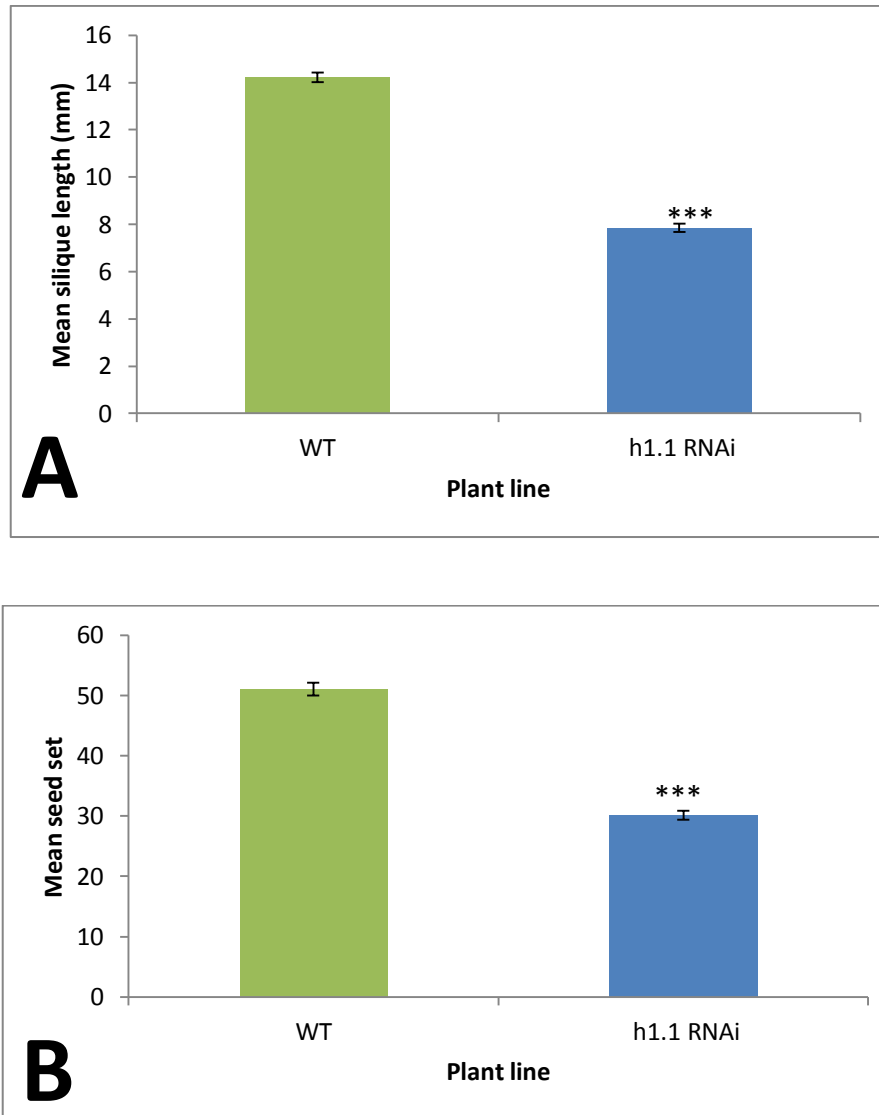


Figure (4.24): Fertility of *Ath1.1*^{RNAi} mutant plants in comparison to Wild-type plants. (A) Silique length Average (N=50). (B) Seed set mean (N=50). *** = P<0.005. Error bars = Standard error of the mean.

4.2.7. Characterisation of the *Arabidopsis* AtH1.2 isoform

The role of *AtH1.2* gene was studied by analysing a T-DNA mutant line (N321948-GK-116E08) (NASC) and comparing it with wild-type plants. The T-DNA insertion is localised in the first exon of the gene at nucleotide position 544 (**Figure 4.25**). Genotyping analysis for both the mutant and wild-type plants was carried out using

PCR with primers which were specific for the *Ath1.2* gene and the TDNA. (LP-RP) (Table 2.2) and (RP-BP (Table 2.3)) primer pairs were used for identifying wild-type and mutant genome bands respectively, and showing bands of 876 kb and 776 kb respectively. Plants with confirmed homozygosity for the T-DNA insertion selected for further studies. Parameters of fertility and phenotypic changes were assessed to give a clear view about the role of *Ath1.2* locus.

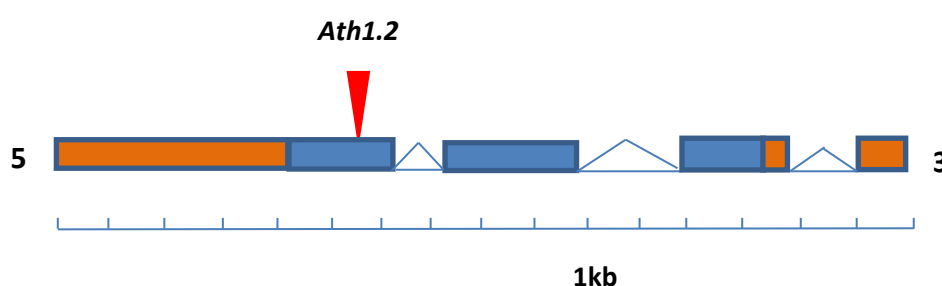


Figure (4.25): Schematic diagram of AT2G30620 locus showing T-DNA insertion localisation. 1.581 kb of *Ath1.2* gene sequence organisation into exons, introns and UTRs. Exons are represented with blue blocks, introns are shown as triangles and UTRs are diagrammed as orange blocks. The T-DNA insertion position; N321948-GK-116E08 (*Ath1.2*), is diagrammed as inverted red triangle.

4.2.7.1. Phenotypic characterisation of *Ath1.2* mutant plants

By studying the vegetative growth appearance of the *Ath1.2* and wild-type plants a noticeable phenotypic difference was observed. 100% of *Ath1.2* mutants (n=6) have a noticeable delayed flowering referring to the parallel sown wild-type plants. This delay continued to be seen up to the later mature stage. The *Ath1.2* plants needed about three more weeks to reach the mature stage seen in the WT plants.

4.2.7.2. Fertility of *Ath1.2* mutant plants

Fertility was slightly affected in *Ath1.2* mutant plants in comparison to wild-type plants. A reduction in the *Ath1.2* mean of silique length (**Figure 4.26 A**) was recorded showing 13.31 mm and 14.14 mm values for *Ath1.2* and wild-type plants siliques respectively. Statistically, P-value (T-test) of 0.003 indicated that the reduction in silique length is significant. Moreover, the mean seed count per silique of *Ath1.2* comparable to the wild-type was 47.56 and 51.06 respectively (**Figure 4.26 B**). Although P-value of 0.048 (T-test) indicates a significant reduction in seed count, but the P-value is not so far from 0.05 (the significance level), suggesting that *AtH1.2* loss is most likely not necessary in *Arabidopsis* seed production.

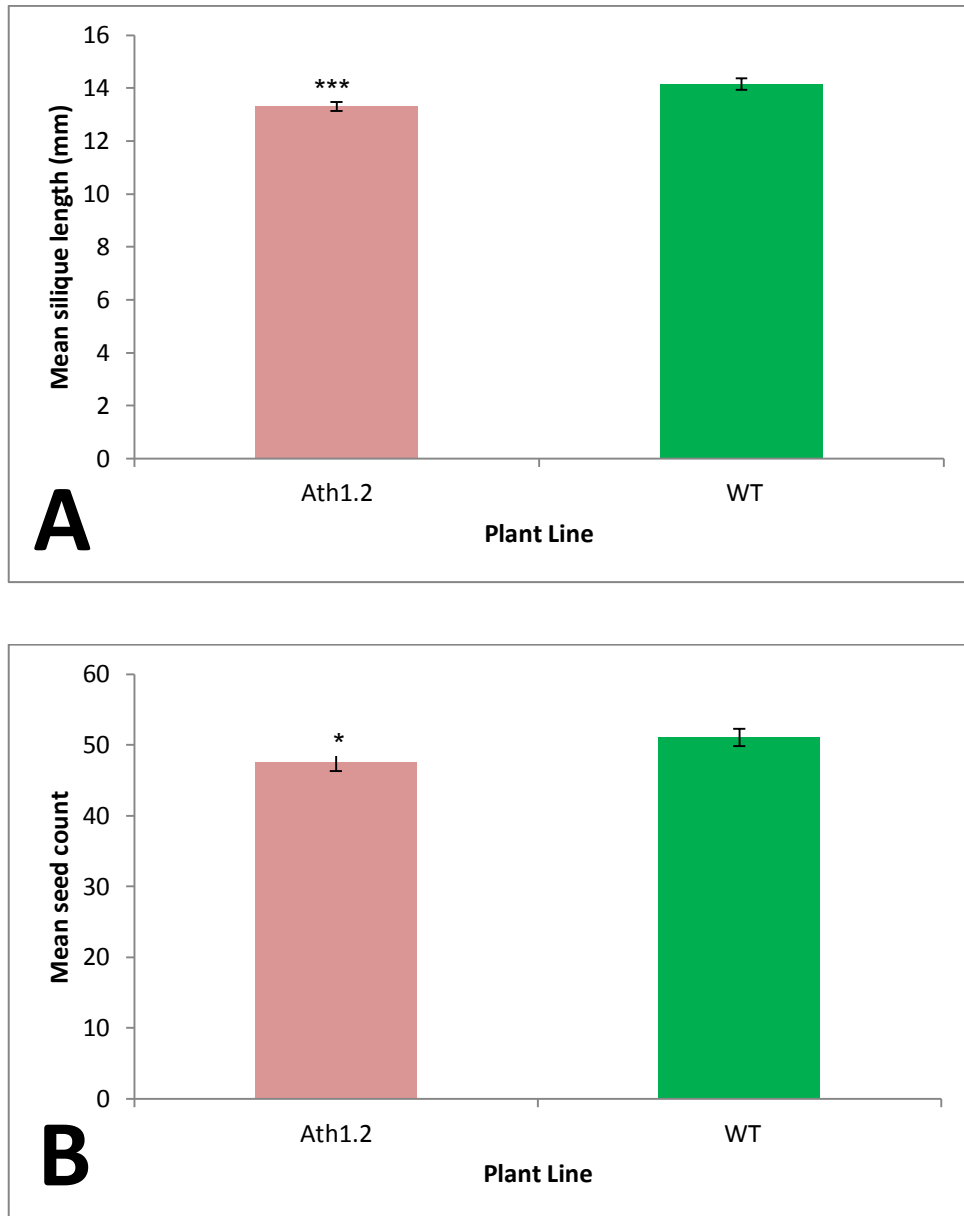


Figure (4.26: Fertility of *Ath1.2* mutant plants in comparison to Wild-type plants. (A) Silique length Average (N=50). (B) Seed set mean (N=50). *=P<0.05, *** = P<0.005. Error bars = Standard error of the mean.

4.2.8. Characterisation of the *Arabidopsis* AtH1.3 isoform

The genetic analysis of *Arabidopsis* histone AtH1.3 was carried out in order to characterise its role. N665594-Salk_025209 *Ath1.3* T-DNA mutant; line plants with T-DNA inserted at 300 nucleotide upstream the 5' UTR was characterised (**Figure**

4.27). The genotype of the plants analysed by PCR using specific *AtH1.3* primers at both sides of the predicted T-DNA insertion (LP-RP, **Table 2.2**). Whereas, the *Ath1.3* T-DNA insertion was genotyped using the RP and BP (**Table 2.3**) primers pair. The *Ath1.3* homozygous T-DNA genotype showed 0.436 kb band size on an agarose gel. The confirmed *Ath1.3* homozygous insertion mutant plants were used to study their appearance, growth rate and fertility, compared to the wild-type plants.

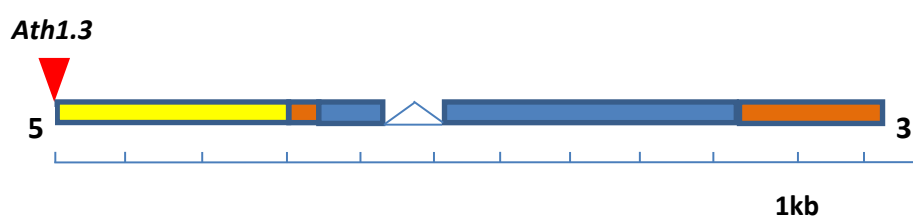


Figure (4.27): Schematic diagram of *At2g18050* locus showing T-DNA insertion localisation. 0.835 kb of *AtH1.3* organisation into UTRs, exons and introns. Exons are represented with blue boxes. Introns are shown as triangles and UTRs are diagrammed as orange blocks. The UTR upstream sequence is represented with yellow block. And *Ath1.3* N665594-Salk_025209 T-DNA insert with inverted red triangle.

4.2.8.1. Phenotypic characterisation of *Ath1.3* mutant plants

The study of *Ath1.3* plants development in parallel with wild-type plants indicated differences. A clear delay in the inflorescences appearance was observed in *Ath1.3* mutant plants in comparison to WT plants (**Figure 4.28**). The *Ath1.3* showed 75% delay in their flowering timing if compared to the wild-type plants sown next to it at same time and under the same conditions.



Figure (4.28): Phenotypic characterisation of *Ath1.3* mutant plants
75% delay in flower appearance was recorded comparable to wild-type plants.

4.2.8.2. Fertility of *Ath1.3* mutant plants

The analysis of *Ath1.3* mutants fertility was assessed by the length of the siliques (seed pods) and the number of seeds per silique. It was found that fertility is affected in *Ath1.3* mutant plants in comparison to wild-type plants. A reduction in the *Ath1.3* silique length (**Figure 4.29 A**) was recorded showing 12.3mm comparable to 14.14mm in WT plant silique. Statistically, P-value (T-test) of 3.44639E-11 indicated that *Ath1.3* reduction in silique length is significant. Moreover, seed count per silique of *Ath1.3* comparable to the wild-type was 39.62 and 51.06 respectively (**Figure 4.29 B**). The statistical analysis of the seeds average per pod in the mutant and the WT indicated a significant decline in *Ath1.3* seed production (P-value= 4.19519E-10) (T-test), suggesting that *AtH1.3* is needed for normal level of seed production in *Arabidopsis*.

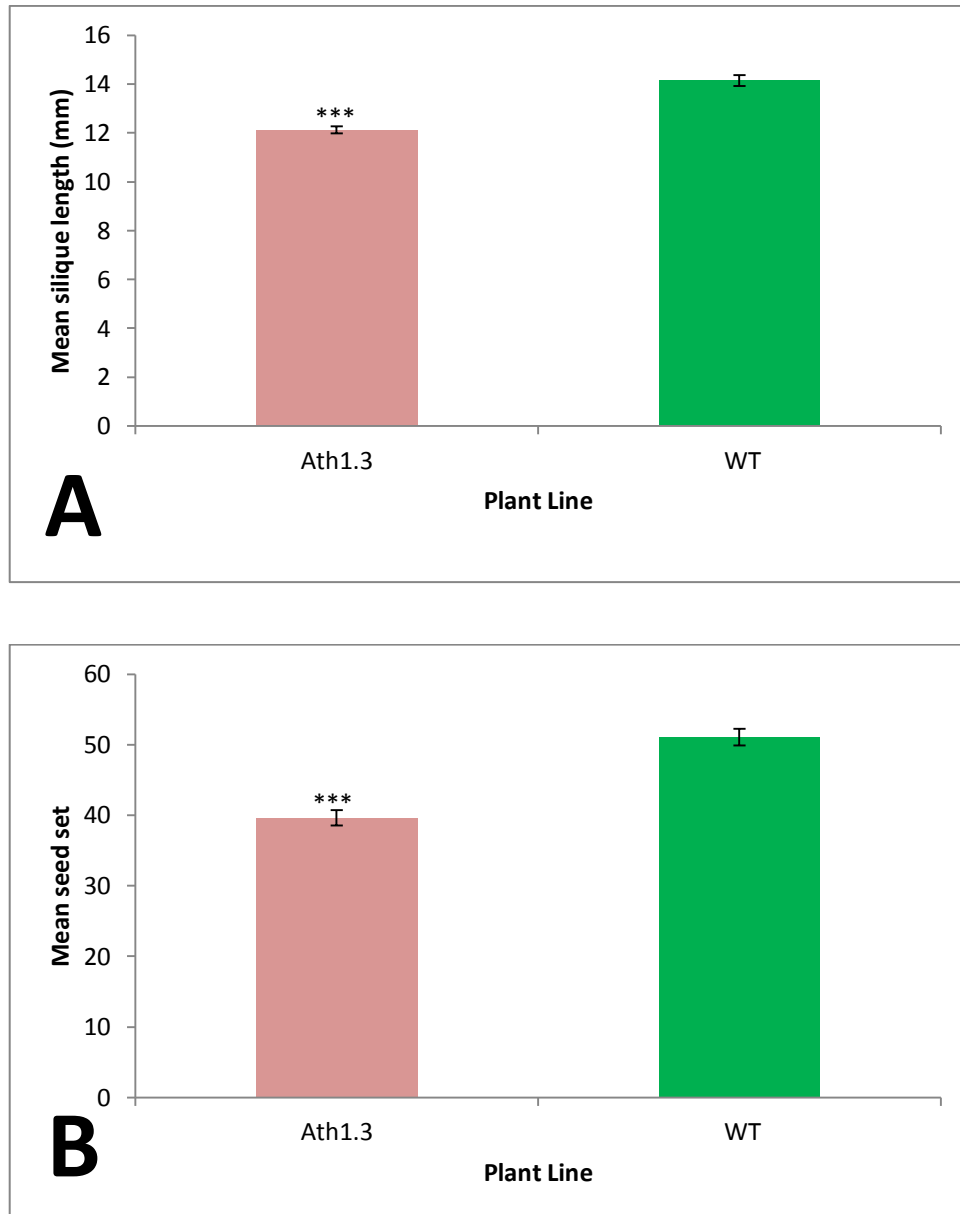


Figure (4.29): Fertility of *Ath1.3* mutant plants in comparison to WT plants. (A) Silique length average (N=50). (B) Seed set mean (N=50). ***= P<0.005. Error bars = Standard error of the mean.

4.2.9. Characterisation of the *Arabidopsis* AtHON4 isoform

To understand AtHON4 importance within the nuclear activity of *Arabidopsis*, *Athon4* T-DNA insertion line; N599887-Salk_099887 (NASC) was obtained and grown in parallel to wild-type plants. *Athon4* T-DNA insertion is localised in exon four of

AtHON4 gene at nucleotide positioned 2.094 from gene start (**Figure 4.30**). PCR products corresponding to the wild type were 1.145 kb in size whereas the T-DNA insertion product was 0.390 kb long in size on an agarose gel. The homozygous plants for the insertion were used to analyse their phenotype; plant growth, development and fertility progress.

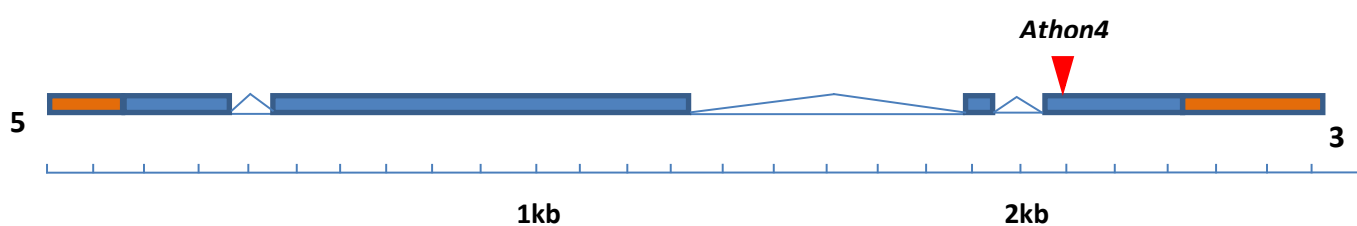


Figure (4.30): Schematic diagram of At3g18035 locus showing T-DNA insertion localisation. 2.635 kb of *AtHON4* organisation into UTRs, exons and introns. Exons are represented with blue boxes. Introns are shown as triangles and UTRs are diagrammed as orange blocks. And *Athon4*; N599887-Salk_099887 T-DNA insert as inverted red triangle.

4.2.9.1. Phenotypic characterisation of *Athon4* mutant plants

The confirmed homozygous *Athon4* mutants were screened during their life cycle for any unusual phenotype. The homozygous *Athon4* mutant showed a 50% delay in their flowering time to that showed by the wild-type plants (**Figure 4.31**). The delay persists up to three weeks. Later the mutant plants were able to flower in a similar way to that observed on the wild-type plants.



Figure (4.31): Phenotypic characterisation of *Athon4* mutant plants. 50% delay in *Athon4* mutants development and flowering was recorded.

4.2.9.2. Fertility of *Athon4* mutant plants

The *Athon4* mutants were studied to see if *AtHON4* gene has a role on the plant ability to produce healthy gametes with potential to develop to zygotes. To do this seed pods (siliques) were assessed in the *Athon4* mutants and compared to wild-type plants. Quantification of seeds per pod in both *Athon4* and the wild-type plants showed that the *Athon4* presented a normal level of fertility with average seed sets per pod of 50.80 compared to 51.06 in the wild-type (**Figure 4.32 B**) with P value of 0.870 (T-test). However, the length of silique pods was decreased significantly in the *Athon4* in reference to their wild-type. The *Athon4* had an average silique length of 13.22 mm compared to 14.14 mm in wild-type (**Figure 4.32 A**) (P-value=0.000867).

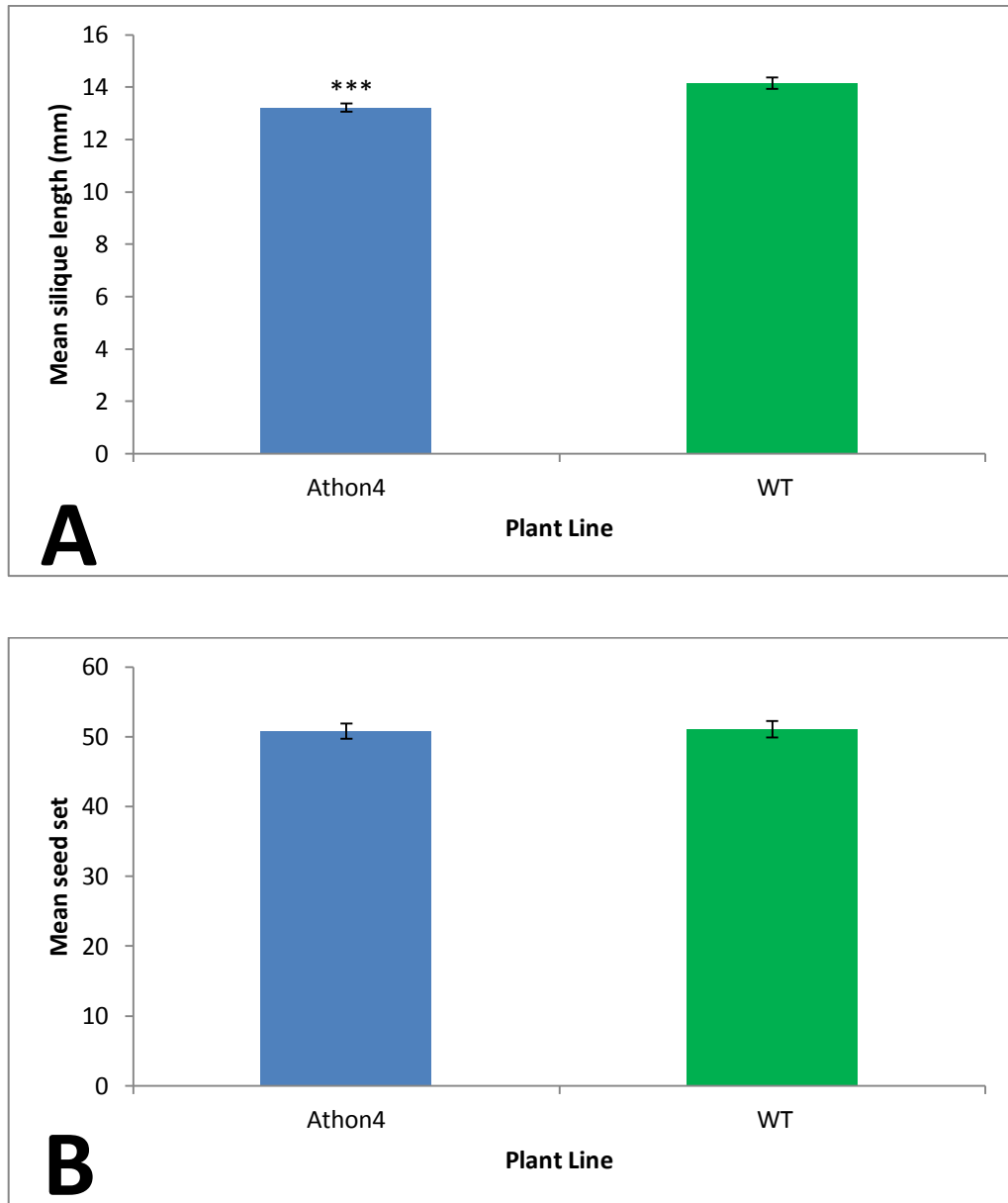


Figure (4.32): Fertility of *Athon4* in comparison to WT plants.

(A) Average silique length (N=50). (B) Seed set mean (N=50).). ***= P<0.005. Error bars = Standard error of the mean.

4.2.10. Characterisation of the *Arabidopsis* AtHON5 isoform

The analysis of AtHON5 in *Arabidopsis* was carried out by studying *Athon5* T-DNA insertion mutant line (N656137-salk_007422) (NASC) and compare it to the wild-type plants. The salk_007422 line has the T-DNA inserted within the first intron of *AtHON5*

gene at nucleotide position 1824 (**Figure 4.33**). The plants genotype was checked by PCR using specific primers for *AtHON5* (1.019 kb band) and for the T-DNA insertion (0.383 kb band). Homozygous *Athon5* mutants were obtained and watched on a weekly basis for any phenotypic difference with that of the wild-type.

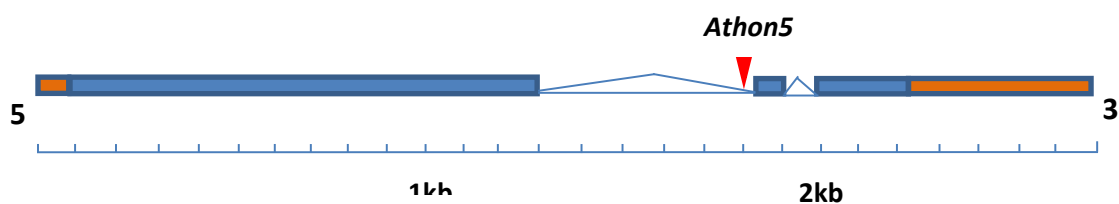


Figure (4.33): Schematic diagram of *At1g48620* locus showing T-DNA insertion localisation . 2.693 kb of *AtHON5* organisation into UTRs, exons and introns. Exons are represented with blue boxes. Introns are shown as triangles and UTRs are diagrammed as orange blocks. And the *Athon5*; N656137-salk_007422, T-DNA insert, as inverted red triangle.

4.2.10.1. Phenotypic characterisation of *Athon5* mutant plants

The phenotypic characterisation of *Athon5* mutant plants showed that 55.5% of the homozygous T-DNA plants were delayed in the flowering time (**Figure 4.34**). *Athon5* mutant plants which were delayed in their flowering development managed to complete normal flowering after two to three weeks delay compared to that of the wild-type plants.



Figure (4.34): Phenotypic characterisation of *Athon5* mutant plants.

55.5 % of *Athon5* mutants showed flowering delay and slow plant development phenotype at the beginning of development.

4.2.10.2. Fertility of *Athon5* mutant plants

Athon5 mutant fertility was analysed by assessing their seed sets and silique lengths in comparison with the wild-type plants. The Average silique length of *Athon5* and wild type were 13.07mm and 14.14mm respectively (**Figure 4.35 A**). P value of 0.000181 (T-test) confirmed that the difference seen in the silique length between *Athon5* and wild-type was significant. However, the seed set average of *Athon5* and wild-type were 54.04 and 51.06 respectively (**Figure 4.35 B**). The calculated P-value was 0.074 (T-test), indicating that seed production in *Athon5* is not different from the WT.

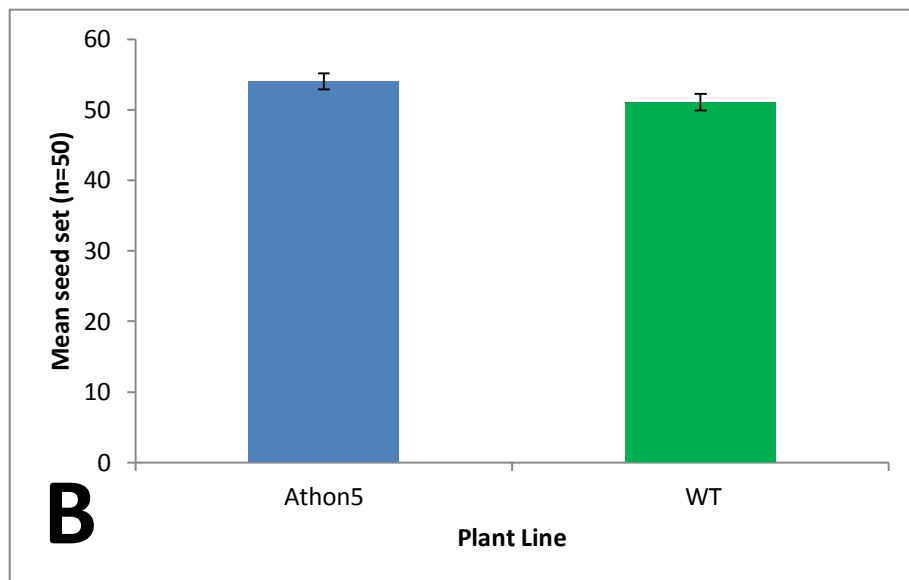
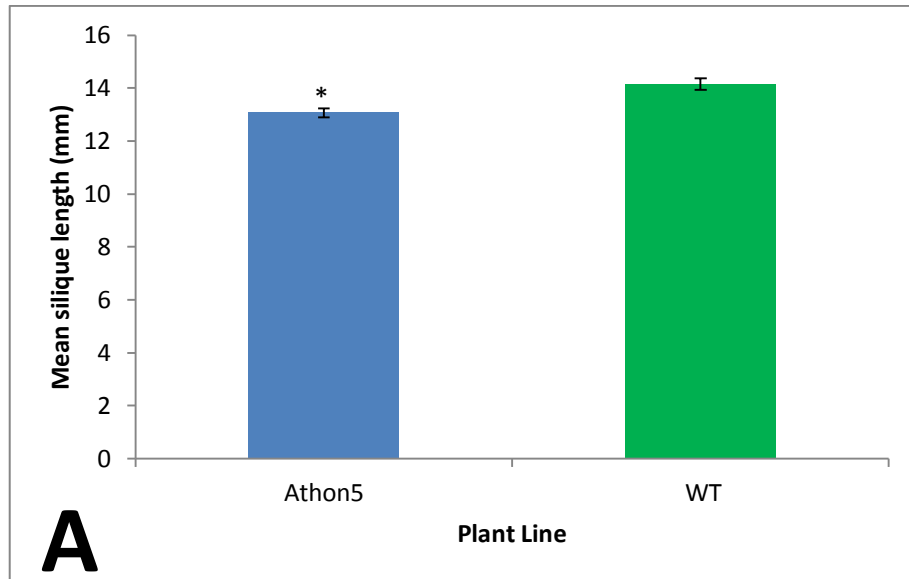


Figure (4.35): Fertility of *Athon5* mutant plants in comparison to WT plants.
 (A) Siliqua length (N=50). (B) Mean of seed set (N=50). *= P<0.05. Error bars= Standard error of the mean.

4.3 Discussion

4.3.1 *Arabidopsis* Linker histone H1 isoforms affect the flowering time of the plant

Our investigation has showed that seven out of ten histone linker H1 mutant lines have significant delay in flowering time; *Ath1.1-1*, *Ath1.2*, *Ath1.3*, *Ath1b*, *Ath1c*, *Athon4*, and *Athon5*. From these lines just three of them presented a significantly reduced fertility (*Ath1.1-1*, *Ath1.2* and *Ath1.3*). Our observations of the flowering time delay might be due to the impact of H1 deletion on transcription, which could be one of the major causes for the developmental switch from vegetative to reproductive growth. Flowering time delay has been reported as a consequence of reduction in transcription (Zhang and Nocker, 2002; Zhang *et al.*, 2003; He *et al.*, 2004; Oh *et al.*, 2004). Additionally, a number of histone modifications or remodelling activities regulated by H1 at the 3' position of genes can have consequences in transcription (Selth *et al.*, 2010). Several studies have showed that, Flowering locus C (FLC) protein, which possess a MADS box domain, can regulate the vegetative phase to converge to the reproductive phase in plants (Creville`n and Dean, 2011). The flowering process is a consequence of two pathways: environmental cues and developmental cues, which regulate the floral pathway integrator. Paf1c is a specific site at *FLC* locus with high importance. It was found that mutations at this locus both in yeast and mammalian cells causes dramatic changes on the process of transcription either by affecting histone modifications or chromatin-remodelling, transcriptional elongation, in addition to its impact on the recruitment of processing factor at the 3' end (Selth *et al.*, 2010). Some reports showed that, mutations of Paf1c at the *FLC* locus reduce transcription. A reduction in both H3K4me3 at 5' end

and H3K36me2/3 was recorded together with an increase in the H3K27me3 (Oh *et al.*, 2008). These findings emphasize that the delay in flowering time in different *Ath1* mutant lines might be due to an interference with the transcription machinery affecting flower development, and probably the *FLC* transcription.

4.3.2 Histones play a role in proper timing of plant development

The presence of multi copies for linker histone proteins in eukaryotes makes it highly difficult to study each single gene even with the different advanced technologies in producing mutants with different gene expression. Gene redundancy could deal with any single gene loss and produce the wild-type like phenotype. Cutting down the H1s community into groups sharing characteristics, and studying each in more detail eases their study, and so, this is what we have done in this project.

The single gene knock-out technology used for analysing each of the ten *Arabidopsis* histone H1s have showed us developmental timing defects in reference to their wild-type. The delayed pattern in flower formation existed in *Ath1s* mutants; *Ath1b*, *Ath1c*, *Ath1.1-1*, *Ath1.2*, *Ath1.3*, *Athon4*, and *Athon5* at earlier stages did reduce the plant development to their fully mature organ phenotype with a delayed period ranges between two to three weeks in reference to their parallel grown wild-type plants. The *Ath1s* mutant plants can be divided into two categories according to their flowering phenotype; delayed and non-delayed. Data indicated that all of the *Ath1s* mutants belonging to HMG-like protein domain were found to show a delayed flowering phenotype, whereas the ones belonging to H1-like and MYB-like protein domains showed both delayed and non-delayed phenotypes as shown in **Figure (4.36)**.

These observations together with the data obtained from genevestigator where all H1s are expressed constitutively during plant organogenesis give us a hint that these proteins are needed for the normal plant development. Moreover, each of the single H1s mutants showed a kind of abnormality either at developmental timing level or at fertility level suggesting the necessity of each single H1 protein in the *Arabidopsis* nuclei in controlling the vital processes of the plants.

Additionally, the ability of plants to skip delay in flowering, and proceed to the normal like mature stage reflects somehow that H1s proteins could be redundant functionally. This belief is further acceptable since H1s protein alignment showed a pair like homology relying on their amino acid sequence. A proteomic screening for single H1 proteins within each single null H1 mutant line will add more data to the real relation between *Arabidopsis* H1s isoforms. Furthermore, cytological analysis of their corresponding single mutants as well as the development of higher level mutants where two or more of H1s proteins are null will enhance drawing a clear conclusion for their supposed redundancy and or specificity within nucleus context.

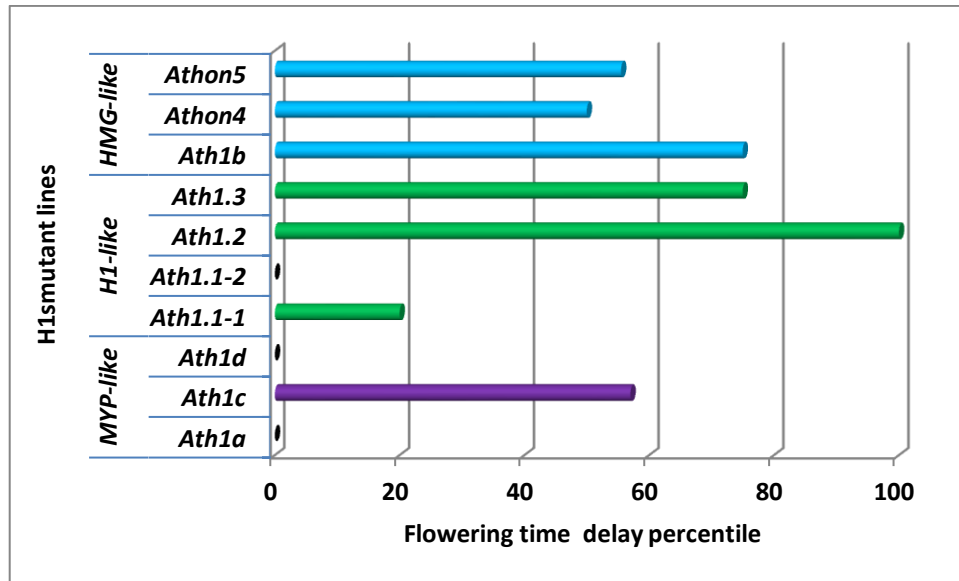


Figure (4.36): Comparison between *Arabidopsis Ath1s* single T-DNA mutants and wild-type plants in flowering time delay.

4.3.3. Histone H1 gene duplication allows H1 compensation in the single *Ath1* null mutants

Our study of the *Ath1s* single mutants (*Ath1b*, *Athon4*, *Athon5*, and *Ath1d*) showed that although each of them got delayed flowering at the beginning, their phenotype would mature to that of the wild-type after some days, suggesting a putative redundancy effect for the different H1 variants in *Arabidopsis*. An error in one gene can be substituted by activating other variants. Our *in silico* analysis of histone H1 proteins which showed that it has a pair wise order according to their protein sequences homology might support this conclusion. Moreover, previous findings by Wierzbicki and Jerzmanoski (2005) reported that the *in vivo* examination of globular linker histone in plants is difficult due to the presence of several isoforms. In addition to Fan *et al.* (2001) results that H1 has several compensating variants. Moreover,

Hanada *et al.* (2009) reported that *A. thaliana* is known in having duplicated genes that are functionally equivalent. And so knocking out one of the gene copies do not cause plant death, since gene loss is rescued by its duplicates.

4.3.4 Loss of H1-like proteins prevents normal fertility

Our analysis to the ten histone *Ath1s* mutant lines showed variation in its loss impact on the plant fertility level. Seven *Ath1s* mutant lines: *Ath1.1-1*, *Ath1.1-2*, *Ath1.2*, *Ath1.3*, *Ath1a*, *Ath1c* and *Athon4*, showed reduction in fertility parameters assessment in comparison to the WT plants. Of these, four *Ath1* T-DNA lines; *Ath1.1-1*, *Ath1.1-2*, *Ath1.2* and *Ath1.3*, and one RNAi line; *h1.1*, showed significant fertility reductions (**Figure 4.37**). Our findings come together with previous studies by (Prymakowska-Bosak *et al.*, 2002; Slusarczyk *et al.*, 2003) on *Nicotiana tabacum* L (Tobacco), who found that inactivation of histone H1 variant caused abnormalities in the flower development and male gametophyte formation leading to male sterile plants.

Fertility level reduction in the *Ath1.1-1*, *Ath1.1-2*, *Ath1.2* and *Ath1.3* could be as a consequence of defects during meiotic chromosomes segregation. Meiosis errors are mostly the direct cause of fertility loss (Osman *et al.*, 2011). Moreover, several reports indicated that defects in homologous chromosomes alignment (Shen *et al.*, 2008), pairing and synapsis (Dernburg *et al.*, 1998; Higgins *et al.*, 2005; Sanchez-Moran *et al.*, 2007), might cause defects in chromosome segregation. Hence, lead to sterile plant phenotype. The meiotic stages in *Ath1.1-1* (**Figure 5.4**), *Ath1.1-2* (**Figure 5.6**)

and *h1.1^{RNAi}* (Figure 5.7) were analysed for these mutant lines in comparison to the WT (Figure 5.3) as will be discussed later in chapter five.

From another point of view, an epigenetic switch might have arisen due to a certain H1 protein loss. And so, this could have been the cause for the developmental defects, and even the silique length and seed numbers. Still all of these are possibilities and further cytological, immunocytological, and proteomics analysis are necessary to be able to get a clear view on defects observed in these mutants.

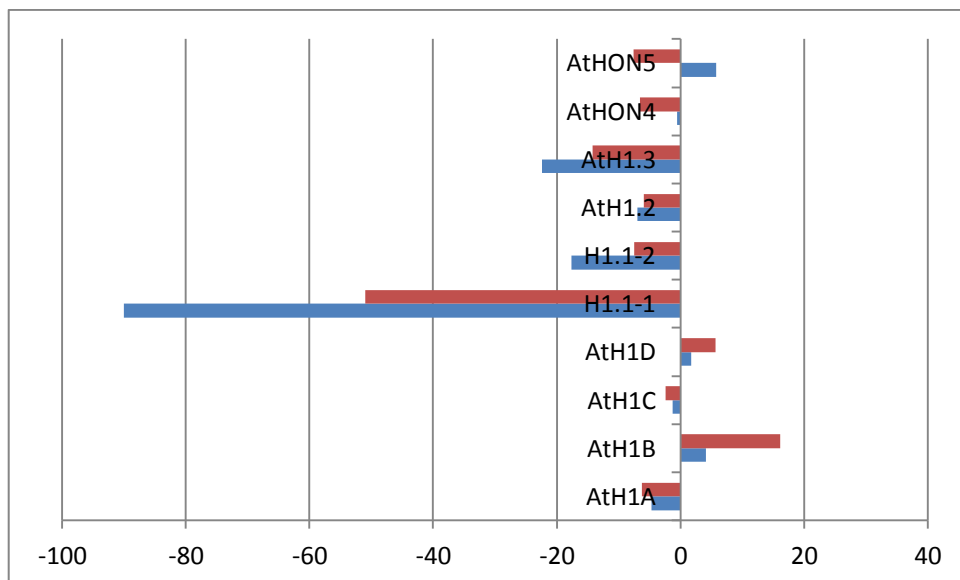


Figure (4.37): Fertility change in percentage for *Arabidopsis* histone *Ath1s* single mutant lines. Red block resembles changes in silique length. The blue block represents changes in seed set count per silique. Horizontal axis line resembles fertility change in percentage. Positive values shows increase in fertility. Negative value resembles reduction in fertility.

H1	Gene Locus	T-DNA Line Locus	T-DNA Position	Flowering delay	Fertility Changes
Ath1a	At1g54260	N877696- Sail_883_F09	3 rd intron	0 %	(A) 4.65 % ↓ (B) 6.20 % ↓
Ath1b	At5g08780	N659488- salk_090072	3 rd exon	75%	(A) 4.13 % ↑ (B) 16.12 % ↑
Ath1c	At1g48610	N586260- Salk_086260	2 nd Intron	43 % - 57%	(A) 1.29 % ↓ (B) 2.40 % ↓
Ath1d	At1g72740	N65754- Salk_065267	5 th intron	0 %	(A) 1.76 % ↑ (B) 5.65 % ↑
Ath1.1-1	At1g06760	N521410-salk_021410	Upstream UTR	5%	(A) 90 % ↓ (B) 51 % ↓
Ath1.1-2	At1g06760	N-654890- salk_128430	1 st exon	0 %	(A) 17.6 % ↓ (B) 7.50 % ↓
Ath1.2	AT2G30620	N321948- GK-116E08	1 st exon	100%	(A) 6.9 %* ↓ (B) 5.9% ↓
Ath1.3	At2g18050	N665594- Salk_025209	300-UTR	75%	(A) 22.4 % ↓ (B) 14.2% ↓
Athon4	At3g18035	N599887- Salk_099887	Exon 4	50%	(A) 0.51 % ↓ (B) 6.5% ↓
Athon5	At1g48620	N656137- Salk_007422	2 nd intron	55.5%	(A) 5.51 % ↑ (B) 7.57 % ↓

Table (4.2): Summary of *Arabidopsis* histone *Ath1s* mutant lines phenotypic changes.

A= Seed data. B= Silique data. Arrows represents change in fertility parameter, upper arrows represents increase and lower arrows represents decrease. Black arrows represent non-significant change and red arrow represents significant change. Purple shade represents MYP-like H1s. Blue shades represents HMG-like H1s, and Grey shades represents H1-like H1s.

4.4. Future work

4.4.1 H1s Redundancy effect

The normal plants phenotype in the single *Ath1s* mutants in the studied T-DNA lines implied that *Arabidopsis* H1s seem to be functionally redundant. This result was supported with the H1s proteomics homology amino acid sequence similarity (**Figure 4.3**). Since *in silico* H1s protein sequence analysis suggested that H1s are grouped into pair-like manor, so this might imply that these pairs are functionally similar, hence, in order to understand their cellular role demands creating double, triple or higher *Ath1s* T-DNA mutants. For that, **Table 4.3** was created showing the possible *Ath1s* T-DNA double mutants that could be created, from single *Ath1* T-DNA mutants crosses, depending on the H1 protein sequence similarity. This prediction needs more investigation.

T-DNA line	Locus	Crosses
N659488-Salk_090072	At5g08780 H1B	
N877696-Sail_883_F09	At1g54260 H1A	
N599887-Salk_099887	At3g18035 <i>HON4</i>	
N665594-Salk_025209	At2g18050 <i>H1.3</i>	
N656137-Salk_007422	At1g48620 HON5	
N521410-Salk_021410	At1g06760 <i>H1.1-1</i>	
N654890-Salk_128430	At1g06760 <i>H1.1-2</i>	
N321948-GK-116E08	At2g30620 H1.2	
N586260-Salk_086260	At1g48610 H1C	
N657654-Salk_065267	At1g72740 H1D	

Table (4.3): Suggested double Histone *Ath1* mutant lines crosses based on protein sequence homology.

Lines with the same colour (show high sequence homology) are crossed together.

CHAPTER 5

H1.1 ROLE IN MITOTIC AND MEIOTIC CHROMOSOME AXIS ORGANIZATION

5.1. Introduction

The linker histone (H1) role in the chromatin organisation have been addressed in several reports. Thoma *et al.* (1979) reported that the *in vitro* addition of histone H1 to the 10 nm nucleosome fibre leads to the formation of the 30 higher order chromatin fibre structure. But on another hand other studies showed that the zigzag two start helix model of the higher order chromatin fibre structure could be formed by interactions form between the H2A acidic amino acids and the amino terminal residues on H4 (Schalch *et al.*, 2005). Thus, H1 role is not yet confirmed in the higher order chromatin structure and in the chromatin organisation, and more studies and analysis are still required to reveal that. Several defects were observed and recorded in the mutants lacking the normal active histone H1 gene products from yeast (Downs *et al.*, 2003), to *Ascobolus immerses* (Barra *et al.*, 2000), *Tobacco* (Prymakowska-Bosak *et al.*, 1999) and *Xenopous* (Maresca *et al.*, 2005). But the presence of different isoforms for the linker histone H1 (Fan *et al.*, 2001) makes it difficult to study each isoform individually. Since gene redundancy could interfere with the phenotype appearance in the single mutants. Interestingly, the link between linker histone H1 and the chromatin organisation *in vivo* came from a study on *Xenopus*. Maresca *et al.* (2005) showed that *in vivo* depletion of histone H1 in *Xenopus* resulted in two times longer mitotic chromosomes. Furthermore, when the H1 was overexpressed, the interphase chromatin was highly compacted (Freeman and Heald, 2010).

In this chapter we will analyse two T-DNA insertion mutants, *Ath1.1-1* and *Ath1.1-2*, and *h1.1^{RNAi}* using cytological, FISH and immunocytological techniques to assess H1.1 role during mitotic and meiotic chromosome organization. We will provide clear evidences for the H1.1 importance for preserving normal homologous recombination levels by allowing the correct formation of the homologous chromosomes axes and thus the proper synapsis and crossover maturation.

5.2. Cytological analysis of mitosis in *Ath1.1* mutants

DAPI stained mitotic cells of *Ath1.1-1* T-DNA plants showed that mitotic metaphase chromosomes appeared to condense differently in 50% metaphase nuclei (n=100) (**Figure 5.1 B&D**). This defect was also recorded in 30% *h1.1^{RNAi}* mutant nuclei (**Figure 5.1 I**). The mitotic metaphase chromosomes appeared to be longer in these mutants than in the wild-type (**Figure 5.1 A**). This abnormality was followed by defects in chromosome segregation at anaphase, in which sister chromatid separation was affected producing lagging chromosomes. Anaphase bridges were observed in *Ath1.1-1* (**Figure 5.1 E**). Anaphase bridges were observed in 3% of cells in *Ath1.1-1* (n=100) (**Figure 5.1 F**)

Mitosis was also checked in the double heterozygote mutant *Ath1.1-2^{-/+}/Ath1.1-1^{-/+}*. DAPI-stained mitotic cells showed abnormal sister chromatid separation in 2% anaphase nuclei (n=50) (**Figure 5.1 J**). Leading to an abnormal chromosome orientation (**Figure 5.1 K**) and anaphase bridges (**Figure 5.1 L**). Furthermore, 2% of the nuclei showed anaphase bridges present at telophase (n=50) (**Figure 5.1 M**).

This finding was consistent in all *Ath1.1* mutants. As anaphase bridges were observed in *Ath1.1-1*, *Ath1.1-2* and *h1.1^{RNAi}*.

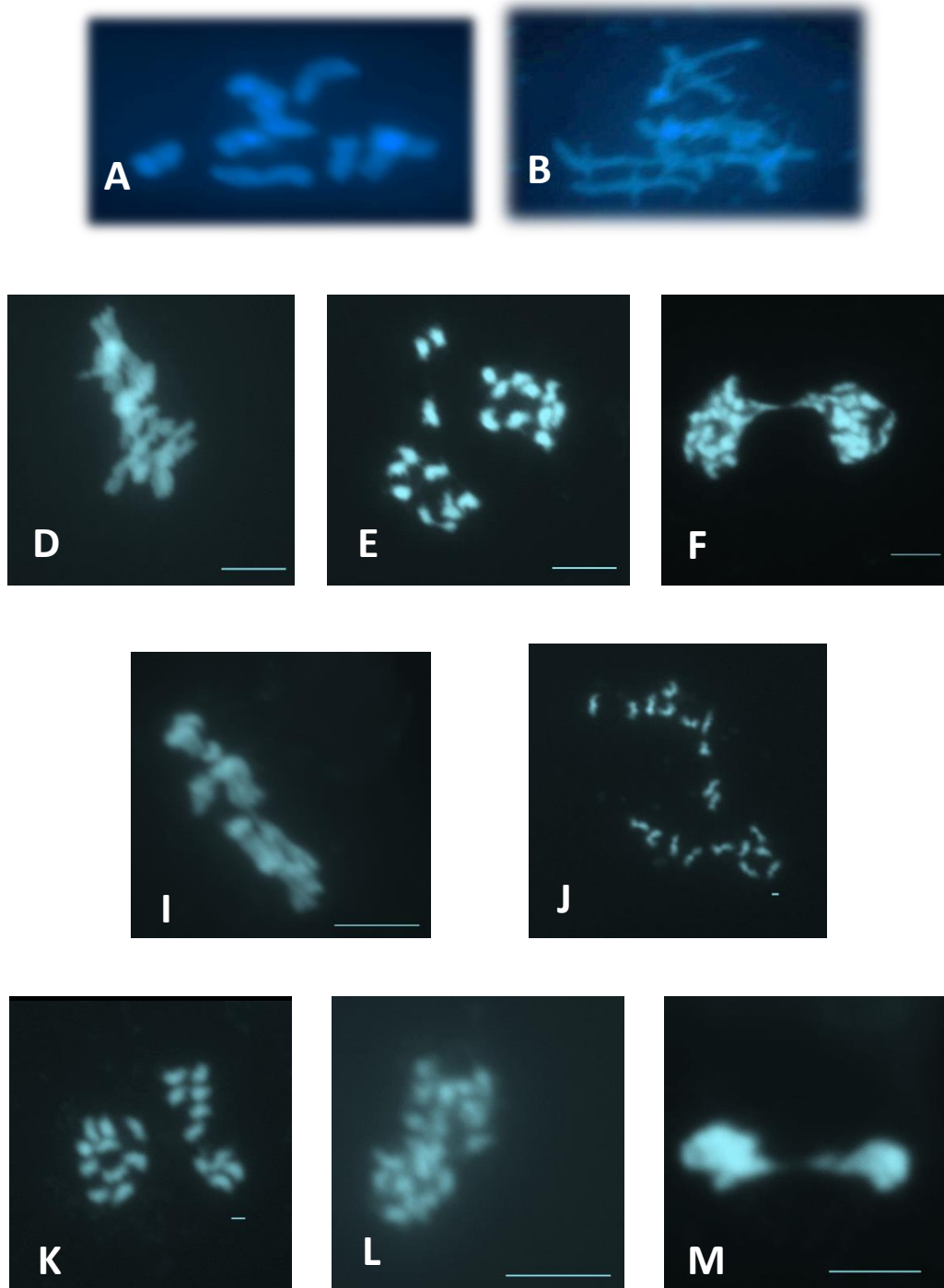


Figure (5.1): Mitotic defect analysis in *Ath1.1* mutants; *Ath1.1-1*, *Ath1.1-2* and *h1.1RNAi*, in comparison to WT.

(A) WT. (B-F) *Ath1.1-1*. (I) *h1.1^{RNAi}*. (J-M) *Ath1.1-2^{+/+}/Ath1.1-1^{+/+}*. (D&I) Metaphase: Long chromosomes indicating that chromosomes condensation is abnormal comparable to WT metaphase (A). (E&J)

Anaphase: sister chromatid separates but unable to orient in a way that give two equal nuclei. One nuclei with normal ten chromosomes whereas the other with seven, however, three chromosomes are lagging comparable to the balanced sister chromatids separation in WT (B). (F&L&M) Anaphase-telophase: anaphase-bridge is obvious between the two nuclei indicating that lagging chromosomes are still stuck in between the newly formed daughter nuclei in comparison to the balanced daughter nuclei at telophase in WT (C).

Mitotic defects	Plant line			
	<i>Ath1.1-1</i>	<i>Ath1.1-2</i>	<i>h1.1^{RNAi}</i>	<i>Ath1.1-2^{+/-}</i> <i>/Ath1.1-1^{+/-}</i>
Chromosome compaction defect (Metaphase)	√ 50%		√ 30%	
Mis-oriented chromosomes (Anaphase)	√ 10%			√ 10%
Anaphase-bridge (Telophase)	√ 10%	√ 10%		√ 20%

Table (5.1): Summary of defects seen in the mitosis of *Ath1.1* mutants

5.3. *AtH1.1* expression is not specific to meiosis

AtH1.1 microarray data has showed that its expression is carried out in all types of *Arabidopsis* tissues (Figure 5.2). *AtH1.1* is expressed in cotyledon, seedling, rosette, seeds, leaf, root, stamen, shoot, inflorescence, flower bud, ovary and silique. Hence, *AtH1.1* is expressed in both vegetative and reproductive tissues.

● AT100700

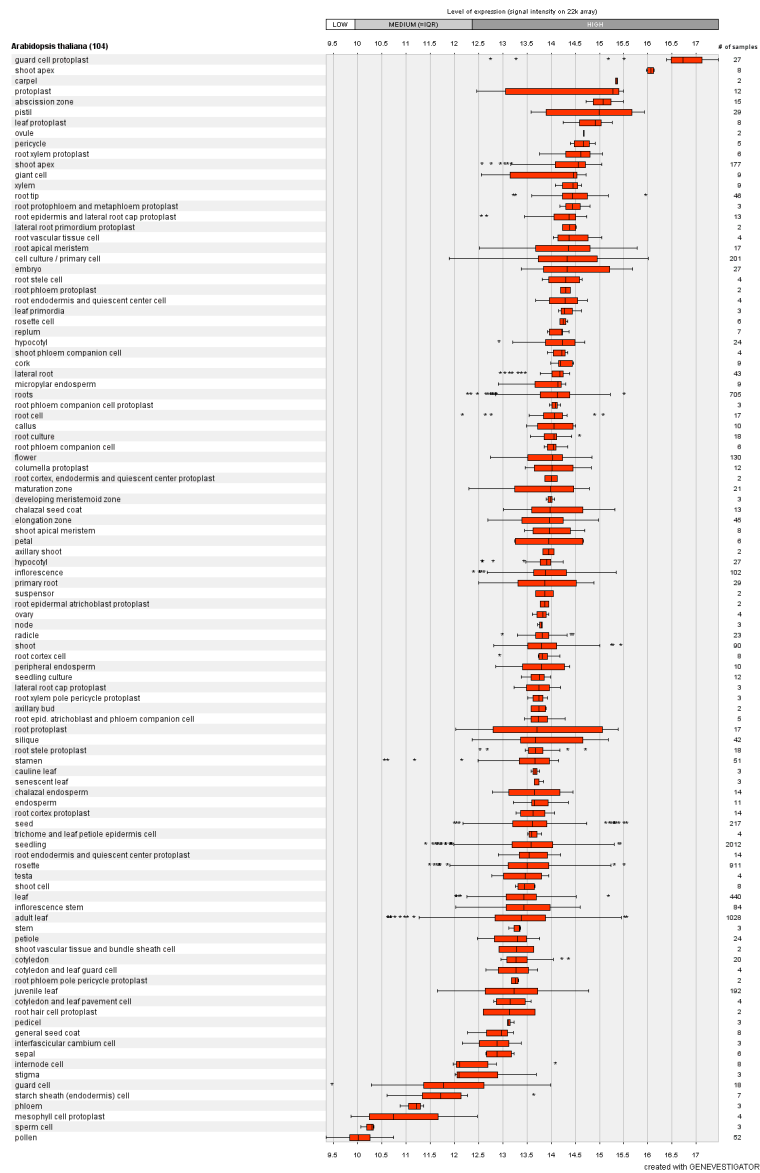


Figure (5.2): Genevestigator expression profile of *Arabidopsis Ath1.1* gene. Microarray data showed that *Ath1.1* is expressed in both vegetative and reproductive tissues. Results show rate of expression in each tissue in reference to the number of samples used for calculating expression mean value. (Hruz *et al.*, 2008).

5.4. Cytological analysis of meiosis in *Arabidopsis* wild-type and *Ath1.1* mutants

To confirm that the fertility defect observed in *Ath1.1* mutant lines (**Figures; 4.19, 4.20, 4.21**) was due to meiotic errors, cytological studies were carried out in pollen mother cells (PMCs) in parallel with the wild-type.

5.4.1. Meiotic cytology of *Arabidopsis* wild-type

The wild-type *Arabidopsis* (Col-0) was analysed for the different meiotic stages using DAPI stained PMCs. The process of meiosis undergoes two divisions, meiosis I and meiosis II. Each can be divided into four stages (prophase, metaphase, anaphase and telophase). Meiosis I initiates at prophase I with discriminative five substages: leptotene, zygotene, pachytene, diplotene and diakinesis. Before meiosis takes place a premeiotic stage termed interphase occur, in which chromosomes initiates to condense, and the sister chromatids are held together after the DNA is replicated prior to enter meiosis. Meiosis I start with leptotene (**Figure 5.3 A**), in which condensed chromosomes become clearly visible. It is followed with zygotene (**Figure 5.3 B**), when the pairing of homologous chromosomes starts, with synapsis and recombination at certain regions of the chromosomes. The chromosomes in this stage have often a discriminative dense knot configuration at one side of the nucleus. Chromosomes then enter pachytene (**Figure 5.3 C**) stage, in which homologous chromosomes are fully synapsed. Hence, homologous chromosomes appear as thick strands with densely stained centromeres. In Diplotene (**Figure 5.3 D**), the chromosomes continue to condense and de-synapsis occur leading to the appearance of extended (sometimes diffused) long chromosomes. Diakinesis

(**Figure 5.3 E**) proceeds later when five bivalents of homologous chromosomes are visually clear. Each bivalent is held by a chiasma at each crossover site. At metaphase I (**Figure 5.3 F**), the five bivalents are aligned at the equatorial region of the cell. And at anaphase I (**Figure 5.3 G**) homologous chromosomes separate, and move towards the opposite poles of the cell. At telophase I (Dyad stage) (**Figure 5.3 H**) the haploid set of chromosomes is present at each pole of the cell separated by a distinguishable wall of granules (cell's organelles, mitochondria and chloroplasts). The chromosomes start re-condensing at prophase II. And at metaphase II (**Figure 5.3 K**), fully condensed chromosomes align at the meiotic spindle equator and at anaphase II (**Figure 5.3 L**), sister chromatids separate and the two sets of chromatids divide to opposite poles. Finally, at telophase II (tetrad stage) (**Figure 5.3 M**) four nuclei are formed, each with a haploid set of the whole genome.

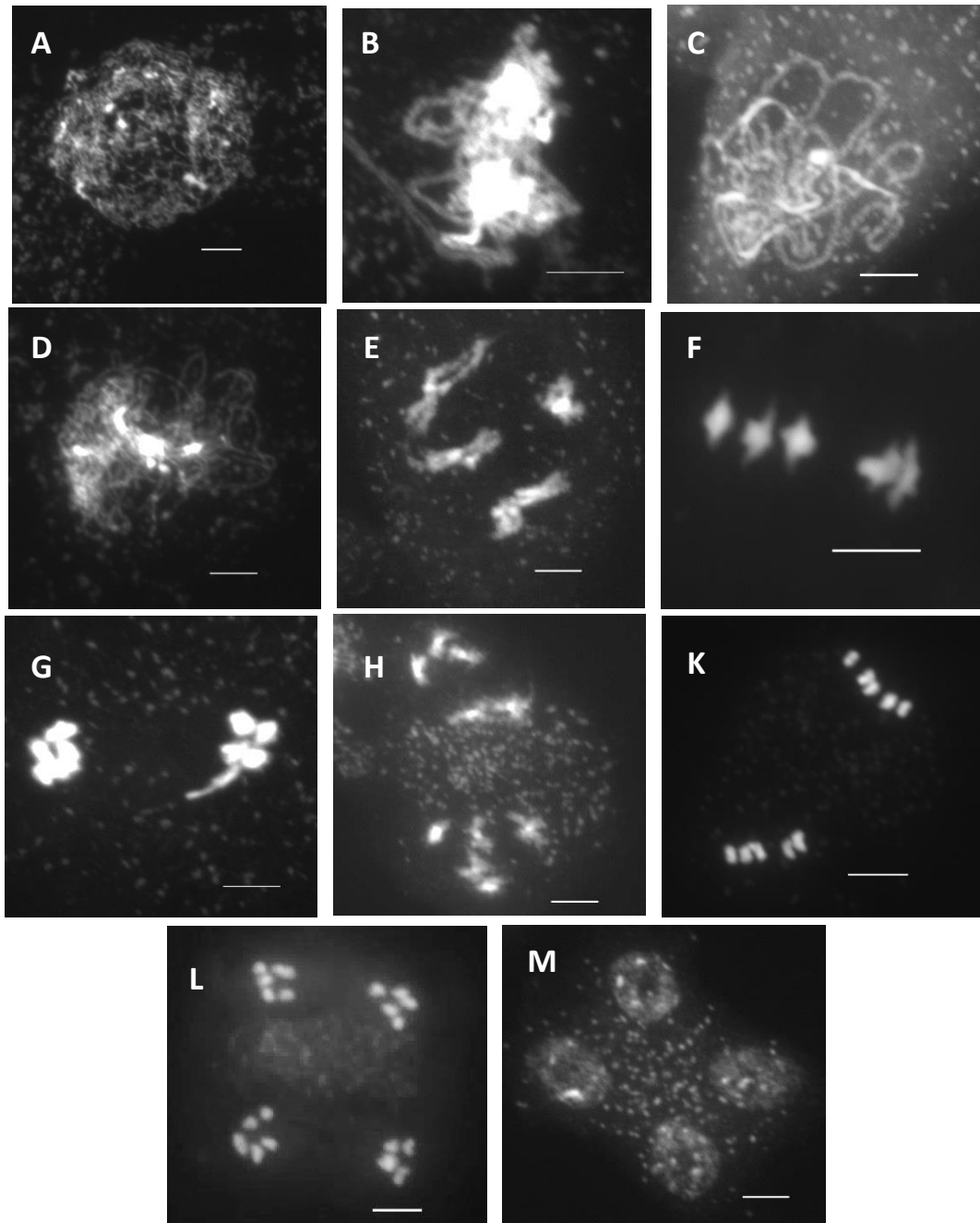


Figure (5.3): Meiotic atlas of wild-type PMCs.

(A-H) Represents meiosis I. (I-M) Represents meiosis II. Meiosis I initiates with prophase I (A-E). (A) Leptotene: chromosomes condense, then homologous chromosomes pairing initiates. (B) Zygotene: pairing between homologous chromosomes continues. (C) Pachytene: full synapsis forms between homologous chromosomes. (D) Diplotene: homologous chromosomes DE synapse. (E) Diakinesis: Homologous chromosomes cross over, with an obvious 9-10 COs. (F) Metaphase I: Five bivalents are observed. (G) Anaphase I: homologous chromosomes separate and move towards the opposite poles of the cell. (H) Dyad stag: The haploid set of chromosomes is present at each pole of the cell separated by a distinguishable wall of granules. (K) Metaphase II: fully condensed chromosomes align at the cell equatorial region. (L) Anaphase II: sister chromatids separate and the two sets of chromatids divide and move to opposite poles. (M) Telophase II: four balanced haploid tetrad nuclei are formed. Cells are DAPI stained. Bar 5 μ m

5.4.2. Meiotic cytology of *Ath1.1-1*

The 90% reduction in fertility within *Ath1.1-1* mutants could be due to meiotic errors. DAPI-stained chromosome spreads were prepared from *Ath1.1-1* PMCs. The cytological analysis of the *Ath1.1-1* line showed severe chromosomal abnormalities during different meiotic stages. Although the initial meiotic stages of leptotene (**Figure 5.4 A**) and zygotene (**Figure 5.4 B**) showed no differences with the wild-type, however, chromosome abnormalities start to appear after those stages. At pachytene (**Figure 5.4 C**) homologous chromosomes did not synapse completely along the full length of the homologues, in contrast to the fully synapsed homologues in the wild-type. Defects are more obvious at diakinesis (**Figure 5.4 E**). Chiasma frequency between homologous chromosomes was highly reduced, leading to early appearance of univalents, comparable to five bivalents in the wild-type meiocytes. The number of chiasma per cell observed in the *Ath1.1-1* ranged from 0 (**Figure 5.4 F**) to 5, in contrast to the 8 to 12 range in the wild-type. In addition, we observed some meiocytes showing early sister chromatid separation at metaphase I (**Figure 5.4 F**). Around 6% of *Ath1.1-1* metaphase I (n=100 cells) showed early sister chromatid separation (**Figure 5.5 A**), showing a mean value of 0.06 (**Figure 5.5 B**), which resembles significant increase comparable to WT. Moreover, 9% of *Ath1.1-1* metaphase I nuclei (n=100) showed some chromosome fragments (**Figure 5.5 C**), with 0.12 fragment per nuclei (**Figure 5.5 D**), indicating significant differences from WT. Moreover, 100% of cells showed univalents (**Figure 5.5 E**), with a mean value of 7.98 univalents per nuclei (**Figure 5.5 F**), showing a significant increase comparable to WT. The consequences of chiasmata deficiency were obvious at anaphase I (**Figure 5.4 G**), where a clear lagging of the chromosomes movement towards the

opposite poles of the cell were visualised, which resulted in the incorrect number and or set of chromosomes be settled at opposite poles. Chromosome mis-segregation defects continued to second meiotic division (**Figure 5.4 H**), where two big nuclei missing the complete set of chromosomes, and small nuclei with few chromosomes appeared. As meiosis I outcome was abnormal, hence, meiosis II follows on initiating with abnormal prophase II (**Figure 5.4 I**), unbalanced nuclei were formed due to chromosomes mis-segregation. At metaphase II (**Figure 5.4 J**) condensed chromosomes aligned at the nucleus equator with some defects; in which the number of chromosomes is unequal on the two poles due to chromosome lagging or chromosome loss. And at anaphase II (**Figure 5.4 K**) and telophase II (**Figure 5.4 L**) unbalanced chromosome segregation was clearly observed.

It is interesting to notice that the *Ath1.1-1* meiotic chromosomes showed defects at the level of chromosome compaction. Some of the mutant chromosomes were not fully condensed at diakinesis (**Figure 5.4 E**). Also, we observed asynchronous chromosomes re-condensation pattern at prophase II (**Figure 5.4 I**). This is very different in the wild-type which presented a very synchronous pattern of chromosomes condensation and re-condensation during the meiotic process. Moreover, an early sister chromatid separation at metaphase I proceeding to metaphase II stages, might suggest a role for *AtH1.1* in preserving the chromosome structure organisation and chromatid cohesion. To further characterise these meiotic defects observed we carried out immunolocalisation studies in the *Ath1.1-1* mutant as well as the WT.

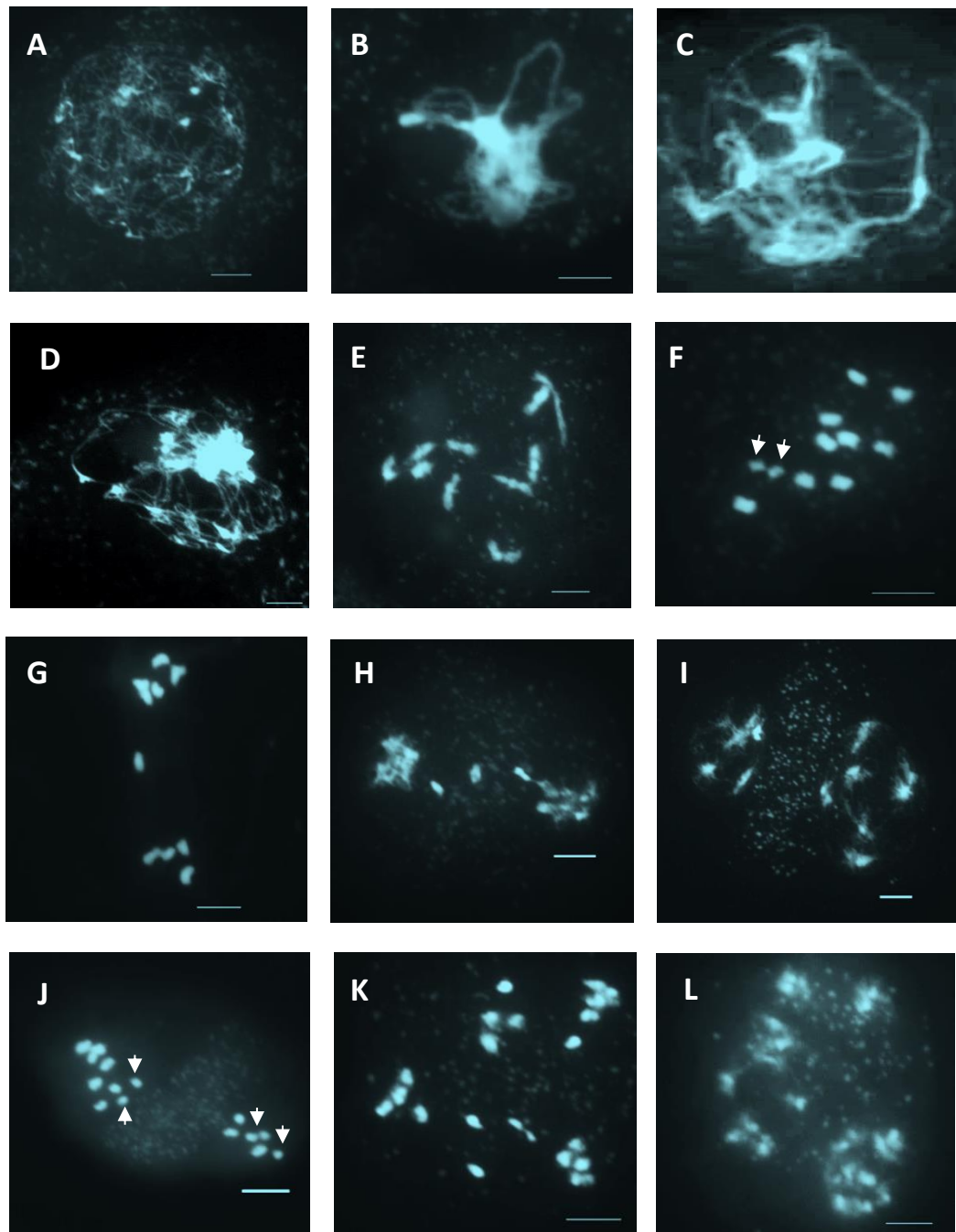


Figure (5.4): Meiotic atlas of *Ath1.1-1* PMCs.

(A) Leptotene and (B) zygotene stages show the wild-type phenotype, whereas, at pachytene (C) the homologous chromosomes are partially synapsed. Diplotene: (D) desynapsed homologous chromosomes. Hence, at (E) diakinesis significant reduction in COs is obvious, with early univalents appearance. (F) At metaphase I COs significant decline was confirmed. Chiasmata range per meiocyte in the *Ath1.1-1* was 0-5 with mean value of 1.06 chiasmata. In contrast, the wild-type showed 8-10 COs, with mean of 9.46 chiasmata. As a result of this, chromosomes missegregation were clear at (G) anaphase I, (H) dyad stage as well as meiosis II stages; (I) prophase II, (J) metaphase II, (K) anaphase II, and ending up with aneuploidy at (L) tetrad stage. Moreover, early sister chromatid separation was obvious in meiosis at different meiotic stages, and here at (F) metaphase I and at (J) metaphase II. Cells are DAPI stained. White arrows indicates early sister chromatid separation. Bar 5 μ m

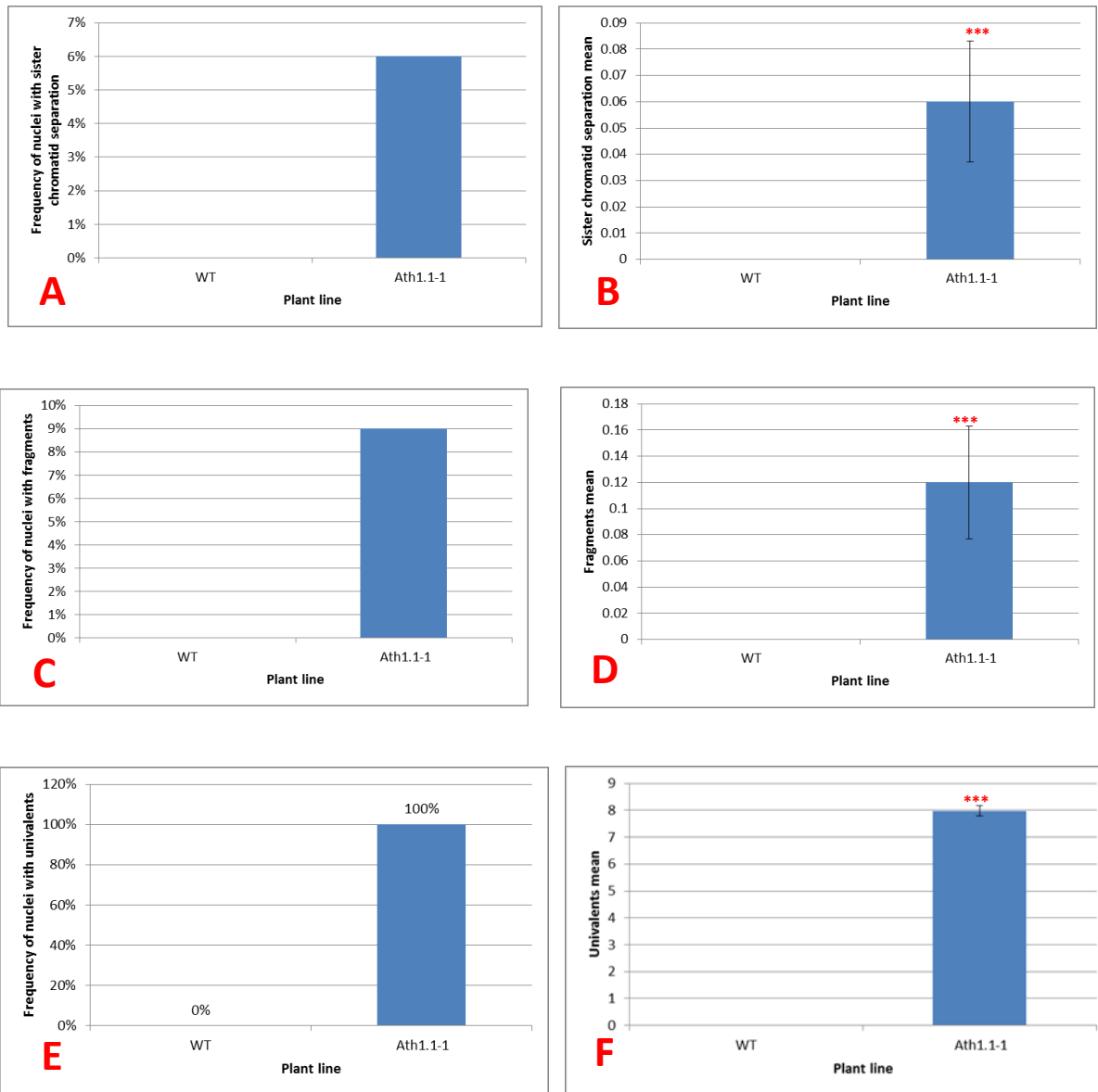


Figure (5.5): Metaphase I Defects observed in *Ath1.1-1* in comparison to WT.

(A) 6% *Ath1.1-1* showed sister chromatid separation while WT is null. (B) *Ath1.1-1* has significantly different phenotype comparable to WT. (C) 9% of *Ath1.1-1* nuclei showed fragments, however WT nuclei were fragments-free. (D) Fragments presence in *Ath1.1-1* showed a mean of (0.12) indicating significant difference from WT. (E) 100% *Ath1.1-1* nuclei showed univalents presence. So, (F) *Ath1.1-1* showed 7.98 univalents per nuclei, indicating significant increase comparable to WT. Triple red asters represent significant difference ($P < 0.05$).

5.4.3. Meiotic cytology of *Ath1.1-2*

The two TDNA mutant lines for *Ath1.1* gene; *Ath1.1-1* and *Ath1.1-2*, showed significant reduction in fertility parameters compared to the WT. Nevertheless, both mutant lines showed different levels of fertility (the parameter that was used is seed count per pod (n=50)) *Ath1.1-1* restored 10% of the WT fertility whereas the *Ath1.1-2* restored 82%. This difference in seed production potential was statistically significant (P-value=1.404E-41, T-test). Fertility changes usually arise due to errors incidence during meiosis. And this seems to be the case for *Ath1.1-1* mutant. To further characterise *Ath1.1-2* mutant, a meiotic atlas of PMCs was prepared.

The results showed that *Ath1.1-2* early prophase I stages; leptotene (**Figure 5.6 A**) and zygotene (**Figure 5.6 B**), were similar to those appeared in *Ath1.1-1* and wild-type. However, meiosis defects were recorded thereafter in comparison to that observed in the wild-type. At pachytene (**Figure 5.6 C-G**) different abnormalities were observed; defects appeared during the chromosome search for their homologue, causing interlocking-like structures to appear (**Figure 5.6 C&D**). Nevertheless, we never observed these structures in *Ath1.1-1* mutants. Partial synapsis between homologous chromosomes (**Figure 5.6 E**) was observed, similar to that seen in *Ath1.1-1*. Moreover, some chromatin breaks (**Figure 5.6 F**) were visible in this mutant line, whereas they were not observed in *Ath1.1-1* pachytenes. Besides that it seemed that pairing between nonhomologues was seen in some cells (**Figure 5.6 G**). Later on at diakinesis (**Figure 5.6 H**) chiasmata between homologous chromosomes were observed but different homologues were interlocked together in

an abnormal manner. Synapsis defects resulted in univalent appearance at metaphase I (**Figure 5.6 I**) causing significant reduction in chiasma frequency with a mean of 8.39 chiasmata per cell. However, the *Ath1.1-1 mutant* showed 1.06 chiasma frequency. At anaphase I and second meiotic divisions, chromosome mis-segregation was observed (**Figure 5.6 J&K&L&M**). Meiotic anaphase bridges were observed in 1% cells (Figure 5.6 K), however such a defect was not viewed in the *Ath1.1-1* meiosis. Moreover, defects in chromosome compaction was visualised also at diakinesis (**Figure 5.6**), similarly to that observed in the *Ath1.1-1* mutant line.

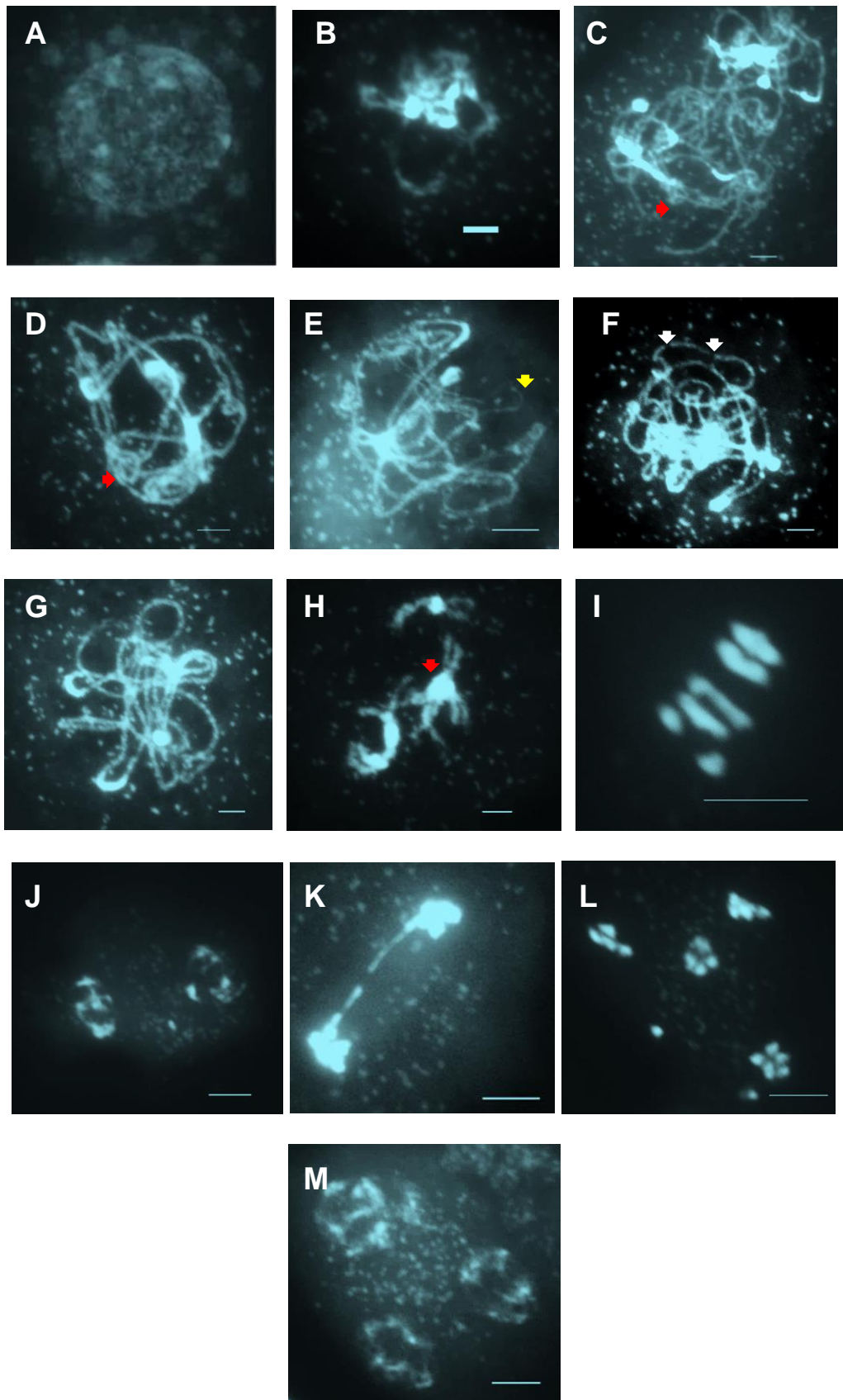


Figure (5.6): Meiotic atlas of *Ath1.1-2* PMCs.

(A) Leptotene and (B) zygotene were similar to wild-type. (C-G) pachytene showed several defects; (C&D) interlocking structure, (E) asynaptic phenotype, (F) chromatin breakage, (G) pairing between nonhomologous chromosomes. (H) diakinesis interlocking structure is still observed. C&D&F&H phenotypes were not seen in *Ath1.1-1*. Synapsis defects resulted in significantly reduced COs at (I) metaphase I. *Ath1.1-2* showed 6-10 COs per meiocyte with an estimated chiasmata mean of 8.39 comparable to 8-10 COs in wild-type with chiasmata mean of 9.46. Although, both *Ath1.1-1* and *Ath1.1-2* showed significant reduction in chiasmata, but *Ath1.1-1* showed 88.79% whereas, *Ath1.1-2* showed 11.3%. Hence, *Ath1.1-2* has 87.4% more COs than *Ath1.1-1*. Chromosome missegregation were consistent at later stages; (J) anaphase-telophase I, (K) dyad, (L) anaphase II, and ending up with aneuploidy at (M) tetrad. Cells are DAPI stained. White arrows indicate chromatin breakage. Red arrows indicate interlocking structures. Yellow arrow indicates unsynapsed chromatin. Scale Bar= 5µm.

5.4.4. Meiotic cytology of *h1.1^{RNAi}* mutant lines

To confirm the meiotic defect seen in the *Ath1.1* TDNA mutant lines; *Ath1.1-1* and *Ath1.1-2*, a knockdown mutant line for histone H1.1 was obtained (N23980-CS23980). The plants were assessed for their fertility. Our results showed a reduction of 41% in seed production in the *h1.1^{RNAi}* comparable to the 90% observed in *Ath1.1-1* and the 17.6% in *Ath1.1-2*. Hence, meiosis analysis was carried out in the *h1.1^{RNAi}* lines using PMCs, to verify for similar defects observed in the meiocytes of *Ath1.1* TDNA mutant lines.

The early prophase stages, leptotene (**Figure 5.7 A**) showed no differences to the wild-type. However, at pachytene (**Figure 5.7**) several defects were recorded. Homologous chromosomes fail to synapse completely similarly to *Ath1.1-1* and *Ath1.1-2* mutants (**Figures B&C**). Interlocking structures were visualised (**Figure 5.7 D**) mimicking that observed in the *Ath1.1-2* mutant. At Diakinesis, early univalents appearance was observed (**Figure 5.7 F&G**) as well as chromosome compaction defects (**Figure 5.7 F&G**), similarly to that observed in both *Ath1.1-1* and *Ath1.1-2* mutants. Chromosome fragmentation (**Figure 5.7 H**) was also recorded. At

metaphase I (**Figure 5.7 I**) a significant reduction in the number of chiasma was observed. Chiasma reduction resulted in the failure of proper homologues disjunction at anaphase I, so chromosomes failed to segregate equally to the opposite poles at anaphase I. Thereafter, chromosome mis-segregation continued to be present at second meiotic divisions (**Figure 5.7 J-O**). The random chromosome segregation at anaphase I and meiosis II observed in the *h1.1^{RNAi}* were similar to the defects shown in the *Ath1.1* TDNA lines.

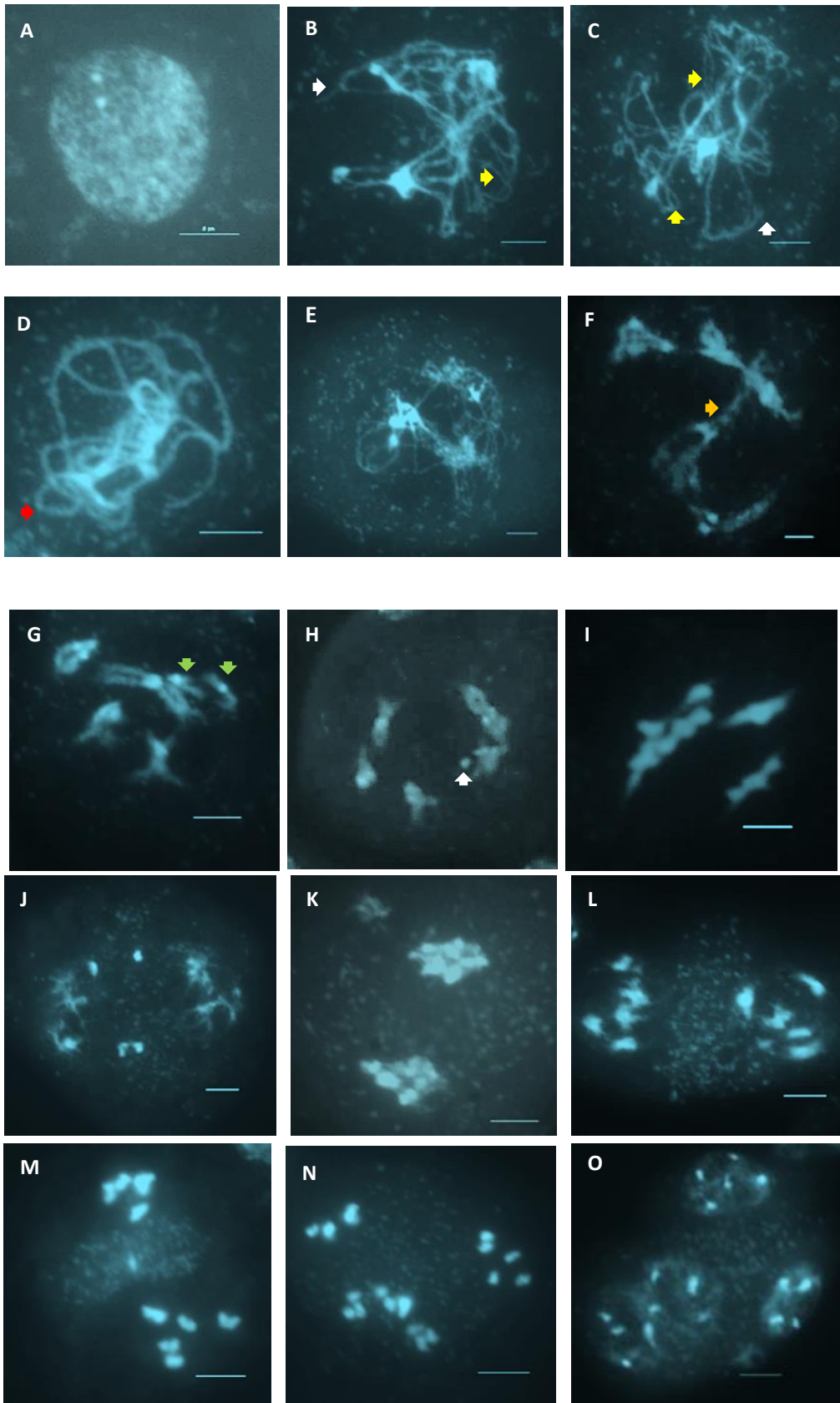


Figure (5.7): Meiotic atlas of *Ath1.1*^{RNAi} PMCs.

(A) Leptotene stage was normal in phenotype, however defects were clearly observed at (B-D) pachytene stage, (F&G&H) diakinesis stage, (I) metaphase I stage, (J) anaphase I stage, (K) dyad stage, (L) prophase II stage, (M) metaphase II stage and (N) anaphase II stage, (O) tetrad stage. (C&D) Interlocking structures. (B&H) Chromosome breakage. (B&C) Asynaptic phenotype. (F&G) defect in chromosome compaction. (I) Chiasmata frequency was reduced, recording chiasmata mean of 7.84 in *h1.1*^{RNAi} comparable to 9.46 in wild-type. (J-N) Chromosome mis-segregation. (O) Tetrad aneuploidy. Cells are DAPI stained. White arrows indicate chromatin breakage. Red arrows indicate interlocking structures. Yellow arrows indicate asynaptic chromatin. Copmpaction defect is represented by orange arrow. Univalents are represented by green arrows. Bar= 5µm.

5.5. Verification of *Ath1.1* mutants phenotype

5.5.1. Fluorescence *in situ* hybridization (FISH) analysis of the T-DNA insertion

in *Ath1.1* mutants

The phenotypic and cytological analysis of *Ath1.1* mutants; *Ath1.1-1* and *Ath1.1-2*, showed that their fertility deficiency arise from similar meiosis defect. Moreover, the *h1.1*^{RNAi} line cytology confirms these *Ath1.1* mutant phenotypes and that are most likely due to mutation in the *AtH1.1* gene. And to confirm that the phenotype observed in these mutant lines were due to the T-DNA insertion in the *AtH1.1* gene, FISH analysis using a T-DNA- labelled probe was used. Signals observed at zygotene and pachytene chromosome spreads from both *Ath1.1-1* and *Ath1.1-2* TDNA mutants showed the presence of only one insertion in both mutants. The FISH results of *Ath1.1-1* showed the presence of two red foci (dot signals) at zygotene (**Figure 5.8 A**) and one red focus (dot signal) at pachytene (**Figure 5.8 B**). Hence, this confirms the presence of one TDNA insert in homozygosis, one in each of the homologous chromosomes, as homologues completely synapsed at pachytene, so the T-DNA signal is reduced to only one focus. Moreover, The FISH analysis of *Ath1.1-2* (**Figure 5.8**) showed similar results to that seen in *Ath1.1-1*. A pair of TDNA

probe signals appeared at zygotene (**Figure 5.8**), however, at pachytene (**Figure 5.8**) the signal was reduced to only one focus.

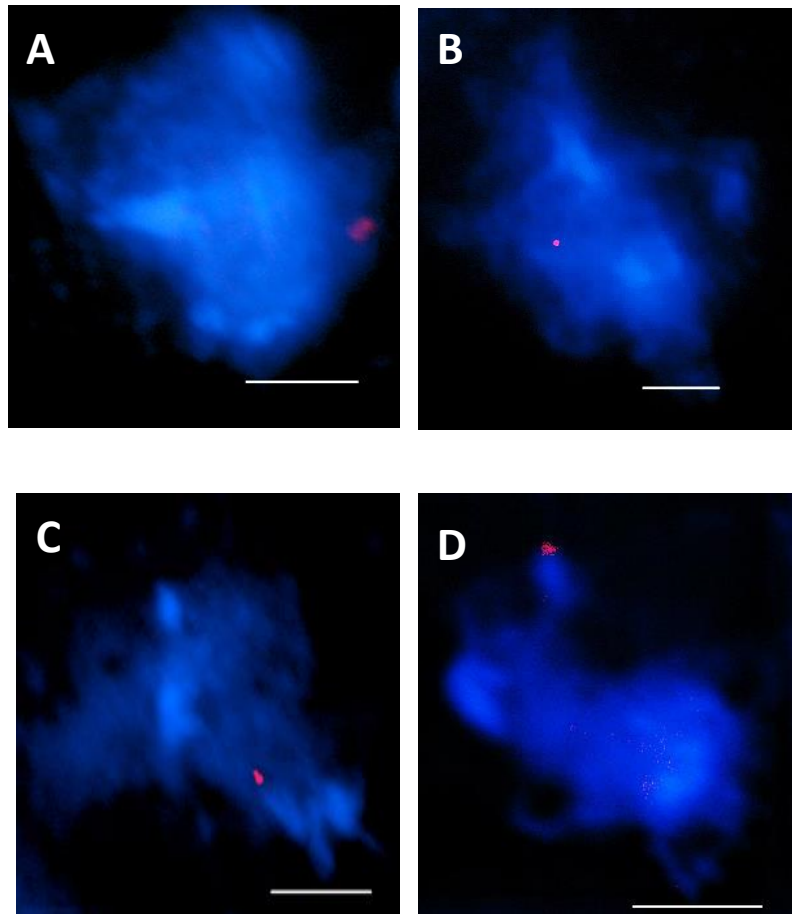


Figure (5.8): FISH verification of *Ath1.1* TDNA insert.

FISH analysis of DAPI stained meiocytes of *Ath1.1* TDNA mutants; (A&B) *Ath1.1-1* and (C&D) *Ath1.1-2*, showed the presence of two pairing signals at (A&C) zygotene, showing one TDNA insert in each of the homologous chromosomes which pair at this stage, and one signal at (B&D) pachytene, as homologues synapse. Red signal indicate *Ath1.1* TDNA- Biotin labelled probe. Bar= 5µm.

5.5.2. Allelism test

To verify that *Ath1.1-1* and *Ath1.1-2* mutant phenotypes are due to a mutation in *Ath1.1* gene, an allelism test was carried out by crossing both mutant alleles with each other. More than six time trials to pollinate *Ath1.1-1* T-DNA stigma with *Ath1.1-2* anthers ended unsuccessfully, producing just empty siliques. However, a reciprocal cross; using *Ath1.1-2* mutant as the female plant and *Ath1.1-1* mutant as the pollinator allowed us to obtain three seeds. These seeds were put to grow, and one plant developed successfully. Its genotype was checked, using the *Ath1.1-1* and *Ath1.1-2* primers, for both the wild-type and the TDNA insert. As expected, the plant genotype was a double heterozygote for *Ath1.1-2/Ath1.1-1*

5.5.2.1 Phenotypic observation of *Ath1.1-2*^{+/-}/*Ath1.1-1*^{+/-} double heterozygote plant

Development and growth of the *Ath1.1-2/Ath1.1-1* double heterozygote T-DNA plants was comparable to that observed in the wild-type. Nevertheless, the double heterozygote plant showed a delay in flowering time, about a week delay compared to WT (**Figure 5.9 A-B**). Furthermore, *Ath1.1-2/Ath1.1-1* double heterozygote mature silique pods showed variation in length that ranged between short siliques (7mm) up to about normal ones (15 mm) (**Figure 5.9 B**). Moreover, some siliques lacked entirely seed sets and others showed a reduction in the number of seed sets with spaces in between them (**Figure 5.9 D**). These results show that *Ath1.1-2/Ath1.1-1* double heterozygote plants showed an intermediate phenotype between the null *Ath1.1-1* and *Ath1.1-2* TDNA mutants.

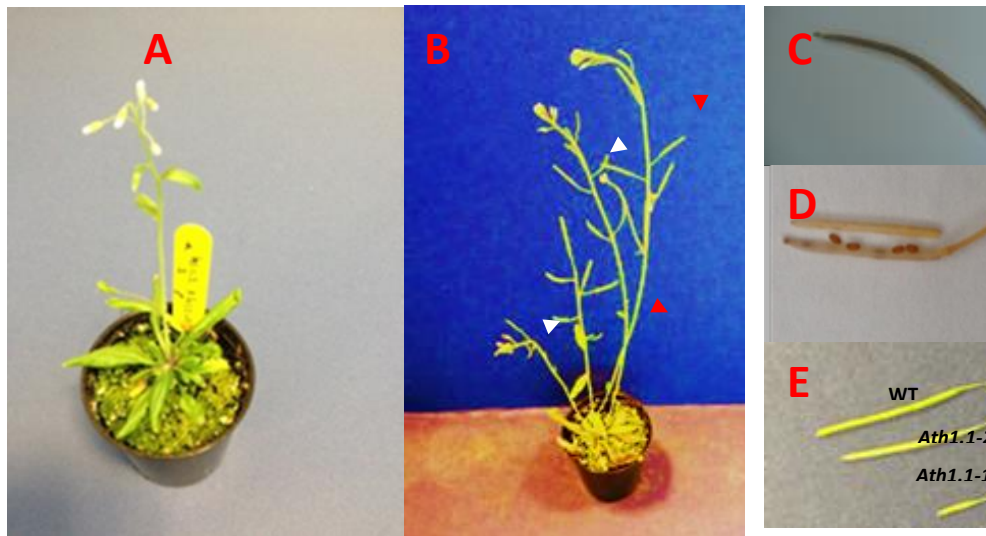


Figure (5.9): Phenotypic observation of *Ath1.1-2*^{+/-}/*Ath1.1-1*^{+/-}.

(A&B&D) Double homozygote *Ath1.1-2/Ath1.1-1*. (C) WT. (A) Flowering time at five weeks. (B) Mature stage. (C&D) Mature silique. (E) Comparison between; WT, null *Ath1.1-2* and null *Ath1.1-1*, in silique length. White arrows show reduced siliques. Red arrow show normal-like siliques

5.5.2.2. Fertility analysis of *Ath1.1-2*^{+/-}/*Ath1.1-1*^{+/-}

Fertility was assessed in the double heterozygote *Ath1.1-2/Ath1.1-1* plants, by measuring their siliques lengths, and quantifying their seeds in parallel to wild-type plant. The *Ath1.1-2*^{+/-}/*Ath1.1-1*^{+/-} plants had a mean of 12.99 mm (n=50) silique length compared to a mean of 14.28 mm (n=50) observed in the wild-type under identical conditions of growth. T-Test analysis showed that this difference was significant (P= 0.0002). These results coincide with a significant reduction in the number of seeds per silique in *Ath1.1-2*^{+/-}/*Ath1.1-1*^{+/-} compared to the wild-type, with a mean of 32.56 (n=50) and 51.88 (n=50) seeds per silique respectively (P= 9.048E-24, T-test)(Figures (5.10 A and B))

The double heterozygote *Ath1.1-2*^{+/-}/*Ath1.1-1*^{+/-} presented a 37.24% reduction in fertility, which is in between the two single mutant alleles; 90% reduction in *Ath1.1-1*^{-/-} and 17.6% in *Ath1.1-2*^{-/-}. Moreover, the differences between the two single mutants *Ath1.1-1*^{-/-} and *Ath1.1-2*^{-/-} were significant, showing 88% difference in seed set (P=1.40415E-41, T-test), and 47.1% difference in silique length (P=1.28496E-40, T-test). These results suggest that the *AtH1.1-1* and *AtH1.1-2* are different mutant alleles, affected at different levels. The allelism test showed us that both phenotypes observed were due to mutations on *AtH1.1* gene, since the loss of one copy of each allele could not be compensated by the other allele in the *Ath1.1-2/Ath1.1-1* double heterozygote plants.

Furthermore, a knock-down *h1.1*^{RNAi} mutant line showed a 41% fertility reduction, which is very similar to that observed in the double heterozygote mutant *Ath1.1-2*^{+/-}/*Ath1.1-1*^{+/-} (P=0.05) (P=0.0489, T-test). This result might indicate that the single mutant *Ath1.1-2* allele is not a null mutant but a knock-down mutant.

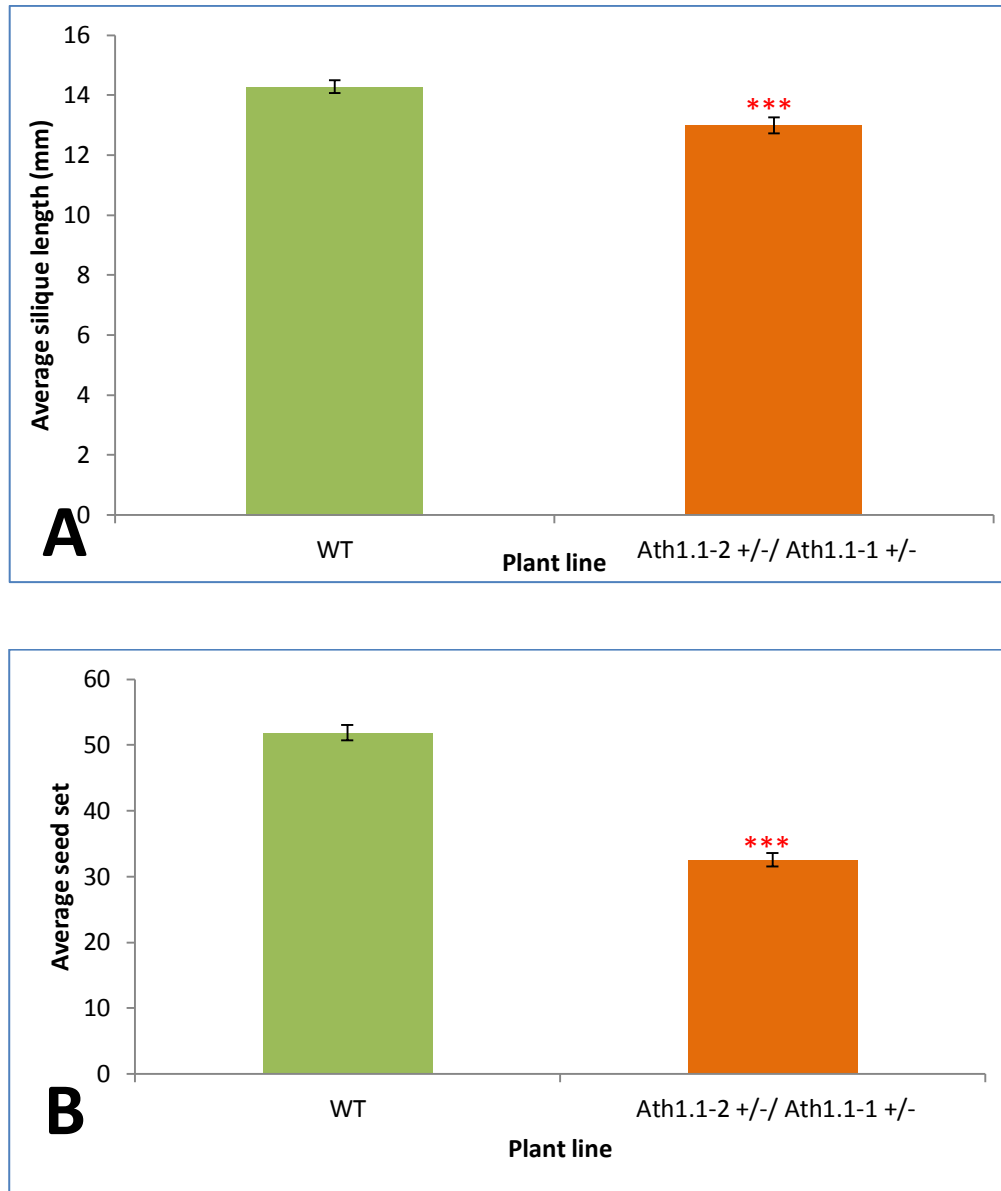


Figure (5.10): Fertility of *Ath1.1-2*^{+/-}/*Ath1.1-1*^{+/-} in comparison to Wild-type plants. (A) Silique length Average (N=50). (B) Seed set mean (N=50). ***= P<0.05. Error bars= Standard error of the mean.

5.5.2.3. Meiotic cytology of *Ath1.1-2*^{+/-}/*Ath1.1-1*^{+/-}

The cytological analysis of DAPI stained meiocytes for the double heterozygote *Ath1.1-1/Ath1.1-2* plants revealed different defects during meiosis (**Figure 5.11**). Fully synapsis was not completed at pachytene (**Figure 5.11 A&B**). Moreover, chiasma frequency was reduced

at metaphase I (**Figure 5.11 C**), which later provided abnormal homologous chromosome segregation at anaphase I (**Figure 5.9 11**), and unbalanced tetrads (**Figure 5.11 E&F**). The meiotic scenario seen in the double heterozygote mutant *Ath1.1-1/Ath1.1-2* plants is very similar to that observed in the single null *Ath1.1* mutants. Thus, meiotic chromosomes behaviour in the *Ath1.1-1^{-/-}/Ath1.1-2^{-/-}* is alike to the original parental lines. From all of these results, we can conclude that the phenotypes observed in these mutants are due to the functional disruption of *AtH1.1* gene.

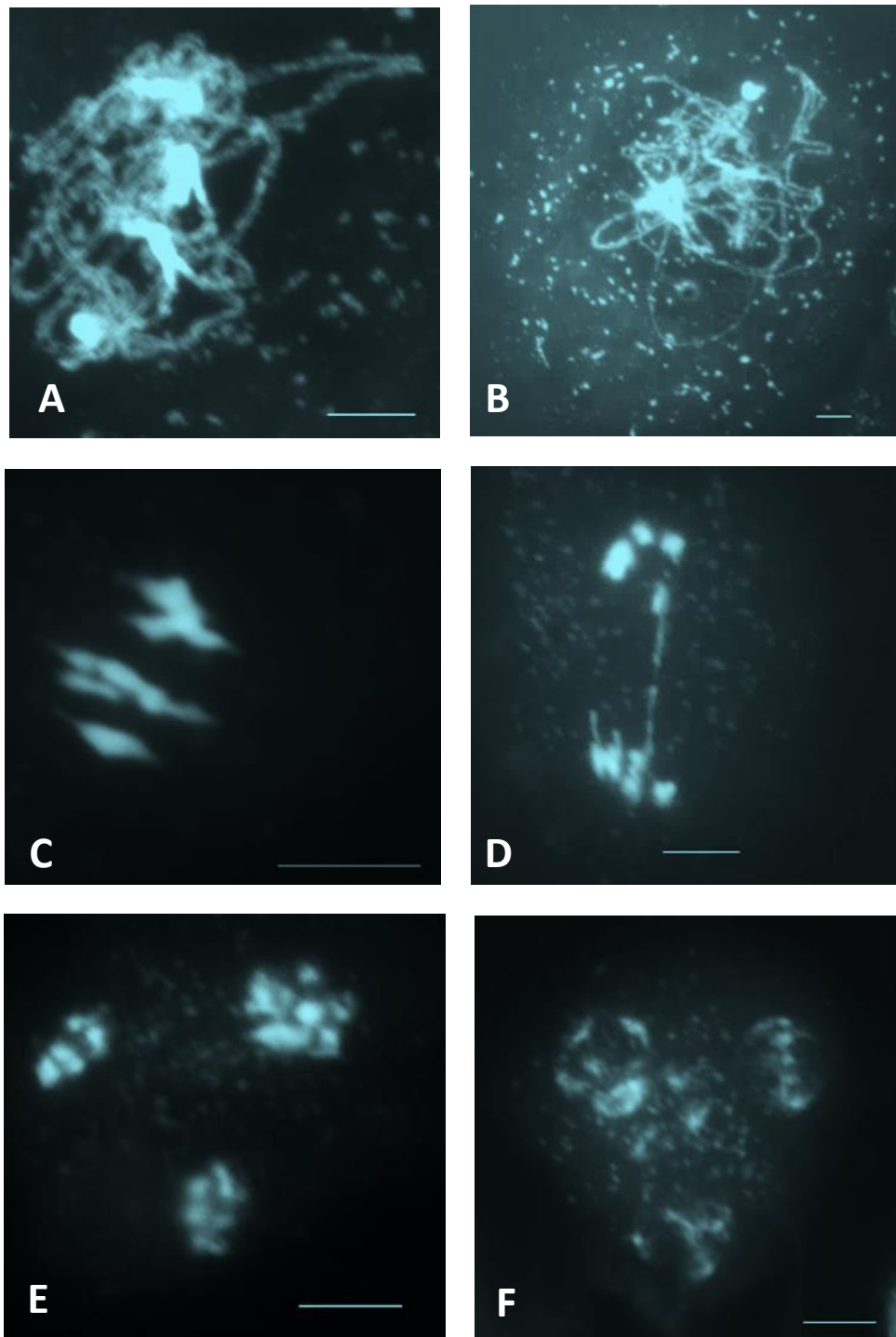


Figure (5.11): Meiotic defects of *Ath1.1-2*^{+/-}/*Ath1.1-1*^{+/-}

(A&B) Pachytene. (C) Metaphase I. (D) Anaphase I. (E&F) Tetrad. Asynaptic phenotype was observed at pachytene. Reduced COs lead to low chiasmata, so univalents present at metaphase I. Hence, defects in homologues disjunction and segregation appear at anaphase I. As a result of that, aneuploidy phenotype appear at tetrad stage. DAPI stained meiocytes. Scale Bar= 5µm.

5.6 Analysis of meiotic chromosome axis and SC proteins localisation in wild-type and *Ath1.1-1* mutant

In order to study chromosome axis organisation on the wild-type meiocytes we carried out immunolocalization of the chromatin axis proteins using antibodies for the axes proteins; anti-ASY1, anti-ASY3 and the synaptonemal complex transverse filament; anti-ZYP1. Prepared chromosome spreads were investigated by epifluorescence microscopy. These meiotic specific chromatin axis proteins start to load as early as late G2. ASY1 starts loading onto the chromatin as numerous foci at G2 which will polymerase at leptotene (**Figure 5.12 A**) and proceed with a linear signal at zygotene (**Figure 5.12 B**). At pachytene, a thick continuous linear signal is observed (**Figure 5.12 C**). Localization of ZYP1 on chromatin starts at early zygotene showing a foci pattern. As zygotene advances and so synapsis, ZYP1 signals are elongated as ZYP1 polymerizes from short stretches to longer ones. These stretches indicate that pairing and synapsis between homologous chromosomes is taking place. At pachytene, ZYP1 signal is fully polymerized along the homologous chromosomes and confirms the successful completed synaptonemal complex formation (**Figure 5.12 D**).

The immunolocalization of chromosome axis and SC proteins in the *Ath1.1-1* mutant revealed different changes from that observed in the wild-type. The ASY1 loading on the chromatin axis was abnormal, instead of ASY1 polymerisation along the chromosome axis at leptotene-zygotene, in the mutant, ASY1 signal was irregularly localized and diffused on the chromatin (**Figure 5.13**). At pachytene, ASY1 signal appeared diffused and fragmented persisting on the axes longer than in the wild-type. The ZYP1 foci appeared at early zygotene like in the wild-type, and cells

showing stretches at late zygotene could be found. Most of the meiocytes had partial polymerization of ZYP1 and very limited number showed fully synapsed chromosomes at pachytene (2 cells in 100). Moreover, the ASY1/ZYP1 colocalisation was observed at zygotene-pachytene in the mutant (**Figure 5.13**). **Figure (5.14)** shows larger view for the ASY1 on the axes compared to wild-type.

On another hand, analysis of ASY3 localization on the wild-type meiocytes showed that it is axes associated at zygotene. And that, the ASY3 colocalization with ASY1 during zygotene (**Figure 5.15**). In the *Ath1.1-1* mutants ASY3 were found to colocalize with ASY1 at zygotene also, but the pattern of ASY3 localization on the axes was not as regular and as well-defined site as that observed in the WT. Although ASY3 seems to show a more linear polymerization on the axes, but it still showing a wider signal on the axes compared to the well organised and defined axes in the wild-type (**Figure 5.15**).

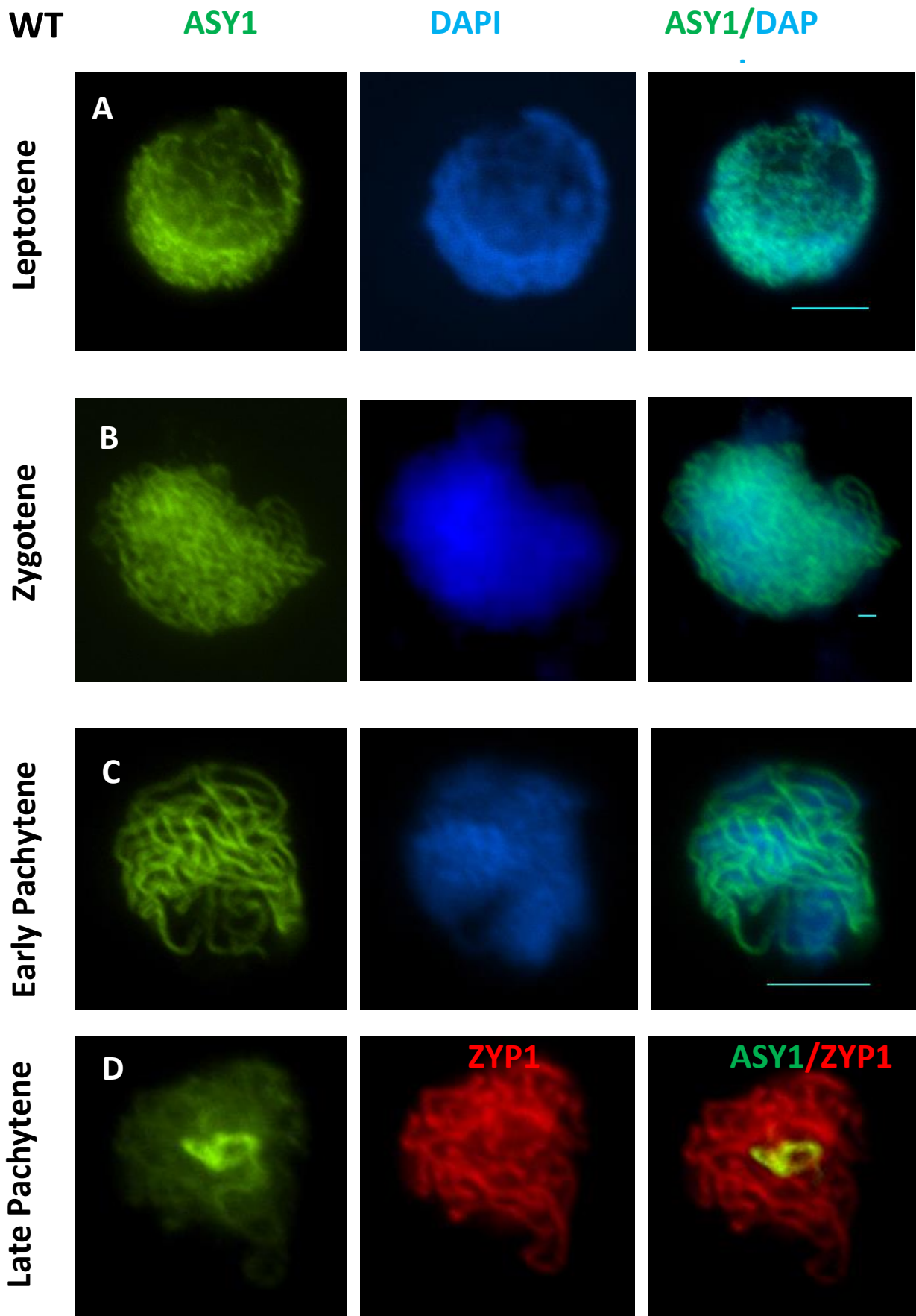
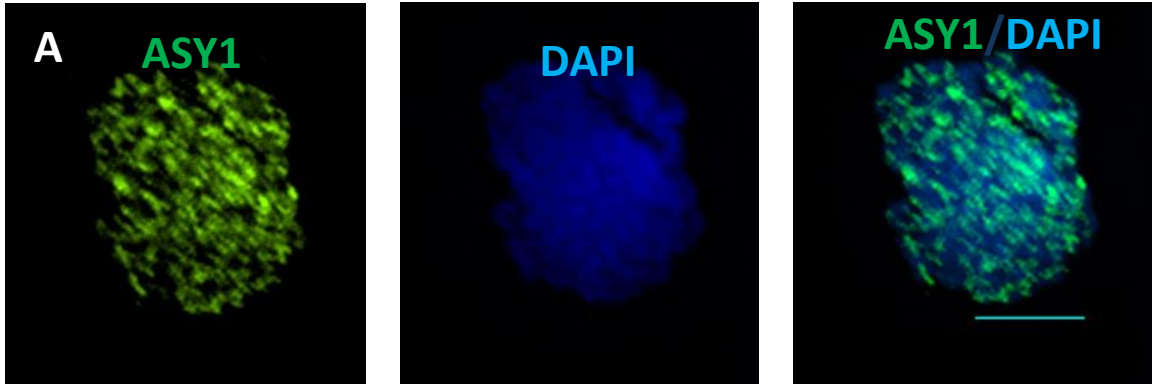


Figure (5.12): Dual Immunolocalization of ASY1, ZYP1 in WT meiocytes.

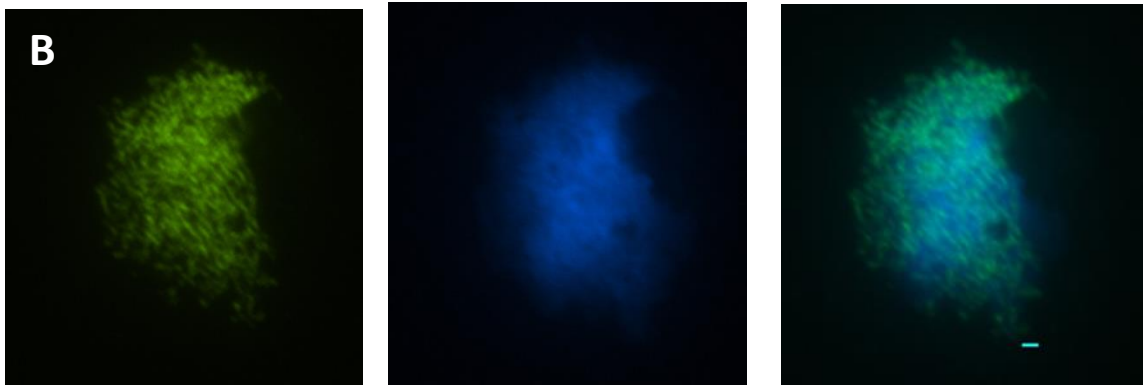
(A) Leptotene: ASY1 present as numerous foci. **(B)** Zygotene: ASY1 present as a linear signal. **(C)** Pachytene: ASY1 is present as thick linear signal. **(D)** Pachytene: As ZYP1 linearize ASY1 signal diffuse. ASY1 signal is in green. DAPI is in blue. ZYP1 signal is in red. Scale bar= 5 μ m.

Ath1.1-1

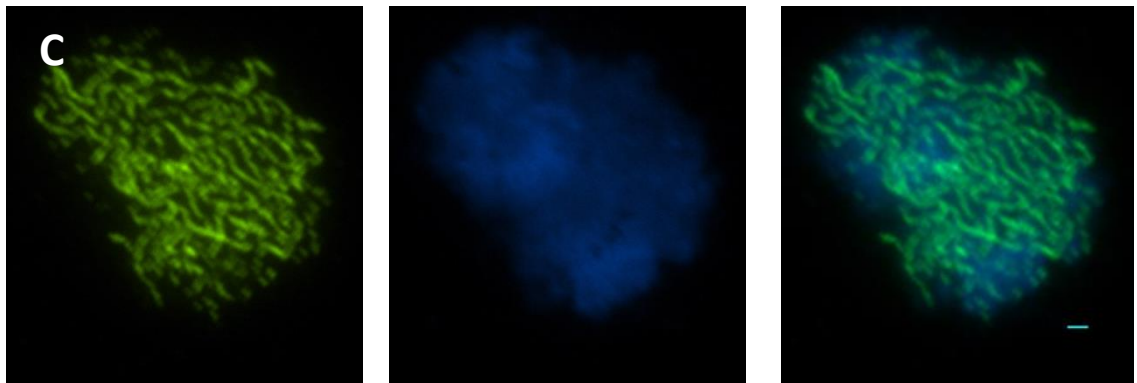
Leptotene



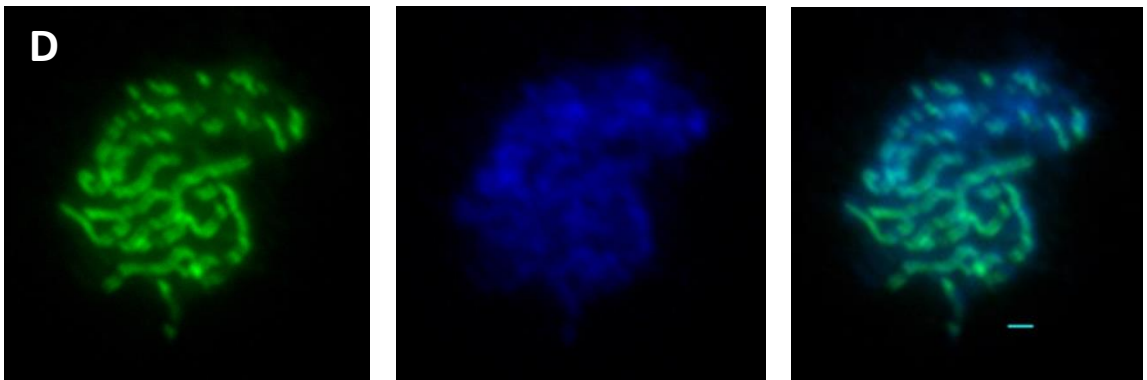
Zygotene



Early Pachytene



Late Pachytene



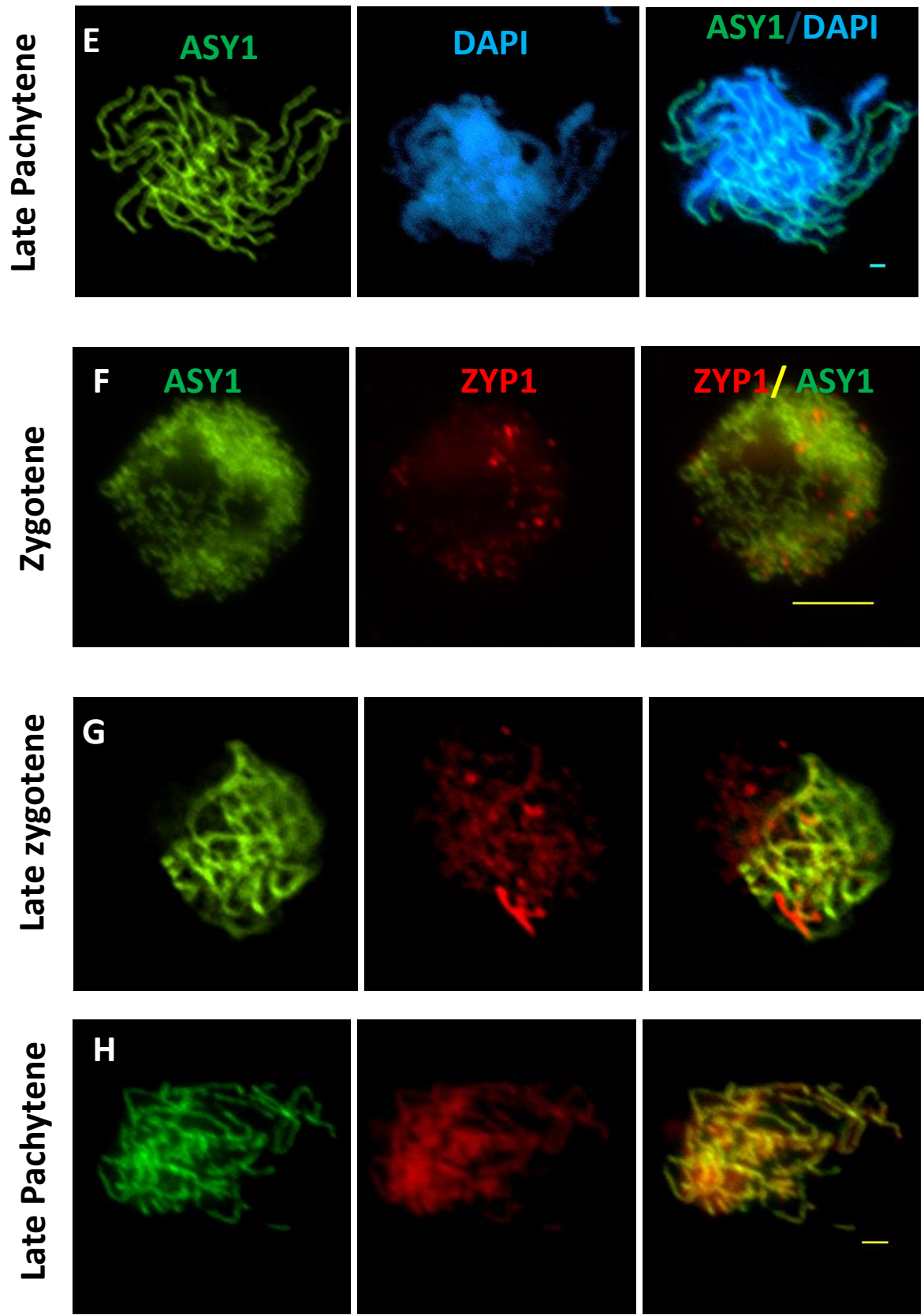


Figure (5.13) : Dual Immunolocalization of ASY1 and ZYP1 on *Ath1.1-1* meiocytes.

(A) Leptotene: ASY1 foci is abnormal. **(B&F&G)** Zygotene: ASY1 appear as diffuse signal. **(C&D&E)** Pachytene: ASY1 signal is fragmented and discontinuous, and never appear as continuous. **(D)** Pachytene: As ZYP1 linearize, ASY1 signal colocalize with ZYP1 on the chromosome axis. ASY1 signal is in green. DAPI is in blue. ZYP1 signal is in red. Scale bar= 5 μ m.

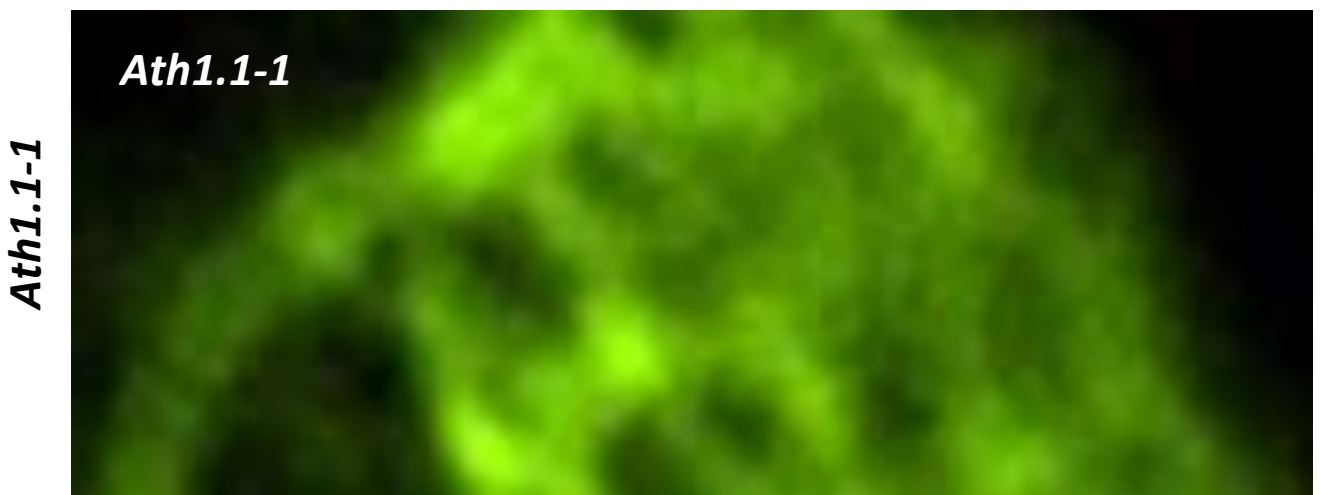
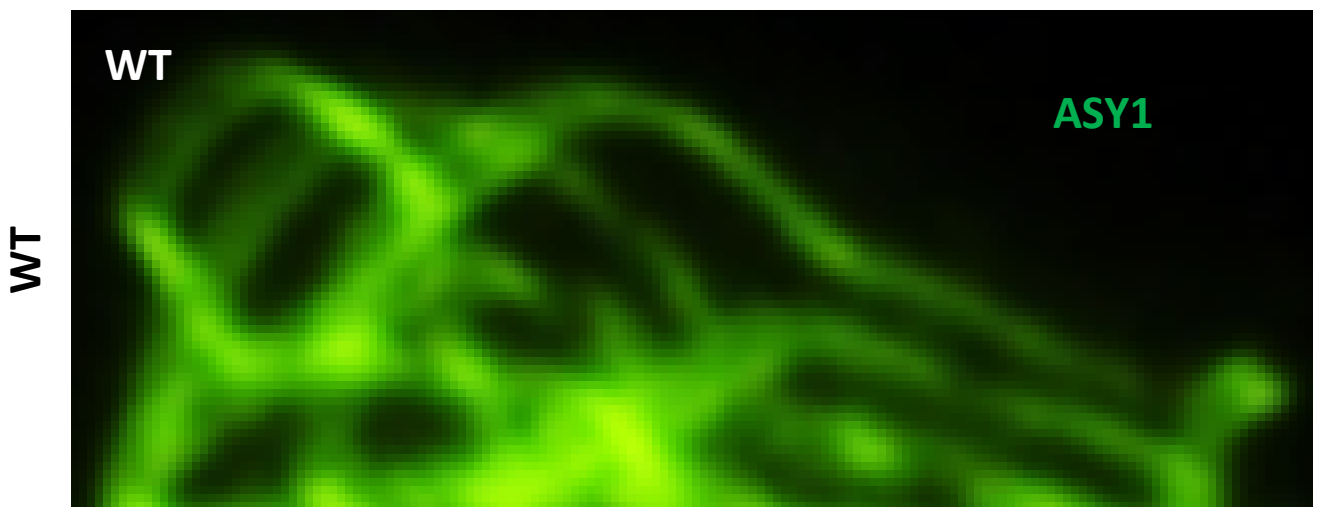
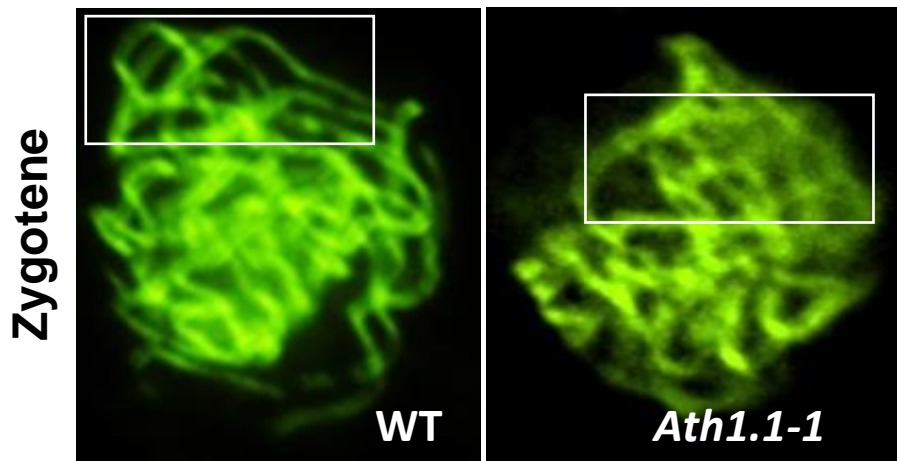


Figure (5.14): Immunolocalization of ASY1 (green) at zygotene on *Ath1.1-1* compared to WT cell.

The results show that ASY1 (green) signal in the *Ath1.1-1* is abnormal, showing diffuse signal at some sites, and strong distinct signal in others, whereas in WT ASY1 polymerize along the axes in a full linear pattern. White boxes defines region selected for larger view (below). Scale bar= 5 μ m.

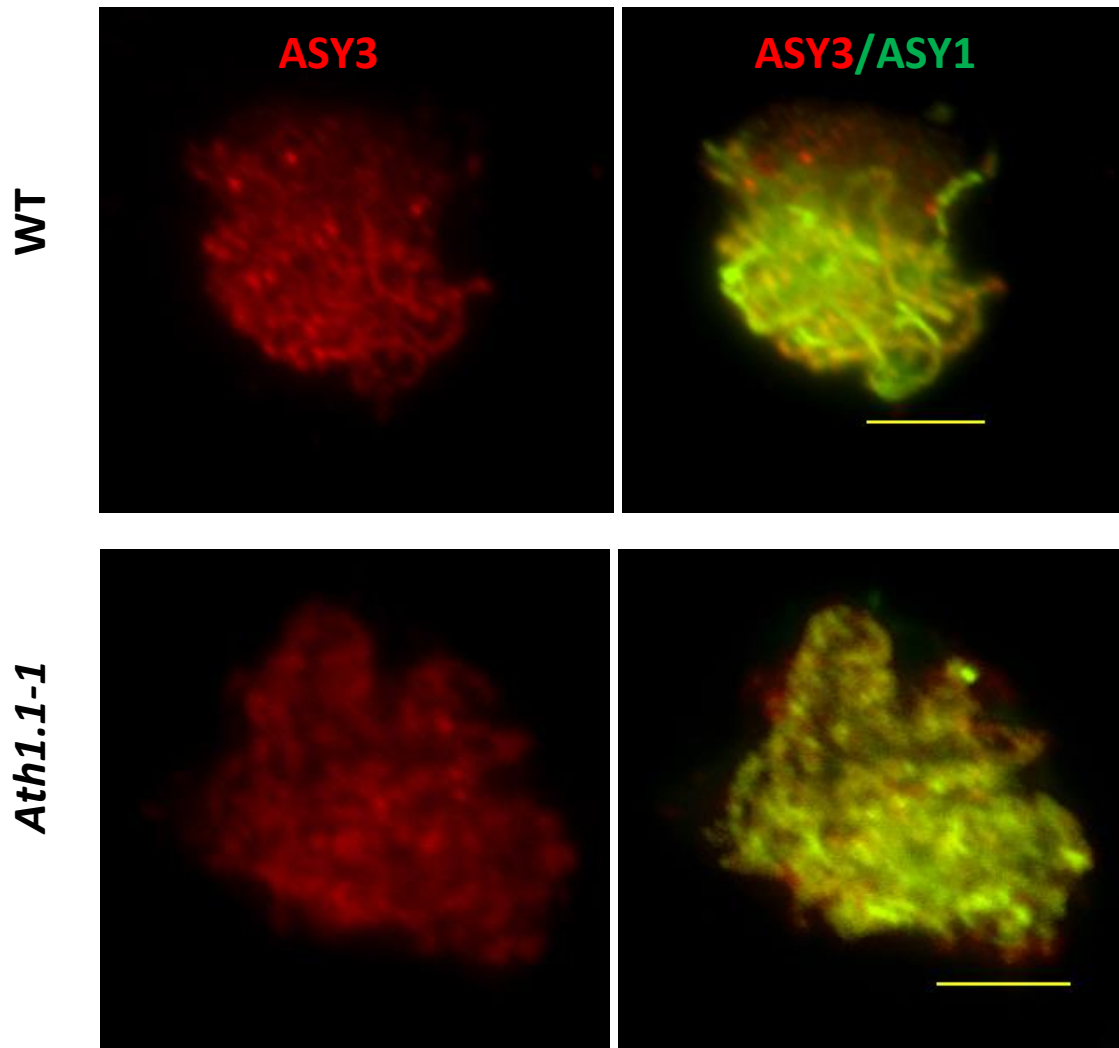


Figure (5.15): Dual Immunolocalization of ASY3 and ASY1 in WT and *Ath1.1-1* meiocytes. (A) Leptotene: ASY1 present as numerous foci. (B) Zygotene: ASY1 present as a linear signal. (C) Pachytene: ASY1 is present as thick linear signal. (D) Pachytene: As ZYP1 linearize ASY1 signal diffuse. ASY1 signal is in green. DAPI is in blue. ZYP1 signal is in red. Scale bar= 5µm.

5.7. Meiotic cohesion components ATSYN1, AtSMC1 and ATSMC3 are normally localized in *Ath1.1-1*

Cohesion proteins AtSMC3, AtSMC1 and AtSYN1 immunolocalization within meiosis was carried in the wild-type and mutant. The localization pattern of all of the cohesion

proteins; AtSMC1, AtSMC3 and SYN1 in wild-type meiocytes showed similar patterns in which these proteins appear initially as foci at early G2, which extends to form linear stretches through leptotene-zygotene. At zygotene-pachytene, cohesion proteins co-localized showing a continuous linear polymerization and co-localization along the chromosome length. The meiotic *Ath1.1-1* chromosome spreads showed that all cohesins; AtSMC1, AtSMC3 and AtSYN1 localization was not altered from that observed in the wild-type. Both cohesins showed fully linearized chromosome axis signal (**Figure5.15**).

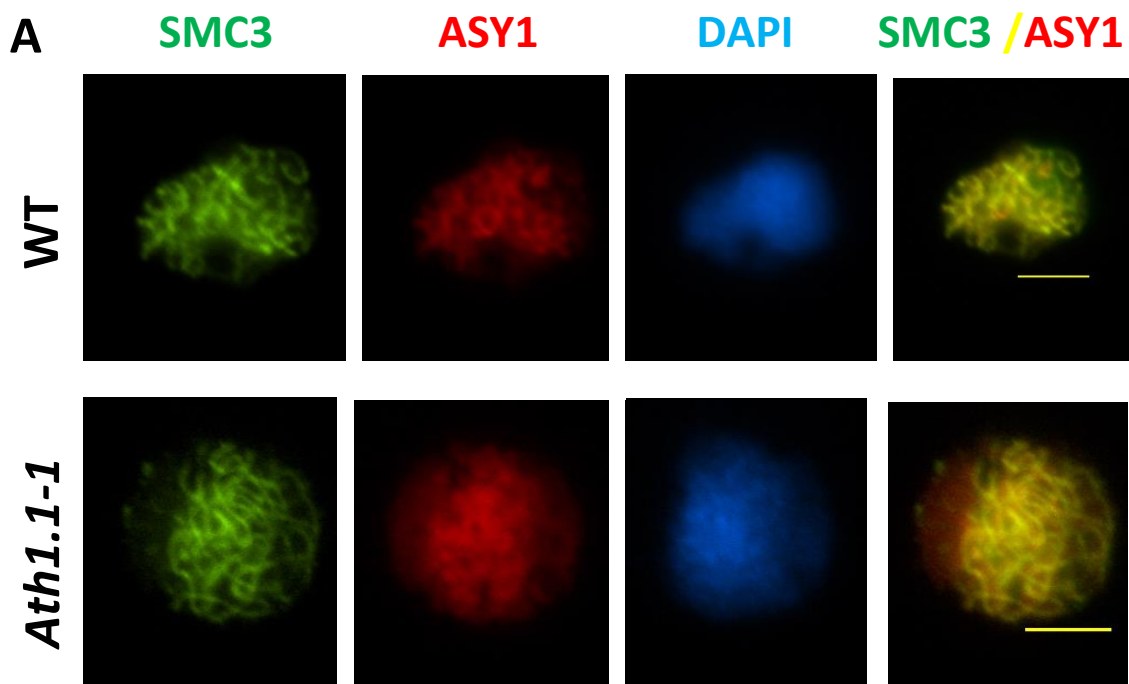


Figure (5.15 A): Immunolocalization of cohesion proteins SMC3 in the *Ath1.1-1* comparable to WT.

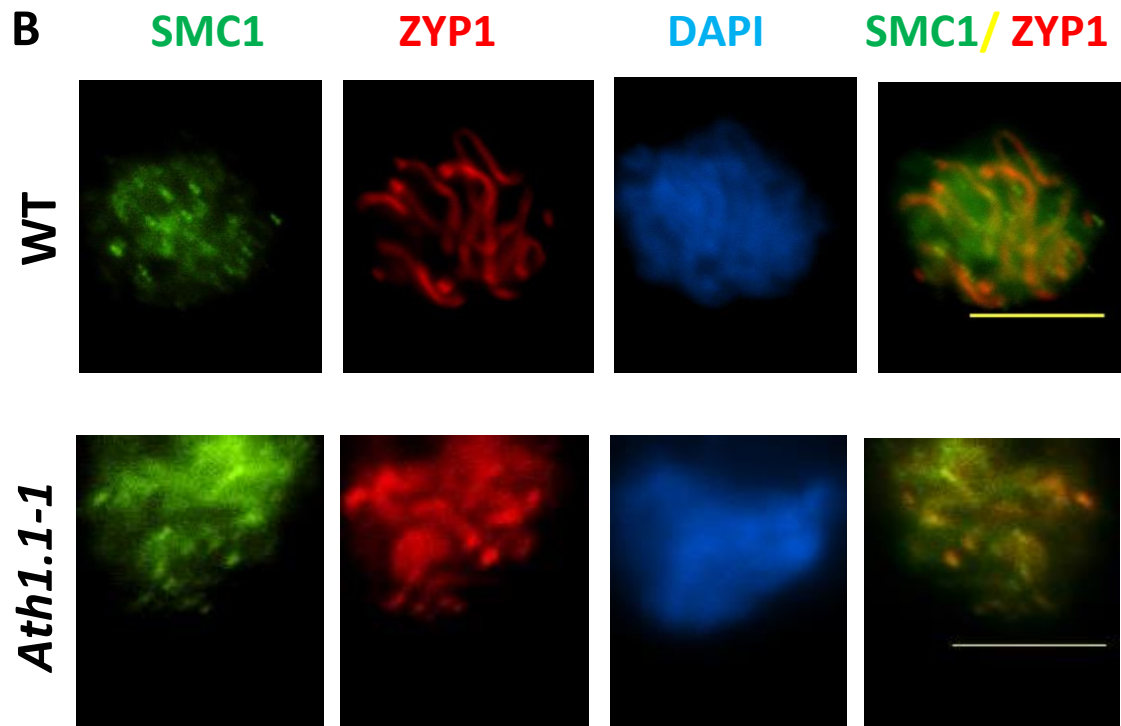


Figure (5.15 B): Immunolocalization of cohesion proteins SMC1 in the *Ath1.1-1* comparable to WT.

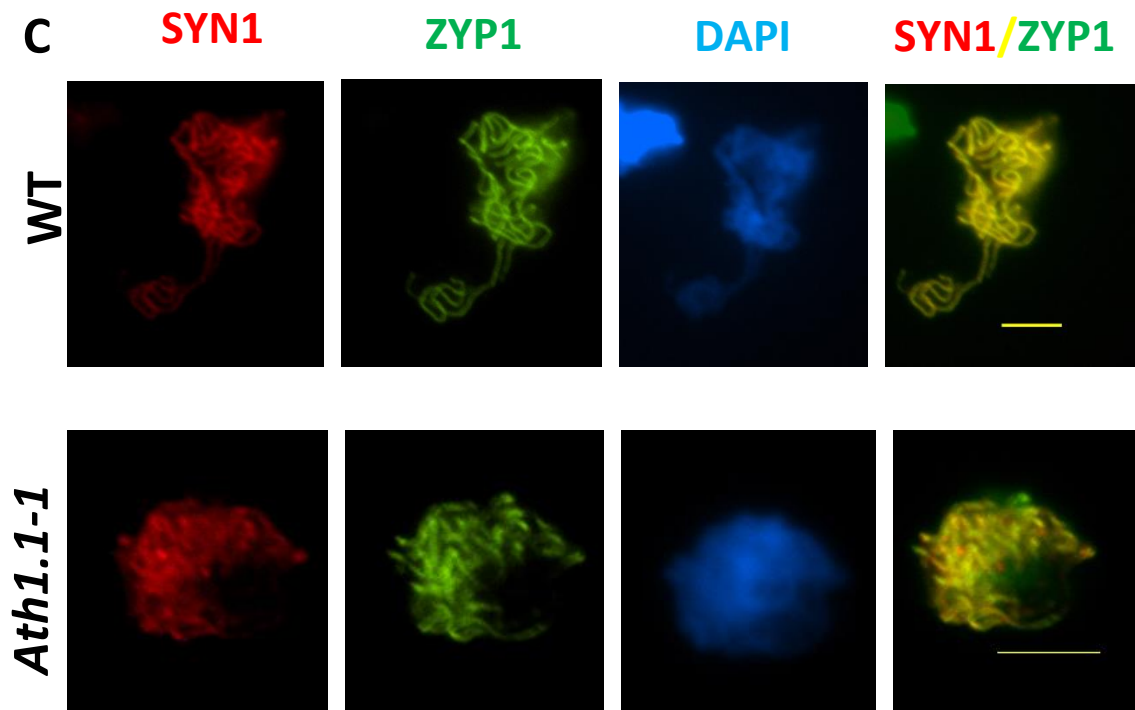


Figure (5.15 C): Immunolocalization of cohesion proteins SYN1 in the *Ath1.1-1* comparable to WT.

5.8. Chiasma frequency analysis in wild-type and *Ath1.1* mutants

The cytological defects observed at pachytene show that *Ath1.1* mutants could be categorized as asynaptic mutants, where full synapsis is not completed. This asynaptic phenotype obviously leads to the presence of univalents at diakinesis and metaphase I stages in the *Ath1.1* mutants. Thus, AtH1.1 might have a role in synapsis and in COs formation. To verify this, chiasma frequency was analyzed using FISH (**Figure 5.17**) in the *Ath1.1* mutants as well as the wild-type, using DAPI stained metaphase I stage meiocytes.

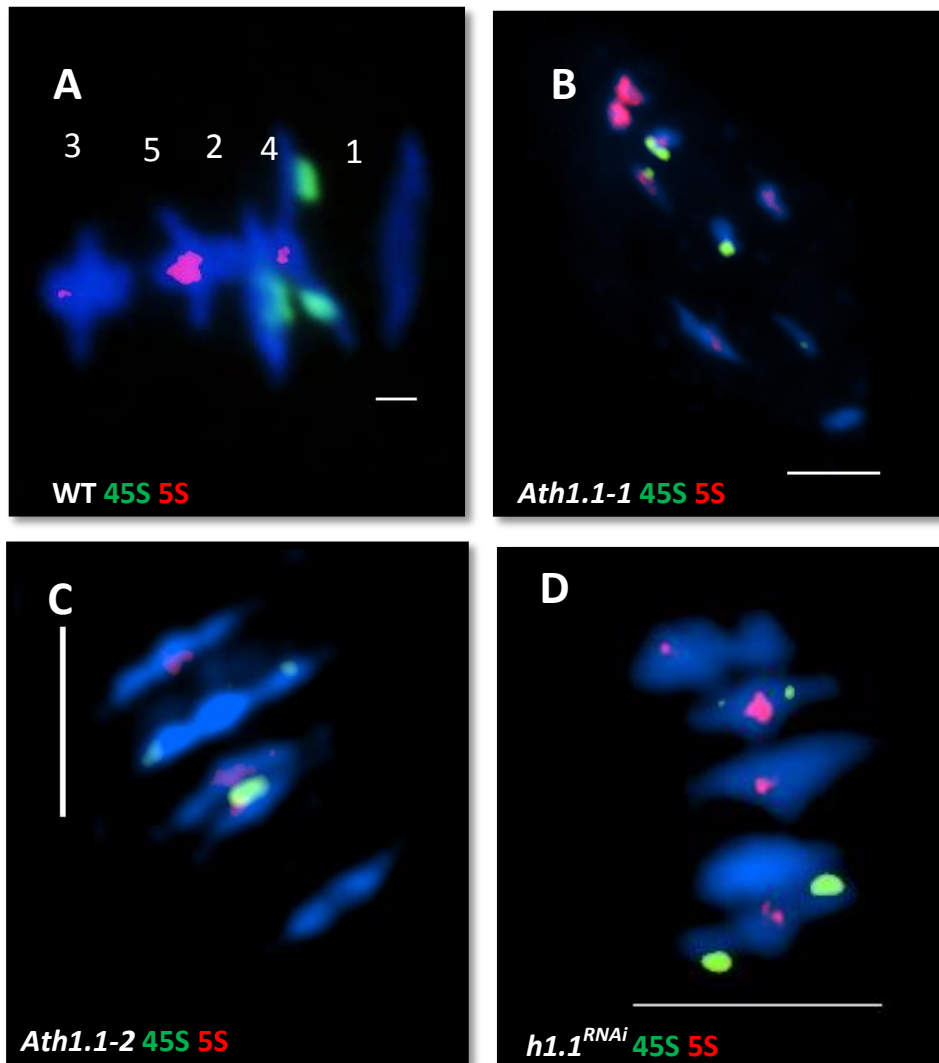


Figure (5.17): FISH analysis of chiasmata in Arabidopsis WT and *Ath1.1* mutants at metaphase I.

(A) Chiasma frequency analysis at metaphase I meiocytes for WT showed 9.25 (n=50) chiasmata per meiocyte, however, although all the *Ath1.1* mutants showed significant reduction in chiasmata formation, but at different levels. (B) *Ath1.1-1* showed ~88.8% decline in COs, with 1.06 (n=100) chiasma per meiocyte. Whereas, (C) *Ath1.1-2* showed 11.3% reduction in COs with 8.39 (n=61) chiasma mean. Besides that, (D) the *h1.1^{RNAi}* recorded 17.12% decline in COs with chiasma frequency mean of 7.84 (n=50). Scale Bar= 5µm.

5.8.1. Chiasma frequency analysis in *Arabidopsis* wild-type metaphase I meiocytes

The wild-type metaphase I meiocytes showed around 8-10 chiasmata per cell (**Figure 5.16 A**), with a chiasma frequency mean of 9.46 (n=50). These results come along with (9.24) chiasma frequency per meiocyte obtained by (Sanchez-Moran *et al.*, 2001).

5.8.2. Chiasma frequency analysis in *Ath1.1-1* metaphase I meiocytes

The cytological analysis of *Ath1.1-1* meiocytes revealed persistent occurrence of univalents as early as diakinesis, and persisting at metaphase I (**Figure 5.18 B**). To analyse if *Ath1.1* might affect meiotic recombination, chiasma frequency and its distribution was characterised in the mutants (**Table 5.2**). Chiasma frequency evaluation in a hundred metaphase I male DAPI-stained meiocytes confirmed a defect, showing univalents in 100% *Ath1.1-1* nuclei, however this phenotype was not seen in the wild-type nuclei (n=50) (**Figure 5.18 A**). Univalents mean in *Ath1.1-1* was 7.98 (n=100) showing a significant increase compared to wild-type (**Figure 5.18 B**). The range of total chiasmata recorded in *Ath1.1-1* varied from 0 up to 5 per nuclei, resulting in a chiasma frequency mean of 1.06 (n=100) (**Table 5.1**). This reduction in the chiasma frequency was significant with a P value of 1.57E-84 (T-test). The *Ath1.1-1* T-DNA meiocytes retained 11.21 % of the normal chiasma frequency observed in the wild-type (**Figure 5.18 C**).

Moreover, analysis of chiasmata distribution at metaphase I showed a significant reduction in the number of ring bivalent configurations, showing (0.05) in *Ath1.1-1*

comparable to (4.46) in WT ($P=1.529E-39$, T-test). However, rod bivalents were significantly increased in *Ath1.1-1*, with (0.96) rods comparable to (0.52) in WT ($P=0.0036$, T-test) (**Figure 5.18 D**). Chiasmata distribution in the *Ath1.1-1* mutant showed a significant increase in the distal chiasmata localised on telomeric positions with a mean of 0.47 ($P=4.036E-06$, T-test). However, sub-telomeric, interstitial and proximal localised chiasmata were not significantly increase or decrease with P values of (0.350, 0.372, 0.319, T-test) respectively (**Figure 5.18 E**). The wild-type showed a significant tendency towards ring bivalents with chiasmata localised at subtelomeric ($P=2.47E-17$, T-test), telomeric ($P= 6.15E-16$, T-test, T-test) and interstitial (0.0036, T-test) positions comparable to *Ath1.1-1* (**Figure 5.18 F**).

Genotype	Configurations			Chiasma mean (COs)	Chiasmata distribution							
	Univalents	Bivalents			Telomeric		Subtelomeric		Interstitial		Proximal	
		Rings total	Rods total		Ring	Rod	Ring	Rod	Ring	Rod	Ring	Rod
WT (n=50)	0	4.46	0.52	9.46 (8-10)	3.82	0.1	4.62	0.28	0.48	0.16	0.0	0.0
<i>Ath1.1-1</i> (n=100)	7.98	0.05	0.96	1.06 (0-5)	0.08	0.47	0.0	0.38	0.0	0.1	0.02	0.01
P-value (T-test)		1.5E-39 ***	0.003 ***	1.5E-84 ***	6.1E-16 ***	4.03E-06 ***	2.47E-17 ***	0.35	0.003 ***	0.37	0.31	0.31

Table (5.2): Chiasma distribution in wild-type and *Ath1.1-1*

The chiasma distribution was evaluated at metaphase I using DAPI stained meiocytes. ***<0.005

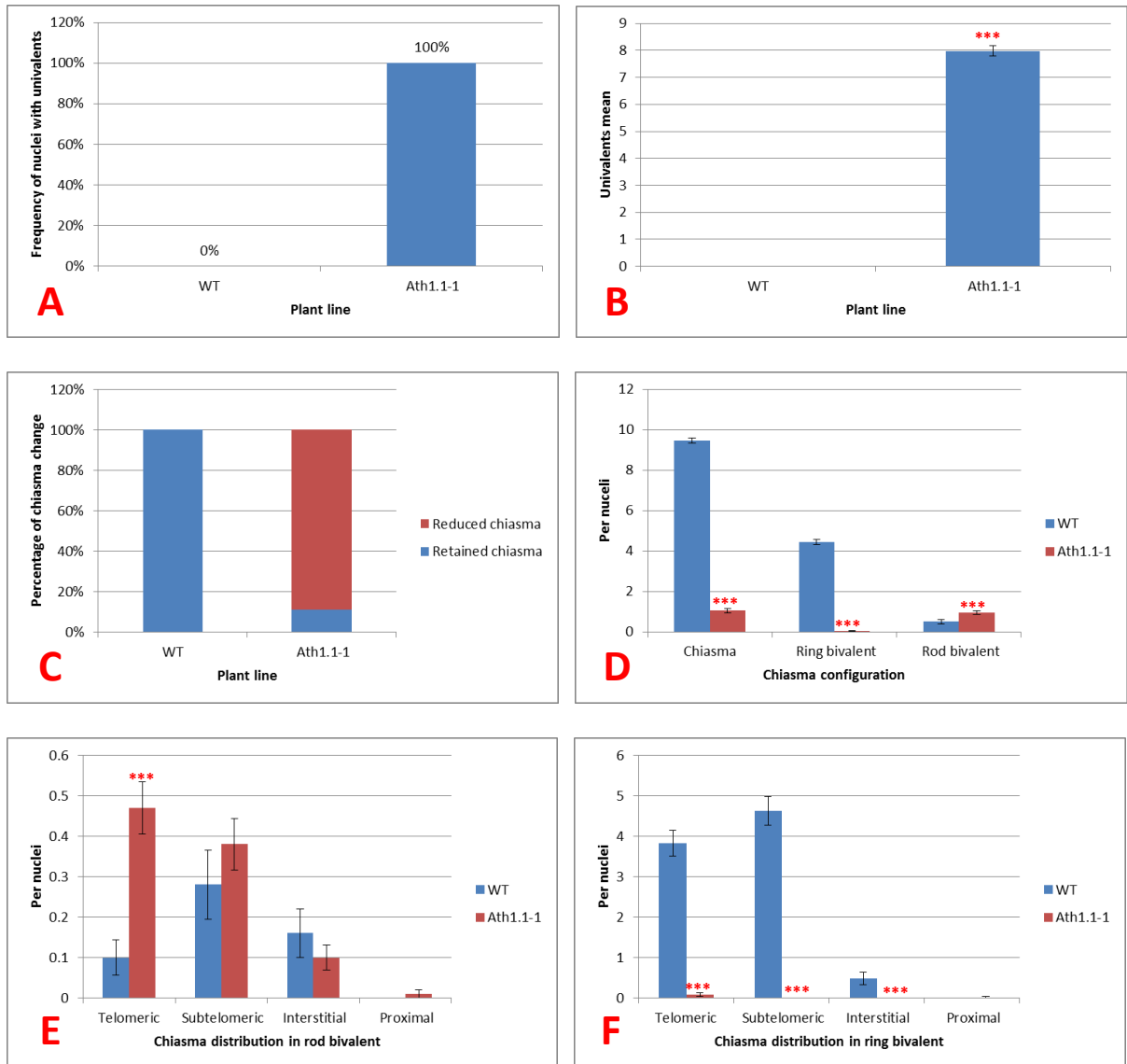


Figure (5.18): Chiasma analysis in *Ath1.1-1* in comparison to WT

(A) 100% nuclei showed univalent in *Ath1.1-1*, whereas WT nuclei were univalent-free. (B) *Ath1.1-1* showed significant appearance of univalent with 7.98 univalents per nuclei comparable to non-univalents phenotype in WT ($P=6.35E-66$). Hence, (C) *Ath1.1-1* showed 88.19% reduction in chiasma comparable to WT. And (D) *Ath1.1-1* scored 1.06 ($n=100$) chiasma per nuclei comparable to 9.46 ($n=50$) in WT showing significant difference ($P=1.5E-84$). Chiasma configuration in *Ath1.1-1* showed significantly reduced ring bivalent ($P=1.5E-39$) in comparison to WT, however, rod bivalents increased significantly ($P=0.003$) comparable to WT. (E) Single chiasma distribution per bivalent showed significant increase in *Ath1.1-1* telomeric chiasma in comparison to WT ($P=4.03E-06$), whereas, non-significant difference observed at subtelomeric, interstitial and proximal chiasma. However, (F) double chiasma distribution per bivalent (ring bivalent) in *Ath1.1-1* was significantly reduced at telomeric ($P=6.1E-16$), Subtelomeric ($P=2.47E-17$), and interstitial ($P=0.003$) chiasma comparable to WT. Significance level $P<0.05$. ***= $P<0.005$. Statistical analysis was done by T-test.

5.8.3. Chiasma frequency analysis in *Ath1.1-2* metaphase I meiocytes

Chiasma frequency in *Ath1.1-2* T-DNA mutant line (**Table 5.3**) was also assessed (**Figure 5.17 C**). The analysis of metaphase I chromosomal spreads of *Ath1.1-2* meiocytes showed that 4.9% of nuclei contain some univalents (**Figure 5.19 A**). The observed PMCs showed 6-10 chiasmata per nuclei in *Ath1.1-2* with a mean chiasma frequency of 8.39 (n=61) (**Figure 5.19 C**). Statistical analysis indicated that this decline in chiasma frequency was significant (P=1.26E-07, T-test). Analysis of the different bivalent configurations in *Ath1.1-2* showed a significant decrease in the frequency of ring bivalents, showing 3.475 in *Ath1.1-2* comparable to 4.46 in WT (P=1.223E-07, T-test). However, the number of rod bivalents was significantly increased showing 1.475 in *Ath1.1-2* comparable to 0.52 in WT (P=1.670E-07, T-test) (**Figure 5.19 D**). Chiasma distribution per rod bivalent showed a significant increase in telomeric chiasmata (P=0.0042, T-test) and interstitial chiasmata (P=5.980E-05, T-test). Whereas, non-significant difference was observed at subtelomeric (P=0.05, T-test) and proximal (P=0.321, T-test) chiasmata (**Figure 5.19 E**). Chiasma distribution in ring bivalents showed a significant decrease in the subtelomeric chiasmata (P=0.0003, T-test). However, non-significant changes were observed in the telomeric (P=0.555, T-test), interstitial (P=0.349, T-test), and proximal (P=0.321, T-test) chiasmata (**Figure 5.19 F**).

Moreover, the configuration of chiasma distribution in *Ath1.1-1* and *Ath1.1-2* null mutants showed that they differ significantly (**Table 5.4**). The *Ath1.1-1* showed 81.42 times increase in the number of univalents compared to *Ath1.1-2* (P=1.24E-70). *Ath1.1-2* showed a significant increase in bivalents configuration, showing 1.536

times increase in rod bivalent ($P=0.00091$) and 69.5 times increase in ring bivalents ($P=1.807E-36$). Hence, overall *Ath1.1-2* showed an increase of 7.9 times in the chiasma frequency ($P=6.557E-48$). And so, chiasmata distribution in ring bivalents showed a significant increase in *Ath1.1-2* compared to *Ath1.1-1* at telomeric ($P=1.524E-23$), subtelomeric ($P=5.464E-20$) and interstitial ($P=0.000605$) positions. Whereas, proximal chiasmata numbers were non-significant ($P=0.889$). Chiasmata distribution in rod bivalents showed that *Ath1.1-2* had a significant increase in interstitial rod frequency ($P=6.901E-07$). Whereas, non-significant differences were observed in telomeric ($P=0.122$), subtelomeric ($P=0.189$) and proximal ($P=0.739$) chiasma distribution.

Genotype	Configurations			Chiasma mean (COs)	Chiasmata distribution							
	Univalents	Bivalents			Telomeric		Subtelomeric		Interstitial		Proximal	
		Rings total	Rods total		Ring	Rod	Ring	Rod	Ring	Rod	Ring	Rod
WT (n=50)	0	4.46	0.52	9.46 (8-10)	3.82	0.1	4.62	0.28	0.48	0.16	0.0	0.0
<i>Ath1.1-2</i> (n=61)	0.098	3.475	1.475	8.39 (6-10)	3.590	0.327 8	3.03	0.52	0.311	0.606	0.016	0.016
P-value (T-test)		1.22E-07 ***	1.67E-07 ***	1.266E-07 ***	0.5559	0.0042 ***	0.00031 ***	0.05	0.349	5.98E-05 ***	0.321	0.321

Table (5.3): Chiasma distribution in wild-type and *Ath1.1-1*

The chiasma distribution was evaluated at metaphase I using DAPI stained meiocytes. ***<0.005

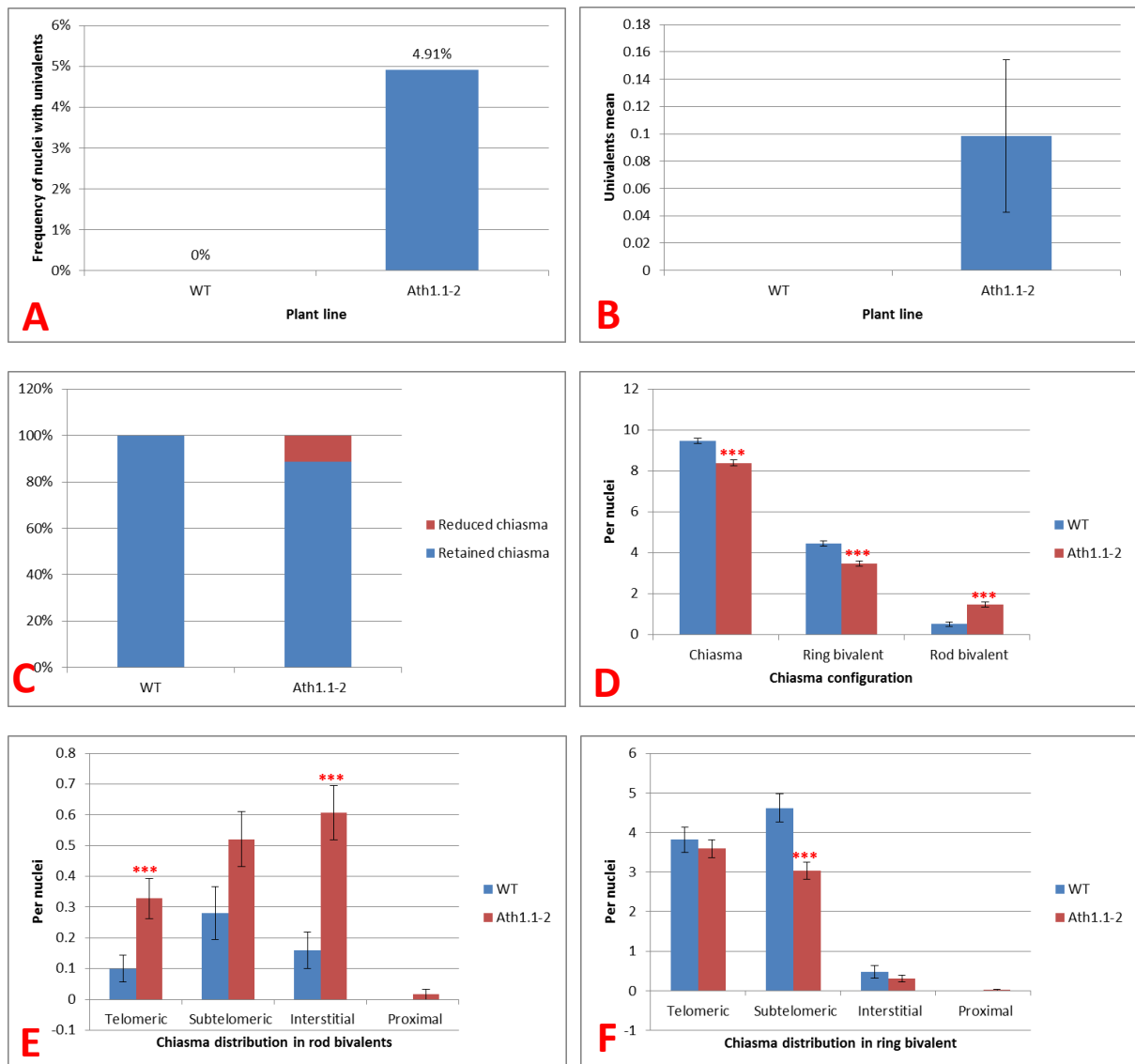


Figure (5.19): Chiasma analysis in *Ath1.1-2* in comparison to WT

(A) 4.91% was the *Ath1.1-2* frequency of nuclei with univalents in comparison to WT nuclei free-univalents. (B) *Ath1.1-2* showed non-significant appearance of univalents with 0.098 univalents mean. (C) *Ath1.1-2* showed 11.31% reduction in chiasma comparable to WT. And (D) *Ath1.1-2* scored 8.39 (n=61) chiasma per nuclei comparable to 9.46 (n=50) in WT showing significant difference ($P=1.266E-07$). Chiasma configuration in *Ath1.1-2* showed significantly reduced ring bivalent ($P=1.22E-07$) in comparison to WT, however, rod bivalents increased significantly ($P=1.67E-07$) comparable to WT. (E) Single chiasma distribution per bivalent showed significant increase in *Ath1.1-2* telomeric ($P=0.0042$), and interstitial ($P=5.98E-05$) chiasma in comparison to WT, whereas, non-significant difference observed at subtelomeric and proximal chiasma. However, (F) double chiasma distribution per bivalent in *Ath1.1-2* was significantly reduced at subtelomeric ($P=0.00031$), whereas non-significant difference was estimated at telomeric, interstitial and proximal chiasma comparable to WT. Significance level $P<0.05$. ***= $P<0.005$. Statistical analysis was done by T-test.

Genotype	Configurations			Chiasma mean (COs)	Chiasmata distribution							
	Univalents	Bivalents			Telomeric		Subtelomeric		Interstitial		Proximal	
		Rings total	Rods total		Ring	Rod	Ring	Rod	Ring	Rod	Ring	Rod
	<i>Ath1.1-1</i> (n=100)	7.98	0.05		0.96	1.06 (0-5)	0.08	0.47	0.0	0.38	0.0	0.1
<i>Ath1.1-2</i> (n=61)	0.098	3.475	1.475	8.39 (6-10)	3.590	0.327 8	3.03	0.52	0.311	0.606	0.016	0.016
P-value (T-test)	1.24E-70 ***	1.80E-36 ***	0.0009 ***	6.55E-48 ***	1.52E-23 ***	0.122	5.46E-20 ***	0.189	0.0006 ***	6.90E-07 ***	0.889	0.735

Table (5.4): Comparison of chiasma frequency and distribution in *Ath1.1-1* and *Ath1.1-2* null mutants.

The chiasma distribution was evaluated at metaphase I using DAPI stained meiocytes. ***<0.005

5.8.4. Chiasma frequency analysis in *h1.1^{RNAi}* metaphase I meiocytes

Cytological analysis of metaphase I of a *h1.1^{RNAi}* mutant line showed some meiocytes with affected homologous chromosomes recombination, showing reduced number of chiasmata (**Figure 5.17 D**). Hence, chiasma frequency and distribution were quantified in DAPI stained meiocytes at metaphase I in the *h1.1^{RNAi}* mutant (n=50) (**Table 5.5**) and compared to wild-type (n=50). Univalents appeared in 4% of *h1.1^{RNAi}* nuclei (**Figure 5.20 A**), with a mean value of 0.08 (**Figure 5.20 B**). The result revealed variation in the chiasma frequency in *h1.1^{RNAi}* line with a chiasmata range varying from 6 up to 10, with a mean chiasma frequency of 7.84 (n=50). This implied a 17.12% reduction in chiasma frequency compared to wild-type meiocytes (**Figure 5.20 C**). This chiasma frequency reduction observed in *h1.1^{RNAi}* is statistically significant (P=8.321E-13, T-test) (**Figure 5.20 D**). Bivalent configuration analysis in the *h1.1^{RNAi}* (**Figure 5.18 D**) showed a significant decrease in ring bivalents, showing a mean of 2.88 in *h1.1^{RNAi}* comparable to 4.46 in WT (P=9.81E-13, T-

test). However, the number of rod bivalents showed a significant increase, showing a mean of 2.08 in $h1.1^{RNAi}$ comparable to 0.52 in the wild-type ($P=1.80E-12$, T-test). Chiasmata distribution in $h1.1^{RNAi}$ rod bivalents (**Figure 5.20 E**) showed a significant increase in both telomeric ($P=7.11E-06$, T-test) and subtelomeric ($P=8.51E-07$, T-test) chiasmata. Whereas, non-significant differences were observed in the interstitial ($P=0.122$, T-test) and proximal rod chiasma frequency. Chiasma distribution in $h1.1^{RNAi}$ ring bivalents (**Figure 5.20 F**) showed a significant decrease in subtelomeric chiasmata per nuclei comparable to WT ($P=1.38E-08$, T-test), whereas, non-significant changes were observed in the telomeric ($P=0.329$, T-test), interstitial ($P=0.508$, T-test) and proximal ring chiasma frequency.

Genotype	Configurations			Chiasm a mean (COs)	Chiasmata distribution							
	Univalen ts	Bivalents			Telomeric		Subtelomeric		Interstitial		Proximal	
		Rings total	Rods total		Ring	Rod	Ring	Rod	Ring	Rod	Ring	Rod
WT (n=50)	0	4.46	0.52	9.46 (8-10)	3.82	0.1	4.62	0.28	0.48	0.16	0.0	0.0
$Ath1.1^{RNAi}$ (n=50)	0.08	2.88	2.08	7.84 (6-10)	3.44	0.64	1.96	1.08	0.36	0.03 6	0	0
P-value (T-test)		9.81E-13 ***	1.80E-12 ***	8.321E-13 ***	0.329	7.11E-06 ***	1.38E-08 ***	8.51E-07 ***	0.508	0.122		

Table (5.5): Chiasma distribution in wild-type and $Ath1.1^{RNAi}$
The chiasma distribution was evaluated at metaphase I using DAPI stained meiocytes. ***<0.005

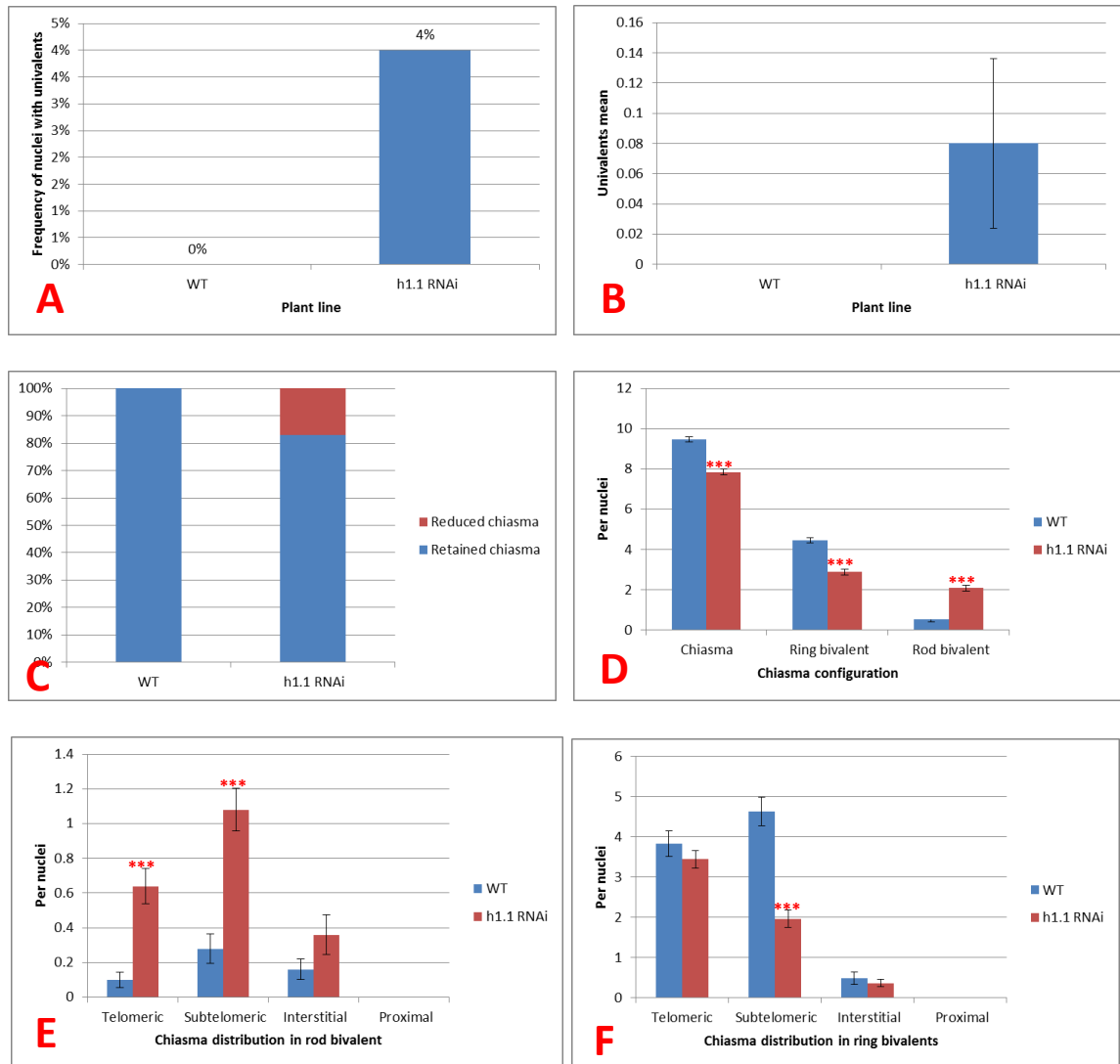


Figure (5.20): Chiasma analysis in $h1.1^{RNAi}$ in comparison to WT

(A) 4% of $h1.1^{RNAi}$ nuclei showed univalents in comparison to WT nuclei free-univalents. (B) $h1.1^{RNAi}$ showed non-significant appearance of univalents with 0.08 univalents mean. (C) $h1.1^{RNAi}$ showed 17.12% reduction in chiasma comparable to WT. And (D) $h1.1^{RNAi}$ scored 7.84 (n=50) chiasma per nuclei comparable to 9.46 (n=50) in WT showing significant decrease ($P=8.321E-13$). Chiasma configuration in $h1.1^{RNAi}$ showed significantly reduced ring bivalent ($P=9.81E-13$) in comparison to WT, however, rod bivalents increased significantly ($P=1.80E-12$) comparable to WT. (E) Single chiasma distribution per bivalent showed significant increase in $h1.1^{RNAi}$ telomeric ($P=7.11E-06$), and subtelomeric ($P=8.51E-07$) chiasma in comparison to WT, whereas, non-significant difference observed at interstitial and proximal chiasma. However, (F) double chiasma distribution per bivalent in $h1.1^{RNAi}$ was significantly reduced at subtelomeric ($P=1.38E-08$), whereas non-significant difference was estimated at telomeric, interstitial and proximal chiasma comparable to WT. Significance level $P<0.05$. ***= $P<0.005$. Statistical analysis was done by T-test.

5.9 ANALYSIS OF RECOMBINATION PROTEINS IN *Ath1.1-1*

Investigation of the recombinases proteins; RAD51 and DMC1, localization during early prophase I showed multi-foci pattern along the chromosome axes during leptotene. The *Ath1.1-1* showed normal-like pattern of AtRAD51 localization similar to that observed in the wild-type (**Figure 3.21 A**), however, the AtDMC1 signal was altered. *Ath1.1-1* pachytenes show more reduced AtDMC1 foci than that observed in the wild-type (**Figure 3.21 B**). About 6 foci (n=3) were observed at pachytene in *Ath1.1-1* mutants.

The Arabidopsis MSH4 (AtMSH4) protein, homologue of yeast MutS, is required for preserving interference sensitive COs normal level. It was reported that AtMSH4 show multi foci at leptotene, which decrease gradually to 9-10 foci per meiocyte at pachytene (Higgins *et al.*, 2008b). And that the mature AtMSH4 foci colocalize with AtZYP1 on the synapsed homologous chromosomes (Higgins *et al.*, 2008b). The immunolocalization of MSH4 on *Ath1.1-1* showed a strange pattern of foci (**Figure 5.22**). The many foci observed at leptotene were decreased at pachytene, but showing foci in different sizes; 4-12 big foci with a mean of 6.8 foci (n=5), 0-12 small with a mean of 5.6 foci (n=5) besides to 1-4 foci with a mean of 1 foci (n=5), compared to 12 equally-sized foci in the wild-type, which all localize on the axis. From these results arose the question; Does the *Ath1.1-1* affect the dHj fate to develop to CO. Previous studies reported that MLH1/MLH3 heterodimers play a role in meiotic crossovers in yeast (Wang *et al.*, 1999). The *Arabidopsis* recombination protein AtMLH1, which is the homologue of *E. coli* MutL (Jean *et al.*, 1999) was also analysed in our study as CO marker. Immunocytology was applied using two antibodies; anti-MLH1 and anti ZYP1, in both the *Ath1.1-1* null mutant and in their

corresponding wild-type plants. The localization of MLH1 in the wild-type showed 8-11 foci in the wild-type at pachytene (Jackson *et al.*, 2006). However, the foci pattern in the *Ath1.1-1* mutant was severely reduced showing a range of 1-5 foci with a mean number of ~2.4 foci (n=5) compared to 8 foci (n=5) in the wild-type (**Figure 5.23**). This number confirms the reduction of chiasmata frequency observed previously.

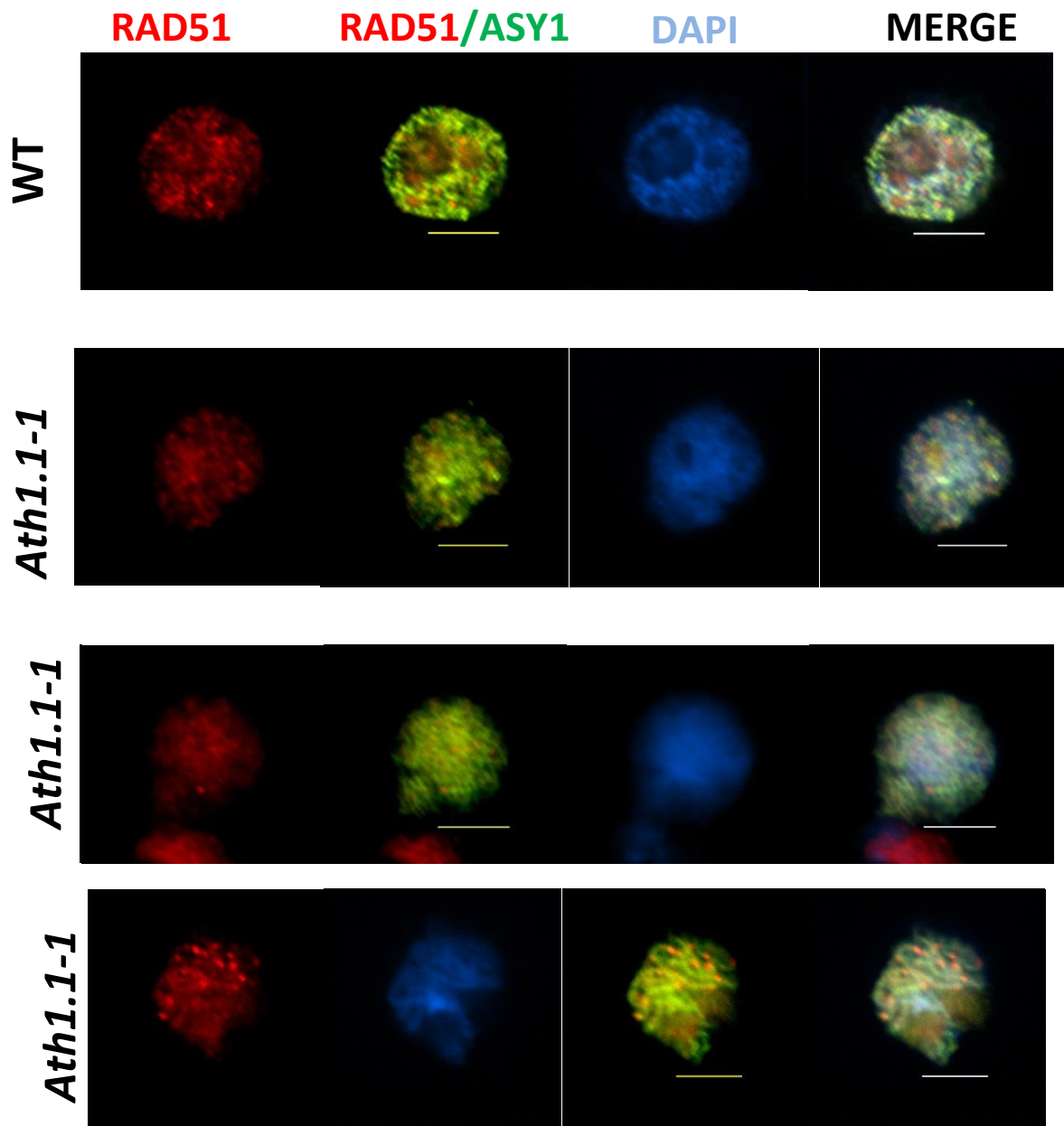


Figure (5.21 A): Dual immunolocalization of RAD51 and ASY1 in the *Ath1.1-1* and WT

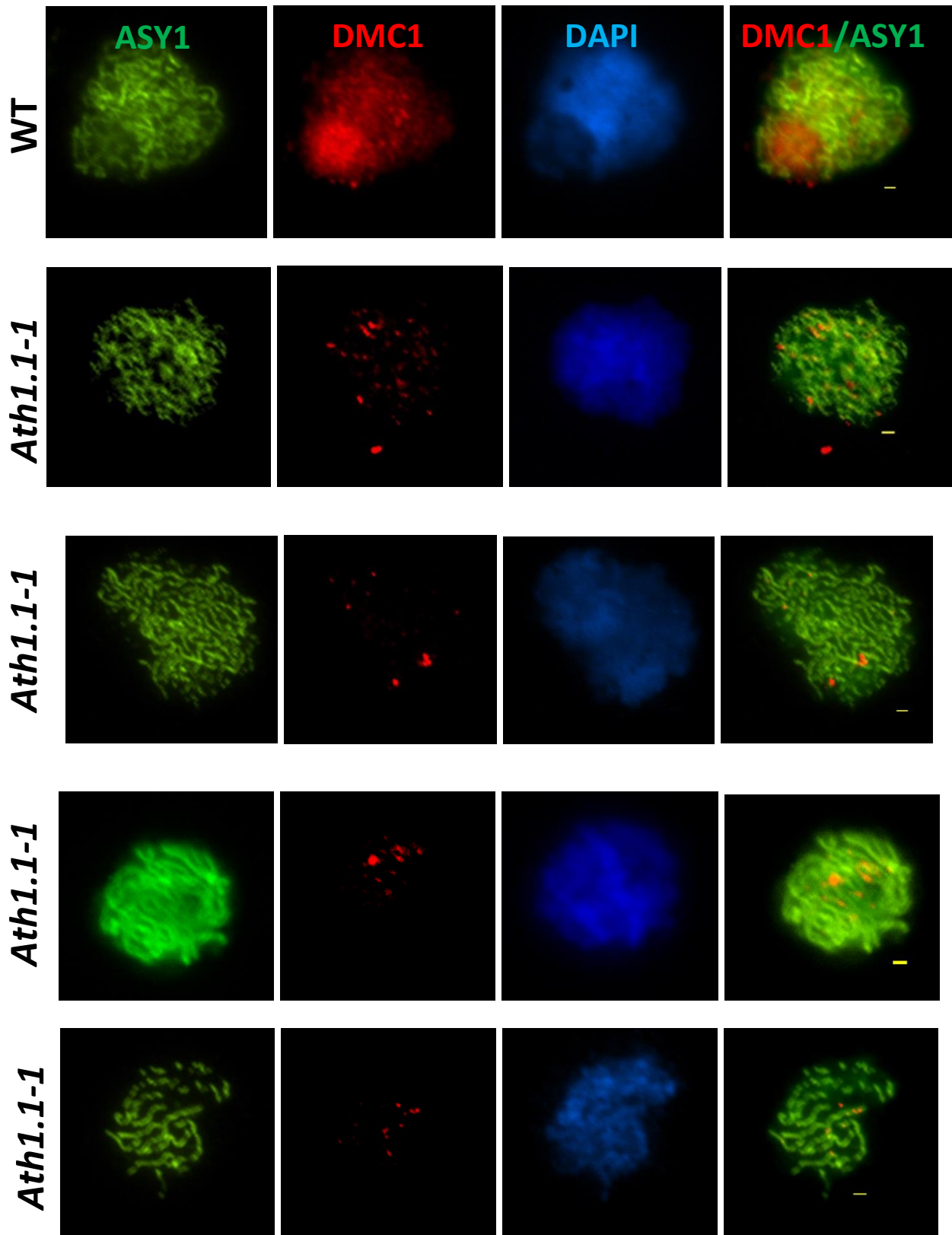


Figure (5.21 B): Dual immunolocalization of DMC1 and ASY1 in the *Ath1.1-1* and WT

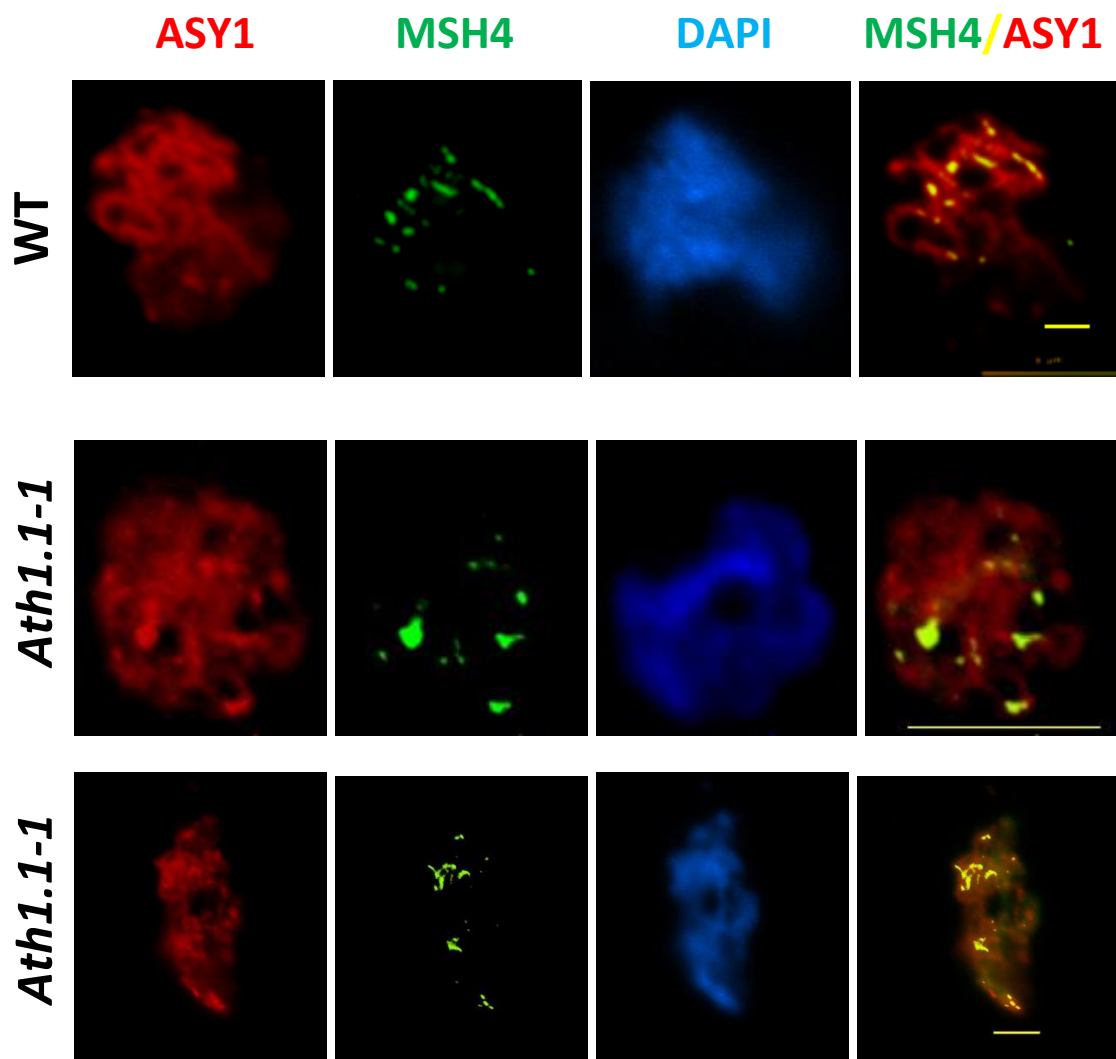


Figure (5.22): Dual immunolocalization of MSH4 and ASY1 in the *Ath1.1-1* and WT

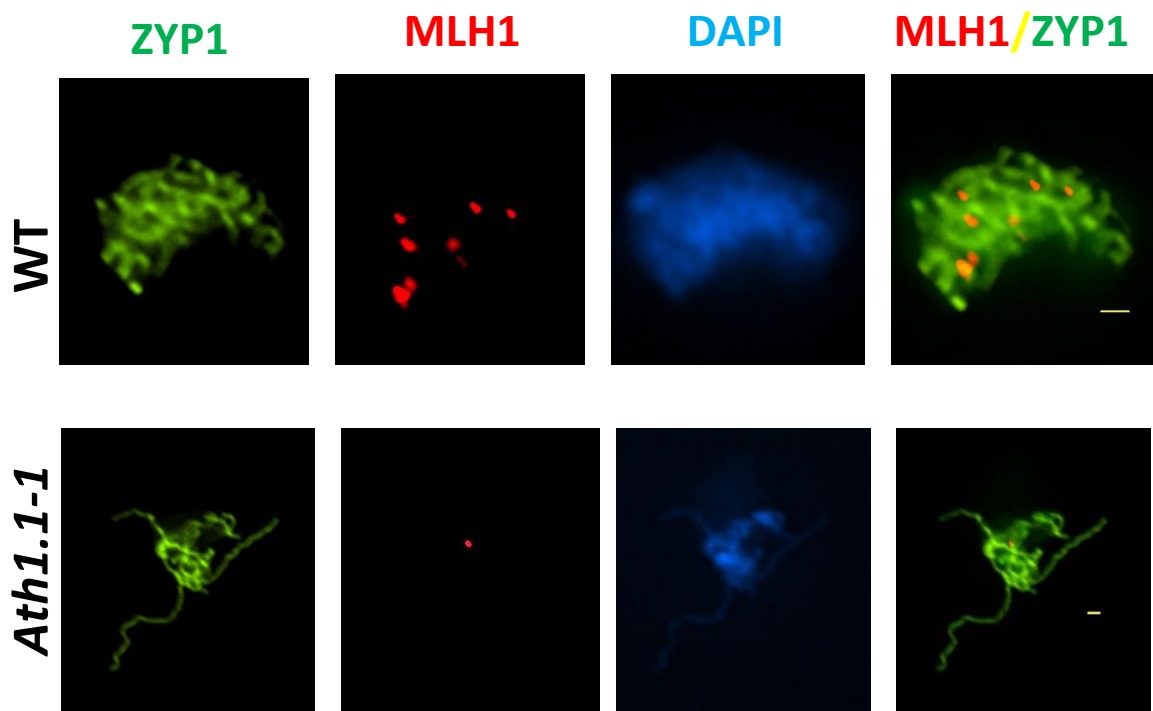


Figure (5.23): Dual immunolocalization of MLH1 and ZYP1 in the *Ath1.1-1-1* and WT

5.10. Discussion

5.10.1. Developmental defects in *Ath1.1* mutants could be a consequence of epigenetic changes

Altered *Ath1.1* mutant phenotype reflects different developmental defects. Several phenotypic changes were recorded in the *Ath1.1* mutants; delayed development, reduced plant size and reduced leaves. Furthermore, fasciated stems were observed in the *h1.1^{RNAi}* mutant line. These defects showed different severity levels among different mutant lines for this gene, suggesting that H1 loss or depletion might cause a different epigenetic switch in different lines. Linker histone role in development was addressed before (Fan *et al.*, 2003; Wierzbicki and Jerzmanowski, 2005). Reduction in more than 90% of *H1* expression in *Arabidopsis* by using dsRNA resulted in several developmental defects; altered stems, leaves, flowers and siliques (Wierzbicki and Jerzmanowski, 2005). These defects were also recorded in mutants for DNA hypomethylation mutants (Finnegan *et al.*, 1996; Kakutani *et al.*, 1996) besides to the ATP-dependent chromatin remodeler *snf2* mutant (Brzeski and Jerzmanowski, 2003). Interestingly, H1 down regulation in *Arabidopsis* was found to cause DNA hypermethylation at DNA repetitive and single-copy sequences (Wierzbicki and Jerzmanowski, 2005). Moreover, Barra *et al.*, (2000) reported that H1 loss in *Ascobolus* resulted in DNA hypermethylation of pre-methylated DNA. These results, besides to the “pleiotropic character” of the H1-dsRNA mutants, and H1 dsRNA mutant defects non-Mendelian pattern of inheritance, allowed Wierzbicki and Jerzmanowski (2005) to suggest that H1 down regulation could cause epigenetic effects. Moreover, (Fan *et al.*, 2003) reported that loss of three somatic H1 isoforms in mice caused embryonic lethality on day 10, which was coupled with H1/

nucleosome ratio decrease by 47% compared to wild-type. From all of that, and in reference to H1 role in preserving H1/nucleosomal ratio in mice Wierzbicki and Jerzmanowski, (2005) proposed that H1 might stabilize the chromatin internal folding by affecting certain chromatin structures (Jerzmanowski, 2004). Moreover Horn *et al.*, (2002) study that H1 phosphorylation mediates higher order chromatin remodelling by triggering SWI/SNF chromatin remodelers. And that chromatin fibre compacts merely when linker histone associates to chromatin fibre (Karymov *et al.*, 2001). Thus, suggesting that H1 stabilizes the overall chromatin higher order chromatin structures in a way permitting the proper DNA and core histones modification (Wierzbicki and Jerzmanowski, 2005). Further analysis is required to clarify if the *Ath1.1* mutants observed phenotypic defects are linked to change in either *H1.1* epigenetic code or related chromatin remodelling complexes functionality.

5.10.2. Chromosome axis architecture is aberrant in the *Ath1.1* mutants; *Ath1.1-1*, *Ath1.1-2*, *h1.1^{RNAi}*

Interestingly, the developmental defects observed in the *Ath1.1* mutants phenotypes were linked to alteration in mitosis. The delayed development reduced whole plant size and reduced leaves observed in the *Ath1.1-1*, as well as fasciated stems in the *h1.1^{RNAi}* plants, were coupled with abnormal mitosis. Some mitotic chromosomes were unable to condense properly at metaphase, showing longer chromosomes, leading to un-proper chromosome segregation and anaphase bridges formation. These defects were known in mutants in one or more of the linker histone *H1* isoforms (Hohmann, 1983; Maresca *et al.*, 2005). H1 link to chromosome compaction

was addressed in *Tetrahymena thermophila* (Shen *et al.*, 1995) and in *Xenopus* (Maresca *et al.*, 2005). A study on *Xenopus laevis* egg extract showed that H1 immuno-depletion resulted in about 50% longer chromosomes, which were unable to align properly at metaphase, and hence showed abnormal chromosome segregation at anaphase (Maresca *et al.*, 2005). Defects in *Xenopus*-depleted H1 chromosomes were coupled with normal condensins and chromokinesins normal structural and localization phenotype, besides to that, H1 addition to the H1-depleted chromosomes consequently rescued chromosomes compaction and alignment at metaphase, suggesting that H1 depletion in *Xenopus* affects the mitotic chromosome architecture directly and not the kinetochore (Maresca *et al.*, 2005). These results allowed Maresca *et al.* (2005) to propose that aberrant alignment of the elongated chromosomes resulted from alteration in the chromosomes connection to microtubules. In addition to that, segregation defect observed arise from the inter-elongated chromosomes twisting and folding. Imposing that H1 has a possible role in chromosomes plasticity and rigidity. The link between mitotic chromosome components and structure yet to be addressed (Maresca *et al.*, 2005). Several reports clarified H1 role in the chromatin structure at interphase (Thoma *et al.*, 1979; Boggs *et al.*, 2000; Woodcock and Dimitrov, 2001; Hansen, 2002). Hence, Maresca *et al.* (2005) proposed that H1 depletion in *Xenopus* interfere with higher order chromatin fibre (30 nm) stability, leading to aberrant longer chromatin template at interphase, which condense to longer metaphase chromosomes. Condensin I and topoisomerase II normal loading pattern in the H1-depleted chromosomes suggest that factors influence chromosome compaction (condensins) are loaded during interphase in a DNA-interval (kilobases) dependant manner rather than chromatin-

interval dependant manner (Maresca *et al.*, 2005). Previous reports showed that condensins and cohesins loads on the chromatin based on DNA intervals (Earnshaw *et al.*, 1985; Kimura and Hirano, 1997; Laloraya *et al.*, 2000; Poirier and Marko, 2002; Hudson *et al.*, 2003; Glynn *et al.*, 2004). Further analysis is required to clarify at which mitotic stage H1 mediates chromosome compaction, through H1-rescue experiments in a time-scale manner (Maresca *et al.*, 2005).

5.10.3. Homologous chromosome pairing and synapsis is aberrant in *Ath1.1* mutants

In order to understand the fertility deficiency observed in *Ath1.1* mutants a comprehensive atlas for the mutant and the wild-type meiotic stages was prepared. *Ath1.1* mutants presented clear defects which cause abnormal gamete formation, thus, fertility problems. During the wild-type meiosis pairing and synapsis of homologous chromosomes initiated at early prophase I is completed by pachytene stage, then homologous chromosomes de-synapse along the chromosomes except for some regions where they are linked by the chiasmata at diplotene. At diakinesis, an increase in chromosome condensation allows the observation of the five bivalents. Then at metaphase I bivalents align in the nucleus equator in a way that would allow the homologous chromosomes to segregate to opposite poles during anaphase I. Afterwards chromosomes alignment at metaphase II allows the proper orientation of chromosomes and the sister chromatids segregation at anaphase II to form balanced haploid gametes. These results were confirmed by the *Arabidopsis* wild-type meiotic atlas produced by Armstrong and Jones (2003).

In *Ath1.1-1* mutant, synapsis defect appeared clearly at pachytene. Incomplete homologous chromosome synapsis is indicated by visible regions of thin chromatin threads. This lack of synapsis is also accompanied by a lack of chiasmata in these regions producing univalents at diakinesis, and hence lacking the normal bivalent orientation at metaphase I, causing problems in chromosome segregation at anaphase I, and ending up with unbalanced dyads and gametes later on. These defects in gametes formation was confirmed by the severe reduction recorded in the percentage of viable pollen in the *Ath1.1-1* mutant (21.28%) comparable to the wild-type (78.71%). Similar meiotic defects observed in *Ath1.1-1* T-DNA line were also observed in the *Ath1.1-2* T-DNA and *h1.1^{RNAi}* mutant lines but to less severe defect phenotype. Moreover results obtained from the allelism test using the double heterozygote line *Ath1.1-1 / Ath1.1-2* showed similar synapsis defects at pachytene, leading to univalents at metaphase I. In all these mutants the meiotic products appeared to have an imbalanced chromosome number due to chromosome missegregation at anaphase I and II. Thus, these meiotic errors produced imbalanced gametes, reducing the correct fertility yield in the plant (seed count per silique). In conclusion, these facts indicate that these defects observed during meiosis are due to the mutations at the *AtH1.1* gene.

Synapsis defects were observed in maize mutants with defects in: homologous chromosomes pairing (e.g. *phs1*), homologous recombination (e.g. *rad51*) axial elements (e.g. *afd1*) and bouquet (e.g. *pam1*) (Golubovskaya *et al.*, 2002, 2006; Pawlowski *et al.*, 2004; Li *et al.*, 2007). Abnormal synapsis had been recorded in several mutants in *Maize* presented as early univalents appearance at diakinesis;

asynaptic 1 (as1) (Beadle, 1930), two *desynaptic 1 (dsy1)* alleles *dsy1-1* and *dsy1-9101* (Golubovskaya and Mashnenkov, 1976; Timofejeva and Golubovskaya, 1991; Bass *et al.*, 2003), *desynaptic2 (dsy2)* (Golubovskaya, 1989; Franklin *et al.*, 2003), *mei*N2415* Golubovskaya *et al.* (2010) , *mtm99-14b*, *mtm99-25*, *mtm00-10*, *mtm99-30* and *mtm00-09* (Golubovskaya *et al.*, 2003), and *desynapticCS* (Staiger and Cande, 1990; Golubovskaya *et al.*, 2003). Interestingly, a study by Golubovskaya *et al.* (2010) using transmission electron microscopy TEM of silver stained chromosome spreads, FISH with telomere probes and immunostaining techniques using antibodies that recognize proteins needed for proper synapsis (ASY1, ZYP1 and AFD1) showed that the maize mutants could be grouped into two categories according to their synapsis defect; improper synapsis and non-homologous chromosomes synapsis. The first group contained all mutants that showed synaptonemal complex maintenance defects, SC kinetics delayed and SC-free cells (e.g. the *asynaptic (as1)* mutants and the *desynaptic (dsy1-1, dsy1-9101, dsy2)* mutants (Golubovskaya *et al.*, 2010). These mutants showed several ZYP1 signal pattern ranging from complete SC loss (*dsy2*) to slowed down synapsis (*mei*N2415*). However the other mutants group (*mtm99-25* and *mtm00-10*) showed false ZYP1 loading arise from either individual chromosomes folding back upon themselves or homologous chromosomes switch to non-homologues partners during the synaptonemal complex progress (Golubovskaya *et al.*, 2010). Suggesting that non-homologous chromosomes synapsis arise from altered chromosome morphology; elongated zygotene chromosome axes (*mtm00-10*) and less compact heterochromatin (*mtm99-25*) (Golubovskaya *et al.*, 2010). Interestingly, previously published papers showed that the central element (CE) can form between two lateral

elements (LEs), even though if not on homologues (Ting, 1971; Jenkins, 1985; Pawlowski and Cande, 2005). Thus, these results besides to Golubovskaya *et al.* (2010) results on *Maize* mutants suggested that the mechanism of homologues pairing and synapsis during meiosis are uncoupled Golubovskaya *et al.* (2010).

Meiotic stage	Defects	Plant line			
		<i>Ath1.1-1</i>	<i>Ath1.1-2</i>	<i>h1.1^{RNAi}</i>	<i>Ath1.1-2^{+/-}/Ath1.1-1^{+/-}</i>
Zygotene	Chromatin breakage		√		
Pachytene	Chromatin breakage		√	√	
	Interlocking-structure		√	√	
	Asynaptic phenotype	√	√	√	√
Diplotene	Chromatin breakage		√		
	Univalents	√			
Diakinesis	Chromosome compaction defect		√	√	
	Chromatin breakage			√	
	Interlocking-structure		√	√	
	Univalents (low COs)	√		√	
Metaphase I	Univalents (low chiasma)	√	√	√	√
	Early sister chromatid separation	√			
	Fragments	√			
Meiosis II	Chromosome mis-segregation	√	√	√	√
	Aneuploidy (Tetrad)	√	√	√	√

Table (5.6): Summary of meiotic defects seen in the *Ath1.1* mutants.

Metaphase I	Plant line			
	WT (N=50)	<i>Ath1.1-1</i> (N=100)	<i>Ath1.1-2</i> (N=61)	<i>h1.1^{RNAi}</i> (N=50)
Early sister chromatid separation	X	√ F= 6% R= (0-1) M= 0.06 ***	X	X
Chromatin fragments	X	√ F= 9% R= (0-3) M= 0.12 ***	X	X
Univalents	X	√ F=100% R=(4-10) M= 7.98 ***	√ F= 4.9 % R= (0-2) M= 0.098 ***	√ F= 4% R=(0-2) M= 0.08 ***

Table (5.7): Metaphase I defects seen in *Ath1.1* mutants comparable to WT.
N= number of cells. F=frequency of nuclei. R= range. M= the mean.

5.10.4. *Ath1.1-1* differ significantly in chiasma frequency and their distribution from *Ath1.1-2* and *h1.1^{RNAi}*

The overall chiasma frequency and distribution in the *Ath1.1* T-DNA null mutants showed significant differences with the wild-type. *Ath1.1-1* and *Ath1.1-2*, showed a significant difference in their chiasma frequency, whereas, the null *Ath1.1-2* and *h1.1^{RNAi}*, had similar chiasma frequencies. The null *Ath1.1-1* showed univalents in

100% metaphase I nuclei, whereas only a 4.91% of metaphase I cells in *Ath1.1-2* and 4% in *h1.1^{RNAi}* (**Figure 5.24 A**). This big difference in the frequency of nuclei with univalents between null *Ath1.1-1* and *Ath1.1-2* mutants reflected significant difference in their univalent mean ($P=1.24E-70$, T-test), similarly *Ath1.1-1* has significant increase in the univalent mean comparable to *h1.1^{RNAi}* ($P=1.25E-70$, T-test), whereas, non-significant difference was observed between *Ath1.1-2* and *h1.1^{RNAi}* ($P=0.816$, T-test) (**Figure 5.24 B**). So, chiasma frequency analysis revealed 88.79% decrease in *Ath1.1-1*, whereas 11.31% in *Ath1.1-2* and 17.12% in *h1.1^{RNAi}* (**Figure 5.24 C**). This indicated significant difference between the different mutant alleles *Ath1.1-1* and *Ath1.1-2* ($P=6.557E-48$, T-test), similarly to *Ath1.1-1* and *h1.1^{RNAi}* ($P=6.545E-57$, T-test). Furthermore, the configuration of ring bivalents (**Figure 5.24 D**) of *Ath1.1-1* showed a significant decrease comparable to *Ath1.1-2* ($P=1.807E-36$, T-test) and *h1.1^{RNAi}* ($P=1.368E-24$, T-test). Also, the configuration of rod bivalents of *Ath1.1-1* showed significant decrease in comparison to *Ath1.1-2* ($P=0.00091$, T-test), and *h1.1^{RNAi}* ($P=8.359E-09$, T-test). Moreover, chiasma configuration in *Ath1.1-2* in comparison to *h1.1^{RNAi}* showed significant difference in both ring bivalents ($P=0.0031$, T-test) and rod bivalents ($P=0.0024$, T-test).

The difference in chiasma frequency between the *Ath1.1* mutants might be a reflection of their difference in their meiotic phenotype defect. So, the *Ath1.1-1* pachytenes showed asynaptic phenotype along the entire chromosome, resulted from abnormal chromosome axes formation, which was observed as abnormal ASY1 polymerization along the axis compared to wild-type, similarly, the *Arabidopsis*

chromosome axes ASY1 mutant, *asy1*, showed very close chiasma frequency of 1.39 (Sanchez Moran *et al.*, 2001), hence a suggestion could be made that *Ath1.1-1* in *Arabidopsis* is required to preserve normal chromosome axes stability/ and or related recombination proteins stability/loading during cell CO phase or process (recombination). For that, further analysis has been carried out on the CO-associated proteins loading on the axes (MSH4 and MLH) besides to the recombinase (DMC1) and all were abnormal similarly to that seen in the *asy1* mutant as discussed in 5.10.6. On the other hand the *Ath1.1-2* early prophase I cells showed persistent abnormal interlocking chromosomes presented at zygotene, pachytene and diakinesis, besides to asynaptic bubbles and chromosomes cutting. Chromosomes interlock is also known as “relational coiling/twisting” arise from chromosomes axes coiling (Moens, 1972; 1974; Zickler and Kleckner 1999). Gelei (1921) reported that homologues coiling during synapsis in zygotene chromosomes lead to be entangled within other synapsing pairs, thus forming interlocks. Two types of chromosomes coiling were observed: type I interlock forms from a bivalent being entangled between un-synapsed AEs whereas type II interlock results from one un-synapsed chromosome being stuck between un-synapsed AEs. In maize “complex interlocks” originated from Interlock I and II coupled in one cell. Interlock I and II are trapped by the SC progress on both sides of the loop (Gillies 1981). Several scenarios had been set for interlocks-removal in meiotic nuclei, of these: by coordinated chromosomes breakage and re-ligation (Holm *et al.*, 1982; Rasmussen, 1986; Moens, 1990). Another strategy is by chromosome movement meanwhile SC disassembly during zygotene and pachytene (Conrad *et al.*, 2008; Koszul *et al.*, 2008), possibly by interlocking chromosomes separation at telomeres (Rasmussen and Holm, 1980).

Analysis of the *mei*^{N2415}* mutant in maize showed a delayed synapsis phenotype resembled as some chromosomes with desynaptic bubbles (intermediate stages in homologous synapsis) were observed, whereas the rest of chromosomes showed normal synapsis (Golubovskaya *et al.*, 2010). The desynaptic chromosomes precede into chiasma-free chromosomes (univalents) at metaphase I however the other chromosomes showed normal phenotype. Suggesting that the *mei*^{N2415}* phenotype arise from defects either in the CE kinetics or regulation (Golubovskaya *et al.*, 2010). The phenotype of improper meiosis phenotype coupled with synapsis delay or full blockage results from abnormal recombination events as is observed in the yeast *zmm* mutants (Borner *et al.*, 2004). Showing delay in chiasma resolution at metaphase I as well longer prophase I.

Homologue recombination demands the proper localization of DNA replication (“recombinosomes”) complexes on chromatin axes (Borner *et al.*, 2004; Anderson and Stack, 2005; Henderson and Keeney, 2005; Franklin *et al.*, 2006; Moens *et al.*, 2007; Oliver-Bonet *et al.*, 2007; Wang *et al.*, 2009). Recombination initiates as early as programmed double-strand breaks (DSBs) occurrence (Blat *et al.*, 2002; Tesse *et al.*, 2003). Afterwards, DNA recombination plays a role in homologues axes pairing and juxtaposition in a way which permits proper synapsis.

A study by Storlazzi *et al.* (2010) on the chromosome organization and pairing during recombination in the filamentous fungus *Sordaria macrospora* by analysing mutants for axes associated recombination proteins, *mer3*, *msh4* and *mlh1*, showed that MLH1 is a demand for chromosomes entanglements “Interlocks” resolution at

zygotene. Mutants for *Mer3*, *Msh4* and *Mlh1* showed reduced COs (Borner *et al.*, 2004). Foci of MLH1 are observed when synapsis is completed, however foci of MER3 and MSH4/5 are observed during SC progress (Higgins *et al.*, 2004; de Boer *et al.*, 2006; Franklin *et al.*, 2006; Jackson *et al.*, 2006; Oliver-Bonet *et al.*, 2007; Moens *et al.*, 2007; Wang *et al.*, 2009). MLH1 role in the recombinational interactions resolution as COs during pachytene was implicated in several reports (Franklin *et al.*, 2006; Hunter, 2006). As MLH1 mediates removal of MSH4/5 from dHJ intermediates (Snowden *et al.*, 2004), hence, Storlazzi *et al.* (2010) reported that the presence of “DNA interlocks” in *mlh1* mutants in *Sordaria macrospora* suggests that MLH1 could similarly play a role in interlocks disassembly. A role for MLH1 in meiotic basepair mismatches recombination intermediates resolution was implicated in some reports (Hunter and Kleckner, 2001; Argueso *et al.*, 2003)

Moreover, the *Ath1.1* mutants showed anaphase defects. Anaphase bridges were observed in both *Ath1.1-2* mutants. Several reports showed that anaphase bridges were observed in condensin mutants (Yu and Koshland, 2003; Chan *et al.*, 2004; Resnick *et al.*, 2008), suggesting that connections arise between chromosomes at anaphase due to defects in chromosomes concatenation removal (Chen *et al.*, 2004). Moreover, defects in cohesion removal at COs could also be another possibility for anaphase bridge formation (Yu and Koshland, 2005).

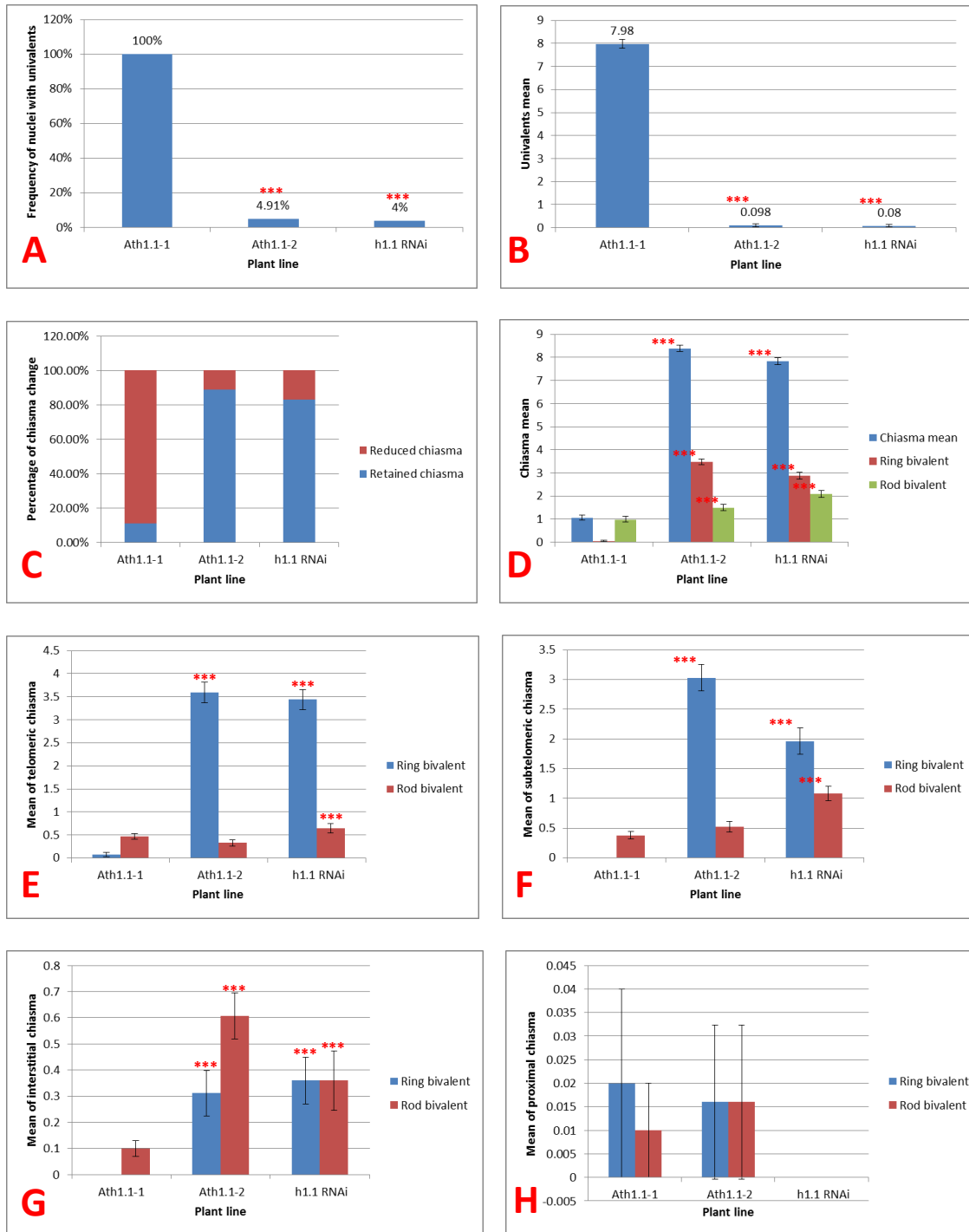


Figure (5.24): Comparison of chiasma frequency and distribution between *Ath1.1* mutants.

5.10.5. AtH1.1-1 and chromosome axes morphogenesis

The immunolocalization analysis for cohesins; SMC3, SMC1 and SYN1, loading on the chromosome axes is similar to that in the wild-type, suggesting that chromosome axes morphology is detectable in the *Ath1.1-1* even though ASY1 localization is aberrant, showing diffuse signal in some cells and discontinuous polymerization in other cells. Interestingly, *asy1* mutants showed normal AtSCC3 and AtSMC3 localization on the axis (Sanchez-Moran *et al.*, 2007), hence chromosome axis was observed (Pradillo *et al.*, 2007). Besides to this, previously published report by Armstrong *et al.* (2002) indicated that ASY1 loading on the chromatin is biased to chromatin sites, which are defined by the axial element (AE). From all of that, Sanchez-Moran *et al.* (2008) proposed that ASY1 has vital role in the chromosome axes maturity, rather than defining chromosome axes morphology. On the other hand, the ASY1 localization on *Ath1.1-1* meiocytes showed linear stretches which are evenly spaced. Since H1 has a confirmed role in higher order chromatin formation, whereas its depletion mediates lower order chromatin, we could propose that the observed evenly spaced ASY1 stretches at early pachytene cells in the *Ath1.1-1* mutant could be due to longer axes arise from less compact chromatin, consequently to H1.1-1 loss. Further analysis for chromosome axes length via deconvolution software is needed to allow new insights if the observed ASY1 localization change is dependent on AtH1.1-1-mediated higher order chromatin structure change. At the moment we could propose that H1.1-1 might be needed to mediate spacial ASY1 localization on the AE-associated axes defined by chromatin loops. More analysis, for ASY1 domains in the mutant in comparison to that in wild-

type might give a clue if the defects resulted from ASY1-axes defined sites change or its spacial shift.

5.10.6. AtH1.1 is required for normal ASY1 localization on the axes to allow normal meiotic recombination progression

The cytological and immunolocalization analysis revealed that the *Ath1.1-1* mutants lack proper ASY1 loading on the axes during early prophase I. *Ath1.1* mutants were never showed full ASY1 polymerization along the chromosome axes. These defects were coupled with severe reduction (~90%) in COs, resulted from aberrant CO type-I mediated-recombination, presented as reduced DMC1, MSH4 and MLH1 foci numbers, however, the DSB dependent protein γ H2AX and the RAD51 were indistinguishable from the wild-type. Interestingly, ~15% residual chiasmata were recorded in the *asy1* mutant in *Arabidopsis* (Sanchez-Moran *et al.*, 2007). Recombination progression defects observed in the *Ath1.1-1* mutants were similar to some degree to recombination defects reported in the *asy1* mutant (Sanchez-Moran *et al.*, 2007). Time coarse labelling experiment showed that reduced COs observed in the *asy1* mutants were linked to aberrant meiosis specific recombinase AtDMC1 stability beyond loading, suggesting that ASY1 is vital for meiotic interhomolog recombination by stabilizing AtDMC1-chromosome axes intermediate structures (Sanchez-Moran *et al.*, 2007, 2008). The ~10% residual chiasmata observed in the *Ath1.1-1* indicates that the interhomolog recombination is not fully constrained. Moreover, the detected AtDMC1 and AtMLH1 foci numbers reduction was corresponding to the residual chiasmata observed. The residual chiasmata number

observed in the *asy1* mutant were linked to residual AtDMC1 foci numbers presence corresponding to AtMLH3 (Sanchez-Moran *et al.*, 2007). Interestingly, *Atdmc1/asy1* double mutant lacking residual chiasmata indicated that chiasmata observed in *asy1* are AtDMC1-dependent (Sanchez-Moran *et al.*, 2007). On another hand, the residual chiasmata observed in the *Ath1.1-1* mutants were biased to telomeric position, however *asy1* residual chiasmata were subtelomeric mostly (Sanchez-Moran *et al.*, 2007). Since ASY1 is not a prerequisite for telomeres of homologous chromosomes pairing in *Arabidopsis* at G2, and nor prior to synapsis or meanwhile synapsis (Armstrong *et al.*, 2001) Sanchez-Moran *et al.* (2007) suggested that, in *asy1* telomere pairing mediates spatial subtelomeric regions on the homologs to come closer, and hence leading to interhomolog recombination mediated by At-DMC1 even though ASY1 absence (Sanchez-Moran *et al.*, 2008). Hence, it is wrathful to analyse chiasmata frequency and distribution in the double *Atdmc1/Ath1.1-1* mutants to understand if the residual chiasmata observed in the *Ath1.1-1* are AtDMC1-dependent similarly to that in *asy1*. The presence of 15% residual chiasmata in *asy1* and 10% in *Ath1.1-1* although that ASY1 is absent in *asy1*, whereas discontinuous (fragmented signal) in the *Ath1.1-1*, suggests that the extra 5% reduction in chiasmata in *Ath1.1-1* is due to AtH1.1 extra role in mediating the interhomologue recombination. The *Ath1.1-1* recombination defects observed were similar to that in *asy1*, suggesting that *AtH1.1* is most likely to allow biased interhomolog recombination by directing ASY1-mediated chromosome axes organization during early prophase I. Future analysis of histone AtH1.1 loading as well as ASY1 and AtDMC1 in the *Ath1.1-1* compared to wild-type through a time course labelling in conjugation with EdU labelling, besides to confocal microscopy analysis of the

mutant meiocytes, will help to address how could AtH1.1 loss affects chromatin structure spatially.

A study by Ferdous *et al.* (2012) showed that in *Arabidopsis* the meiotic chromosome axes proteins, AtASY3 and ASY1, have a vital role in allowing biased-interhomolog recombination, in a functionally similar way to that in budding yeast homologs, RED1 and HOP1, (Ferdous *et al.*, 2012). AtASY1 localize on the axes in an AtASY3-dependent manner, mimicking HOP1 in relation with RED1 (Ferdous *et al.*, 2012). The interplay between chromosome axes proteins and recombination progress indicated that ASY3 and ASY1 behave differently (Ferdous *et al.*, 201). Interestingly, *asy3* mutants showed 3.2 COs, whereas, 1.39 COs in *asy1*. This reduction in COs in the *asy3* mutants was found to be due to 33% reduction in DSBs. Time course labelling of the AtDMC1 protein in the *asy3* compared to *asy1*, showed normal-like AtDMC1 loading pattern per time in *asy3*, however, in *asy1*, AtDMC1 normal loading observed at the beginning do not persist, and declines severely. Suggesting that *asy3* bias towards inter sister recombination is due to reduced DSBs, whereas, reduced COs in *asy1* are linked with AtDMC1 stability on the axis (Ferdous *et al.*, 201). Moreover, *asy3* showed residual ASY1 localisation, suggesting that, AtDMC1 foci are stabilized by the residual AtASY1 domains detected (Ferdous *et al.*, 201). ASY3 localization on the axes in *Ath1.1-1* seems normal-like in terms of foci linearization, but still well defined axes signal is not observed, showing thicker axes identity compared to well defined and organized linear ASY3 signal in wild-type. From all of that, analysis of ASY3 localization in the *Ath1.1-1* prophase I will rule out

the interplay between AtH1.1-1 and chromosome axes progress if it is mediated by ASY3 localization.

5.10.7. H1.1 and meiotic chromosome axes organization within the homologous recombination context

Interphase chromatin switch to a compact organized chromosome in meiosis cannot be understood without discussing recombination-associated chromosome axis context. Several reports confirmed that recombination proteins associate with chromosome axes (Tarsounas *et al.*, 1999; Moens *et al.*, 2002). Kleckner (2006) proposed a model for meiotic chromosome organization which represents the “Dual loop model”. In this model sister chromatids of homologous chromosomes arrange into dense loops of 20 loops per μm , oriented in a way that permits homolog chromosomes joining at the axis. Loops base binding along the chromatin permit the formation of arrays of linear and equally distributed spaces. Chromosome axes protein ASY1 as well as cohesins SMC3, and SMC1 are used as a marker for chromosome axis morphogenesis (Sanchez-Moran *et al.*, 2007). Besides to ASY3 which colocalize with ASY1 (Ferdous *et al.*, 2012). Both *asy1* and *asy3* T-DNA mutants showed that SMC3 localization during prophase 1 is normal, suggesting that chromosome axes morphogenesis is normal. In these mutants normal chromosome axes is compromised, leading to asynaptic homologous chromosome phenotype, since the residual transverse AtZYP1 observed fail to progress, and hence reduced CO frequency was recorded, 1.39 in *asy1* (Sanchez-Moran *et al.*, 2007) and 3.2 in *asy3* (Ferdous *et al.*, 2012), suggesting that chromosome axes proteins; ASY1 and

ASY3, establish structural axes which mediates recombination to occur. Interestingly, analysis of *Ath1.1-1* T-DNA mutant showed that chiasmata were reduced severely showing 1.06 COs per cell. Immunolocalization analysis of chromosome axes morphogenesis using cohesion proteins; SMC3, SMC1 and SYN1 indicated that is normal. However, although ASY1 and ASY3 could be still occurring on the axes, ASY1 localization pattern was altered from the WT, whereas ASY3-were more normal, but still both ASY1 and ASY3 are showing disorganized chromosome axes identity. ASY1/SMC3 colocalization showed that, the diffuse and discontinuous ASY1-axis polymerisation defines thicker disorganised chromosome axes compared to that observed in the ASY1/SMC3 localization in wild-type. Besides that, ASY1 signal during zygotene-early pachytene appear as two aligned and interspaced stretches along the chromosomes axes, rather than one thick signal. Moreover, chiasmata decline observed in the *Ath1.1-1* mutant resulted from decline in the AtDMC1 foci number, whereas RAD 51 seems to be normal, leading to a bias towards inter sister chromatid recombination rather than inter homologous recombination. These, results indicate that, *Ath1.1-1* play a role in the meiotic chromosome axes organization as well as maturity to allow recombination machinery to progress normally. And that, H1.1-1 might allow higher order chromatin organization of the chromatin loops and in the chromatin connecting chromatin loops base sites (ASY1-AE associated axis). Thus resulting in an increase in the spaces forms between AE along chromosome axes. Hence, ASY1 appears discontinuous. Besides, there is a possibility of a delayed axes formation in the *Ath1.1-1* mutants, represented as ASY1 signal staying to late pachytene, showing colocalization with AtZYP1 signal. Furthermore, Although ZYP1 polymerization is more normal than

ASY1 signal, but it seems that ZYP1 polymerization does not indicate efficient recombination, with a possibility that delayed and improper chromosome axes organization is a consequence for ASY1 local delayed shift to chromosome axes, leading to synapsis starting from non-mature AE structure, lacking recombinases, hence synapsis precede, but not recombination. All of these scenarios are still suggestion, and more analysis is still needed.

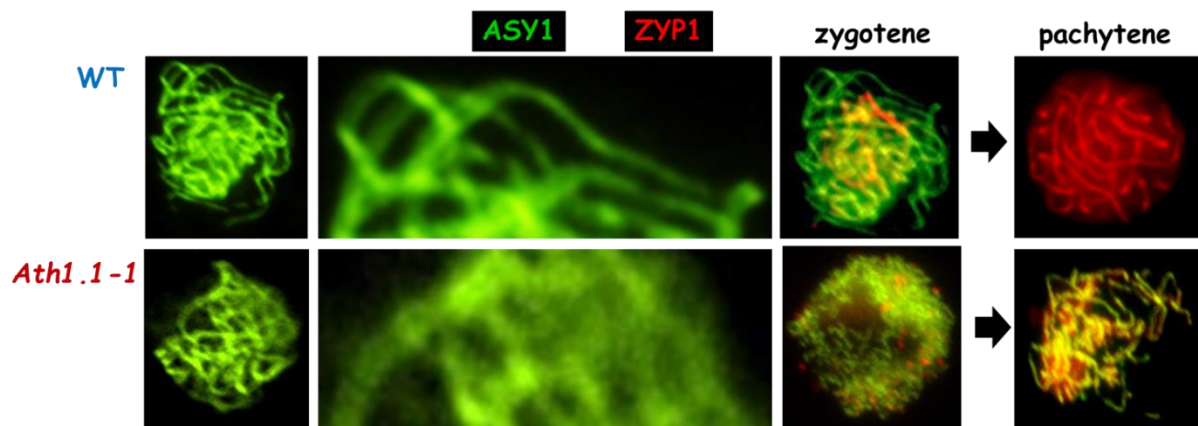


Figure (5.25): Comparison of ASY1 and ZYP1 localisation on the *Ath1.1-1* and WT meiocytes. Chromosome axes defects were observed in the *Ath1.1-1* mutants represented as diffuse and discontinuous ASY1 signal showing improper chromatin-axes organisation, which is also accompanied with delayed abnormal synaptonemal complex TF protein loading on the axes, and ending in ASY1-ZYP1 colocalization at late pachytene, whereas in wild-type ZYP1 signal replaces ASY1 signal at late pachytene.

CHAPTER 6

GENERAL DISCUSSION

6.1. Introduction

The aim of International Food Security Programs is to provide enough food for the planet's inhabitants. The great increase in the population annually imposes challenges on researchers worldwide to develop techniques which could increase crop production and provide the desired traits and quality. Scientists have achieved several different strategies for crop breeding like; heterosis (Hochholdinger, 2007; Springer and Stupar, 2007; Stupar *et al.*, 2008; Fernandez-Silva *et al.*, 2009; Wei *et al.*, 2009), backcross breeding (Vogel, 2009) and reverse breeding (Dirks *et al.*, 2003; Wijnker *et al.*, 2012), which vary in their outcome prediction. Reverse breeding is the most modern breeding strategy (Dirks *et al.*, 2009). This technique stands on two steps; the first is suppression of cross over recombination in the plant of interest, and the second is the reproduction of double haploid plants from spores with achiasmatic chromosomes (Dirks *et al.*, 2009). Hence, genes that affect meiotic recombination are of interest for this technique like SPO11 and DMC1 whose mutant alleles show achiasmatic chromosomes at metaphase I (Ross *et al.*, 1997; Couteau *et al.*, 1999; Caryl *et al.*, 2000; Nonomura *et al.*, 2004; Stacey *et al.*, 2006). These genes could be suppressed through several strategies; RNA interference (RNAi), posttranscriptional gene silencing like (siRNAs) or virus induced gene silencing, or even by the action of specific chemicals to suppress meiotic COs (e.g. mirin, an inhibitor for Mre11-Rad50-Nbs1 complex) (Dupre *et al.*, 2008). Therefore, studies on meiotic genes which control the CO-recombination pathway are of a great value as a tool to manipulate genome recombination (Dirks *et al.*, 2009). There have been very few reports on higher eukaryotes showed that linker histones might play a role in DNA repair and recombination up to date (Rosidi *et al.*, 2008). Our research might

shed some light on a linker histone which seems to have a role in preserving meiotic recombination at normal levels in *Arabidopsis*. Hence, the combination of our results besides to other achiasmatic mutants could provide some basic genetic tools for plant breeders to manipulate recombination. The use of histone *h1* mutants in different crops like the mutant studied in this thesis could be a source of haploids due to the missegregation of chromosomes, and thus, these mutants could be used to obtain desirable double haploid crop plants. Furthermore, we have observed that *h1* mutants have a considerable delay in flowering time opposite to *h4* mutants which possess an early flowering time. By themselves, these two characteristics have been exploded in different occasions by plant breeders.

The main aim of this research was to study different histones role in chromosome organisation during meiosis and mitosis in *Arabidopsis*. Thus, my project focused in studying two types of histones; the linker histone (H1) and the core histone H4 and their role on the global chromosome organisation during cell division and gamete production in *Arabidopsis*. *Arabidopsis* has ten variants for the linker histone H1 and eight identical copies for histone H4 (for more details see the homology search studies done via *in silico* analysis in previous chapters). We carried out a screening study for different histone *h1* T-DNA insertion mutants corresponding to the different isoforms of H1 coded by the *Arabidopsis* genome. Furthermore, a single available RNAi mutant line for a specific locus *H1.1* was also analysed. On the other hand, *Arabidopsis* genome contains 8 loci for histone *H4* which encode for eight identical histone H4s. These copies and their nearly identical expression profiles show their redundant effect, so a knockdown RNAi mutant line was used for the genetic analysis of all these histone H4s.

6.2. Core histone H4

6.2.1. Meiosis is affected in H4 mutants

The analysis of a histone *Ath4^{RNAi}* line in *Arabidopsis* showed a significant semi-sterile phenotype in these plants. This semi-sterile phenotype is derived from meiotic errors (**Table 6.1**), since the meiocytes clearly showed defects as early as prophase I. Different chromatin breakage sites were obvious at zygotene-pachytene stages, followed with defects in chromosome segregation, which in total ended with unbalanced and non-viable gametes. Nevertheless, due to time constraints no further analysis could be carried out. More research is still needed to have a clear view on the histone H4 role during meiosis and DNA repair and recombination. The extra work on H4 should take in consideration different issues: The first, at the epigenetic code level (histone H4 modifications and interactions). The second, at the nucleosome structural level, as H4 is one of the core histones which build up the nucleosome. The errors observed in the *Arabidopsis Ath4^{RNAi} kd* mutant line might be the consequence of disturbing the whole nucleosome particle, due to the loss of its main constituents, as histone H4 binds to H3 and forms (H4-H3)₂ hetero-tetramers, rather than the specific H4 loss merely. To analyse this theory, two different histones chaperons were preliminary analysed; CAF1 and NAP1.

Nucleosome assembly demands that histone chaperons deposit histones onto DNA. Chromatin Assembly Factor 1 (CAF1) deposits histones H3/H4 on the DNA either in a replication dependent manner (Smith and Stillman, 1989, 1991; Shibahara and Stillman, 1999; Tagami *et al*, 2004) and or beyond nucleotide excision repair (NER)

(Ridgeway and Almouzni, 2000). Several studies indicated that CAF1 is evolutionary conserved among species (Smith and Stillman, 1989; Verreault *et al.*, 1996; Kaufman *et al.*, 1997; Kaya *et al.*, 2001). Plants have three subunits for CAF1: Fasciata 1 and 2 (FAS1 & FAS2) and Multicopy Suppressor of IRA1 (MSI1) (Kaya *et al.*, 2001). The tripartite CAF1 in plants were found to correspond to Chromatin Assembly Complex proteins (CAC1& CAC2 & CAC3) in budding yeast (*Saccharomyces cerevisiae*) (Kaufman *et al.*, 1997), and to p155, p60, and p48 in humans (Smith and Stillman, 1989; Verreault *et al.*, 1996). CAF1 structural conservation in plants, yeast, and animals had showed also that it is functionally similar (Kaufman *et al.*, 1997; Tyler *et al.*, 1999; Kaya *et al.*, 2001; Tyler *et al.*, 2001).

The CAF1 in *Arabidopsis* was studied by analysing the two FAS subunits; FAS 1-2 and FAS 2-3. We analysed T-DNA insertion mutant alleles for both subunits; *fas1-3* and *fas 2-3* respectively. Both *fas1-3* and *fas 2-3* mutant lines showed similar defects to that observed in the *h4 kd* mutant line (**Table 6.1**). The mutants showed that the massive reduction in fertility arose from cytological chromosome fragmentation at pachytene followed by chromosome missegregation. The third CAF1 subunit, MSI1, was not successfully studied as the mutants did not survive very well. Moreover, another histone chaperones like the Nucleosome Assembly Protein 1 (NAP1), the H2A-H2B replication dependent major chaperon should be analysed through my future work. NAP1 is evolutionary conserved from yeast to human (Ishimi *et al.*, 1984; Dong *et al.*, 2003; Ohkuni *et al.*, 2003; Park and Luger, 2006a). NAP1 in yeast (yNAP1) has the best studied NAP1 protein. The yNAP1 (48 KDa protein) allow nucleosome assembly in vitro by binding to the H2A-H2B and to H3-H4 (Ishimi *et al.*,

1983; Ishimi and Kikuchi, 1991; Ito *et al.*, 1996; McBryant *et al.*, 2003; Steer *et al.*, 2003). It has been reported that amino acid residues 74-365 are responsible in maintaining nucleosomes original structure and function during its assembly (Fujii-Nakata *et al.*, 1992; McBryant *et al.*, 2003). Studies on HeLa cells reported that NAP1 binds to newly formed H2A-H2B to allow chromatin assembly (Chang *et al.*, 1997). Furthermore, the NAP1 role exceeds H2A-H2B association/disassociation from the nucleosome to its substitution by H2A-H2B variants (Park *et al.*, 2005), suggesting that NAP1 is vital for both replication-dependent and replication-independent chromatin assembly as well as for nucleosome sliding resulting from H2A-H2B dimer exchange (Park *et al.*, 2005).

The importance of both *fas* and *nap* mutants analysis is that it will clarify if the hypothesis that *Ath4*^{RNAi} meiotic defects, as were shown previously, are due to H4 level decline merely or it is the whole nucleosome blockage. Hence, cytological and proteomics analysis for histone H4 protein within meiotic context of *nap* and *fas* mutants as well as cytological analysis for *nap* mutants and their core histones content in relation to histone H4 will shed more light on the real role of H4 within *Arabidopsis* nucleus in meiosis.

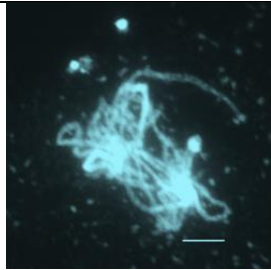
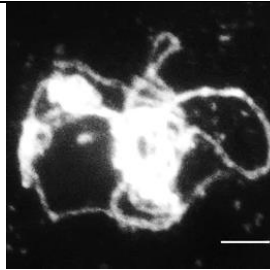
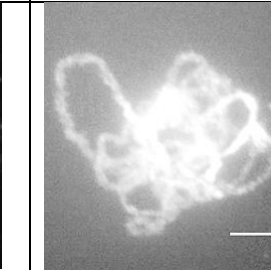
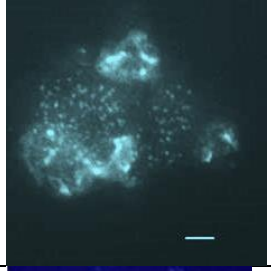
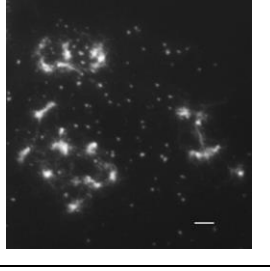
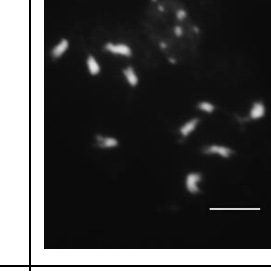
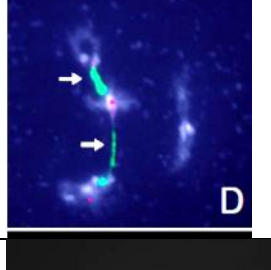
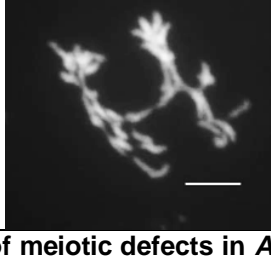

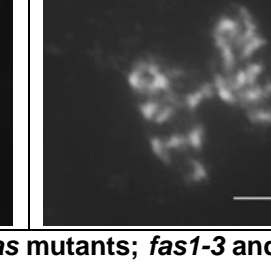
Plant line		<i>h4^{RNAi}</i>	<i>fas 1-3</i>	<i>fas 2-3</i>
Fertility		52.7%	20.7%	21.4%
Meiosis defects	Chromatin fragments			
	Abnormal chromosome segregation			
	Ectopic recombination			
Mitosis defects	Anaphase-Bridge			

Table (6.1): Summary of meiotic defects in *Arabidopsis Ath4* and *fas* mutants; *fas1-3* and *fas 2-*

3.

6.2.2. Histone H4 is needed for proper meiotic chromosome organisation

The chromosome phenotype observed in the *Ath4^{RNAi}* line showed consistent chromatin fragmentation at pachytene stage. Suggesting that histone H4 is needed for proper chromosome organization and maintenance in meiosis. Since the *Ath4^{RNAi}* showed tangled and abnormal nucleolus, FISH analysis was done to see the impact on the 45S rDNA and 5SrDNA regions. The *Ath4^{RNAi}* mutants showed that most of

the chromatin fragmentation occurred at the 45S/5S rDNA regions at pachytene. Furthermore, chromosome interactions between non-homologous chromosomes were clear at diakinesis and metaphase I also involving chromatin from the rDNA regions, suggesting that histone H4 is important to preserve the rDNA region during *Arabidopsis* meiotic recombination. This fragmentation observed in the rDNA regions in *h4^{RNAi}* mutants might be the result of ectopic recombination; abnormal recombination results from cross over between nonhomologous chromosomes at loci with sequence homology at least as 2.2Kb DNA (Licthen *et al.*, 1986; Montgomery *et al.*, 1987) among these regions. Thus, H4 in *Arabidopsis* could play a role to prevent ectopic recombination normally. The 45S rDNA role in genome instability was addressed in different reports (Butler, 1992; Thomas *et al.*, 1996). Histone H4 has been suggested to have a role in DNA double strand break repair (Kothapalli *et al.*, 2005; Corsini and Sattler, 2007). Hence further research is needed to understand if the chromatin breakage in the *Ath4^{RNAi}* mutant is due to defect in DSB processing during meiosis or it is a result to structural defects in the meiotic chromosome. Moreover, defects observed in the *fas* mutants in *Arabidopsis* at the cytological level suggest a role for FAS in DSB either directly or as a consequence of histone H4 indirect loss. FAS suggested role in DSB was addressed previously by Endo *et al.* (2006).

Arabidopsis and human histone H4 proteins are 98% identical so we could predict that the studies done here in *Arabidopsis* could add more value for understanding the histone H4 role in chromatin organization and its functional status within the different processes like DNA repair, meiosis and mitosis in other eukaryotes including

humans. As several studies showed that histone H4 proteins are subjected to several posttranslational modifications. And since the H4 epigenetic code previously showed an impact on the functional progress of the nucleus (Loidl, 1988; Loidl, 1994; Garcia-Ramirez *et al.*, 1995). Hence, we ran screening of two histone modifiers mutants; a histone deacetylase mutant *Athda6-7* and a histone methylase triple mutant *Atdrm1xdrm2xmet* (data not shown), and both have showed a preliminary semi-sterile phenotype compared to the normal fertility level seen in WT. The further analysis of these mutants at both meiotic and mitotic levels, through the usage of both cytological and proteomics will help understanding H4 posttranslational modifications specificity, if any, during cell nucleus. Besides that, histones H4 immuno-precipitations will add more value on the nucleus H4 networking.

6.2.3. Histone H4 is needed for mitotic chromosome architecture

A defect seen in the mitotic cells of the *Ath4^{RNAi}* mutants suggests a role for histone H4 in preserving the structural chromosomes integrity. Anaphase bridges were consistent in the *Ath4^{RNAi}* as well as in the *Atfas* mutants showing a possibility of chromosome fragmentation or defects in the inter sister chromatid homologous recombination. Few reports suggested a link between histone H4 and cell cycle (Megee *et al.*, 1995). Furthermore, Shogren-Knaak and Peterson (2006) proposed that histone H4 acetylation either has a role on the higher order chromatin organisation or cause alteration in the chromatin proteins interactions. Moreover, the *Ath4^{RNAi}* mutant's growth on 30µM cisplatin plates was abnormal. The *Ath4^{RNAi}* mutants showed delayed vegetative growth as well as reduction in the number of

viable seeds comparable to wild-type, suggesting that some DSBs induced in the *Ath4^{RNAi}* mutants were unable to repair.

6.3. Linker histones H1

6.3.1. Linker histones are involved in plant development

The screening of ten isoforms for histone H1 in *Arabidopsis* showed that histone H1s are needed for proper plant development. The presence of several isoforms for histone H1 in higher eukaryotes suggests that the different variants are needed for the different cell types formation as well as the different developmental stages (Newrock *et al.*, 1977). The delayed pattern in flower formation existed in H1s mutants; *Ath1b*, *Ath1c*, *Ath1.1-1*, *Ath1.2*, *Ath1.3*, *Athon4*, and *Athon5*, suggested that histone H1 loss might affect the flower regulatory genes. The tobacco deficient histones H1A and H1B showed sterile phenotype, which showed aberrations in plant development; in which stamens and collars were abnormal, defects in flower development were linked with temporal change in the stimulation of the regulatory genes; Nap3 and Ta29, through flower bud development (Prymakowska-Bosaka *et al.*, 1999). Nap3, the homologue of *Arabidopsis* APETALA3 (AP3) gene were found to have a major role in flower development through its mere expression in the stamens and petals (Hill *et al.*, 1998), whereas Ta29 encodes tapetum-specific glycerine rich protein (Golberg *et al.*, 1993). Although Nap3 and Ta29 expression phenotype in the mature flowers of H1A and H1B deficient tobacco plants were normal, but their expression at earlier stages were abnormal, showing early termination of Nap3 transcription at stage 3 and 4 which is not the case in the control

plants, however, Ta29 was induced at stage 1 rather than the normal induction at stage 3. So, H1A and H1B deficiency in tobacco was thought to impede normal flower bud development and functional pollen grain formation by affecting Nap3 and Ta29 genes temporally rather than spatially (Prymakowska-Bosaka *et al.*, 1999).

6.3.2. Chromosome axis architecture is disturbed in *Ath1.1* mutants; *Ath1.1-1*, *Ath1.1-2*, *Ath1.1*^{RNAi}

The cytological analysis of mitotic cells in the *Ath1.1* mutants showed abnormal mitotic metaphase chromosome condensation compared to wild-type chromosomes (**Table 6.2**). *Ath1.1* mutants were unable to show full chromosome compaction at metaphase I. The link between linker histones and mitosis was addressed in several reports (Hohmann, 1983; Maresca *et al.*, 2005). It was reported that Cdk1 and Cdk2 phosphorylates histone H1 in a cell-cycle dependent manner in protozoa and mammals (Bhattacharjee *et al.*, 2001; Langan *et al.*, 1989; Roth *et al.*, 1991; Gurley *et al.*, 1995), whereas the mitotic Cdk homologues, Cdc2⁺/CDC28 in yeast and frog (Langan *et al.*, 1989). In mammals H1 phosphorylation starts at G2 prior to mitosis, and peaks at mitosis (Hohmann, 1983). Eukaryotic histone H1 phosphorylation was found to permit chromatin condensation (Maresca *et al.*, 2005). Besides to this, a study on *Xenopus* showed that H1 depletion resulted in longer chromosomes, which were unable to align properly at metaphase, and hence showed abnormal chromosome segregation at anaphase (Maresca *et al.*, 2005). These defects in *Xenopus*-depleted H1 chromosomes showed that mitotic condensins and chromokinesins have normal structural and functional phenotype, suggesting that H1

depletion in *Xenopus* affects the mitotic chromosome architecture directly (Maresca *et al.*, 2005).




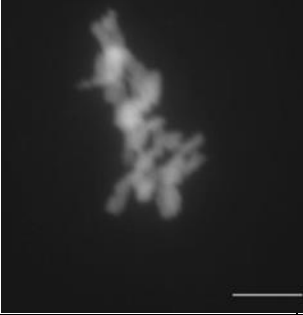
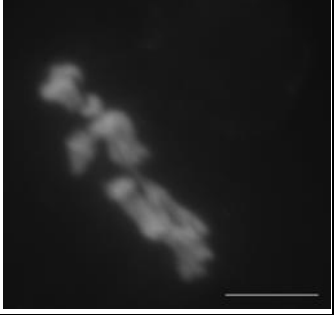
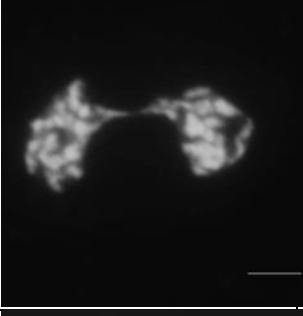
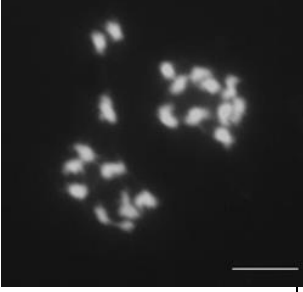
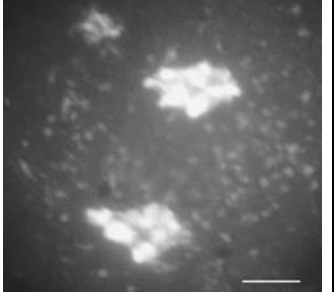
		<i>h1.1-1</i>	<i>h1.1-2</i>	<i>h1.1^{RNAi}</i>
Mitosis defects	Plant phenotype			
	Chromosome compaction defect			
	Anaphase-Bridge			
				

Table (6.2): Summary of mitotic defects in *Ath1.1* mutants

6.3.3. AtH1.1 is needed for proper meiosis

Analysis of *Ath1.1* mutants; *Ath1.1-1*, *Ath1.1-2* and *h1.1^{RNAi}* showed that seed production is constrained. Analysis of PMCs showed that fertility defects arise due to defects in meiosis (**Figure 6.1**). Cytological and immunolocalization spreads of the *Ath1.1* mutants indicated synapsis defects at early prophase I. Also, univalents were present as early as diakinesis, chiasma frequency was significantly reduced compared to wild-type plants. And so, chromosome missegregation was consistent at anaphase I and afterwards resulting in unbalanced tetrads forming nonviable gametes. Several reports showed that histone H1 variants play a role in preserving normal meiosis. A study by Prymakowska-Bosaka *et al.* (1999) showed that chromosomal defects were related to deficiency in the linker histones H1A and H1B in Tobacco. Tobacco plants showed defects at metaphase and onwards, showing micronuclei at later stages, suggesting that chromosomes were unable to separate to the poles or chromosomes were broken (Prymakowska-Bosaka *et al.*, 1999). These results were thought to be as a result of defect in synaptonemal complex formation or in sister chromatid cohesion (Peirson *et al.*, 1997).

Moreover, other studies showed that fertility defects are linked to abnormal behavior of meiotic chromosomes due to defect in one of the proteins involved in DNA repair (reviewed by Osman *et al.*, 2011), suggesting a possible link between the linker histone H1 role and the DSB processing within meiosis in *Arabidopsis*. This possibility was confirmed through the immunolocalization analysis using antibodies

that recognize some proteins involved in homologous recombination. It showed that loading of some of these proteins was highly reduced in the *Ath1.1* mutant.

On the other hand, several studies implied a role for heterochromatin regions in maintaining homologous chromosomes alignment during meiosis (Derenburg *et al.*, 1996; Karpen *et al.*, 1996; Renauld and Gasser, 1997). A link between histone H1 and heterochromatin regions establishment was addressed previously by Prymakowska-Bosaka *et al.* (1999). Overexpression of somatic H1 in tobacco caused increase in the heterochromatin within the nuclei (Prymakowska-Bosak *et al.*, 1996). Moreover, histone H1 had been addressed to permit the chromatin transition from 10 nm nucleosome fibre to 30 nm fibre structure, hence H1s are associated with higher order structure formation (Thoma *et al.*, 1979).

Moreover, the *Ath1.1-2* mutants showed anaphase defects (**Table 6.3**). Anaphase bridges were observed in *Ath1.1-2* mutants. Several reports showed that anaphase bridges were observed in condensin mutants (Yu and Koshland, 2003; Chan *et al.*, 2004; Resnick *et al.*, 2009), suggesting that connections arise between chromosomes at anaphase due to defects in chromosomes concatenation removal (Chen *et al.*, 2004). Moreover, defects in cohesion removal at COs could also be another possibility for anaphase bridge formation (Yu and Koshland, 2005).





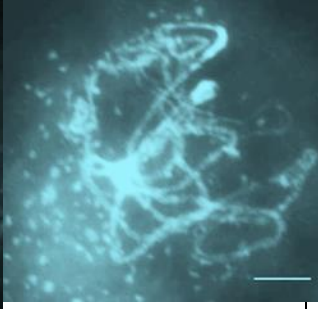
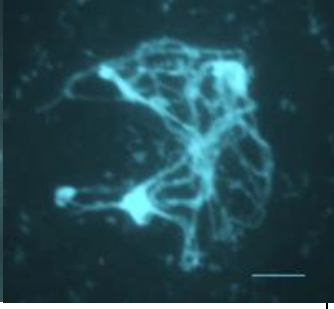
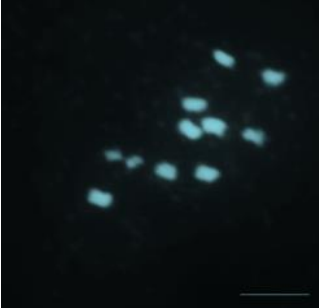

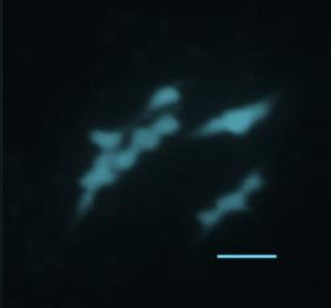
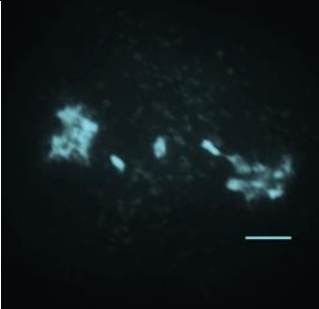
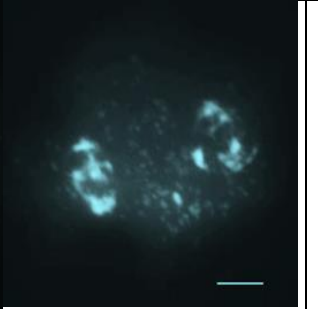
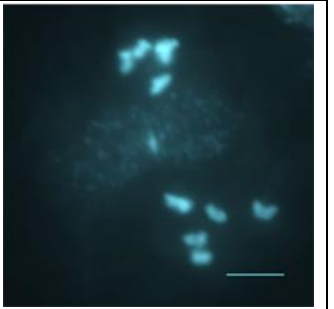
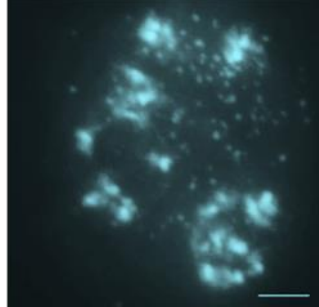
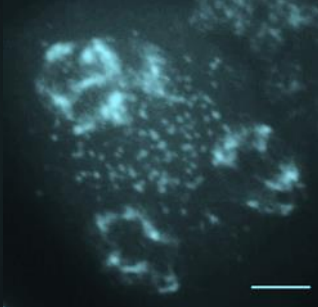
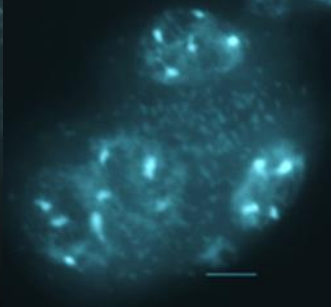
Plant line		<i>Ath1.1-1</i>	<i>Ath1.1-2</i>	<i>h1.1^{RNAi}</i>
Fertility defect	Silique Phenotype			
	Seed-set reduction	90% ↓	17.6% ↓	41% ↓
Meiosis defects	Asynapsis (Pachytene)			
	Chiasma frequency reduction (Metaphase I)			
		88.79% ↓	11.31% ↓	17.12% ↓
	Chromosome mis-segregation (Telophase I)			
Aneuploidy at Tetrad				

Table (6.3): Summary of meiosis defects in the *Ath1.1* mutants

6.3.4. *Ath1.1-1* mutants show disturbed meiotic chromosome axes

Analysis of DAPI stained chromosomal spreads of the *Ath1.1* mutants showed defects during early prophase I. Synapsis defects were confirmed at pachytene in the *Ath1.1* mutants. In order to understand the basis of this defect an immunolocalization analysis was done for the *Ath1.1-1* mutant line using antibodies that recognize the chromosome axes proteins; ASY1, ASY3 besides to the Synaptonemal complex component TF, AtZYP1. The results showed that the chromosome axes proteins ASY1 and ASY3 showed abnormal signal on the chromosome axes. Defects were seen in the ASY1 polymerization as early as leptotene were consistent, showing diffuse signal at zygotene in some cases, and abnormal stretches in others, which continues to show unequal fragmented linear ASY1 signal at pachytene. Besides to this ASY3/ASY1 colocalization showed that the ASY3 signal were more diffuse than ASY1 at zygotene, suggesting that *Ath1.1-1* loss imbed ASY1 and ASY3 proper polymerization, suggesting a role for histone *Ath1.1-1* in preserving the meiotic chromosome axes through directing ASY1 and ASY3 proper loading on the axes and or affecting chromosome organization required to permit ASY1 and or ASY3 to polymerize. On the other hand AtZYP1 signal showed that cells were able to show more normal linear polymerisation at pachytene comparable to ASY1 signal, but cells showed that AtZYP1 signal do not polymerize fully along the axes as some regions were AtZYP1 signal-free. Moreover, some pachytene cells showed ASY1/ZYP1 full co-localization, a thing which never seen in the wild-type pachytenes. The link between linker histones and meiotic chromosome axes proteins were never

addressed before in other species, which makes this research unique in its results from one side, and it opens the gate wide for similar analysis to be carried out on plants as well as animals to be able to understand the role of histone H1 variants on the organisation of meiotic chromosome. A recent study on the *Arabidopsis* pachytene checkpoint AtPCH2 showed a link between chromosome axes remodelling and CO formation. *Atpch2* mutants showed reduction in COs resulted from synapsis defects at early prophase I. Interestingly, *Atpch2* mutants showed ASY1-ZYP1 proteins colocalization at pachytene stage, suggesting that, may be, delayed ASY1 loading on the meiotic chromosome axis, impedes the proper spatial homologous axis organization required for the programmed recombination machinery to progress normally (Personal communication with C.FK).

Moreover, previously it was reported that lack of ASY1 in *Arabidopsis* affected the maintenance of DMC1 association with the chromosome axes during prophase I, which reduces the ability of homologous chromosomes recombination (Sanchez-Moran *et al.*, 2007). Similarly, it was observed that *Ath1.1-1* mutant showed reduction in the DMC1 foci in the early prophase I comparable to the wild-type. The reduced DMC1 foci and the diffuse ASY1 signal at zygotene-pachytene suggest that AtH1.1-1 is needed for proper ASY1 polymerization and DMC1 stabilization. A time course labelling BrdU analysis of the DMC1 foci in the *Ath1.1-1* mutant could show if the AtH1.1-1 loss affects temporal DMC1 stabilization on the axes or not (Sanchez-Moran *et al.*, 2007).

6.3.5. AtH1.1 is needed for proper COs

The asynaptic phenotype observed in the *Ath1.1* mutants; *Ath1.1-1*, *Ath1.1-2*, and *h1.1^{RNAi}*, indicated a possible inter-homologue recombination defect. This was confirmed as meiocytes showed reduction in COs as early as diakinesis, expressed as early univalents. Chiasmata frequency quantification at metaphase I in all of the *Ath1.1* mutants showed significant reduction. Moreover, immunolocalization analysis of the recombination proteins in the *Ath1.1-1* mutants revealed defects in their foci numbers comparable to wild-type. Significant reduction was recorded in the foci of *Arabidopsis* recombination proteins; AtDMC1, AtMSH4 and AtMLH3, comparable to wild-type, a thing which confirms *AtH1.1* role in preserving normal COs. Interestingly, the *Ath1.1-1* showed ~10% COs per nuclei, which is somehow so close to the 1.39 COs per meiocyte recorded in the *Arabidopsis asy1* mutant (Sanchez-Moran *et al.*, 2001), suggesting a link between the linker histone AtH1.1-1 protein presence and ASY1 proper loading and or polymerization on the chromosome axes. Furthermore, *Ath1.1-1* mutant show diffuse ASY1 localization. Moreover, it was reported that *asy1* mutants have unstable DMC1 foci (Sanchez-Moran *et al.*, 2007). DMC1 is vital for COs formation since *dmc1* mutants showed chiasma-free chromosomes (univalent) at metaphase I (Couteau *et al.*, 1999).

6.4. Overview of chromatin associated-histones and chromatin

Analysis of histone mutants; *Ath1.1* and *Ath4^{RNAi}* showed that both AtH1.1-1 and AtH4 have a vital role in preserving the vegetative as well as the reproductive phases of the cell. Developmental defects, represented as changed growth rate, altered plant size and change in flower bud appearance rate, were linked with aberrant mitosis. However, lower seed production resulted from abnormal meiosis.

Cytological assessment of the chromosomes phenotype within *Arabidopsis* linker histone mutants (*Ath1.1*) showed chromosome compaction defects, resembled as longer and less compact mitotic chromosomes, similarly, to H1-depleted mitotic chromosomes in *Xenopus leavis* (Maresca *et al.*, 2005) Interestingly, it was reported that “linker histone binding to nucleosomal arrays in vitro causes linker DNA to form an apposed stem motif, which stabilizes extensively folded secondary chromatin structures, and promotes self-association of individual nucleosomal arrays into oligomeric tertiary chromatin structures” (Lu and Hansen, 2004). Moreover, analysis of condensation ability of linker histones with mutation in the recombinant mouse linker H C-terminus indicated that its function is due to specific amino acids subdomains (Lu and Hansen, 2004). And that these domains show “intrinsic disorder” pattern of spreading like that reported previously (Wright and Dyson; 1999; Dunker *et al.*, 2001, 2002). Indicating that proteins with such character show “molten globule-like” characteristics at their original phase (reviewd by Lu and Hansen, 2004) and switch to its structural phase upon their association with cellular macromolecules (reviewd by Lu and Hansen, 2004) and that one domain is able to play a role in different functions by interacting with different cellular components.

Moreover, the aberrant segregation of meiotic chromosomes in the *Ath1.1* mutants were linked with immature chromosome axes-recombination stage, leading to severe consequences on efficient COs formation. It is yet not well understood how could H1 preserve/stabilize the chromosome axis further cytological and biochemical analysis (as discussed in 4.5.2) will help in resolving its mysterious role in chromatin compaction associated with axes formation dynamics.

On the other hand, the *Ath4*^{RNAi} mutants fragmented chromatin at the rDNA sites clarified H4 role in protecting the nucleolus rDNA content integrity.

6.5. Future work

6.5.1. Core histone H4

Analysis of the *Ath4*^{RNAi} mutants suggests a role for histone H4 in maintaining the organization of the rDNA region during meiosis in *Arabidopsis*. Moreover, the possibility that the defect observed in *Ath4*^{RNAi} mutants arise from constrains in the nucleosome structure, due to loss in its constituents rather than histone H4 mere loss, hence, analysis of NAP (histone chaperone) should be done to analyse if the loss of nucleosomes on the nuclei by other means could produce the same phenotype. Thus, analysing corresponding *nap* mutants will broaden our view about nucleosome specific role within the meiotic chromatin landscape.

The chromosome fragmentation phenotype observed in the *Ath4*^{RNAi} mutants address a very important question, this fragmentation is originated by the wrong repair of DSBs during meiosis. These DSBs could be Spo11-dependent, and to reiterate this, we would need to cross the *Ath4*^{RNAi} line with a null *Atspo11* mutant (*spo11.1* or *spo11.2*). Then if the *Atspo11xAth4*^{RNAi} double mutant is still showing fragmentation, then these breaks would be SPO11 independent probably originated by DNA replication errors. DNA replication errors can be repair by producing DSBs and problems on the repair of these could lead to the chromatin fragmentation observed during meiosis. In order to check if H4 depletion interfere with the proper

DSBs DNA repair pathways like for example the homologous recombination pathway we could analysed *Atdmc1xAth4^{RNAi}* and *Atrad51xAth4^{RNAi}* double mutants.

Furthermore, immunolocalization analysis using Anti-H4 antibodies to study H4 behaviour in the wild-type plants will help to understand its role within chromatin context. Since H4 acetylation and methylation was addressed to play a role in chromosome organization and recombination in other species, so the usage of antibodies to recognised acetylated and methylated forms of histone H4 to investigate further the defects observed in the *Ath4^{RNAi}* mutants as well as *caf1* mutants.

6.5.2. Linker histone H1

On the other hand, the chromosome axes and architecture defects linked to the *Ath1.1* mutation should be further analysed. Homologues pairing and synaptonemal complex (SC) formation is highly important for proper meiotic recombination, chromosome segregation and the formation of viable gametes. Our analysis of *Ath1.1* mutants have showed defects in the chromatin localization of ASY1 (meiotic chromosome axis/SC lateral element component) and ZYP1 (SC central element component). Thus there are some further questions that come to our mind; 1) Does histone AtH1.1 affect proper axes formation spatially or on a time-point bases during meiosis? 2) Is histone AtH1.1 needed to stabilize ASY1 localization directly or indirectly (e.g through ASY3)? Are the defects observed in the *Ath1.1* mutants arise from H1 loss/absence, or it happened because of the changes in the global amount

of H1 posttranslational modifications? Furthermore, the ~90% COs reduction in the *Ath1.1-1* mutants coupled with severe reduction of DMC1, MSH4 and MLH1 foci localization on the chromosome axes, whereas RAD51 and γ H2AX signals are similar to the WT, suggests that AtH1.1 might be needed to stabilize homologues recognition intermediates by either preserving the homologues sequences in a structural physical pattern to allow their 2nd end invasion mediated by DMC1 continuation or by affecting DMC1-axes stability (Sanchez-Moran et al., 2007). Hence, it would be very important to develop specific antibodies to recognise the histone AtH1.1, and/or produced recombinant proteins tagged with a fluorescent protein like GFP (AtH1.1-GFP) and analysed the exact localisation of AtH1.1 *in vivo* and its relation with the chromosome axes as well as with the meiotic recombination machinery. Moreover, the conjugation of immunolocalization for the chromosome axes (ASY1, ASY3, ZYP1) and meiotic recombinases (DMC1) with BrdU or EdU labelling experiments in both *Ath1.1-1* mutant and WT would show if the discontinuous axes defects observed in the *Ath1.1-1* is caused by either delayed axis-proteins spatial loading, or as a result of destabilised axes formation which could cause unstable chromatin structures with lower efficiency in responding to the meiotic-programmed recombination machinery. Furthermore, AtH1.1 protein extraction from plant tissues, particularly meiocytes, would allow us to carry out immune-precipitation (IPs) experiments which could add further insights on the associations of AtH1.1 with other proteins, and would allow us a better understanding of the AtH1.1 role in the nuclear chromatin context. Moreover, analysis of the AtH1.1 epigenetic modifications could help us to understand the dynamics of AtH1.1 during different nuclear stages and its multiprotein associations.

6.6. Conclusions

- This research has led new insights into the roles of H1 linker histones and H4 nucleosome core histone in preserving chromosome structure and functional genome integrity in *Arabidopsis*.
- The *Arabidopsis* genome possesses eight histone H4 loci expressing equally and ubiquitously at all different stages of the plant development. These eight loci encode for histone H4 proteins with identical amino acid sequence that is only 2 amino acids different from that in the human H4 histone.
- The use of RNAi technology has allowed us to analyse an *Ath4*^{RNAi} knock-down mutant line which showed different phenotypes:
 - Mutant plants presented an early flowering time development with respect to the wildtype.
 - Mutant plants were semi-sterile, with a significant reduction in the number of seeds per silique (fruit/seed pod) due to meiotic errors.
 - Mutant plants presented chromosome fragmentation on early prophase I meiotic stages (Zygotene/Pachytene) and chromosome connections between non-homologous chromosomes. These connections produced chromosome missegregation after anaphase I.
 - The fragmented and non-homologous connected regions were mostly affecting the repeated sequences of the 45S and 5S rDNA and therefore the Nucleolus Organising Regions (NORs) on the

chromosomes suggesting a defect in the repair of DSBs on these highly repeated sequences among the *Arabidopsis* genome.

- The characterisation of *Arabidopsis* mutants for CAF1 chaperon subunits AtFAS1 and AtFAS2 has shown that the rDNA regions in *Arabidopsis* are also affected suggesting that H4 presence and dynamics on the nucleosomes are highly important for maintaining the integrity of these regions in *Arabidopsis*.
- We have also carried out a characterization of all the different histone linker H1 proteins presented in *Arabidopsis*. Some of these H1 isoform mutants (*Ath1b*, *Ath1c*, *Ath1.1-1*, *Ath1.2*, *Ath1.3*, *Athon4*, and *Athon5*) presented a delayed patterning in the flowering time, suggesting that these histone H1 isoforms might have important effects on the regulation of flower development.
- The cytological analysis of mitotic cells in the *Ath1.1* mutants showed us abnormal mitotic metaphase chromosome condensation compared to wild-type chromosomes presenting longer chromosomes than the WT which in some cases delayed the mitotic divisions and translated on some mitotic aberrations like anaphase bridges. Some plants presented a dwarf vegetative growth probably as a consequence of this mitotic errors.
- *Ath1.1* mutants presented different levels of plant semi-sterility. A cytological analysis of meiotic stages showed different errors:
 - Chiasma frequency was highly reduced on null mutant *Ath1.1-1*.

- A significant reduction on the number of loci for meiotic recombinase AtDMC1 and later recombination machinery AtMSH4 and AtMLH1 was observed in the null mutant *Ath1.1-1*.
 - Fully synapsis was not properly completed on *Ath1.1-1* mutant. ZYP1 polymerization showed abnormal pattern, ASY1 signal is diffused on the chromatin and does not seem to localise to the meiotic chromosome axis suggesting that the meiotic axis are not properly assemble on the mutant.
-
- Histone linker isoform AtH1.1 seems to be highly important for the assembling of the meiotic chromosome axis and thus for the proper pairing, synapsis and crossover formation during meiotic prophase I.
 - Our results could be further analysed in order to obtain different tools to allow plant breeders to manipulate meiotic recombination to generate new combination of agronomically interesting genes in different plant crops.

CHAPTER 7

REFERENCES

- Adolph, K.W., Cheng, S.M. and Laemmli, U.K.** (1977). Electron microscopic observation on whole mount mitotic human chromosomes. *J Anat*, **103**: 143-150.
- Agalioti, T., Chen, G. and Thanos, D.** (2002) Deciphering the transcriptional histone acetylation code for a human gene. *Cell*, **111**: 381–392.
- Ahmad, K. and Henikoff, S.** (2002a) Histone H3 variants specify modes of chromatin assembly. *Proc Natl Acad Sci*, **99** (Suppl 4): 16477–16484.
- Ahmad, K. and Henikoff, S.** (2002) The histone variant H3.3 marks active chromatin by replication-independent nucleosome assembly. *Mol Cell*, **9**: (6):1191-200.
- Akey, C.W. and Luger, K.** (2003) Histone chaperones and nucleosome assembly. *Curr Opin Struct Biol*, **13**: 6–14.
- Alani, E., Thresher, R., Griffith, J.D. and Kolodner, R.D.** (1992) Characterization of DNA-binding and strand-exchange stimulation properties of γ -RPA, a yeast single-strand-DNA-binding protein. *J Mol Biol*, **227**: 54-71.
- Albig, W., Meergans, T. and Doenecke, D.** (1997) Characterisation of the H1.5 gene completes the set of H1 subtype genes. *Gene*, **184**:141-148.
- Alexander, M.P.** (1969) Differential staining of aborted and nonaborted pollen. *Stain Technol*, **44**: (3): 117-122.
- Allan, J., Staynov, D.Z. and Gould, H.** (1980) Reversible dissociation of linker histone from chromatin with preservation of internucleosomal repeat. *Proc Natl Acad Sci USA*, **77**: 885–889.
- Alva, V., Ammelburg, M., Lupas, A.N.** (2007). On the origin of the histone fold. *BMC Struct Biol*, **7**: 17.
- An, W., Leuba, S.H., van Holde, K. and Zlatanova, J.** (1998) Linker histone protects linker DNA on only one side of the core particle and in a sequence-dependent manner. *Proc Natl Acad USA*, **95**: 3396-3401.
- An, W., van Holde, K. and Zlatanova, J.** (1998) Linker histone protection of chromatosomes reconstituted on 5S rDNA from *Xenopus borealis*: a reinvestigation. *Nucleic Acids Res*, **26**: 4042-4046.
- Anderson, L.K., Hooker, K.D. and Stack, S.M.** (2001) The distribution of early recombination nodules on zygotene bivalents from plants. *Genetics*, **159**: 1259–1269.
- Anderson, L.K. and Stack, S.M.** (2005) Recombination nodules in plants. *Cytogenet Genome Res*, **109**:198–204.
- Annunziato, A.** (2008) DNA packaging: Nucleosomes and chromatin. *Nature Education*, **1**: (1): 26.
- Arents, G., Burlingame, R.W., Wang, B.C., Love, W.E. and Moudrianakis, E.N.** (1991) The nucleosomal core histone octamer at 3.1 Å resolution: a tripartite protein assembly and a left-handed superhelix. *Proc Natl Acad Sci U S A*, **88**: (22):10148-52.
- Arents, G. and Moudriankis, E.N.** (1993) Topography of the histone octamer surface: repeating structural motifs utilized in the docking of nucleosomal DNA. *Proceedings of the National Academy of Science of the USA*, **90**: 10489-10493.
- Argueso, J.L., Kijas, A.W., Sarin, S., Heck, J., Waase, M. and Alani, E.** (2003) Systematic mutagenesis of the *Saccharomyces cerevisiae* MLH1 gene reveals distinct roles for Mlh1p in meiotic crossing over and in vegetative and meiotic mismatch repair. *Mol Cell Biol*, **23**:873–886.

- Armstrong, S.J., Caryl, A.P., Jones, G.H. and Franklin, F.C.** (2002) Asy1, a protein required for meiotic chromosome synapsis, localizes to axis-associated chromatin in *Arabidopsis* and *Brassica*. *J Cell Sci*, **115**: 3645-3655.
- Armstrong, S.J., Franklin, F.C.H. and Jones, G.** (2001) Nucleolus-associated telomere clustering and pairing precede meiotic chromosome synapsis in *Arabidopsis thaliana*. *J. Cell Sci.* **114**: 4207-4217.
- Armstrong, S.J., Franklin, F.C.H. and Jones, G.H.** (2003) A meiotic time-course for *Arabidopsis thaliana*. *Sexual Plant Reproduction*, **16**: (3): 141-149.
- Armstrong, S.J. and Jones, G.H.** (2003) Meiotic cytology and chromosome behaviour in wild-type *Arabidopsis thaliana*. *J Exp Bot*, **54**: (380): 1-10.
- Armstrong, S.J. and Jones, G.H.** (2001) Female meiosis in wild-type *Arabidopsis thaliana* and in two meiotic mutants. *Sex Plant Reprod*, **13**: 177–183.
- Aubin, R.J., Dam, V.T., Miclette, J., Brousseau, Y., Huletsky, A. and Poirier, G.G.** (1982) Hyper (ADP-ribosyl)ation of histone H1. *Can J Biochem*, **60**: 1085-1094.
- Ausio, J. and Abbott, D.W.** (2004) The role of histone variability in chromatin stability and folding. Amsterdam, the Netherlands. Elsevier, vol. 39. Elsevier, Amsterdam, The Netherlands
- Axel, R., Melchior, W.J.R., Sollner-Webb, B. and Felsenfeld, G.** (1974) Specific Sites of Interaction Between Histones and DNA in Chromatin. *Proc Nat Acad Sci USA*, **71**: (10): 4101-4105.
- Bai, X., Peirson, B.N., Dong, F., Xue, C. and Makaroff, C.A.** (1999) Isolation and characterisation of SYN1 a RAD21-like gene essential for meiosis in *Arabidopsis*. *Plant Cell*, **11**: (3): 417-430.
- Bakkenist, C.J. and Kastan, M.B.** (2003) DNA damage activates ATM through intermolecular autophosphorylation and dimer dissociation. *Nature*, **421**: (6922):499–506.
- Bannister, L.A., Reinholdt, L.G., Munroe, R.J. and Schimenti, J.C.** (2004) Positional cloning and characterization of mouse mei8, a disrupted allele of the meiotic cohesin Rec8. *Genesis*, **40**, 184-194.
- Barra, J.L., Rhounm, L., Rossigmol, J.L. and Faugeron, G.** (2000) Histone H1 is dispensable for methylation-associated gene silencing in *Ascobolus immerses* and essential for long life span. *Mol Cell Biol*, **20**:61-69.
- Barrett, T. and Gould, H.J.** (1973) Tissue and species specificity of non-histone chromatin proteins. *Biochem Biophys Acta*, **294**: 165-170.
- Bass, H.W., Bordoli, S.J. and Foss, E.M.** (2003) The desynaptic (dy) and desynaptic1 (dys1) mutations in maize (*Zea mays* L.) cause distinct telomere-misplacement phenotypes during meiotic prophase. *Journal of Experimental Botany*, **54**: 39–46.
- Bass, H.W., Riera-Lizarazu, O., Ananiev, E.V., Bordoli, S.J., Rines, H.W., Phillips, R.L., Sedat, J.W., Agard, D.A. and Cande, W.Z.** (2000) Evidence for the coincident initiation of homolog pairing and synapsis during the telomere-clustering (bouquet) stage of meiotic prophase. *J Cell Sci*, **113** (Pt 6): 1033-1042.
- Bassett1, A., Cooper, S., Wu, C. and Travers, A.** (2009) The folding and unfolding of eukaryotic chromatin. *Current Opinion in Genetics & Development*, **19**: 159-165.
- Beadle, G.W.** (1930) Genetic and cytological studies of a Mendelian asynaptic in *Zea mays*. *Cornell Agriculture Experimental Station Memorandum*, **129**: 1–23.

Belayev, N.D., Keohane, A.M. and Turner, B.M. (1996). Differential underacetylation of histones H2A, H3, and H4 on the inactive X chromosome in human female cells. *Hum Genet*, **97**: 573–578.

Belmont, A.S. (2006) Mitotic chromosome structure and condensation. *Current Opinion in Cell Biology*, **18**: (6):632-638.

Bendar, J., Horowitz, R.A., R.A., Grigoryev, S.A., Carruthers, L.M., Hansen, J.C., Koster, A.J. and Woodcock, C.L. (1998) Nucleosomes, linker DNA, and linker histone form a unique structural motif that directs the higher-order folding and compaction of chromatin. *Proc Natl Acad Sci USA*, **95**: 14173-14178.

Bennett, M.D., Leitch, I.J., Price, H.J. and Johnston, J.S. (2003) Comparisons with *Caenorhabditis* (100 Mb) and *Drosophila* (175 Mb) using Flow Cytometry shows genome size in *Arabidopsis* to be 157 Mb and thus 25% larger than the *Arabidopsis* genome initiative estimate of 125 Mb. *Annals of Botany*, **91**: (5): 547-557.

Berchowitz, L.E. and Copenhaver, G.P. (2008) Fluorescent *Arabidopsis* tetrads: a visual assay for quickly developing large crossover and crossover interference data sets. *Nat Protoc*, **3**: 41-50.

Berchowitz, L.E., Francis, K.E., Bey, A.L. and Copenhaver, G.P. (2007) The role of AtMUS81 in interference-insensitive crossovers in *A.thaliana*. *PLoS Genet*, **3**: 1355-1364.

Berchowitz, L.E., Hanlon, S.E., Lieb, J.D. and Copenhaver, G.P. (2009) A positive but complex association between meiotic double-strand break hotspots and open chromatin in *Saccharomyces cerevisiae*. *Genome Res*, **19**: 2245-2257.

Berger, S.L. (2002) Histone modifications in transcriptional regulation. *Curr Opin Genet Dev*, **12**: 142–148.

Berkowitz, E.M. and Riggs, E.A. (1981) Characterization of rat liver oligonucleosomes enriched in transcriptionally active genes: evidence for altered base composition and a shortened nucleosome repeat. *Biochemistry*, **20**: 7284- 7290.

Bhatt, A.M., Lister, C., Page, T., Fransz, P., Findlay, K., Jones, G.H., Dickinson, H.G. and Dean, C. (1999). The DIF1 gene of *Arabidopsis* is required for meiotic chromosome segregation and belongs to the REC8/RAD21 cohesin gene family. *Plant J*, **19**: 463-472.

Bhattacharjee, R.N., Banks, G.C., Trotter, K.W., Lee, H.L. and Archer, T.K. (2001) Histone H1 phosphorylation by Cdk2 selectively modulates mouse mammary tumor virus transcription through chromatin remodeling. *Mol Cell Biol*, **21**: 5417-25.

Bird, A.W., Yu, D.Y., Pray-Grant, M.G., Qiu, Q., Harmon, K.E., Megee, P.C., Grant, P.A., Smith, M.M., Christman, M.F. (2002) Acetylation of histone H4 by Esa1 is required for DNA double-strand break repair. *Nature*, **419**: 411–415.

Birkenbihl, R.P. and Subramani, S. (1995). The rad 21 gene product of *Schizosaccharomyces pombe* is a nuclear, cell cycle-regulated phosphoprotein. *J Biol Chem*, **270**: 7703-7711.

Bishop, D.K., Park, D., Xu, L. and Kleckner, N. (1992) DMC1: a meiosis-specific yeast homolog of *E. coli* recA required for recombination, synaptonemal complex formation, and cell cycle progression. *Cell*, **69**: (3): 439-456.

Bishop, D.K. and Zickler, D. (2004) Early decision; meiotic crossover interference prior to stable strand exchange and synapsis. *Cell*, **117**: (1): 9-15.

Blat, Y., Protacio, R.U., Hunter, N. and Kleckner, N. (2002) Physical and functional interactions among basic chromosome organizational features govern early steps of meiotic chiasma formation. *Cell*, **111**: 791-802.

- Bleuyard, J.Y., Gallego, M.E., Savigny, F. and White, C.I.** (2005) Differing requirements for the Arabidopsis Rad51 paralogs in meiosis and DNA repair. *Plant J*, **41**: 533-545.
- Bleuyard, J.Y., Gallego, M.E. and White, C.I.** (2004) Meiotic defects in the Arabidopsis rad50 mutant point to conservation of the MRX complex function in early stages of meiotic recombination. *Chromosoma*, **113**, 197-203.
- Bleuyard, J.Y. and White, C.I.** (2004) The Arabidopsis homologue of Xrcc3 plays an essential role in meiosis. *EMBO J*, **23**: 439-449.
- Boddu J, Cho S, Kruger WM, Muehlbauer GJ.** (2006) Transcriptome analysis of the barley–Fusarium graminearum interaction. *Mol Plant Microbe Interact.* **19**: 407–417.
- Boggs, B.A., Allis, C.D. and Chinault, A.C.** (2000) Immunofluorescent studies of human chromosomes with antibodies against phosphorylated H1 histone. *Chromosoma*, **108**: 485-490.
- Borde, V., Robine, N., Lin, W., Bonfils, S., Geli, V. and Nicolas, A.** (2009) Histone H3 lysine 4 trimethylation marks meiotic recombination initiation sites. *EMBO J*, **28**: 99-111.
- Borner, G.V., Barot, A. and Kleckner, N.** (2008) Yeast Pch2 promotes domainal axis organization, timely recombination progression, and arrest of defective recombinosomes during meiosis. *P Natl Acad Sci USA*, **105**: 3327-3332.
- Borner, G.V., Kleckner, N. and Hunter, N.** (2004) Crossover/noncrossover differentiation, synaptonemal complex formation, and regulatory surveillance at the leptotene/zygotene transition of meiosis. *Cell*, **117**: 29-45.
- Briggs, G.C., Osmont, K.S., Shindo, C., Sibout, R. and Hardtke, C.S.** (2006) Unequal genetic redundancies in *Arabidopsis*- a neglected phenomenon? : *TRENDS in Plant Science*, **11**: (10): 492-498; doi: 10.1016/j.tplants.2006.08.005
- Brzeski, J., and Jerzmanowski, A.** (2003) Deficient in DNA methylation 1 (DDM1) defines a novel family of chromatin remodeling factors. *J Biol Chem*, **278**: 823–828.
- Bruno, M., Flaus, A., Stockdale, C., Rencurel, C. and Ferreira, H.** (2003) Histone H2A/H2B dimer exchange by ATP dependent chromatin remodeling activities. *Mol Cell*, **12**: 1599–1606.
- Budhavarapu, V.N., Chavez, M. and Tyler, J.K.** (2013) How is epigenetic information maintained through DNA replication. *Epigenetics & Chromatin*, **6**:32.
- Bundock, P. and Hooykaas, P.** (2002) Severe developmental defects, hypersensitivity to DNA-damaging agents, and lengthened telomeres in Arabidopsis MRE11 mutants. *Plant Cell*, **14**: 2451-2462.
- Bustin, M., Catez, F., Lim, J-H.** (2005) The Dynamics of Histone H1 Function in Chromatin. *Molecular Cell*, **17**: 617–620.
- Butler, D.K.** (1992) Ribosomal DNA is a site of chromosome breakage in aneuploid strains of *Neurospora*. *Genetics*, **131**: 581–592.
- Buzek, J., Riha, K., Siroky, J., Ebert, I., Greilhuber, J. and Vyskot, B.** (1998) Histone H4 underacetylation in plant facultative heterochromatin. *Biol. Chem*, **379**: 1235-1241.
- Cai, X., Dong, F., Edelman, R.E. and Makaroff, C.A.** (2003) The Arabidopsis SYN1 cohesin protein is required for sister chromatid arm cohesion and homologous chromosome pairing. *J Cell Sci*, **116**: 2999-3007.

- Cairns, B.R., Lorch, Y., Li, Y., Zhang, M., Lacomis, L., Erdjument-Bromage, H., Tempst, P., Du, J., Laurent, B., Kornberg R.D.** (1996) RSC, an essential, abundant chromatin-remodeling complex. *Cell*, **87**: 1249–1260.
- Caldecott, K.W.** (2003) XRCC1 and DNA strand break repair. *DNA Repair* (Amsterdam) **2**: 955–969.
- Cam, H.P., Sugiyama, T., Chen, E.S., Chen, X., FitzGerald, P.C. and Grewal, S.I.S.** (2005) Comprehensive analysis of heterochromatin- and RNAi-mediated epigenetic control of the fission yeast genome. *Nat Genet*, **37**: 809–819.
- Camporeale, G., Oommen, A.M., Griffin, J.B., Sarath, G. and Zemleni, J.** (2007) K12-biotinylated histone H4 marks heterochromatin in human lymphoblastoma cells. *J Nutr Biochem*, **18**: (11):760–8.
- Camporeale, G., Shubert, E.E., Sarath, G., Cerny, R. and Zemleni, J.** (2004) K8 and K12 are biotinylated in human histone H4. *Eur J Biochem*, **271**: 2257–2263
- Carmen, A.A., Milne, L. and Grunstein, M.** (2002) Acetylation of the yeast histone H4 N terminus regulates its binding to heterochromatin protein SIR3. *J Biol Chem*. **277**: 4778–4781.
- Carpenter, A.T.** (1975) Electron microscopy of meiosis in *Drosophila melanogaster* females: II. The recombination nodule—a recombination-associated structure at pachytene? *P Natl Acad Sci USA*, **72**: 3186–3189.
- Caryl, A.P., Armstrong, S.J., Jones, G.H. and Franklin, F.C.H.** (2000) A homologue of the yeast HOP1 gene is inactivated in the *Arabidopsis* meiotic mutant *asy1*. *Chromosoma*, **109**: 62–71.
- Catez, F., Yang, H., Tracey, KJ, Reeves, R., Misteli, T. and Bustin, M.** (2004) Network of dynamic interactions between histone H1 and high-mobility-group proteins in chromatin. *Moll Cell Biol*, **24**:4321–4328.
- Celerin, M., Merino, S.T., Stone, J.E., Menzie, A.M. and Zolan, M.E.** (2000) Multiple roles of Spo11 in meiotic chromosome behavior. *EMBO J*, **19**, 2739–2750.
- Chai, B., Huang, J., Cairns, B.R., Laurent, B.C.** (2005) Distinct roles for the RSC and Swi/Snf ATP-dependent chromatin remodelers in DNA double-strand break repair. *Genes Dev*, **19**: 1656–1661.
- Chan, R.C., Severson, A.F. and Meyer, B.J.** (2004) Condensin restructures chromosomes in preparation for meiotic divisions. *J Cell Biol*, **167**: 613–625.
- Chang, L., Loranger, S.S., Mizzen, C., Ernst, S.G., Allis, C.D. and Annunziato, A.T.** (1997) Histones in transit: cytosolic histone complexes and diacetylation of H4 during nucleosome assembly in human cells. *Biochemistry*, **36**: 469–480.
- Chaubet N., Clement, B. and Gigot, C.** (1992) Genes encoding a histone H3.3-like variant in *Arabidopsis* contain intervening sequences. *J Mol Biol*, **225**: 569–574.
- Chelysheva, L.** (2005) AtREC8 and AtSCC3 are essential to the monopolar orientation of the kinetochores during meiosis. *Journal of Cell Science*, **118**: (20): 4621–4632.
- Cheung, W.L., Briggs, S.D. and Allis, C.D.** (2000). Acetylation and chromosomal functions. *Curr Opin Cell Biol*, **12**: 326–333.
- Cimini, D., Mattiuzzo, M., Torosantucci, L. and Degrossi, F.** (2003) Histone hyperacetylation in mitosis prevents sister chromatid separation and produces chromosome segregation defects. *Molecular Biology of the Cell*, **14**: 3821–3833,

- Clavente, A., Viera, A., Page, J., Parra, M.T., Gomez, R., Suja, J.A., Rufas, J.S. and Santos, J.L.** (2005) DNA double-strand breaks and homology search: inferences from a species with incomplete pairing and synapsis. *J Cell Sci*, **118**: 2957-2963.
- Clore, G.M., Gronenborn, A.M., Nilges, M., Sukumaran, D.K. and Zarbock, J.** (1987) The polypeptide fold of the globular domain of histone H5 in solution. A study using nuclear magnetic resonance, distance geometry and restrained molecular dynamics. *EMBO J*, **6**: 1833-1842.
- Clough, S.J. and Bent, A.F.** (1998) Floral dip: a simplified method for *Agrobacterium*-mediated transformation of *Arabidopsis thaliana*. *Plant J*, **16**: (6): 735-743.
- Cnudde, F. and Gerats, T.** (2005) Meiosis: inducing variation by reduction. *Plant Biol (Stuttg)*, **7**: 321-341.
- Copenhaver, G.P., Browne, W.E. and Preuss, D.** (1998) Assaying genome-wide recombination and centromere functions with *Arabidopsis* tetrads. *P Natl Acad Sci USA*, **95**: 247-252.
- Conrad, M.N., Lee, C.Y., Chao, G., Shinohara, M., Kosaka, H., et al.,** (2008) Rapid telomere movement in meiotic prophase is promoted by NDJ1, MPS3, and CSM4 and is modulated by recombination. *Cell*, **133**: 1175–1187.
- Corsini, L. and Sattler, M.** (2007) Tudor hooks up with DNA repair. *Nature Structural & Molecular Biology* **14**: 98 – 99.
- Costelloea, K., FitzGerald, J., Murphya, N.J., Flausb, A. and Lowndesa, N.F.** (2006) Chromatin modulation and the DNA damage response. *Experimental Cell Research*, **312**: (14): 2677-2686.
- Cota, P., Shafa, M. and Rancourt, E.** (2013) Stem cells and epigenetic reprogramming, pluripotent stem cells, Dr. Deepa Bhartiya (Ed.), ISBN: 978-953-51-1192-4, InTech, DOI: 10.5772/55983.
- Couteau, F., Belzile, F., Horlow, C., Grandjean, O., Vezon, D. and Doutriaux, M.P.** (1999) Random chromosome segregation without meiotic arrest in both male and female meiocytes of a *dmc1* mutant of *Arabidopsis*. *Plant Cell*, **11**: 1623-1634.
- Couture, J.F., Collazo, E., Brunzelle, J.S. and Trievel, R.C.** (2005) Structural and functional analysis of SET8, a histone H4 Lys-20 methyltransferase. *Genes Dev.* **19**, 1455-1465.
- Cox, M; Nelson, D. R. and Lehninger, A. L.** (2005) Lehninger principles of biochemistry. San Francisco: WH Freeman. ISBN, 0:7167-4339-6.
- Crevillen, D. and Dean, C.** (2011) Regulation of the floral repressor gene FLC: the complexity of transcription in a chromatin context. *Current Opinion in Plant Biology*, **14**:38-44.
- Dai, J., Sultan S., Taylor, S.S. and Higgins,J.M.** (2005) The kinase haspin is required for mitotic histone H3 Thr 3 phosphorylation and normal metaphase chromosome alignment. *Genes Dev*, **19**: 472-488.
- Daniel, K., Lange, J., Hached, K., Fu, J., Anastassiadis, K., Roig, I., Cooke, H.J., Stewart, A.F., Wassmann, K., Jasin, M., Keeney, S. and Toth, A.** (2011) Meiotic homologue alignment and its quality surveillance are controlled by mouse HORMAD1. *Nat Cell Biol*, **13**: 599-610.
- Davey, C.A., Sargent, D.F. and Luger, K.** (2002) Solvent mediated interactions in the structure of the nucleosome core particle at 1.9 a resolution. *Journal of Molecular Biology*, **319**: (5): 1097-1113.
- De, S., Brown, D.T., Lu, Z.H., Leno, G.H., Wellman, S.E. and Sittman, D.B.** (2002) Histone H1 variants differentially inhibit DNA replication through an affinity for chromatin mediated by their carboxyl-terminal domains. *Gene*, **292**: (1-2):173-81.

- de Boer, E., Stam, P., Dietrich, A.J., Pastink, A. and Heyting, C.** (2006) Two levels of interference in mouse meiotic recombination. *Proc Natl Acad Sci USA*, **103**:9607–9612.
- de los Santos, T., Hunter, N., Lee, C., Larkin, B., Loidl, J. and Hollingsworth, N.M.** (2003) The Mus81/Mms4 endonuclease acts independently of double holliday junction resolution to promote a distinct subset of crossovers during meiosis in budding yeast. *Genetics*, **164**: 81-94.
- De Muyt, A., Pereira, L., Vezon, D., Chelysheva, L., Gendrot, G., Chambon, A., Laine-Choinard, S., Pelletier, G., Mercier, R., Nogue, F. and Grelon, M.** (2009) A high throughput genetic screen identifies new early meiotic recombination functions in *Arabidopsis thaliana*. *PLoS Genet*, **5**: (9): e1000654.
- Deal, R.B. and Henikoff, S.** (2010) Capturing the dynamic epigenome. *Genome Biology*, **11**:218.
- Dej, K.J. and Orr-Weaver, T.L.** (2000). Separation anxiety at the centromere. *Trends Cell Biol*, **10**:392-399.
- Dernburg, A.F., McDonald, K., Moulder, G., Barstead, R., Dresser, M. and Villeneuve, A.M.** (1998) Meiotic recombination in *C-elegans* initiates by a conserved mechanism and is dispensable for homologous chromosome synapsis. *Cell*, **94**: 387-398.
- Derenburg, A.F., Sedat, J.W., and Hawley, R.S.** (1996) Direct evidence of a role for heterochromatin in meiotic chromosome segregation. *Cell*, **86**: 136–146.
- Dion, E., Li, L., Jean, M. and Belzile, F.** (2007) An *Arabidopsis* MLH1 mutant exhibits reproductive defects and reveals a dual role for this gene in mitotic recombination. *Plant J*, **51**: 431-440.
- Dion, M.F., Altschuler, S.J., Wu, L.F. and Rando, O.J.** (2005) Genomic characterization reveals a simple histone H4 acetylation code. *Proc Natl Acad Sci*. **102**: 5501–5506.
- Dirks, R.H.G., van Dun, C.M.P. and Reinink, K., Rijk Zwaan Zaadteelt en Zaadhandel, B.V.** (2003) Reverse Breeding, WO/2003/017753.
- Dirks, R., van Dun, K., de Snoo, C.B., Berg, M. Vd., Lelivelt, C.L.C., Voermans, W., Woudenberg, L., de Wit, J.P.C., Reinink, K., Schut, J.W., van der Zeeuw, E., Vogelaar, A., Freymark, G., Gutteling, E.W., Keppel, M.N., van Drongelen, P., Kieny, M., Ellul, P., Touraev, A., Ma, H., Jong, H. and Wijnker, E.** (2009) Reverse breeding: a novel breeding approach based on engineered meiosis. *Plant Biotechnology Journal*, **7**: 837–845.
- Dong, A., Zhu, Y., Yu, Y., Cao, K., Sun, C. and Shen, W.H.** (2003) Regulation of biosynthesis and intracellular localization of rice and tobacco homologues of nucleosome assembly protein 1. *Planta*, **216**: 561–570.
- Dou, Y., Mizzen, C.A., Abrams, M., Allis, C.D. and Gorovsky, M.A.** (1999) phosphorylation of linker histone H1 regulates gene expression *in vivo* by mimicking H1 removal. *Mol Cell*, **4**: 641-647.
- Doutriaux, M.P., Couteau, F., Bergounioux, C. and White, C.** (1998) Isolation and characterisation of the RAD51 and DMC1 homologs from *Arabidopsis thaliana*. *Mol Gen Genet*, **257**: 283-291.
- Downey, M., Durocher, D.** (2006) Chromatin and DNA repair: the benefits of relaxation. *Nat Cell Biol*, **8**: 9–10.
- Downs, J.A., Allard, S., Jobin-Robitaille, O., Javaheri, A., Auger, A., Bouchard, N., Kron, S.J., Jackson, S.P., Cote, J.** (2004) Binding of chromatin-modifying activities to phosphorylated histone H2A at DNA damage sites. *Mol Cell*, **16**: 979–990.
- Downs, J.A., Kosmidou, E., Morgan, A. and Jackson, S.P.** (2003) Suppression of homologous recombination by the *Saccharomyces cerevisiae* linker histone. *Mol Cell*, **11**: 1685-1692.

Dunker, A.K., Brown, C.J., and Obradovic, Z. (2002) Identification and functions of usefully disordered proteins. *Adv Protein Chem*, **62**, 25–49.

Dunker, A.K., Brown, C.J., Lawson, J.D., Iakoucheva, L.M., and Obradovic, Z. (2002) Intrinsic disorder and protein function. *Biochemistry* **41**, 6573–6582.

Dunker, A.K., Lawson, J.D., Brown, C.J., Williams, R.M., Romero, P., Oh, J.S., Oldfield, C.J., Campen, A.M., Ratliff, C.M., Hipps, K.W., Ausio, J., Nissen, M.S., Reeves, R., Kang, C., Kissinger, C. R., Bailey, R.W., Griswold, M.D., Chiu, W., Garner, E.C., and Obradovic, Z. (2001) Intrinsically disordered protein. *J Mol Graph Model*. **19**, 26–59.

Dupraw, E. (1966). Macromolecular organization of nuclei and chromosomes; a folded fiber model based on whole mount electron microscopy. *Nature*, **206**: 338-343.

Dupre, A., Boyer-Chatenet, L., Sattler, R.M., Modi, A.P., Lee, J-H., Nicolette, M.L., Kopelovich, L., Jasin, M., Baer, R., Paull, T.T. and Gautier, J. (2008) A forward chemical genetic screen reveals an inhibitor of the Mre11–Rad50–Nbs1 complex. *Nature Chemical Biology*, **4**: 119 – 125.

Earnshaw, W.C., Halligan, B., Cooke, C.A., Heck, M.M. and Liu, L.F. (1985) Topoisomerase II is a structural component of mitotic chromosome scaffolds. *J Cell Biol*, **100**:1706–1715.

Eijpe, M., Offenberg, H., Jessberger, R., Revenkova, E. and Heyting, C. (2003) Meiotic cohesin REC8 marks the axial elements of rat synaptonemal complexes before cohesins SMC1beta and SMC3. *J Cell Biol*, **160**: 657-670.

Einhorn, L.H. (1994) Salvage therapy for germ cell tumors. *Semin Oncol*, **21**: 47–51.

Eirn-Lopez, J.M., Ruiz, M.F., Gonzalez-Tizon, A.M., Martinez, A., Sanchez, L. and Mendez, J. (2004) Molecular evolutionary characterization of the Mussel mytilus histone multigene family: first record of a tandemly repeated unit of five histone genes containing an H1 subtype with “Orphon” features. *J Mol Evol*, **58**:131–144.

Endo, M., Ishikawa, Y., Osakabe, K., Nakayama, S., Kaya, H., Araki, T., Shibahara, K., Abe, K., Ichikawa, H., Valentine, L., Hohn, B., and Toki, S. (2006) Increased frequency of homologous recombination and T-DNA integration in Arabidopsis CAF-1 mutants. *EMBO J*, **25**: 5579–5590.

Espino, P.S., Drohic, B., Dunn KL. and Davie, J.R. (2005) Histone modifications as a platform for cancer therapy. *J Cell Biochem*, **94**: 1088-1102.

Fan, Y., Nikitina, T., Morin-Kensicki, E.M., Zhao, J., and Magnuson, T.R. (2003) H1 linker histones are essential for mouse development and affect nucleosome spacing in vivo. *Mol Cell Biol*, **13**: 4559–4572.

Fan, Y., Nikitina, T., Zhao, J., Fleury, T.J., Bhattacharyya, R., Bouhassira, E.E., Stein, A., Woodcock, C.L. and Skoultchi, A. (2005) Histone H1 depletion in mammals alters global chromatin structure but causes specific changes in gene regulation. *Cell*, **123**: 1199-1212.

Fan, Y., Sirotkin, A., Russell, R.G., Ayala, J. and Skoultchi, A.I. (2001) Individual somatic H1 subtypes are dispensable for mouse development even in mice lacking the H1 replacement subtype. *Mol Cell Biol*, **21**: 7933-7943.

Fang, J., Feng, Q., Ketel, C.S., Wang, H., Cao, R., Xia, L., Erdjument-Bromage, H., Tempst, P., Simon, J. A. and Zhang, Y. (2002) Purification and functional characterization of SET8, a nucleosomal histone H4-lysine 20 specific methyltransferase. *Curr Biol*, **9**: 1086-1099.

Ferdous, M.1., Higgins, J.D., Osman, K., Lambing, C., Roitinger, E., Mechtler, K., Armstrong, S.J., Perry, R., Pradillo, M., Cuñado, N. and Franklin, F.C. (2012) Inter-homolog crossing-over and

synapsis in Arabidopsis meiosis are dependent on the chromosome axis protein AtASY3. *PLoS Genet.* **8**: (2):e1002507. doi: 10.1371/journal.pgen.1002507.

Fernandez-Capetillo, O., Allis, C.D. and Nussenzweig, A. (2004) Phosphorylation of histone H2B at DNA doublestrand breaks. *J Exp Med*, **199**:1671–7.

Fernandez-Capetillo, O., Celeste, A. and Nussenzweig, A. (2003) Focusing on foci: H2Ax and recruitment of DNA-damage response factors. *Cell Cycle*, **2**: 426-427.

Fernandez-Capetillo, O., Lee, A., Nussenzweig, M. and Nussenzweig, A. (2004) H2AX: the histone guardian of the genome. *DNA Repair (Amst)*, **3**: 959–967.

Fernandez-Silva, I., Moreno, E., Eduardo, I., Arus, P., Alvarez, J.M. and Monforte, A.J. (2009) On the genetic control of heterosis for fruit shape in melon (*Cucumis melo L.*). *J Hered*, **100**: 229–235.

Fillingham, J., Keogh, M.C. and Krogan, N.J. (2006) GammaH2AX and its role in DNA double-strand break repair. *Biochem Cell Biol*, **84**: 568-577.

Finch, J.T. and Klug, A. (1976) Solenoidal model for superstructure in chromatin. *Proc Natl Acad Sci U S A*. **73**: (6):1897-901.

Finkel, T. and Holbrook, N.J. (2000) Oxidants, oxidative stress and the biology of ageing. *Nature*, **408**: 239–247.

Finnegan, E.J., Peacock, W.J. and Dennis, E.S. (1996) Reduced DNA methylation in Arabidopsis thaliana results in abnormal plant development. *Proc Natl Acad Sci USA*, **93**: 8449–8454.

Foster, E.R. and Downs, J.A. (2005) Histone H2A phosphorylation in DNA double-strand break repair. *FEBS J*, **272**: 3231–3240.

Fraga, M.F., Ballestar, E., Villar-Garea, A., Boix-Chornet, M., Espada J., Schotta, G., Bonaldi, T., Haydon, C., Roperio, S., Petrie, K., Iyer, N.G., Pérez-Rosado, A., Calvo, E., Lopez, J.A., Cano, A., Calasanz, M.J., Colomer, D., Piris, M.A., Ahn4, N., Imhof, A., Caldas, C., Jenuwein T. and Esteller, M. (2005) Loss of acetylation at Lys16 and trimethylation at Lys20 of histone H4 is a common hallmark of human cancer. *Nature Genetics*, **37**: 391 – 400.

Franklin, A.E., McElver, J., Sunjevaric, I., Rothstein, R., Bowen, B. and Cande, W.Z. (1999) Three-dimensional microscopy of the Rad51 recombination protein during meiotic prophase. *Plant Cell*, **11**: 809-824.

Franklin, A.E., Golubovskaya, I.N., Bass, H.W. and Cande, W.Z. (2003) Improper chromosome synapsis is associated with elongated RAD51 structures in the maize desynaptic2 mutant. *Chromosoma*, **112**: 17–25.

Franklin, F.C.H., Higgins, J.D., Sanchez-Moran, E., Armstrong, S.J., Osman, K.E., Jackson, N. and Jones, G.H. (2006) Control of meiotic recombination in Arabidopsis: role of the MutL and MutS homologues. *Biochem Soc T*, **34**: 542-544.

Fransz, P., Armstrong, S., Alonso-Blanco, C., Fischer, T.C., Torres- Ruiz, R.A., and Jones, G.H. (1998). Cytogenetics for the model system *Arabidopsis thaliana*. *Plant J*, **13**: 867–876.

Freedman, B. S. and Heald, R. (2010) Functional comparison of H1 histones in *Xenopus* reveals isoform-specific regulation by CDK1 and RanGTP. *Current Biology*, **20**: (11): 1048-1052.

Friedberg, E. C. (2003) DNA damage and repair. *Nature*, **421**: 436–440.

- Fujii-Nakata, T., Ishimi, Y., Okuda, A. and Kikuchi, A.** (1992) Functional analysis of nucleosome assembly protein, NAP-1. The negatively charged COOH-terminal region is not necessary for the intrinsic assembly activity. *J Biol Chem*, **267**: 20980–20986.
- Fung, J.C., Rockmill, B., Odell, M. and Roeder, G.S.** (2004) Imposition of crossover interference through the nonrandom distribution of synapsis initiation complexes. *Cell*, **116**: 795-802.
- Gallego, M.E. and White, C.I.** (2005) DNA repair and recombination functions in Arabidopsis telomere maintenance. *Chromosome Res*, **13**: 481-491.
- Garcia, V., Bruchet, H., Comescaisse, D., Granier, F., Bouchez, D. and Tissier, A.** (2003) AtATM is essential for meiosis and the somatic response to DNA damage in plants. *Plant Cell*, **15**: 119–132.
- Garcia-Ramirez, M., Rocchini, C., and Ausio, J.** (1995) Modulation of chromatin folding by histone acetylation. *J Biol Chem*, **270**: 17923-17928.
- Gelei, J.** (1921) Weitere studien iiber die oogenese des dendrocoelum lacteum II. Die langskonjugation der chromosomen Arch. *Zellforsch*, **16**: 88–169.
- Geradia, R. J., and David, B. K.** (1977). Banding and spiralization of human chromosomes. *Hum Genet*, **36**: 155-160.
- Gernand, D., Demidov, D. and Houben, A.** (2003) The temporal and spatial pattern of histone H3 phosphorylation at serine 28 and serine 10 is similar in plants but differs between mono- and polycentric chromosomes. *Cytogenet Genome Res*, **101**: 172-176.
- Giannattasio, M., Lazzaro, F., Plevani, P., Muzi-Falconi, M.** (2005) The DNA damage checkpoint response requires histone H2B ubiquitination by Rad6–Bre1 and H3 methylation by Dot1. *J Biol Chem*, **280**: 9879–9886.
- Gillies, C.B.** (1981) Electron microscopy of spread maize pachytene synaptonemal complexes. *Chromosoma*, **83**: 575–591.
- Glynn, E.F., Megee, P.C., Yu, H.G., Mistrot, C., Unal, E., Koshland, D.E., DeRisi, J.L. and Gerton, J.L.** (2004) Genome-wide mapping of the cohesin complex in the yeast *Saccharomyces cerevisiae*. *PLoS Biol*, **2**: 1325-1339.
- Goldberg, R.B., Beals, T.P. and Sanders, P.M.** (1993) Anther development: Basic principles and practical applications. *Plant Cell*, **5**:1217–1229.
- Goll, M.G. and Bestor, T.H.** (2002) Histone modification and replacement in chromatin activation. *Genes Dev*, **16**: 1739-1742.
- Golubovskaya, I.N.** (1989) Meiosis in maize: mei genes and conception of genetic control of meiosis. *Advanced Genetics*, **26**: 149–192.
- Golubovskaya, I.N., Hamant, O., Timofejeva, L., Wang, C.J., Braun, D., Meeley, R. and Cande, W.Z.** (2006) Alleles of *afd1* dissect REC8 functions during meiotic prophase I. *Journal of Cell Science*, **119**: 3306–3315.
- Golubovskaya, I.N., Harper, L.C., Pawlowski, W.P., Schichnes, D. and Cande, W.Z.** (2002) The *pam1* gene is required for meiotic bouquet formation and efficient homologous synapsis in maize (*Zea mays* L.). *Genetics*, **162**: (4): 1979-1993.
- Golubovskaya, I.N. and Mashnenkov, A.S.** (1976) Genetic control of meiosis: II A desynaptic mutant in maize induced by N-nitroso-Nmethylurea. *Genetika* (Russ), **12**: 7–14.

- Golubovskaya, I.N., Wang, C.J.R., Timofejeva, L. and Cande, W.Z.** (2010) Maize meiotic mutants with improper or non-homologous synapsis due to problems in pairing or synaptonemal complex formation. *Journal of Experimental Botany*. doi:10.1093/jxb/erq292
- Gontijo, A.M., Green, C.M. and Almouzni, G.** (2003) Repairing DNA damage in chromatin. *Biochimie*, **85**: 1133–1147.
- Graziano, V., Gerchman, S.E., Wonacott, A.J., Sweet, R. M , Wells, J. R., White, S. W. and Ramakrishnan, V.** (1990) Crystallization of the globular domain of histone H5. *J Mol Biol*, **212**: (2): 253-257.
- Grelon, M., Gendrot, G., Vezon, D. and Pelletier, G.** (2003) The Arabidopsis MEI1 gene encodes a protein with five BRCT domains that is involved in meiosis-specific DNA repair events independent of SPO11-induced DSBs. *Plant J*, **35**: 465–475.
- Grelon, M., Vezon, D., Gendrot, G. and Pelletier, G.** (2001) AtSPO11-1 is necessary for efficient meiotic recombination in plants. *EMBO J*, **20**: 589-600.
- Grigoryeva, S.A., Aryab, G., Correll, S., Woodcock, C.L. and Schlick, T.** (2009) Evidence for heteromorphic chromatin fibres from analysis of nucleosome interactions. *Proceedings of National Academy of Sciences of the USA*, **106**: 13317-13322.
- Grunstein, M.** (1997). Histone acetylation in chromatin structure and transcription. *Nature*, **389**: 349–352.
- Guacci, V., Hogan, E. and Koshland, D.** (1994). Chromosome condensation and sister chromatid pairing in budding yeast. *J Cell Biol*, **125**: 517-530.
- Gunjan A, Paik J and Verreault A.** (2005) Regulation of histone synthesis and nucleosome assembly. *Biochimie*, **87**: 625–635.
- Gunjan, A. and Verreault, A.** (2003) A Rad53 kinase-dependent surveillance mechanism that regulates histone protein levels in *S. cerevisiae*. *Cell*, **115**: 537–549.
- Gurley, L.R., Valdez, J.G. and Buchanan, J.S.** (1995) Characterization of the mitotic specific phosphorylation site of histone H1. Absence of a consensus sequence for the p34cdc2/cyclin B kinase. *J Biol Chem*, **270**: 27653-60.
- Haering, C.H., Lowe, J., Hochwagen, A. and Nasmyth, K.** (2002). Molecular architecture of SMC proteins and the yeast cohesin complex. *Mol Cell*, **9**: 773-788.
- Haering, C. H., Schoffnegger, D., Nishino, T., Helmhart, W., Nasmyth, K. and Lowe, J.** (2004). Structure and stability of cohesin's Smc1-kleisin interaction. *Mol Cell*, **15**: 951-964.
- Han, M., Chang, M., Kim,U.J. and Grunstein, M.** (1987) Histone H2B repression causes cell-cycle-specific arrest in yeast: Effects on chromosomal segregation, replication, and transcription. *Cell*, **48**: 589–597.
- Hanada, K., Kuromori, T., Myouga, F., Toyoda, T., Li, W. and Shinozaki, K.** (2009) Evolutionary persistence of functional compensation by duplicate genes in Arabidopsis. *Genome Biol Evol.* **2009**: 409-414; doi: 10.1093/gbe/evp043
- Handzel, M.J., Lever, M.A., Crawford, E. and Th`ng, J.P.** (2004) The C-terminal domain is the primary determinant of H1 binding to chromatin in vivo. *J Biol Chem*, **279**: 20028-20034.
- Hans, F. and Dimitrov, S.** (2001) Histone H3 phosphorylation and cell division. *Oncogene*, **20**: 3021–3027.

- Hansen, J.C.** (2002) Conformational dynamics of the chromatin fiber in solution: determinants, mechanisms and functions. *Ann Rev Biophys Biomol Struct*, **31**: 361-392.
- Happel, N. and Doenecke, D.** (2009) Histone H1 and its isoforms: contribution to chromatin structure and function. *Gene*, **15**:431 (1-2):1-12. doi: 10.1016/j.gene.2008.11.003. Epub
- Happel, N., Schulze, E. and Doenecke, D.** (2005) Characterisation of human histone H1x. *Bio Chem*, **386**: 541-551.
- Harper, L., Golubovskaya, I. and Cande, W.Z.** (2004) A bouquet of chromosomes. *J Cell Sci*, **117**: (Pt 18): 4025-4032.
- Hartsuiker, E., Neale, M.J. and Carr, A.M.** (2009a) Distinct requirements for the Rad32 (Mre11) nuclease and Ctp1(CtIP) in the removal of covalently bound topoisomerase I and II from DNA. *Mol Cell*, **33**: 117-123.
- Hartung, F. and Puchta, H.** (2000) Molecular characterisation of two paralogous SPO11 homologues in *Arabidopsis thaliana*. *Nucleic Acids Res*, **28**: 1548-1554.
- Hartung, F., Suer, S., Knoll, A., Wurz-Wildersinn, R. and Puchta, H.** (2008) Topoisomerase 3alpha and RMI1 suppress somatic crossovers and are essential for resolution of meiotic recombination intermediates in *Arabidopsis thaliana*. *PLoS Genet*, **4**: (12): e1000285.
- Hashimoto, H., Takami, Y., Sonoda, E., Iwasaki, T., Iwano, H., Tachibana, M., Takeda, S., Nakayama, T., Kimura, H. and Shinkai, Y.** (2010) Histone H1 null vertebrate cells exhibit altered nucleosome architecture. *Nucleic Acids Res*, **38**: 3533-3545.
- Hassan, Y.I. and Zemleni, J.** (2006) Epigenetic Regulation of Chromatin Structure and Gene Function by Biotin. *J Nutr*, **136**: (7): 1763-1765.
- Haushalter, K.A. and Kadonaga, J.T.** (2003) Chromatin assembly by DNA-translocating motors. *Nat Rev Mol Cell Biol*, **4**: 613-620
- Hayes, J.J.** (1996) Site-directed cleavage of DNA by a linker histone-Fe (II) EDTA conjugate: localization of a globular domain binding site within a nucleosome. *Biochemistry*, **35**: 11931-11937.
- Hayes, J.J., Pruss, D. and Wolffe, A.P.** (1994) Contacts of globular domain of histone H5 and core histones with DNA in a "chromatosome". *Proc Natl Acad USA*, **91**: 7817-7821.
- Hayes, J.J. and Wolffe, A.P.** (1993) Preferential and asymmetric interaction of linker histones with 5S DNA in the nucleosome. *Proc Natl Acad Sci USA*, **90**: 6415-6419.
- He, Y., Doyle, M.R. and Amasino, R.M.** (2004) PAF1-complex-mediated histone methylation of FLOWERING LOCUS C chromatin is required for the vernalization-responsive winter-annual habit in *Arabidopsis*. *Genes Dev*, **18**: 2774-2784.
- Henderson, K.A. and Keeney, S.** (2004) Tying synaptonemal complex initiation to the formation and programmed repair of DNA double-strand breaks. *Proc Natl Acad Sci USA*, **101**: 4519-4524.
- Henderson, K.A. and Keeney, S.** (2005) Synaptonemal complex formation: where does it start?. *Bioessays*, **27**:995-998.
- Hendzel, M.J., Wei, Y., Mancini, M.A., Van Hooser, A., Ranalli, T., Brinkley, R.P., Bazett-Jones, D.P. and Allis, C.D.** (1997) Mitosis-specific phosphorylation of histone H3 initiates primarily within pericentromeric heterochromatin during G2 and spreads in an ordered fashion coincident with mitotic chromosome condensation. *Chromosoma*, **106**: 348-360.

- Henikoff, S., Ahmad, K. and Malik, H.S.** (2001) The centromere paradox: stable inheritance with rapidly evolving DNA. *Science*, **293**: 1098-1102.
- Hennig, L., Taranto, P., Walser, M., Schonrock, N. and Gruissem, W.** (2003) Arabidopsis MSI1 is required for epigenetic maintenance of reproductive development. *Development*, **130**: 2555–2565
- Hewish, D.R. and Burgoyne, U.A.** (1973) Chromatin sub-structure: the digestion of chromatin DNA at regularly spaced sites by a nuclear deoxyribonuclease. *Biochemical and Biophysical Research Communication*, **52**: 504-510.
- Higgins, J.D., Armstrong, S.J., Franklin, F.C.H. and Jones, G.H.** (2004) The Arabidopsis MutS homolog AtMSH4 functions at an early step in recombination: evidence for two classes of recombination in *Arabidopsis*. *Gene Dev*, **18**: 2557-2570.
- Higgins, J.D., Buckling, E.F., Franklin, F.C.H. and Jones, G.H.** (2008b) Expression and functional analysis of AtMUS81 in Arabidopsis meiosis reveals a role in the second pathway of crossing-over. *Plant J*, **54**: 152-162.
- Higgins, J.D., Perry, R.M., Barakate, A., Ramsay, L., Waugh, R., Halpin, C., Armstrong, S.J. and Franklin, F.C.H.** (2012) Spatiotemporal Asymmetry of the Meiotic Program Underlies the Predominantly Distal Distribution of Meiotic Crossovers in Barley. *The Plant Cell*. **24**: 4096 - 4109
- Higgins, J.D., Sanchez-Moran, E., Armstrong, S.J., Jones, G.H. and Franklin, F.C.H.** (2005) The Arabidopsis synaptonemal complex protein ZYP1 is required for normal fidelity of crossing-over and chromosome synapsis. *Genes and Development*, **19**: 2488-2500.
- Higgins, J.D., Vignard, J., Mercier, R., Pugh, A.G., Franklin, F.C. and Jones, G.H.** (2008a) AtMSH5 partners AtMSH4 in the class I meiotic crossover pathway in Arabidopsis thaliana, but is not required for synapsis. *Plant J*, **55**: 28-39.
- Higgins, J.D., Vignard, J., Mercier, R., Pugh, A.G., Franklin, F.C.H. and Jones, G.H.** (2008b) AtMSH5 partners AtMSH4 in the class I meiotic crossover pathway in Arabidopsis thaliana, but is not required for synapsis. *The Plant Journal*, **55**: (1): 28-39.
- Hill, T.A., Day, C.D., Zondlo, S.C., Thackeray, A.G. and Irish, V.F.** (1998) Discrete spatial and temporal cis-acting elements regulate transcription of the *Arabidopsis* floral homeotic gene *APETALA3*. *Development*, **125**: 1711–1721.
- Hirano, T.** (2000). Chromosome cohesion, condensation, and separation. *Annu Rev Biochem*, **69**: 15-144.
- Hochholdinger, F. and Hoecker, N.** (2007) Towards the molecular basis of heterosis. *TRENDS in Plant Science*, **12**: (9): 427-432.
- Hohmann, P.** (1983) Phosphorylation of H1 histones. *Mol Cell Biochem*, **57**: 81-92.
- Hollingsworth, N.M. and Byers, B.** (1989) HOPI: a Yeast Meiotic Pairing Gene. *Genetics*, **121**: (3): 445-462.
- Holm, P.B., Rasmussen, S.W. and von Wettstein, D.** (1982) Ultrastructural characterization of the meiotic prophase. A tool in the assessment of radiation damage in man. *Mutat Res*, **95**: 45–59.
- Horn, P.J., Carruthers, L.M., Logie, C., Hill, D.A., Solomon, M.J., et al.,** (2002) Phosphorylation of linker histones regulates ATP- dependent chromatin remodeling enzymes. *Nat Struct Biol*, **9**: 263-267.

Hruz, T., Laule, O., Szabo, G., Wessendorp, F., Bleuler, S., Oertle, L., Widmayer, P., Gruissem, W. and Zimmermann, P. (2008) Genevestigator v3: a reference expression database for the meta-analysis of transcriptomes. *Adv Bioinformatics*, **2008**: 420747.

Huang, J. and Berger, S.L. (2008) The emerging field of dynamic lysine methylation of non-histone proteins. *Current Opinion in Genetics & Development*, **18**:152–158.

Hudson, D.F., Vagnarelli, P., Gassmann, R. and Earnshaw W.C. (2003) Condensin is required for nonhistone protein assembly and structural integrity of vertebrate mitotic chromosomes. *Dev Cell*, **5**: 323–336.

Hulten, M.A. (2011) On the origin of crossover interference: A chromosome oscillatory movement (COM) model. *Mol Cytogenet*, **4**: 10.

Hunter, N. (2006) Meiotic recombination. In: Aguilera, A.; Rothstein, R., editors. *Molecular Genetics of Recombination*. Springer Berlin; Heidelberg. 381-442.

Hunter, N. and Kleckner, N. (2001) The single-end invasion: an asymmetric intermediate at the double-strand break to double-holliday junction transition of meiotic recombination. *Cell*, **106**: 59–70.

Huyen, Y., Zgheib, O., Ditullio Jr, R.A., Gorgoulis, V.G., Zacharatos, P., Petty, T.J., Sheston, E.A., Mellert, H.S., Stavridi, E.S., Halazonetis, T.D. (2004) Methylated lysine 79 of histone H3 targets 53BP1 to DNA double-strand breaks. *Nature*, **432**: 406–411.

Iguchi, N., Tnaka, H., Yomogida, K. and Nishimune, Y. (2003) Isolation and characterization of a novel cDNA-binding protein (Hils1) specifically expressed in testicular haploid germ cells. *Int J Androl*, **26**: 354-365.

Integra8-A.thaliana-genome-statistics.

<http://www.ebi.ac.uk/integr8/OrganismStatsAction.do;jsessionid=08E9058B5B688A4F7FF7D161CB9E36A4?orgproteomeld=3>

Ip, S.C., Rass, U., Blanco, M.G., Flynn, H.R., Skehel, J.M. and West, S.C. (2008) Identification of Holliday junction resolvases from humans and yeast. *Nature*, **456**: 357-361.

Irvine, D.V., Amor, D.J., Perry, J., Sirvent, N., Pedeutour, F., Choo, K.H.A. and Saffery, R. (2004) Chromosome size and origin as determinants of the level of CENP-A incorporation into human centromeres. *Chromosome Res*, **12**: 805-815.

Ishimi, Y., Hirosumi, J., Sato, W., Sugawara, K., Yokota, S., Hanaoka, F., and Yamada, M. (1984) Purification and initial characterization of a protein which facilitates assembly of nucleosome-like structure from mammalian cells. *Eur J Biochem*, **142**: 431–439.

Ishimi, Y. and Kikuchi, A. (1991) Identification and molecular cloning of yeast homolog of nucleosome assembly protein I which facilitates nucleosome assembly in vitro. *J Biol Chem*, **266**: 7025–7029.

Ishimi, Y., Yasuda, H., Hirosumi, J., Hanaoka, F. and Yamada, M. (1983) A Protein which Facilitates Assembly of Nucleosome-like Structures In Vitro in Mammalian Cells. *J Biochem*, (Tokyo) **94**: 735–744.

Ito, T., Bulger, M., Kobayashi, R. and Kadonaga, J.T. (1996) Drosophila NAP-1 is a core histone chaperone that functions in ATP-facilitated assembly of regularly spaced nucleosomal arrays. *Mol Cell Biol*, **16**: 3112–3124.

- Ito, T., Ikehara, T., Nakagawa, T., Kraus, W.L. and Muramatsu, M.** (2000) p300-mediated acetylation facilitates the transfer of histone H2A–H2B dimers from nucleosomes to a histone chaperone. *Genes Dev*, **14**: 1899–1907.
- Izzo, A., Kamieniarz, K. and Schneider, R.** (2008) The histone H1 family: specific members, specific functions. *Biol Chem*, **389**: 333–343.
- Jackson, N., Sanchez-Moran, E., Buckling, E., Armstrong, S.J., Jones, G.H. and Franklin, F.C.H.** (2006) Reduced meiotic crossovers and delayed prophase I progression in AtMLH3-deficient Arabidopsis. *EMBO J*, **25**: (6): 1315–1323.
- Jean, M., Pelletier, J., Hilpert, M., Belzile, F. and Kunze, R.** (1999) Isolation and characterization of AtMLH1, a MutL homologue from *Arabidopsis thaliana*. *Mol Gen Genet*, **262**: 633–642.
- Jeffreys, A.J., Kauppi, L. and Neumann, R.** (2001) Intensely punctate meiotic recombination in the class II region of the major histocompatibility complex. *Nat Genet*, **29**: 217–222.
- Jenkins, G.** (1985) Synaptonemal complex formation in hybrids of *Lolium temulentum* × *Lolium perenne* (L.). II. Triploid. *Chromosoma*, **92**: 387–390
- Jenuwein, T. and Allis, C.D.** (2001) Translating the histone code. *Science*, **293**: 1074–1080.
- Jeppesen, P., Mitchell, A., Turner, B. and Perry, P.** (1992). Antibodies to defined histone epitopes reveal variations in chromatin conformation and underacetylation of centric heterochromatin in human metaphase chromosomes. *Chromosoma*, **101**: 322–332.
- Jerdrusik, M.A. and Schulze, E.** (2001) A single histone H1 isoform (H1.1) is essential for chromatin silencing and germ line development in *Caenorhabditis elegans*. *Development*, **128**:1069–1080.
- Jerzmanowski, A.** (2004) The linker histones, pp 75–102 in Chromatin Structure and Dynamics: State-of-the-Art, edited by J. Zlatanova and S.H.Leuba. ELSEVIER, Amsterdam/ New York.
- Jin, J., Cai, Y., Li, B., Conaway, R. C., Workman, J. L., Conaway, J.W. and Kusch, T.** (2005) In and out: histone variant exchange in chromatin. *Trends Biochem Sci*, **30**: (12):680–7.
- Jones, G.H. and Franklin, F.C.H.** (2006) Meiotic crossing-over: Obligation and interference. *Cell*, **126**: 246–248.
- Jones, S. and Sgouros, J.** (2001). The cohesin complex: sequence homologies, interaction networks and shared motifs. *Genome Biol*, **2**: 0009.1–0009.12.
- Kakutani, T., Jeddelloh, J.A., Flowers, S.K., Munakata, K. and Richards, E.J.** (1996) Developmental abnormalities and epimutations associated with DNA hypomethylation mutations. *Proc Natl Acad Sci USA*, **93**: 12406–12411.
- Kamakaka, R.T. and Biggins, S.** (2005) Histone variants: Deviants. *Genes Dev*, **19**: 295–310.
- Kanno, T., Kanno, Y., Siegel, R.M., Jang, M.K., Lenardo, M.J. and Ozato, K.** (2004) Selective recognition of acetylated histones by bromodomain proteins visualized in living cells. *Mol Cell*, **13**: 33–43.
- Karachentsev, D., Druzhinina, M. and Steward, R.** (2007) Free and chromatin-associated mono-, di-, and trimethylation of histone H4-lysine 20 during development and cell cycle progression. *Dev Biol*, **304**: 46–52.
- Karpen, G.H., Le, M.-H., and Le, H.** (1996) Centric heterochromatin and the efficiency of achiasmate disjunction in *Drosophila* female meiosis. *Science*, **273**: 118–122.

- Karymov, M.A., Tomschik, M., Leuba, S.H., Caiafa, P. and Zlatanova, J.** (2001) DNA methylation-dependent chromatin fiber compaction in vivo and in vitro, requirement for linker histones. *FASEB J*, **15**: 2631–2641.
- Kasinsky, H.E., Lewis, J.D., Dacks, J.B. and Ausio, J.** (2001) Origin of H1 linker histones. *FASEB J*, **15**:34-41.
- Kastan, M.B. and Bartek, J.** (2004) Cell-cycle checkpoints and cancer. *Nature*, **432**: 316–323.
- Kaufman, P.D., Kobayashi, R., Kessler, N. and Stillman, B.** (1995) The p150 and p60 subunits of chromatin assembly factor I: a molecular link between newly synthesized histones and DNA replication. *Cell*, **81**: 1105–1114
- Kaufman, P.D., Kobayashi, R. and Stillman, B.** (1997) Ultraviolet radiation sensitivity and reduction of telomeric silencing in *Saccharomyces cerevisiae* cells lacking chromatin assembly factor-I. *Genes Dev*, **11**: 345–357.
- Kaya, H., Shibahara, K., Taoka1, K., Iwabuchi1, M., Stillman, B. and Araki1, T.** (2001) Fasciata genes for chromatin assembly factor-1 in *Arabidopsis* maintain the cellular organization of apical meristems. *Cell*, **104**: (1): 131–142.
- Keeney, S., Giroux, C.N. and Kleckner, N.** (1997) Meiosis-specific DNA double-strand breaks are catalyzed by Spo11, a member of a widely conserved protein family. *Cell*, **88**: (3): 375-384.
- Keeney, S.** (2001) Mechanism and control of meiotic recombination initiation. *Curr Top Dev Biol*, **52**: 1-53.
- Kim, K.P., Weiner, B.M., Zhang, L., Jordan, A., Dekker, J. and Kleckner, N.** (2010) Sister cohesion and structural axis components mediate homolog bias of meiotic recombination. *Cell*, **143**, 924-937.
- Kim, U.J., Han, M., Kayne, P. and Grunstein, M.** (1988) Effects of histone H4 depletion on the cell cycle and transcription of *Saccharomyces cerevisiae*. *EMBO J*, **7**: 2211–2219.
- Kimura, A., Umehara, T. and Horikoshi, M.** (2002) Chromosomal gradient of histone acetylation established by Sas2p and Sir2p functions as a shield against gene silencing. *Nat Genet.* **32**: 370–377.
- Kimura, K., and Hirano, T.** (1997) ATP-dependent positive supercoiling of DNA by 13S condensin: a biochemical implication for chromosome condensation. *Cell*, **90**:625–634.
- Kirik, A., Pecinka, A., Wendeler, E. and Reissa, B.** (2006) The chromatin assembly factor subunit FASCIATA1 is involved in homologous recombination in plants. *The Plant Cell*, **18**: 2431–2442
- Kleckner, N.** (2006) Chiasma formation: chromatin/axis interplay and the role(s) of the synaptonemal complex. *Chromosoma*, **115**: 175-194.
- Kleckner, N., Zickler, D., Jones, G.H., Dekker, J., Padmore, R., Henle, J. and Hutchinson, J.** (2004) A mechanical basis for chromosome function. *P Natl Acad Sci USA*, **101**, 12592-12597.
- Klein, F., Mahr, P., Galova, M., Buonomo, S.B., Michaelis, C., Nairz, K. and Nasmyth, K.** (1999) A central role for cohesins in sister chromatid cohesion, formation of axial elements, and recombination during yeast meiosis. *Cell*, **98**: 91-103.
- Klimyuk, V.I. and Jones, J.D.** (1997) AtDMC1, the *Arabidopsis* homologue of the yeast DMC1 gene: characterization, transposon-induced allelic variation and meiosis-associated expression. *Plant J*, **11**: (1): 1-14.

- Kornberg, R.** (1974) Chromatin structure: a repeating unit of histones and DNA. *Science*, **184**: 868-871.
- Kornberg, R.D. and Thomas, J.O.** (1974) Chromatin structure; oligomers of the histones. *Science*, **184**: 865-868.
- Koshland, D.E. and Guacci, V.** (2000). Sister chromatid cohesion: the beginning of a long and beautiful relationship. *Curr Opin Cell Biol*, **12**: 297-301.
- Kosmoski, J.V., Ackerman, E.J. and Smerdon, M.J.** (2001) DNA repair of a single UV photoproduct in a designed nucleosome. *Proc Natl Acad Sci USA*, **98**:10113–8.
- Koszul, R., Kim, K.P., Prentiss, M., Kleckner, N. and Kameoka, S.** (2008) Meiotic chromosomes move by linkage to dynamic actin cables with transduction of force through the nuclear envelope. *Cell*, **133**: 1188–1201.
- Koszul, R. and Kleckner, N.** (2009) Dynamic chromosome movements during meiosis: a way to eliminate unwanted connections? *Trends in Cell Biology*, **19**: (12): 716-724.
- Kothapalli, N., Sarath, G. and Zempleni, J.** (2005) Biotinylation of K12 in histone H4 decreases response to DNA double strand breaks in Human Jar choriocarcinoma cells. *J Nutr*, **135**: 2337-42.
- Kothapalli, N. and Zempleni, J.** (2005) Biotinylation of histones depends on the cell cycle in NCI-H69 small cell lung cancer cells. *FASEB*, **19**: A 55
- Kruhlak, M.J., Hendzel, M.J., Fischle, W., Bertos, N.R., Hameed, S., Yang, X.-J., Verdi D.E. and Bazett-Jones, D.P.** (2001). Regulation of global acetylation in mitosis through loss of histone acetyltransferases and deacetylases from chromatin. *J Biol Chem*, **276**: 38307– 38319.
- Krylov, D., Leuba, S., Van Holde, K. and Zlatanova, J.** (1993) Histones H1 and H5 interact preferentially with crossovers of double-helical DNA. *Proc Natl Acad Sci US*, **90**: 5052-5056.
- Kugou, K., Fukuda, T., Yamada, S., Ito, M., Sasanuma, H., Mori, S., Katou, Y., Itoh, T., Matsumoto, K., Shibata, T., Shirahige, K. and Ohta, K.** (2009) Rec8 guides canonical Spo11 distribution along yeast meiotic chromosomes. *Mol Biol Cell*, **20**: 3064-3076.
- Kurdistani, S.K., Tavazoie, S., and Grunstein, M.** (2004) Mapping global histone acetylation patterns to gene expression. *Cell*, **117**: 721.
- Kuzmichev, A., Jenuwein, T., Tempst, P. and Reinberg, D.** (2004) Different EZH2-containing complexes target methylation of histone H1 or nucleosomal histone H3. *Mol Cell*, **14**: 183-193.
- Laemmli, U.K., Cheng, S.M., Adolph, K.W., Paulson, J.R., Brown, J.A. and Baumbach, W.R.** (1978). Metaphase chromosome structure: the role of non-histone proteins. *Cold Spring Harbor Symp Quant Biol*, **42**: 109-118.
- Laloraya, S., Guacci, V. and Koshland, D.** (2000) Chromosomal addresses of the cohesin component Mcd1p. *J Cell Biol*, **151**:1047–1056.
- Lam, A.L., Boivin, C.D., Bonney, C.F., Rudd, M.K. and Sullivan, B.A.** (2006) Human centromeric chromatin is a dynamic chromosomal domain that can spread over non centromeric DNA. *Proc Natl Acad Sci USA*, **103**: 4185-4191
- Lam, W.S.** (2005) Characterization of Arabidopsis thaliana SMC1 and SMC3: evidence that AtSMC3 may function beyond chromosome cohesion. *Journal of Cell Science*, **118**: (14): 3037-3048.

- Langan, T.A., Gautier, J., Lohka, M., Hollingsworth, R., Moreno, S., Nurse, P., Maller, J. and Sclafani, R.A.** (1989) Mammalian growth-associated H1 histone kinase: a homolog of cdc2+/ CDC28 protein kinases controlling mitotic entry in yeast and frog cells. *Mol Cell Biol*, **9**: 3860-8.
- Lavelle, C., Victor, J.M. and Zlatanova, J.** (2010) Chromatin Fiber Dynamics under Tension and Torsion. *Int J Mol Sci*, **11**: (4): 1557-1579; doi:10.3390/ijms11041557
- Lee, B-H., Lee, H., Xiong, L. & Zhu, J-K.** (2002) A mitochondrial complex I defect impairs cold-regulated nuclear gene expression. *Plant Cell*, **14**: 1235–1251.
- Lee, C.Y., Conrad, M.N. and Dresser, M.E.** (2012) Meiotic chromosome pairing is promoted by telomere-led chromosome movements independent of bouquet formation. *PLoS Genet*, **8**: (5): e1002730.
- Lee, R.C., Feinbaum, R.L. and Ambros, V.** (1993) The *C. elegans* heterochronic gene *lin-4* encodes small RNAs with antisense complementarity to *lin-14*. *Cell*, **75**: 843–854.
- Levchenko, V. and Jackson, V.** (2004) Histone release during transcription: NAP1 forms a complex with H2A and H2B and facilitates a topologically dependent release of H3 and H4 from the nucleosome. *Biochemistry*, **43**: 2359–2372.
- Lever, M.A., Th`ng, J.P., Sun, X. and Hendzel, M.J.** (2000) Rapid exchange of histone H1.1 on chromatin in living human cells. *Nature*, **408**: 873-876.
- Leyser, H.M.O. and Furner, I.J.** (1992) Characterisation of three shoot apical meristem mutants of *Arabidopsis thaliana*. *Development*, **116**: 397–403.
- Li, J., Harper, L.C., Golubovskaya, I., Wang, C.R., Weber, D., Meeley, R.B., McElver, J., Bowen, B., Cande, W.Z. and Schnable, P.S.** (2007) Functional analysis of maize RAD51 in meiosis and double-strand break repair. *Genetics*, **176**: 1469–1482.
- Li, W., Chen, C., Markmann-Mulisch, U., Timofejeva, L., Schmelzer, E., Ma, H. and Reiss, B.** (2004) The *Arabidopsis* AtRAD51 gene is dispensable for vegetative development but required for meiosis. *P Natl Acad Sci USA*, **101**, 10596-10601.
- Li, W.X., Yang, X.H., Lin, Z.G., Timofejeva, L., Xiao, R., Makaroff, C.A. and Ma, H.** (2005) The AtRAD51C gene is required for normal meiotic chromosome synapsis and double-stranded break repair in *Arabidopsis*. *Plant Physiol*, **138**: 965-976.
- Lichten, M.** (2001). Meiotic recombination: breaking the genome to save it. *Curr Biol*, **11**: R253-256.
- Lichten, M, Borts, R.H. and Haber, J.E.** (1986) Meiotic gene conversion and crossing over between dispersed homologous sequences occurs frequently in *saccharomyces cerevisiae*. *Genetics*, **115**: 233-246.
- Lindahl, T. and Wood, R.D.** (1999) Quality control by DNA repair. *Science*, **286**: 1897–1905.
- Lisby, M., Mortensen, U.H. and Rothstein, R.** (2003) Colocalization of multiple DNA double-strand breaks at a single Rad52 repair centre. *NatCell Biol*, **5**:572–577.
- Lisby, M., Rothstein, R. and Mortensen, U.H.** (2001) Rad52 forms DNA repair and recombination centers during S phase. *Proc Natl Acad Sci USA*, **98**:8276–8282.
- Loehrer, P.J. and Einhorn, L.H.** (1984) Cisplatin. *Ann Int Med*, **100**: 704–713.
- Loidl, P.** (1988) Towards an understanding of the biological function of histone acetylation. *FEBS Lett*, **227**: 91-95.

- Loidl, P.** (1994) Histone acetylation: Facts and questions. *Chromosoma*, **103**: 441-449.
- Lorenz, A., West, S.C. and Whitby, M.C.** (2010) The human Holliday junction resolvase GEN1 rescues the meiotic phenotype of a *Schizosaccharomyces pombe* mus81 mutant. *Nucleic Acids Res*, **38**: 1866-1873.
- Losada, A. and Hirano, T.** (2001) Shaping the metaphase chromosome: coordination of cohesion and condensation. *BioEssays*, **23**: 924-935.
- Losada, A. and Hirano, T.** (2005) Dynamic molecular linkers of the genome: the first decade of SMC proteins. *Genes Dev*, **19**: (11): 1269-1287.
- Lowndes, N.F. and Murguia, J.R.** (2005) Sensing and responding to DNA damage. *Curr Opin Genet Dev*, **10**: 17–25.
- Lowndes, N.F. and Toh, G.W.** (2005) DNA repair: the importance of phosphorylating histone H2AX. *Curr Biol*, **15**: R99–R102.
- Lu, X. and Hansen, J.C.** (2004) Identification of specific functional subdomains within the linker H1 C-terminal domain. *J Biol Chem*, **279**: 8701-8707.
- Lu, X., Klonoski, J.M., Resch, M.G. and Hansen, J.C.** (2006) In vitro chromatin self-association and its relevance to genome architecture. *Biochem Cell Biol*, **84**: (4): 411-417.
- Luger, K.** (2001) Nucleosomes: Structure and Function. *Encyclopedia of Life Sciences*.
- Luger, K., Mader, A.W. Richmond, R.K., Sargent, D.F. and Richmond, T.J.** (1997) Crystal structure of the nucleosome core particle at 2.8 Å resolution. *Nature*, **389**: (6684): 251-260.
- Lukaszewski, A.J.** (1997) The development and meiotic behavior of asymmetrical isochromosomes in wheat. *Genetics*, **145**: (4): 1155-1160.
- Lydall, D. and Whitehall, S.** (2005) Chromatin and the DNA damage response. *DNA Repair (Amst)*, **4**: 1195–1207.
- Macalpine, D.M. and Almouzni, G.** (2013) Chromatin and DNA Replication. *Cold Spring Harb Perspect Biol*. doi:10.1101/cshperspect.a010207.
- Maeshima, K., Imai, R., Tamura, S. and Nozaki, T.** (2014) Chromatin as dynamic 10-nm fibers. *Chromosoma*, **123**: (3):225-37.
- | | |
|---|--|
| 1 | |
|---|--|
- Mahadevaiah, S.K., Turner, J.M.A., Baudat, F., Rogakou, E.P., de Boer, P., Blanco-Rodriguez, J., Jasin, M., Keeney, S., Bonner, W.M. and Burgoyne, P.S.** (2001) Recombinational DNA double-strand breaks in mice precede synapsis. *Nat Genet*, **27**: 271-276.
- Malik, H.S. and Henikoff, S.** (2003) Phylogenomics of the nucleosome. *Nat Struct Biol*, **10**: 882–891.
- Maresca, T.J., Freedman, B.S. and Heald, R.** (2005) Histone H1 is essential for mitotic chromosome architecture and segregation in *Xenopus laevis* egg extracts. *J Cell Biol*, **169** (6): 859-869.
- Marnett, L.J. and Plastaras, J.P.** (2001) Endogenous DNA damage and mutation. *Trends Genet*, **17**: 214–221.
- Marsden, M.P.F. and Laemmli, V.K.** (1979) Metaphase chromosome structure: evidence for a radial loop model. *Cell*, **17**:849-858.

- Martianov, I., Brancorsini S., Catena, R., Gansmuller, A., Kotaja, N., Parvinen, M., Sassone-Corsi, P. and Davidson, I.** (2005) Polar nuclear localization of H1T2, a histone H1 variant, required for spermatid elongation and DNA condensation during spermiogenesis. *Proc Natl Acad Sci USA*, **102**: 2808-2813.
- Marzluff, W.F. and Duronio, R.J.** (2002) Histone mRNA expression: Multiple levels of cell cycle regulation and important developmental consequences. *Curr Opin Cell Biol*, **14**: 692–699.
- Maurer-Stroh, S., Dickens, N.J., Hughes-Davies, L., Kouzarides, T., Eisenhaber, F., Ponting, C.P.** (2003) The tudor domain 'Royal Family': tudor, plant agenet, chromo, PWWP and MBT domains. *Trends Biochem Sci*, **28**: 69–74.
- McBryant, S.J., Adams, V.H. and Hansen, J.C.** (2006) Chromatin architectural proteins. *Chromosome Res*, **14**: 39-51.
- McBryant, S.J., Lu X. and Hansen, J.C.** (2010) Multifunctionality of the linker histones: an emerging role for protein-protein interactions. *Cell Res*, **20**: (5): 519-528.
- McBryant, S.J., Park, Y.J., Abernathy, S.M., Laybourn, P.J., Nyborg, J.K. and Luger, K.** (2003) Preferential binding of the histone (H3-H4)₂ tetramer by NAP1 is mediated by the amino-terminal histone tails. *J Biol Chem*, **278**: 44574–44583.
- McKim, K.S., Green-Marroquin, B.L., Sekelsky, J.J., Chin, G., Steinberg, C., Khodosh, R. and Hawley, R.S.** (1998) Meiotic synapsis in the absence of recombination. *Science*, **279**: 876-878.
- McVean, G. and Myers, S.** (2010) PRDM9 marks the spot. *Nat Genet*, **42**, 821-822.
- Meergans, T., Albig, W. and Doenecke, D.** (1997) Varied expression patterns of human H1 histone genes in different cell lines. *DNA Cell Biol*, **16**: 1041-1049.
- Megee, P.C., Morgan, B.A. and Smith, M.M.** (1995) Histone H4 and the maintenance of genome integrity. *Genes Dev*, **9**: 1716-1727.
- Meijer, A.H., van Dijk, E.L. and Hoge, J.H.** (1996) Novel members of a family of AT hook-containing DNA-binding proteins from rice are identified through their in vitro interaction with consensus target sites of plant and animal homeodomain proteins. *Plant Mol Biol*, **31**: (3): 607–18. doi:10.1007/BF00042233. PMID 8790293.
- Melby, T.E., Ciampaglio, C.N., Briscoe, G. and Erickson, H.P.** (1998) The symmetrical structure of structural maintenance of chromosomes (SMC) and MukB proteins: Long, antiparallel coiled coils, folded at a flexible hinge. *J Cell Biol*, **142**: 1595-1604.
- Meneghini, M., Wu, M. and Madhani, H.** (2003) Conserved histone variant H2A.Z protects euchromatin from the ectopic spread of silent heterochromatin. *Cell*, **112**: 725–736.
- Mets, D.G. and Meyer, B.J.** (2009) Condensins Regulate Meiotic DNA Break Distribution, thus Crossover Frequency, by Controlling Chromosome Structure. *Cell*, **139**, 73-86.
- Millan-Arino, L., Islam, A.B., Izquierdo-Bouldstridge, A., Mayor, R., Terme, J-M., Luque, N., Sancho, M., Lopez-Bigas, N. and Jordan, A.** (2014) Mapping of six somatic linker histone H1 variants in human breast cancer cells uncovers specific features of H1.2. *Nucl Acids Res*. doi: 10.1093/nar/gku079
- Misteli, T., Gunjan, A., Hock, R., Bustin, M. and Brown, D.T.** (2000) Dynamic binding of histone H1 to chromatin in living cells. *Nature*, **408**: 877-881.
- Mizuguchi, G., Shen, X., Landry, J., Wu, W.H., Sen, S. and Wu, C.** (2004) ATP-driven exchange of histone H2AZ variant catalyzed by SWR1 chromatin remodeling complex. *Science*, **303**: 343–348

- Moens, P.B.** (1972) Fine structure of chromosome coiling at meiotic prophase in *Rhoeo discolor*. *Can J Genet Cytol*, **14**: 801–808.
- Moens, P.B.** (1974) Quantitative electron microscopy of chromosome organization at meiotic prophase. *Cold Spring Harbor Symp Quant Biol*, **38**: 99–107.
- Moens, P.B.** (1990) Unravelling meiotic chromosomes: topoisomerase II and other proteins. *J Cell Sci*, **97**: (1): 1–3.
- Moens, P.B., Kolas, N.K., Tarsounas, M., Marcon, E., Cohen, P.E. and Spyropoulos, B.** (2002) The time course and chromosomal localization of recombination-related proteins at meiosis in the mouse are compatible with models that can resolve the early DNA-DNA interactions without reciprocal recombination. *J Cell Sci*, **115**: 1611-1622.
- Moens, P.B., Marcon, E., Shore, J.S., Kochakpour, N. and Spyropoulos, B.** (2007) Initiation and resolution of interhomolog connections: crossover and non-crossover sites along mouse synaptonemal complexes. *J Cell Sci*, **120**: 1017-1027.
- Montgomery, E., Charlesworth, B. and Langley, C.H.** (1987) A test for the role of natural selection in the stabilization of transposable element copy number in a population of *Drosophila melanogaster*. *Genet Res*, **49**: 31–41.
- Morrison, A.J., Highland, J., Krogan, N.J., Arbel-Eden, A., Greenblatt, J.F., Haber, J.E., Shen, X.** (2004) INO80 and gamma-H2AX interaction links ATP-dependent chromatin remodeling to DNA damage repair. *Cell*, **119**: 767–775.
- Mozgova, I., Mokros, P. and Fajkusa, J.** (2010) Dysfunction of Chromatin Assembly Factor 1 Induces Shortening of Telomeres and Loss of 45S rDNA in *Arabidopsis thaliana*. *The Plant Cell*, **22**: 2768–2780.
- Muggia, F.M.** (1991) Cisplatin update. *Semin Oncol*, **18**: 1–4.
- Muggia, F.M. and Muderspach, L.** (1994) Platinum compounds in cervical and endometrial cancers: focus on carboplatin. *Semin Oncol*, **21**: 35–41.
- Mukherjee, B., Kessinger, C., Kobayashi, J., Chen, B.P., Chen, D.J., Chatterjee, A. and Burma, S.** (2006) DNA-PK phosphorylates histone H2AX during apoptosis DNA fragmentation in mammalian cells. *DNA Repair (Amst)*, **5**: (5): 575-590.
- Myers, S., Freeman, C., Auton, A., Donnelly, P. and McVean, G.** (2008) A common sequence motif associated with recombination hot spots and genome instability in humans. *Nat Genet*, **40**: 1124-1129.
- Nabatiyan, A., Szuts, D. and Krude, T.** (2006) Induction of CAF-1 expression in response to DNA strand breaks in quiescent human cells. *Molecular and Cellular Biology*, **26**: (5): 1839–1849.
- Nagel, S. and Grossbach, U.** (2000) Histone H1 genes and histone gene clusters in the genus *Drosophila*. *J Mol Evol*. **51**: 286–298.
- Nairz, K. and Klein, F.** (1997) mre11S-a yeast mutation that blocks double-strandbreak processing and permits nonhomologous synapsis in meiosis. *Gene Dev*, **11**: 2272-2290.
- Nakamura, T.M., Moser, B.A., Du, L.L., Russell, P.** (2005) Cooperative control of Crb2 by ATM family and Cdc2 kinases is essential for the DNA damage checkpoint in fission yeast. *Mol Cell Biol*, **25**: 10721–10730.
- Nasmyth, K.** (2001). Disseminating the genome: joining, resolving, and separating sister chromatids during mitosis and meiosis. *Annu Rev Genet*, **35**: 673-745.

- Nasmyth, K.** (2002). Segregating sister genomes: the molecular biology of chromosome separation. *Science*, **297**: 559–565.
- Nasmyth, K., Haering, C.H.** (2009) Cohesin: Its roles and mechanisms. *Annu Rev Genet*, **43**: 525-558.
- Nasmyth, K., Peters, J.M. and Uhlmann, F.** (2000) Splitting the chromosome: cutting the ties that bind sister chromatids. *Science*, **288**: 1379-1384.
- Neale, M.J. and Keeney, S.** (2006) Clarifying the mechanics of DNA strand exchange in meiotic recombination. *Nature*, **442**: 153-158.
- Nelson, D.M., Ye, X., Hall, C., Santos, H., Ma, T., Kao, G.D., Yen, T.J., Harper, J.W. and Adams, P.D.** (2002) Coupling of DNA synthesis and histone synthesis in S phase independent of cyclin/cdk2 activity. *Mol Cell Biol*, **22**: 7459–7472.
- Nelson W.G., Pienta K.J., Barrack E.R. and Coffey D.S.** (1986). The role of the nuclear matrix in the organization and function of DNA. *Annu Rev Biophys Biophys Chem*. **15**: 457–475.
- Newrock, K.M., Alfageme, C.R., Nardi, C.V., and Cohen, L.H.** (1977) Histone changes during chromatin remodeling in embryogenesis. *Cold Spring Harb Symp Quant Biol*, **42**: 421–431.
- Nguyen, G.D., Gokhan, S., Molero, A.E., Yang, S-M., Kim, B-J., Skoutchi, A.I., Mehler, M.F.** (2014) The role of H1 linker histone subtypes in preserving the fidelity of elaboration of mesendodermal and neuroectodermal lineages during embryonic development. *PLoS ONE*, 9: (5): e96858. doi:10.1371/journal.pone.0096858
- Nicolette, M.L., Lee, K., Guo, Z., Rani, M., Chow, J.M., Lee, S.E. and Paull, T.T.** (2010) Mre11-Rad50-Xrs2 and Sae2 promote 5' strand resection of DNA double-strand breaks. *Nat Struct Mol Biol*, **17**: 1478-1485.
- Nilsson, C., Roberg, K., Grafstrom, R.C. and Ollinger, K.** (2010) Intrinsic differences in cisplatin sensitivity of head and neck cancer cell lines: correlation to lysosomal pH. *Head Neck*, **32**: 1185–1194
- Nishioka, K., Rice, J.C., Sarma, K., Erdjument-Bromage, H., Werner, J., Wang, Y., Chuikov, S., Valenzuela, P., Tempst, P., Steward, R., Lis, J.T., Allis, C.D. and Reinberg, D.** (2002) PR-Set7 is a nucleosome-specific methyltransferase that modifies lysine 20 of histone H4 and is associated with silent chromatin. *Mol. Cell*, **9**: 1201-1213.
- Noll, M. and Komberg, R.D.** (1977) Action of micrococcal nuclease on chromatin and the location of histone H1. *Mol Biol*, **109**: 393-404.
- Nonomura, K.I., Nakano, M., Murata, K., Miyoshi, K., Eiguchi, M., Iyao, A., Hirochika, H. and Kurata, N.** (2004) An insertional mutation in the rice PAIR2 gene, the ortholog of Arabidopsis ASY1, results in a defect in homologous chromosome pairing during meiosis. *Mol Genet Genomics*, **271**: 121–129.
- Novak, I., Wang, H., Revenkova, E., Jessberger, R., Scherthan, H. and Hoog, C.** (2008) Cohesin Smc1 beta determines meiotic chromatin axis loop organization. *J Cell Biol*, **180**: 83-90.
- Nowak, M.A., Boerlijst, M.C., Cooke, J. and Smith, J.M.** (1997) Evolution of genetic redundancy. *Nature*, **388**: (6638):167-71.
- Oberg, C., Izzo, A., Schneider, R., Wrangé, O. and Belikov, S.** (2012) Linker histone subtypes differ in their effect on nucleosomal spacing in vivo. *J Mol Biol*, **419**: (3-4): 183-97

- Oh, S.D., Lao, J.P., Taylor, A.F., Smith, G.R. and Hunter, N.** (2008) RecQ helicase, Sgs1, and XPF family endonuclease, Mus81-Mms4, resolve aberrant joint molecules during meiotic recombination. *Mol Cell*, **31**: 324-336.
- Oh, S., Park, S. and van Nocker, S.** (2008) Genic and global functions for Paf1C in chromatin modification and gene expression in Arabidopsis. *PLoS Genet*, **4**:e1000077.
- Oh, S., Zhang, H., Ludwig, P. and van Nocker, S.** (2004) A mechanism related to the yeast transcriptional regulator Paf1c is required for expression of the Arabidopsis FLC/MAF MADS box gene family. *Plant Cell*, **16**:2940-2953.
- Ohkuni, K., Shirahige, K., and Kikuchi, A.** (2003) Genome-wide expression analysis of NAP1 in *Saccharomyces cerevisiae*. *Biochem Biophys Res Commun*, **306**: 5–9.
- Ohsumi, K. and Katagiri, C.** (1991) Occurrence of H1 subtypes specific to pronuclei and cleavage-stage cell nuclei of anuran amphibians. *Dev Biol*, **147**: (1): 110-120
- Ohta, K., Shibata, T. and Nicolas, A.** (1994) Changes in chromatin structure at recombination initiation sites during yeast meiosis. *EMBO J*, **13**: 5754-5763.
- Okada, T., Bhalla, P.L. and Singh, M.B.** (2005) Transcriptional activity of male gamete-specific histone gH3 promoter in sperm cell of *Lilium longiflorum*. *Plant Cell Physiol*, **46**: 797–802.
- Olins, A.L. and Olins, D.E.** (1974) Spheroid chromatin units (v bodies). *Science*, **183**: 330-332.
- Olins, D.E. and Olins, A.L.** (2003) Chromatin history: Our view from the bridge. *Nature Reviews Molecular Cell Biology*, **4**: 809-814.
- Oliver-Bonet, M., Campillo, M., Turek, P.J., Ko, E. and Martin, R.H.** (2007) Analysis of replication protein A (RPA) in human spermatogenesis. *Mol Hum Reprod*, **13**:837–844.
- Onnuki, Y.** (1968) Structure of chromosomes I morphological studies of the spiral structure of human somatic chromosomes. *Chromosoma*, **25**: 402-408.
- Osakabe, K., Yoshioka, T., Ichikawa, H. and Toki, S.** (2002) Molecular cloning and characterization of RAD51-like genes from Arabidopsis thaliana. *Plant Mol Biol*, **50**, 71-81.
- Osman, K., Higgins, J.D., Sanchez-Moran, E., Armstrong, S.J. and Franklin, C.H.** (2011) Pathways to meiotic recombination in *Arabidopsis thaliana*. *New Phytologist*, **190**: 523-544.
- Osman, K., Sanchez-Moran, E., Mann, S.C., Jones, G.H. and Franklin, F.C.H.** (2009) Replication protein A (AtrPA1a) is required for class I crossover formation but is dispensable for meiotic DNA break repair. *EMBO J*, **28**: 394-404.
- Owen-Hughes, T., Utley, R.T., Cote, J., Peterson, C.L., Workman, J.L.** (1996) Persistent site-specific remodeling of a nucleosome array by transient action of the SWI/SNF complex. *Science*, **273**: 513–516.
- Park, Y.J., Chodaparambil, J.V., Bao, Y., McBryant, S.J. and Luger, K.** (2005) Nucleosome assembly protein 1 exchanges histone H2A–H2B dimers and assists nucleosome sliding. *J Biol Chem*, **280**: 1817–1825.
- Park, Y.J. and Luger, K.** (2006a) Structure and function of nucleosome assembly proteins. *Biochem Cell Biol*, **84**: 549–558.
- Parseghian, M.H. and Hamkalo, B.A.** (2001) A compendium of the histone family of somatic subtypes: an elusive cast of characters and their characteristics. *Biochem Cell Biol*, **79**: 289-304.

- Parseghian, M.H., Henschen, A.H., Krieglstein, K.G. and Hamkalo, B.A.** (1994) A proposal for a coherent mammalian correlated with amino acid sequences. *Protein Sci*, **3**: 575-587.
- Pasierbek, P., Jantsch, M., Melcher, M., Schleiffer, A., Schweizer, D. and Loidl, J.** (2001) A *Caenorhabditis elegans* cohesion protein with functions in meiotic chromosome pairing and disjunction. *Genes Dev*, **15**: 1349-1360.
- Patterson, H.G., Landel, C.C., Landsman, D., Peterson, C.L. and Simpson, R.T.** (1998) The biochemical and phenotypic characterization of Hho1p, the putative linker histone H1 of *Saccharomyces cerevisiae*. *J Biol Chem*. **273**: 7268-7276.
- Paull, T.T., Rogakkou, E.P., Yamazaki, V., Kirchgessener, C.U., Gellert, M. and Bonner, W.M.** (2000) A critical role for histone H2AX in recruitment of repair factors to nuclear foci after DNA damage. *Curr Biol*, **10**: 886-895.
- Paulson, J.R. and Laemmli, U.K.** (1977) The structure of histone-depleted metaphase chromosomes. *Cell*, **12**: 817-828.
- Pawlowski, W.P. and Cande, W.Z.** (2005) Coordinating the events of the meiotic prophase. *Trends in Cell Biology*, **15**: 674–681.
- Pawlowski, W.P., Golubovskaya, I.N., Timofejeva, L., Meeley, R.B., Sheridan, W.F. and Cande, W.Z.** (2004) Coordination of meiotic recombination, pairing, and synapsis by PHS1. *Science*, **303**: 89–92.
- Peirson, B.N., Bowling, S.E. and Makaroff, C.A.** (1997) A defect in synapsis causes male sterility in a T-DNA-tagged *Arabidopsis thaliana* mutant. *Plant J*, **11**: 659-669.
- Peoples, T.L., Dean, E., Gonzalez, O., Lambourne, L. and Burgess, S.M.** (2002) Close, stable homolog juxtaposition during meiosis in budding yeast is dependent on meiotic recombination, occurs independently of synapsis, and is distinct from DSB-independent pairing contacts. *Gene Dev*, **16**: 1682-1695.
- Perez-Cadahia, B., Dorbic, B. and Davie, J.** (2009) H3 Phosphorylation: dual role in mitosis and interphase. *Biochem Cell Biol*, **87**: 695-709.
- Perisic, O., Colleparado-Guevara, R. and Schlick, T.** (2010) Modeling studies of chromatin fiber structure as a function of DNA linker length. *J Mol Biol*, **403**: 777- 802.
- Peterson, C.L. and Cote, J.** (2004) Cellular machineries for chromosomal DNA repair. *Genes Dev*, **18**: 602–616.
- Peterson, C.L. and Laniel, M.A.** (2004) Histones and histone modifications. *Curr Biol*, **14**: 546-551.
- Phillip, R.M, Fred, L.B. and Joseph, J.M.** (1977) Subunit structure of chromatin and the organization of eukaryotic highly repetitive DNA: Nucleosomal proteins associated with a highly repetitive mammalian DNA. *Proc. Natl Acad Sci USA*, **74**: (8): 3297-3301.
- Poirier, M.G. and Marko, J.F.** (2002) Mitotic chromosomes are chromatin networks without a mechanically contiguous protein scaffold. *Proc Natl Acad Sci USA*, **99**:15393–15397.
- Polo, S.E. and Almouzni, G.** (2006) Chromatin assembly, a basic recipe with various flavours. *Curr Opin Genet Dev*, **16**: 104–111
- Pradillo, M., Lopez, E., Romero, C., Sanchez-Moran, E, Cunado, N., Santos, J.L.** (2007) An analysis of Univalent segregation in meiotic mutants of *Arabidopsis thaliana*: A possible role for synaptonemal complex. *Genetics*, **175**: 505-511.

- Prado, F. and Aguilera, A.** (2005) Partial depletion of histone H4 increases homologous recombination-mediated genetic instability. *Mol Cell Biol*, **25**: 1526–1536
- Preuss, U., Landsberg, G. and Scheidtmann, K.H.** (2003) Novel mitosis-specific phosphorylation of histone H3 at Thr11 mediated by DIK/ZIP kinase. *Nucleic Acids Res*, **31**:878-885.
- Prieto, I., Tease, C., Pezzi, N., Buesa, J.M., Ortega, S., Kremer, L., Martinez, A., Martinez, A.C., Hulten, M.A. and Barbero, J.L.** (2004) Cohesin component dynamics during meiotic prophase I in mammalian oocytes. *Chromosome Res*, **12**: 197-213.
- Probst, A.V., Dunleavy, E. and Almouzni, G.** (2009) Epigenetic inheritance during the cell cycle. *Nat Rev Mol Cell Biol*, **10**:192–206.
- Prymakowska-Bosak, M., Przewoka, M.R., Iusarczyk, J., Kura, M., Lichota, J., Killa, B. and Jerzmanowski, A.** (1999) Linker histones play a role in male meiosis and the development of pollen grains in Tobacco. *The plant Cell*, **11**: 2317-2329.
- Prymakowska-Bosak, M., Przewloka, M.R., Iwkiewicz, J., Egierszdorff, S., Kuras, M., Chaubet, N., Gigot, C., Spiker, S., and Jerzmanowski, A.** (1996) Histone H1 overexpressed to a high level in tobacco affects certain developmental programs but has limited effect on basal cellular functions. *Proc Natl Acad Sci USA*, **93**: 10250–10255.
- Puizina, J.** (2004) Mre11 Deficiency in Arabidopsis Is Associated with Chromosomal Instability in Somatic Cells and Spo11-Dependent Genome Fragmentation during Meiosis. *The Plant Cell Online*, **16**: (8): 1968-1978.
- Puizina, J., Siroky, J., Mokros, P., Schweizer, D. and Riha, K.** (2004) Mre11 deficiency in Arabidopsis is associated with chromosomal instability in somatic cells and Spo11-dependent genome fragmentation during meiosis. *Plant Cell*, **16**: 1968-1978.
- Qin, S., Parthun, M.R.** (2006) Recruitment of the type B histone acetyltransferase Hat1p to chromatin is linked to DNA double-strand breaks. *Mol Cell Biol*, **26**: 3649–3658.
- Ramakrishnan, V., Finch, J. T., Graziano, V., Lee, P. L. and Sweet, R. M.** (1993) Crystal structure of globular domain of histone H5 and its implications for nucleosome binding. *Nature*, **362**: 219-223.
- Ramirez-Parra, E. and Gutierrez, C.** (2007) The many faces of chromatin assembly factor 1. *Trends in plant science*, **12**: (12): 570-576.
- Ramirez-Parra, E. and Gutierrez, C.** (2007) E2F regulates FASCIATA1, a chromatin assembly gene whose loss switches on the endocycle and activates gene expression by changing the epigenetic status. *Plant Physiol*, **144**: 105–120.
- Ramon, A., Muro-Pastor, M.I., Scazzocchio, C. and Gonzalez, R.** (2000) Deletion of the unique gene encoding a typical histone H1 has no apparent phenotype in *Aspergillus nidulans*. *Mol Microbiol*, **35**: 223-233.
- Rasmussen, S.W.** (1986) Initiation of synapsis and interlocking of chromosomes during zygotene in Bombyx spermatocytes. *Carlsberg Res Commun*, **51**: 401–432.
- Rasmussen, S.W. and Holm, P.B.** (1980) Mechanics of meiosis. *Hereditas*, **93**: 187–216.
- Rattner, J.B. and Hamkalo, B.A.** (1978) Higher order structure of metaphase chromosomes, the 250 A fiber. *Chromosoma*, **69**: 362-372.
- Rattner, J.B. and Lin, C.C.** (1985) Radial loops and helical coils coexist in metaphase chromosomes. *Cell*, **42**: 291-296.

- Rea, M., Zheng, W., Chen, M., Braud, C., Bhangu, D., Rognan, T.N. and Xiao, W.** (2012) Histone H1 affects gene imprinting and DNA methylation in Arabidopsis. *The Plant Journal*, **71**: 776–786.
- Reddy, K.C., Villeneuve, A.M.** (2004) *C. elegans* HIM-17 links chromatin modification and competence for initiation of meiotic recombination. *Cell*, **118**: (4):439–452.
- Redon, C., Pilch, D., Rogakou, E., Sedelikova, O., Newrock, K. and Bonner, W.** (2002) Histone H2A variants H2AX and H2AZ. *Curr Opin Genet Dev*, **12**:162-169.
- Reeves, R.** (2001).Molecular biology of HMGA proteins: hubs of nuclear function. *Gene*, **277**: (1–2): 63–81. doi:10.1016/S0378-1119(01)00689-8. PMID 11602345.
- Reeves, R. and Beckerbauer, L.** (2001). HMGI/Y proteins: flexible regulators of transcription and chromatin structure. *Biochim Biophys Acta*, **1519**: (1–2): 13–29. doi:10.1016/S0167-4781(01)00215-9. PMID 11406267.
- Reeves, R. and Nissen, M.S.** (1990).The A.T-DNA-binding domain of mammalian high mobility group I chromosomal proteins. A novel peptide motif for recognizing DNA structure. *J Biol Chem*, **265**: (15): 8573–82. PMID 1692833.
- Renauld, H., and Gasser, S.M.** (1997) Heterochromatin: A meiotic matchmaker. *Trends Cell Biol*, **7**: 201–205.
- Resnick, T., Dej, K., Xiang, Y., Hawley, R., Ahn, C. and Orr-Weaver, T.** (2009) Mutations in the chromosomal passenger complex and the condensin complex differentially affect synaptonemal complex disassembly and metaphase I configuration in Drosophila female meiosis. *Genetics*, **181**: 875–887.
- Revenkova, E., Eijpe, M., Heyting, C., Hodges, C.A., Hunt, P.A., Liebe, B., Scherthan, H. and Jessberger, R.** (2004) Cohesin SMC1 beta is required for meiotic chromosome dynamics, sister chromatid cohesion and DNA recombination. *Nat Cell Biol*, **6**, 555-562.
- Rice, J.C., Nishioka, K., Sarma, K., Steward, R., Reinberg, D. and Allias, C.D.** (2002) Mitotic-specific methylation of histone H4 Lys 20 follows increased PR-Set7 expression and its localization to mitotic chromosomes. *Genes Dev*, **1**: 2225-2230.
- Richmond, T.J., Finch, J.T., Rushton, B., Rhodes, D. and Klug, A.** (1984) Structure of the nucleosome core particle at 7 Å resolution. *Nature*, **311**: 532-537.
- Ridgway, P.1. and Almouzni, G.** (2000) CAF-1 and the inheritance of chromatin states: at the crossroads of DNA replication and repair. *J Cell Sci*, **113**: (15): 2647-58.
- Rill, R.L. and Nelson, D.A.** (1978) Histone Organization in Chromatin: Comparisons of Nucleosomes and Subnucleosomal Particles from Erythrocyte, Myeloma, and Yeast Chromatin. *Cold Spring Harb Symp Quant Biol*, **42**: 475-482.
- Riqueleme, P.T., Burzio, L.O. and Koide, S.S.** (1979) ADP ribosylation of rat liver lysine-rich histone *in vitro*. *J Biol Chem*, **254**: 3018-3028.
- Robinson, P.J.J. and Rhodes, D.** (2006) Structure of the “30 nm” chromatin fibre: A key role for the linker histone. *Current Opinion in Structural Biology*, **16**:336-343.
- Rockmill, B., Engebrecht, J.A., Scherthan, H., Loidl, J. and Roeder, G.S.** (1995) The yeast MER2 gene is required for chromosome synapsis and the initiation of meiotic recombination. *Genetics*, **141**: 49-59.
- Rockmill, B. and Roeder, G.S.** (1990) Meiosis in Asynaptic Yeast. *Genetics*, **126**: 563-574.

- Rogakou, E.P., Pilch, D.R, Orr, A.H., Ivanova, V.S. and Bonner, W.M.** (1998) DNA double-stranded breaks induce histone H2AX phosphorylation on serine 139. *J Biol Chem*, **273**:5858-5868.
- Ronne, M.** (1977) Induction of uncoiled chromosome with RNase. *Hereditas*, **86**: 245-250.
- Rosidi, B., Wang, M., Wu, W., Sharma, A., Wang, H. and Lliakis, G.** (2008) Histone H1 functions as a stimulatory factor in backup pathways of NHEJ. *Nucleic Acid Research*, **36**: 1610-1623.
- Ross, K.J., Fransz, P., Armstrong, S.J., Vizir, I., Mulligan, B., Franklin, F.C. and Jones, G.H.** (1997) Cytological characterization of four meiotic mutants of *Arabidopsis* isolated from T-DNA-transformed lines. *Chromosome Res*, **5**: 551-559.
- Roth, S.Y. and Allis, C.D.** (1992) Chromatin condensation: does histone H1 dephosphorylation play a role. *Trends Biochem Sci*, **17**: 93-98.
- Roth, S.Y., Collini, M.P., Draetta, G., Beach, D., Allis, C.D.** (1991) A cdc2-like kinase phosphorylates histone H1 in the amitotic macronucleus of *Tetrahymena*. *EMBO J*, **10**: 2069-75.
- Routh, A., Sandin, S. and Rhodes, D.** (2008) Nucleosome repeat length and linker histone stoichiometry determine chromatin fibre structure. *PNAS*, **105**: (26): 8872-8877.
- Rutledge, R.G., Shay, C.E., Brown, G.L. and Neelin, J.M.** (1981) The similarity of histones from turtle erythrocytes and liver. *Can J Biochem*, **59**: (4): 273-279.
- Sadoni, N., Langer, S., Fauth, C., Bernardi, G., Cremer, T., Turner, B.M. and Zink, D.** (1999) Nuclear organization of mammalian genomes: Polar chromosome territories build up functionally distinct higher order compartments. *J Cell Biol*, **146**: 1211-1226.
- Saha, A., Wittmeyer, J., Cairns, B.R.** (2006) Chromatin remodelling: the industrial revolution of DNA around histones. *Nat Rev Mol Cell Biol*, **7**: 437-447.
- Sahasrabudde, C.G. and Van Holde, K.E.** (1974) The effect of trypsin on nuclease-resistant chromatin fragments. *J Biol Chem*, **249**: (1):152-6.
- Saitoh, Y. and Laemmli, U.K.** (1994) Metaphase chromosome structure – bands arise from a differential folding path of the highly at-rich scaffold. *Cell*, **76**: 609-622.
- Sanchez-Moran, E.** (2013) Genomics and chromatin packaging. *Annual Plant Reviews*, **46**: 123-156.
- Sanchez-Moran, E., Alfaro, D., Martinez, M. and Santos, J.L.** (2001) A comparative analysis of chiasma frequencies in different ecotypes of *Arabidopsis thaliana* (L.). *Chromosome Res*, **9**: 132.
- Sanchez-Moran, E., Armstrong, S.J., Santos, J.L., Franklin, F.C.H. and Jones, G.H.** (2002) Variation in chiasma frequency among eight accessions of *Arabidopsis thaliana*. *Genetics*, **162**: 1415-1422.
- Sanchez-Moran, E., Osman, K., Higgins, J.D., Pradillo, M., Cuñado, N., Jones, G.H. and Franklin F.C.H.** (2008) ASY1 coordinates early events in the plant meiotic recombination pathway. *Cytogenet Genome Res*, **120**: 302-312 (DOI: 10.1159/000121079)
- Sanchez-Moran, E., Santos, J.L., Jones, G.H. and Franklin, F.C.H.** (2007) ASY1 mediates AtDMC1-dependent interhomolog recombination during meiosis in *Arabidopsis*. *Gene Dev*, **21**: 2220-2233.
- Schalch, T., Duda, S., Sargent, D.F. and Richmond, T.J.** (2005) X-ray structure of a tetranucleosome and its implications for the chromatin fibre. *Nature*, **436**: 138-141.

- Scherthan, H.** (2001) A bouquet makes ends meet. *Nat Rev Mol Cell Biol*, **2**: (8): 621-627.
- Schonrock, N., Exner, V., Probst, A., Gruissem, W. and Hennig, L.** (2006) Functional genomic analysis of CAF-1 mutants in *Arabidopsis thaliana*. *J Biol Chem*, **281**: 9560–9568.
- Schotta, G., Lachner, M., Sarma, K., Ebert, A., Sengupta, R., Reuter, G., Reinberg, D. and Jenuwein, T.** (2004) A silencing pathway to induce H3-K9 and H4-K20 trimethylation at constitutive heterochromatin. *Genes Dev*, **1**: 1251-1262.
- Sedat, J. and Manuelides, L.** (1977) A direct approach to the structure of eukaryotic chromosomes. *Cold Spring Harbor Symp Quant Biol*, **42**: 331-350.
- Severson, A.F., Ling, L., van Zuylen, V. and Meyer, B. J.** (2009) The axial element protein HTP-3 promotes cohesin loading and meiotic axis assembly in *C. elegans* to implement the meiotic program of chromosome segregation. *Gene Dev*, **23**: 1763-1778.
- Seyedin, S.M. and Kistler, W.S.** (1980) Isolation and characterization of rat testis H1t: An H1 histone variant associated with spermatogenesis. *J Biol Chem*, **255**: 5949-5954.
- Sheehan, M.J. and Pawlowski, W.P.** (2009) Live imaging of rapid chromosome movements in meiotic prophase I in maize. *Proceedings of the National Academy of Sciences*, **106**: (49): 20989-20994
- Shen, X., Mizuguchi, G., Hamiche, A., Wu, C.** (2000) A chromatin remodelling complex involved in transcription and DNA processing. *Nature*, **406**: 541–544.
- Shen, X., YU, L., Weir, J.W. and Gorovsky, M.A.** (1995) Linker histones are not essential and affect chromatin condensation in vivo. *Cell*, **82**: 47-56.
- Shen Y., Tang D., Wang K., Wang M., Huang J., Luo W., Luo Q., Hong L., Li M., Cheng Z .** (2012). The role of ZIP4 in homologous chromosome synapsis and crossover formation in rice meiosis. *J Cell Science*, **125**: 2581–2591.
- Shibahara, K. and Stillman, B.** (1999) Replication-dependent marking of DNA by PCNA facilitates CAF-1-coupled inheritance of chromatin. *Cell*, **96**: 575–585.
- Shim, E.Y., Ma, J.L., Oum, J.H., Yanez, Y., Lee, S.E.** (2005) The yeast chromatin remodeler RSC complex facilitates end joining repair of DNA double-strand breaks. *Mol Cell Biol*, **25**: 3934–3944.
- Shinohara, A., Ogawa, H. and Ogawa, T.** (1992) Rad51 protein involved in repair and recombination in *S. cerevisiae* is a RecA-like protein. *Cell*, **69**: (3): 457-470.
- Shogren-Knaak, M., Ishii, H., Sun, J.M., Pazin, M.J., Davie, J.R. and Peterson, C.L.** (2006) Histone H4-K16 acetylation controls chromatin structure and protein interactions. *Science*, **3**: (11): 844–847.
- Shogren-Knaak, M. and Peterson, C.L.** (2006) Switching on chromatin mechanistic role of histone H4-K16 acetylation. *Cell Cycle*, **5**:13, e1-e5.
- Shroff, R., Arbel-Eden, A., Pilch, D., Ira, G., Bonner, W.M., Petrini, J.H., Haber, J.E. and Lichten, M.** (2004) Distribution and dynamics of chromatin modification induced by a defined DNA double-strand break. *Curr Biol*, **14**: 1703-1711.
- Siaud, N., Dray, E., Gy, I., Gerard, E., Takvorian, N. and Doutriaux, M.P.** (2004) Brca2 is involved in meiosis in *Arabidopsis thaliana* as suggested by its interaction with Dmc1. *EMBO J*, **23**: 1392-1401.
- Singh, M., D'Silva, L. and Holak, T.A.** (2006) DNA-binding properties of the recombinant high-mobility-group-like AT-hook-containing region from human BRG1 protein. *Biol Chem*, **387**: (10–11): 1469–78. doi:10.1515/BC.2006.184. PMID 17081121.

- Singh, R., Mortazavi, A., Telu, K.H., Nagarajan, P., Lucas, D.M., Thomas-Ahner, J.M., Clinton, S.K., Byrd, J.C., Freitas, M.A and Parthun, M.** (2013) Increasing the complexity of chromatin: functionally distinct roles for replication-dependent histone H2A isoforms in cell proliferation and carcinogenesis. *Nucl Acids Res.* doi: 10.1093/nar/gkt736
- Siroky, J., Zluvova, J., Riha, K., Shippen, D.E. and Vyskot, B.** (2003) Rearrangements of ribosomal DNA clusters in late generation telomerase-deficient *Arabidopsis*. *Chromosoma*, **112**: (3):116-23.
- Sjogren, C. and Nasmyth, K.** (2001) Sister chromatid cohesion is required for postreplicative double strand break repair in *Saccharomyces cerevisiae*. *Curr Biol*, **11**: (12): 991-995.
- Sleth, LA., Sigurdsson, S. and Svejstrup, J.Q.** (2010) Transcript elongation by RNA polymerase II. *Ann Rev Biochem*, **79**: 271-293.
- Slusarczyk, J., Wierzbicki, A., Przewloka, M, Tykarska, T., Jerzmanowski, A. and Kuras, M.** (2003) Influence of change in the proportion of H1 histone variants on microsporogenesis and development of male gametophyte in transgenic plants of Tobacco (*Nicotiana tabacum* L.). *Acta Societatis Botanicorum Poloniae*, **72**: (1): 25-35.
- Smith, B.J., Walker, J.M. and Johns, E.W.** (1980) Structural homology between a mammalian H1 O subfraction and avian erythrocyte specific histone H5. *FEBS Lett*, **112**: 42-44.
- Smith, R.C., Dworkin-Rastl, E. and Dworkin, M.B.** (1988) Expression of a histone H1-like protein is restricted to early *Xenopus* development. *Genes Dev*, **2**: 1284-1295
- Smith, M.F., Athey, B.D., Williams, S.P. and Langmore, J.P.** (1990) Radial density distribution of chromatin: evidence that chromatin fibers have solid centers. *J Cell Biol*, **110**: 245–254
- Smith, S. and Stillman, B.** (1989) Purification and characterization of CAF-1, a human cell factor required for chromatin assembly during DNA replication in vitro. *Cell*, **58**: 15–25.
- Smith, S. and Stillman, B.** (1991) Stepwise assembly of chromatin during DNA replication in vitro. *EMBO J*, **10**: 971–980.
- Snowden, T., Acharya, S., Butz, C., Berardini, M. and Fishel, R.** (2004) hMSH4-hMSH5 recognizes Holliday Junctions and forms a meiosis-specific sliding clamp that embraces homologous chromosomes. *Mol Cell*, **15**: 437-451.
- Sobel, R.E., Cook, R.G., Perry, C.A., Annunziato, A.T. and Allis, C.D.** (1995) Conservation of deposition-related acetylation sites in newly synthesized histones h3 and h4. *Proc Natl Acad Sci USA*, **92**: 1237–1241.
- Springer, N.M. and Stupar, R.M.** (2007) Allelic variation and heterosis in maize: how do two halves make more than a whole. *Genome Res*, **17**: 264–275.
- Stacey, N.J., Kuromori, T., Azumi, Y., Roberts, G., Breuer, C., Wada, T., Maxwell, A., Roberts, K. and Sugimoto-Shirasu, K.** (2006) *Arabidopsis* SPO11-2 functions with SPO11-1 in meiotic recombination. *Plant J*, **48**: 206-216.
- Stahl, F.W., Foss, H.M., Young, L.S., Borts, R.H., Abdullah, M.F. and Copenhaver, G.P.** (2004) Does crossover interference count in *Saccharomyces cerevisiae*? *Genetics*, **168**, 35-48.
- Staiger, C.J. and Cande, W.Z.** (1990) Microtubule distribution in dv, a maize meiotic mutant defective in the prophase to metaphase transition. *Developmental Biology*, **138**: 231–242.
- Steer, W.M., Abu-Daya, A., Brickwood, S.J., Mumford, K.L., Jordanaires, N., Mitchell, J., Robinson, C., Thorne, A.W. and Guille, M.J.** (2003) *Xenopus* nucleosome assembly protein

becomes tissue-restricted during development and can alter the expression of specific genes. *Mech Dev*, **120**: 1045–1057.

Stein, G.S., Hunter, G. and Lavie, L. (1974) Non-histone chromosomal proteins evidence for their role in mediating the binding of histones to deoxyribonucleic acid during the cell cycle. *Biochem J*, **139**: (1): 71-76.

Storlazzi, A., Gargano, S., Ruprich-Robert, G., Falque, M., David, M., Kleckner, N. and Zickler, D. (2010) Recombination Proteins Mediate Meiotic Spatial Chromosome Organization and Pairing. *Cell*, **141**: 94-106.

Storlazzi, A., Tesse, S., Gargano, S., James, F., Kleckner, N. and Zickler, D. (2003) Meiotic double-strand breaks at the interface of chromosome movement, chromosome remodeling, and reductional division. *Genes Dev*, **17**: (21): 2675-2687.

Storlazzi, A., Tesse, S., Ruprich-Robert, G., Gargano, S., Poggeler, S., Kleckner, N. and Zickler, D. (2008). Coupling meiotic chromosome axis integrity to recombination. *Genes Dev*, **22**: 796-809.

Stracke, R., Werber, M. and Weisshaar, B. (2001) The R2R3-MYB gene family in *Arabidopsis thaliana*. *Curr Opin Biol*, **4**: (5): 447-456.

Strahl, B.D. and Allis, C.D. (2000) The language of covalent histone modifications. *Nature*, **403**: (6765): 41-45.

Stucki, M. and Jackson, S.P. (2006) gammaH2AX and MDC1: anchoring the DNA-damage-response machinery to broken chromosomes. *DNA Repair (Amst)*, **5**: 534–543.

Stupar, R., Gardiner, J., Oldre, A., Haun, W., Chandler, V. and Springer, N. (2008) Gene expression analyses in maize inbreds and hybrids with varying levels of heterosis. *BMC Plant Biol*, **8**: 33.

Suka, N., Luo, K. and Grunstein, M. (2002) Sir2p and Sas2p opposingly regulate acetylation of yeast histone H4 lysine16 and spreading of heterochromatin. *Nat Genet*. **32**: 378–383.

Sun, H., Treco, D., Schultes, N.P. and Szostak, J.W. (1989) Double-Strand Breaks at an Initiation Site for Meiotic Gene Conversion. *Nature*, **338**: 87-90.

Sym, M. and Roeder, G.S. (1994) Crossover interference is abolished in the absence of a synaptonemal complex protein. *Cell*, **79**: 283-292.

Tagami, H., Ray-Gallet, D., Almouzni, G. and Nakatani, Y. (2004) Histone H3.1 and H3.3 complexes mediate nucleosome assembly pathways dependent or independent of DNA synthesis. *Cell*, **116**: 51–61.

Talbert, P.B., Masuelli, R., Tyagi, A.P., Comai, L. and Henikoff, S. (2002) Centromeric localization and adaptive evolution of an *Arabidopsis* histone H3 variant. *Plant Cell*, **14**: 1053–1066.

Tamburini, B.A., Tyler, J.K. (2005) Localized histone acetylation and deacetylation triggered by the homologous recombination pathway of double-strand DNA repair. *Mol Cell Biol*, **25**: 4903–4913.

Tanaka, M., Hennebold, J. D., Macfarlane, J. and Adashi, E.Y. (2001) A mammalian oocyte-specific linker histone gene H1oo: homology with the genes for the oocyte-specific cleavage stage histone (cs-H1) of sea urchin and the B4/H1M histone of the frog, *Development*, **128**:655-664

Tanaka, M., Kihara, M., Meczekalski, B., King, G.C. and Adashi, E.Y. (2003) H1oo: a preembryonic H1 linker histone in search of a function, *Mol Cell Endocrinol*, **202**: 5-9.

Tanaka, T., Fuchs, J., Loidl, J. and Nasmyth, K. (2000) Cohesion ensures bipolar attachment of microtubules to sister centromeres and resists their precocious separation. *Nat Cell Biol*, **2**:492-499.

Tarsounas, M., Morita, T., Pearlman, R.E. and Moens, P.B. (1999) RAD51 and DMC1 from mixed complexes associated with mouse meiotic chromosome cores and synaptonemal complexes. *J Cell Biol*, **147**: 207-219.

The Arabidopsis Genome Initiative (2000) Analysis of the genome sequence of the flowering plant *Arabidopsis thaliana*. *Nature*, **408**: (6814): 796-815.

Tease, C. and Hulten, M.A. (2004) Inter-sex variation in synaptonemal complex lengths largely determine the different recombination rates in male and female germ cells. *Cytogenet Genome Res*, **107**, 208-215.

Teng, Y., Yu, Y., Waters, R. (2002) The *Saccharomyces cerevisiae* histone acetyltransferase Gcn5 has a role in the photoreactivation and nucleotide excision repair of UV-induced cyclobutane pyrimidine dimers in the MFA2 gene. *J Mol Biol*, **316**: 489–499.

Terasawa, M., Ogawa, H., Tsukamoto, Y., Shinohara, M., Shirahige, K., Kleckner, N. and Ogawa, T. (2007) Meiotic recombination-related DNA synthesis and its implications for cross-over and non-cross-over recombinant formation. *P Natl Acad Sci USA*, **104**: 5965-5970.

Tesse, S., Storlazzi, A., Kleckner, N., Gargano, S. and Zickler, D. (2003) Localization and roles of Ski8p protein in *Sordaria* meiosis and delineation of three mechanistically distinct steps of meiotic homolog juxtaposition. *P Natl Acad Sci USA*, **100**: 12865-12870.

Thiriet, C. and Hayes, J.J. (2005) Chromatin in need of a fix: phosphorylation of H2AX connects chromatin to DNA repair. *Mol Cell*, **18**: 617–622.

Thng, J.P., Sung, R., Ye, M. and Hendzel, M.J. (2005) H1 family histones in the nucleus. Control of binding and localization by the C-terminal domain. *J Biol Chem*, **280**: 27809-27814.

Thoma, F. and Koller, T. (1977) Influence of histone H1 on chromatin structure. *Cell*, **12**: 101-107.

Thoma, F., Koller, T. and Klug, A. (1979) Involvement of histone H1 in the organization of the nucleosome and of the salt-dependent superstructures of chromatin. *J Cell Biol*, **83**: 403-427.

Thomas, H.M., Harper, J.A., Meredith, M.R., Morgan, W.G., Thomas, I.D., Timms, E. and King, I.P. (1996). Comparison of ribosomal DNA sites in *Lolium* species by fluorescence *in situ* hybridization. *Chrom Res*, **4**: 486–490.

Thomas, J.O., Rees, C. and Finch, J.T. (1992) Cooperative binding of the globular domain of histones H1 and H5 to DNA. *Nucleic Acids Res*, **20**:187-194.

Timofejeva, L.P. and Golubovskaya, I.N. (1991) A new type of desynaptic gene in maize revealed by the microspreading method of synaptonemal complexes. *Cytologia (Russ)*, **33**: 3–8.

Ting, Y.C. (1971) Further studies on the synaptonemal complex of haploid maize. *Genetics*, **68**: 67

Toh, G.W., O'Shaughnessy, A.M., Jimeno, S., Dobbie, I.M., Grenon, M., Maffini, S., O'Rourke, A., Lowndes, N.F. (2006) Histone H2A phosphorylation and H3 methylation are required for a novel Rad9 DSB repair function following checkpoint activation. *DNA Repair (Amst)*, **5**: 693–703.

Tremethick, D. J. (2007) Higher-order structures of chromatin: the elusive 30 nm fibre. *Cell*, **128**: 651-654.

- Tsai, C.J., Mets, D.G., Albrecht, M.R., Nix, P., Chan, A. and Meyer, B.J.** (2008) Meiotic crossover number and distribution are regulated by a dosage compensation protein that resembles a condensin subunit. *Gene Dev*, **22**: 194-211.
- Tsukuda, T., Fleming, A.B., Nickoloff, J.A., Osley, M.A.** (2005) Chromatin remodelling at a DNA double-strand break site in *Saccharomyces cerevisiae*. *Nature*, **438**: 379–383.
- Turner, B.M.** (2000) Histone acetylation and an epigenetic code. *Bioassays*, **22**: 836-845.
- Turner, B.M.** (2005) Reading signals on the nucleosome with a new nomenclature for modified histones. *Nat Struct Mol Biol*. **12**: 110–112.
- Tyler, J.K., Adams, C.R., Chen, S.R., Kobayashi, R., Kamakaka, R.T., and Kadonaga, J.T.** (1999). The RCAF complex mediates chromatin assembly during DNA replication and repair. *Nature*, **402**: 555–560.
- Tyler, J.K., Collins, K.A., Prasad-Sinha, J., Amriott, E., Bulger, M., Harte, P.J., Kobayashi, R., and Kadonaga, J.T.** (2001). Interaction between the *Drosophila* CAF-1 and ASF1 chromatin assembly factors. *Mol Cell Biol*, **21**: 6574–6584.
- Uanschou, C., Siwiec, T., Pedrosa-Harand, A., Kerzendorfer, C., Sanchez- Moran, E., Novatchkova, M., Akimcheva, S., Woglar, A., Klein, F. and Schlogelhofer, P.** (2007) A novel plant gene essential for meiosis is related to the human CtIP and the yeast COM1/SAE2 gene. *EMBO J*, **26**: 5061-5070.
- Uhlmann, F.** (2001) Chromosome cohesion and segregation in mitosis and meiosis. *Current Opinion in Cell Biology*, **13**: 754–761.
- Uhlmann, F., Lottspeich, F. and Nasmyth, K.** (1999) Sister-chromatid separation at anaphase onset is promoted by cleavage of the cohesin subunit Scc1. *Nature*, **400**: 37-42.
- Uhlmann, F. and Nasmyth, K.** (1998) Cohesion between sister chromatids must be established during DNA replication. *Curr Biol*, **8**: (20): 1095-1101.
- Unal, E., Arbel-Eden, A., Sattler, U., Shroff, R., Lichten, M., Haber, J.E. and Koshland, D.** (2004) DNA damage response pathway uses histone modification to assemble a double-strand specific cohesin domain. *Molecular Cell*, **16**: 991-1002.
- Ushinsky, S.C., Bussey, H., Ahmed, A.A., Wang, Y., Friesen, J., Williams, B.A. and Storms, R.K.** (1997) Histone H1 in *Saccharomyces cerevisiae*. *Yeast*, **13**:151-161.
- Usui, T., Ohta, T., Oshiumi, H., Tomizawa, J., Ogawa, H. and Ogawa, T.** (1998) Complex formation and functional versatility of Mre11 of budding yeast in recombination. *Cell*, **95**: 705-716.
- van Attikum, H., Fritsch, O., Hohn, B., Gasser, S.M.** (2004) Recruitment of the INO80 complex by H2A phosphorylation links ATP-dependent chromatin remodeling with DNA double-strand break repair. *Cell*, **119**: 777–788.
- van Heemst, D. and Heyting, C.** (2000) Sister chromatid cohesion and recombination in meiosis. *Chromosoma*, **109**: 10-26.
- Van Holde, K.E.** (1988) Chromatin. Series in molecular biology. Springer-Verlag, Newyork
- van Holde, K. and Zlatanova, J.** (2007) Chromatin fiber structure: Where is the problem now. *Semin Cell Dev Biol*, **18**: 651-658.
- van Leeuwen, F., Gafken, P.R., Gottschling, D.E.** (2002) Dot1p modulates silencing in yeast by methylation of the nucleosome core. *Cell*, **109**: 745–756.

- Varga-Weisz, P., van Holde, K. and Zlatanova, J.** (1993) Preferential binding of histone H1 to four-way helical junction DNA. *J Biol Chem*, **268**: 20699-20700.
- Verreault, A.** (2000) De novo nucleosome assembly: new pieces in an old puzzle. *Genes Dev*, **14**: (12):1430-8.
- Verreault, A., Kaufman, P.D., Kobayashi, R., Stillman, B.** (1996) Nucleosome assembly by a complex of CAF-1 and acetylated histones H3/H4. *Cell*, **87**: 95–104
- Vettese-Dadey, M., Grant, P.A., Hebbes, R.T., Crane-Robinson, C., Allis, C.D. and Workman, J.L.** (1996) Acetylation of histone H4 plays a primary role in enhancing transcription factor binding to nucleosomal DNA in vitro. *EMBO J*, **15**: 2508–2518.
- Vila, R., Ponte, I., Collado, M., Arrondo, J. L. R., Jiménez, M. A., Rico, M. and Suau, P.** (2001) DNA-induced α -helical structure in the NH2-terminal domain of histone H1. *J Biol Chem*, **276**: 46429-46435.
- Vogel, K.E.** (2009) Backcross breeding. *Methods Mol Biol*, **526**:161-9. doi: 10.1007/978-1-59745-494-0_14.
- Wade, P.A., Pruss, D. and Wolffe, A.** (1997) Histone acetylation: chromatin in action. *Trends Biochem Sci*, **22**: 128–132.
- Wako, T., Murakami, Y. and Fukui, K.** (2005) Comprehensive analysis of dynamics of histone H4 acetylation in mitotic barley cells. *Genes and Genetic Systems*, **80**: 269-27.
- Wagner, C.R., Kuervers, L., Baillie, D.L. and Yanowitz, J.L.** (2010) xnd-1 regulates the global recombination landscape in *Caenorhabditis elegans*. *Nature*, **467**: (7317): 839–843.
- Walsh, J.B. and Stephan, W.** (2001) Mutigene families evolution. Encyclopedia of life sciences. Nature Publishing Group.
- Walter, P.P., Owen-Hughes, T.A., Cote, J. and Workman, J.L.** (1995) Stimulation of transcription factor binding and histone displacement by nucleosome assembly protein 1 and nucleoplasmin requires disruption of the histone octamer. *Mol Cell Biol*. **15**: 6178–6187
- Wang, C.R., Carlton, P.M., Golubovskaya, I.N., Cande, W.Z.** (2009) Interlock formation and coiling of meiotic chromosome axes during synapsis. *Genetics*, **183**: 905–915.
- Wang, D. and Lippard, S.J.** (2004) Cisplatin-induced post-translational modification of histones H3 and H4. *J Biol Chem*, **279**: 20622–20625.
- Wang, K., Tang, D., Wang, M., Lu, J., Yu, H., Liu, J., Qian, B., Gong, Z., Wang, X., Chen, J., Gu, M., Cheng, Z.** (2009) MER3 is required for normal meiotic crossover formation, but not for presynaptic alignment in rice. *J Cell Sci*, **122**: 2055–2063.
- Wang, M., Wang, K., Tang, D., Wei, C., Li, M., Shen, Y., Chi, Z., Gu, M. and Cheng, Z.** (2010) The central element protein ZEP1 of the synaptonemal complex regulates the number of crossovers during meiosis in rice. *Plant Cell*, **22**: 417-430.
- Wang, T.F., Kleckner, N., and Hunter, N.** (1999). Functional specificity of MutL homologs in yeast: evidence for three Mlh1-based heterocomplexes with distinct roles during meiosis in recombination and mismatch correction. *Proc Natl Acad Sci U S A*, **96**: 13914-13919.
- Watanabe, Y., and Nurse, P.** (1999). Cohesin Rec8 is required for reductional chromosome segregation at meiosis. *Nature*, **400**: 461-464.

- Waterworth, W.M., Altun, C., Armstrong, S.J., Roberts, N., Dean, P.J., Young, K., Weil, C.F., Bray, C.M. and West, C.E.** (2007) NBS1 is involved in DNA repair and plays a synergistic role with ATM in mediating meiotic homologous recombination in plants. *Plant J*: **52**, 41-52.
- Wei, G., Tao, Y., Liu, G., Chen, C., Luo, R., Xia, H., Gan, Q., Zeng, H., Lu, Z., Han, Y., Li, X., Song, G., Zhai, H., Peng, Y., Li, D., Xu, H., Wei, X., Cao, M., Deng, H., Xin, Y., Fu, X., Yuan, L., Yu, J., Zhu, Z. and Zhu, L.** (2009) A transcriptomic analysis of superhybrid rice LYP9 and its parents. *PNAS*, **106**: 7695–7701.
- White, M.J.D.** (1973) *Animal Cytology and Evolution*. (New York: Cambridge University Press), pp. 1-58.
- Wierzbicki, A.T., Jerzmanowski, A.** (2005) Suppression of histone H1 genes in *Arabidopsis* results in heritable developmental defects and stochastic changes in DNA methylation. *Genetics*, **169**:997-1008.
- Wijnker, E., van Dun, k., de Snoo, C.B., Lelivelt, C.L.C., Keurentjes, J.J.B., Naharudin, N.S., Ravi, M., Chan, S.W.L., de Jong, H., and Dirks, R.** (2012) Reverse breeding in *Arabidopsis thaliana* generates homozygous parental lines from a heterozygous plant. *Nature Genetics*, **44**: 467–470. doi:10.1038/ng.2203
- Williamson, R.** (1970) Properties of rapidly labelled deoxyribonucleic acid fragments isolated from the cytoplasm of primary cultures of embryonic mouse liver cells. *Journal of Molecular Biology*, **51**: 157-168.
- Williams, S.P., Athey, B.D., Muglia, L.J., Schappe, R.S., Gough, A.H. and Langmore, J.P.** (1986) Chromatin fibers are left handed double helices with diameter and mass per unit length that depend on linker length. *Biophys J*. **49**:233–248.
- Wisniewski, J.R., Zougman, A., Krüger, S. and Mann, M.** (2007) Mass Spectrometric Mapping of Linker Histone H1 Variants Reveals Multiple Acetylations, Methylations, and Phosphorylation as Well as Differences between Cell Culture and Tissue. *Molecular & Cellular Proteomics*, **6**: 72-87.
- Wojtasz, L., Daniel, K., Roig, I., Bolcun-Filas, E., Xu, H., Boonsanay, V., Eckmann, C.R., Cooke, H.J., Jasin, M., Keeney, S., McKay, M.J. and Toth, A.** (2009) Mouse HORMAD1 and HORMAD2, two conserved meiotic chromosomal proteins, are depleted from synapsed chromosome axes with the help of TRIP13 AAA-ATPase. *PLoS Genet*, **5**, e1000702.
- Wolffe, A.P.** (1998) *Chromatin structure and function*, 3rd edn. London: Academic Press. London
- Wolffe, A.P., Khochbin, S. and Dimitrov, S.** (1997) What do linker histones do in chromatin. *BioEssays*, **19**: 249-255.
- Wolffe, A.P.** (1999) *Chromatin: structure and function*, 3rd ed. Academic Press, San Diego, Calif.
- Wolffe, A.P.** (2000) *Chromatin: Structure and Function* (Academic, San Diego)
- Wong, H., Victor, J.M. and Mozziconacci, J.** (2007) An all-atom model of the chromatin fibre containing linker histones reveals a versatile structure tuned by the nucleosomal repeat length. *PLoS One*, **2**: (9): e877.
- Woodcock, C.L.F.** (1973) Ultrastructure of inactive chromatin. *Journal of Cell Biology*, **59**: 368a.
- Woodcock, C.L.** (2005) A milestone in the odyssey of higher-order chromatin structure. *Nature Structural and Molecular Biology*, **12**: 639.
- Woodcock, C.L., and Dimitrov, S.** (2001) Higher-order structure of chromatin and chromosomes. *Curr Opin Genet Dev*, **11**:130–135.

- Woodcock, C.L., Frado, L.L. and Rattner, J.B.** (1984) The higher-order structure of chromatin: evidence for a helical ribbon arrangement. *J Cell Biol*, **99**: (1 Pt 1):42–52.
- Wright, P.E. and Dyson, H.J.** (1999) Intrinsically unstructured proteins: re-assessing the protein structure-function paradigm. *J Mol Biol*, **293**, 321–331
- Wu, C., Bassett, A. and Travers, A.** (2007) A variable topology for the 30-nm chromatin fibre. *EMBO reports*, **8**: (12): 1129-1134.
- Wu, T.C. and Lichten, M.** (1994) Meiosis-induced double-strand break sites determined by yeast chromatin structure. *Science*, **263**: 515-518.
- Wurtele, H. and Verreault, A.** (2006) Histone post-translational modifications and the response to DNA double-strand breaks. *Curr Opin Cell Biol*, **18**: 137–144.
- Wysocki, R., Javaheri, A., Allard, S., Sha, F., Cote, J. and Kron, S.J.** (2005) Role of Dot1-dependent histone H3 methylation in G1 and S phase DNA damage checkpoint functions of Rad9. *Mol Cell Biol*, **25**: 8430–8443.
- Xiao, B., Jing, C., Killely, G., Walker, P.A., Muskett, F.W., Frenkiel, T.A., Martin, S.R., Sarma, K., Reinberg, D., Gamblin, S.J. and Wilson, J.R.** (2005) Specificity and mechanism of the histone methyltransferase Pr-Set7. *Genes Dev*, **19**: 1444-1454.
- Xu, H., Beasley, M.D., Warren, W.D., van der Horst, G.T. and McKay, M.J.** (2005) Absence of mouse REC8 cohesin promotes synapsis of sister chromatids in meiosis. *Dev Cell*, **8**: 949-961.
- Xu, L.H., Weiner, B.M. and Kleckner, N.** (1997) Meiotic cells monitor the status of the interhomolog recombination complex. *Gene Dev*, **11**: 106-118.
- Yan, W., Ma, L., Burns, K.H. and Matzuk, M. M.** (2003) HILS1 is a spermatid-specific linker histone H1-like protein implicated in chromatin remodeling during mammalian spermiogenesis. *Proc Natl Acad Sci USA*, **100**: 10546-10551.
- Yu, H.G. and Dawe, R.K.** (2000) Functional redundancy in the maize meiotic kinetochore. *J Cell Biol*, **151**: 131-142.
- Yu, H-G. and Koshland, D.E.** (2003) Meiotic condensin is required for proper chromosome compaction, SC assembly, and resolution of recombination-dependent chromosome linkages. *J Cell Biol*, **163**: 937–947.
- Yu, H-G. and Koshland, D.** (2005) Chromosome morphogenesis: Condensin-dependent cohesin removal during meiosis. *Cell*, **123**: 397–407.
- Zempleni, J.** (2005) Uptake localization and non carboxylase roles of biotin. *Annu Rev Nutr*, **25**: 175-96.
- Zhang, H., Ransom, C., Ludwig, P., van Nocker, S.** (2003) Genetic analysis of early flowering mutants in Arabidopsis defines a class of pleiotropic developmental regulator required for expression of the flowering-time switch flowering locus C. *Genetics*, **164**: 347-358.
- Zhang, H. and van Nocker, S.** (2002) The vernalization independence 4 gene encodes a novel regulator of Flowering Locus C. *Plant J*, **31**:663-673.
- Zhang, L., Tao, J., Wang, S., Chong, K. and Wang, T.** (2006). The rice OsRad21-4, an orthologue of yeast Rec8 protein, is required for efficient meiosis. *Plant Mol Biol*, **60**: 533-554.
- Zhang, X., Henriques, R., Lin, S.S., Niu, Q.W. and Chua, N.H.** (2006) Agrobacterium-mediated transformation of *Arabidopsis thaliana* using the floral dip method. *Nat Protoc*, **1**: (2): 641-6.

- Zhang, X.L., Li, X.X., Marshall, J.B., Zhong, C.X. and Dawe, R.K.** (2005) Phosphoserines on maize centromeric histone H3 and histone H3 demarcate the centromere and pericentromere during chromosome segregation. *Plant Cell*, **17**: 572-583.
- Zheng, C. and Hayes, J.J.** (2003) Structures and interactions of the core histone tail domains. *Biopolymers*, **68**: (4): 539-546.
- Zhou, X., Richon, V.M., Wang†, A.H., Yang, X-J., Rifkind, R.A. and Marks, P.A.** (2000) Histone deacetylase 4 associates with extracellular signal-regulated kinases 1 and 2, and its cellular localization is regulated by oncogenic Ras. *Proceedings of the National Academy of Sciences of the United States of America*, **97**: (26): 14329-14333
- Zickler, D. and Kleckner, N.** (1998) The leptotene-zygotene transition of meiosis. *Annu Rev Genet*, **32**: 619-697.
- Zickler, D. and Kleckner, N.** (1999) Meiotic chromosomes: Integrating structure and function. *Annu Rev Genet*, **33**: 603-754.
- Zickler, D., Moreau, P.J., Huynh, A.D. and Slezec, A.M.** (1992) Correlation between pairing initiation sites, recombination nodules and meiotic recombination in *Sordaria macrospora*. *Genetics*, **132**: 135-148.
- Zimmermann, P., Hirsch-Hoffmann, M., Hennig, L., Gruissem, W.** (2004) GENEVESTIGATOR. *Arabidopsis* microarray database and analysis toolbox. *Plant Physiol*, **136**: 2621–2632.
- Zlatanova, J. and Doenecke, D.** (1994) Histone H1 zero: a major player in cell differentiation. *The FASEB Journal*, **8**: (15): 1260-1268.